Imperial College London

Department of Physics

Global Symmetry and Poisson Brackets for Moduli Spaces of Supersymmetric Quiver Gauge Theories with 8 Supercharges

Author:
Kirsty Gledhill

Supervisor:
Amihay Hanany

Submitted in partial fulfilment of the requirements for the degree of Doctor of Philosophy in Physics of Imperial College London and the Diploma of Imperial College

October 5, 2023

Abstract

The study of supersymmetric quantum field theories (SQFTs) has been of high interest in theoretical physics for many years now. It has led to developments in the understanding of many topics such as conformal field theories, the AdS/CFT correspondence and non-supersymmetric QFTs, to name just a few. SQFTs may admit continuous families of vacua, and the continuous vacuum expectation values (VEVs) trace out a geometric space. The space traced out by physically distinct VEVs is termed the moduli space of the theory. Geometric properties of a point on the moduli space of a theory relate to physical properties of the theory in the corresponding vacuum state; one can explore the physics of a theory by studying its moduli space as a mathematical object. The properties of the moduli space that this note contributes to the understanding of are its global symmetry, and its Poisson bracket.

We are concerned with the Coulomb branches of $3d$ $\mathcal{N} = 4$ quiver gauge theories, at their IR fixed point. In particular, the Coulomb branches we focus on have a global symmetry which is a product of the $SU(2)_R$ R-symmetry and the topological global symmetry GS, and are symplectic singularities. The symplectic form induces a Poisson structure, and degenerates at the singularities. The Coulomb branch global symmetry and Poisson bracket are of interest because, as mentioned above, they correspond to physical properties of the theory. In SQFT, particles are understood as excitations of the vacuum state and are labelled by their charges under the global symmetries of the theory. The more massless states that have been integrated out in a particular vacuum state, the more the Poisson bracket degenerates at the corresponding point on the moduli space. This thesis is devoted to recent developments made in the aid of being able to read off these properties from a given $3d$ $\mathcal{N} = 4$ quiver using only simple graph theory operations. In the case of the global symmetry, an attempt at such an algorithm exists, but it does not work unanimously. We help to understand its failure, and suggest an amendment which works on a wider set of quivers. In the case of the Poisson bracket, we provide a conjecture for computing it for quivers of high rank, and in particular for magnetic quivers for certain 5 and $6d$ Higgs branches at infinite coupling.

Declaration

Originality

The new results presented in Chapters 3 and 4 of this thesis are the author's original work, in collaboration with Amihay Hanany. The work in each of these chapters has been published in the following two papers,

- K. Gledhill and A. Hanany, *Coulomb Branch Global Symmetry and Quiver Addition*, *JHEP* **12** (2021) 127 [2109.07237],
- K. Gledhill and A. Hanany, *Poisson Brackets for Coulomb Branches*, *JHEP* **03** (2023) 154 [2210.02966],

respectively. Large parts of the other chapters in this thesis were also drawn from the introductory chapters and appendices of these works. To the best of the author's knowledge, all work present in this thesis that is not the author's own is properly cited and acknowledged.

As these works are published in the Journal of High Energy Physics (JHEP), they are distributed under the terms of the Creative Commons Attribution License (CC-BY 4.0), which permits any use, distribution and reproduction in any medium, provided the original authors and source are credited. Unless stated otherwise, it should be assumed that material adapted from these works has been modified from its original presentation.

Copyright

Acknowledgements

This PhD has not just been about a journey into the world of theoretical physics research for me, but also all the other life that was lived alongside it. While I am incredibly grateful for the opportunity, it has not been an easy ride for me personally: along the way there have been many tricky moments of anxiety and self-doubt. But there has also been an awful lot of fun and love. During my time at Imperial I found running, which has given me a new lease for life. I was lucky enough to live in London, bustling with fun opportunities, lots of different people, and all their stories. The dynamic duo of nature and TV that have brought me peace and belonging ever since childhood remained a firm rock for me throughout. But mainly, as ever, it has been the people who have really shaped and brightened my experience. So many have brought joy and support to me throughout these three years, both in the world of physics, and out of it. With hugs, laughter, empathy, kindness, understanding, or even just a passing smile. I cannot fully express what a difference these people have made to me, and sadly there are too many to name individually here. However there are a select few that I'd like to take the next page or so to give a special mention to.

Firstly and foremostly, I'd like to thank my supervisor Amihay Hanany for being so flexible, accepting, and encouraging. His passion for physics, desire to discover, and the joy he displays in undertaking research are great things to see. I've also learnt far more about etymology from him than I ever thought I would know. Oh, and he's a jolly clever chap – kudos on that Ami.
I'd like to thank Julius and Antoine, who gave up countless hours of their time to help me understand our field. They always did so with kindness, and their explanations enabled me time and time again to understand things a little better. I feel very lucky to have had their company, humour and generosity throughout these three years.
I'd like to thank Zhenghao, Rudolph and Antoine for sharing their coding and computational tips and tricks.
And finally from the field of quivers, I'd like to thank all those who contributed useful discussions or computations for the new work presented in this thesis: Matthew Bullimore, Jacques Distler, Gabi Zafrir, Siyul Lee, Zhenghao Zhong.

In the wider physics world, I would like to thank all my wonderful office-mates at Imperial, all of whom have provided many much-needed laughs and smiles. In particular I would like to thank Torben and Calvin, although I will never be able to do so enough. Lads, I know we are not related, but I think of you both as brothers. Not just each other's brothers either, but mine too. So that's two brothers (you) and one sister (me), to the same hypothetical parents. Time and time again you have taken away my worries and put a huge smile on my face.[1] Thank you for your amazing senses of humour and ability to find fun. For your imaginations, biathlete-themed cards, and willingness to join me on holidays I would otherwise have gone on alone due to buying flights on the wrong week. Thank you for your 100% track record of immediately dropping anything to join me for a much-needed bubble tea or a Tuesday coffee, whether as a celebration or a pick-me-up. Love you both.
And a huge thanks goes to Jacob and Dan. To Jacob for helping me to find peace by affirming, celebrating and joining me in a change in direction, and to Dan for being so supportive, helping to make the change happen, and encouraging me to do it in a way to recognise what had gone before.

[1] You even embrace my excessive caveating and apologising, which is fortunate as I'm sorry to say that I aim to do more of it going forward. But obviously that's just my current take and I can't guarantee I'll feel that way in the future.

Since that April I have felt much stronger and happier.

Lastly I'd like to say a huge thank you to all my wonderful friends and family outside of Imperial. To the Durham and Stourbridge gangs, cheers for it all lads. You know who you are.
I'd like to thank Collins, for always giving me the best advice, and for making me laugh like nobody else. Praise be, lass.
I'd like to give Adon a cursory nod.
I'd like to thank Nanna and Gramps, for all the love, support, kindness and interest. I miss you Nanna.
I'd like to thank Mum and Dad, for everything. From cranking me out in 1997, to always encouraging me to follow my dreams and trust my gut, and a lot of support and looking-after in between. I can never quite get over how kind, moral and loving you guys are, seemingly without even trying.
I'd like to thank Jake, for the updates on Johnson Charles.
And finally, I'd like to thank Croob. For all the hugs, love and care. For making so many days so fun and filled with laughter. For the gyros, for the yes, and for the and.

Dedication

This thesis is dedicated to Mum, Dad, Jake, Nanna and Gramps. I love you all very much.

Contents

Chapter 1

Introduction

In this work, we present recent progress made in two areas: in finding a method for deciphering (a) the global symmetry and (b) the Poisson brackets of a $3d$ $\mathcal{N} = 4$ Coulomb branch $\mathcal{C}$ from its quiver Q. The former is useful as the global symmetries of the Coulomb branch elicit conserved charges in the theory [1], under which the particles in each vacuum state are labelled. The latter relates to the symplectic form of the Coulomb branch, a key ingredient for categorising it as a symplectic singularity [2, 3]. It is of interest to us to study Coulomb branches as mathematical entities, as the geometric properties at a point on the Coulomb branch correspond to physical properties of the vacuum lying at the point. In particular, we will study the IR fixed points[1] of Coulomb branches of "good" or "ugly" [4] $3d$ $\mathcal{N} = 4$ unitary quiver gauge theories with no mass parameters, such that said Coulomb branches are symplectic singularities.

Before diving deeper into our specific area of study, we take a brief step back to ask why such a field is of interest. At surface-level, we are concerned with the moduli spaces of supersymmetric gauge theories. So, why supersymmetry? Why the moduli space?

Supersymmetry is the notion that every boson has a fermionic superpartner and vice versa. The superpartner of a particle has identical mass to it but spin which differs by one half. Supersymmetry was phenomenologically attractive early in its inception as it provided a solution to the so-called *heirarchy problem* of the standard model. It's theoretically viable too, as it evades the Coleman-Mandula postulates; it's an allowed additional global symmetry of a Poincaré-invariant theory. Moreover, it was actually *predicted* by string theory, the theory believed by many to be the best candidate for a "theory of everything". It's clear from the lack of superpartners that supersymmetry is spontaneously broken in the vacuum state of our world, but it is possible that it would emerge at higher energies. As time goes on and evidence for supersymmetry is still yet to be found at higher and higher energies, the hope of finding superpartners (and thus the phenomenological motivation for supersymmetry) is dwindling. However, this does not mean there is a lack of motivation to study supersymmetric theories. The mathematical structure behind supersymmetry is used in many areas of physics, making it still of practical interest. Then there is the theoretical interest. Incorporating supersymmetry simplifies many problems. Theories with it enjoy nice properties, such as the protection of certain quantities under the renormalisation group (RG) flow. This makes supersymmetric theories good toy models for their non-supersymmetric counterparts, helping us to learn of their behaviour in an arena

[1] Note that having an infrared (IR) fixed point implies that the theory contains "sufficient matter" [4].

in which we can actually perform computations.

The moduli space $\mathcal{M}$ of a theory is its set of gauge-inequivalent vacua. This is an important object to study for many reasons, the most obvious of which is that it tells us the possible spectra. In many quantum field theories (QFTs) $\mathcal{M}$ is trivial or rather uninteresting, but in supersymmetric gauge theories there are often continuous families of vacua parameterising a moduli space with rich structure. This is especially prevelant in gauge theories with eight supercharges, where the representations of the superPoincaré algebra give a natural splitting of $\mathcal{M}$ into the *Coulomb branch*, *Higgs branch* and possible *mixed branches*. The Higgs branch at finite coupling remains classically exact all along the RG flow, and is well understood. The Coulomb branch however receives quantum corrections, and in general it's not known how to practically deal with these. However, for the specific case of $3d$ $\mathcal{N} = 4$ theories there is an alternative route that can be pursued to make progress: at the IR fixed point, the Coulomb branch can be described by half-BPS dressed monopole operators. This thesis focuses on using this viewpoint to contribute further developments to the study of $3d$ $\mathcal{N} = 4$ Coulomb branches. The only Higgs branches studied are those taken from 5 and $6d$ theories at infinite coupling, which can be described by the Coulomb branch of a $3d$ $\mathcal{N} = 4$ theory.

It was conjectured in [5] that $3d$ $\mathcal{N} = 4$ Coulomb branches are symplectic singularities[2] in the sense of [2]: roughly speaking, they are algebraic varieties with a symplectic form ω containing zero or more singular points at which ω degenerates. Algebraic geometry then tells us that such an object is described fully by the ring of holomorphic functions over it, which for $3d$ $\mathcal{N} = 4$ Coulomb branches is believed to be isomorphic to the chiral ring. A chiral operator in a theory is an operator which is annihilated by all supercharges of one chirality (it preserves half the supersymmetry). The chiral ring is then the set of all gauge-invariant chiral operators which satisfy the vacuum constraints. It is a commutative ring; the Coulomb branch can be categorised exactly as an algebraic variety if the explicit form of the chiral operators generating it and any relations they satisfy can be found. This is typically too challenging to do, but there are still good steps we can take towards fully categorising $\mathcal{C}$ as a symplectic singularity, as we do have methods to compute many of its properties. Examples of such properties that we take interest in are its dimension, Hilbert series, global symmetry, singularity structure and symplectic form.

At the top of this introduction, we were far more specific with the moduli spaces that we study than simply "$3d$ $\mathcal{N} = 4$ Coulomb branches". However, all the other caveats, for example that we consider only gauge theories and not ones which incorporate gravity, are simply there because it is for these theories that we have been able to develop techniques to successfully study them. Any progress enabling us to drop any of these caveats, for example a method to study the Coulomb branch in the infrared but not at the SCFT, would be most welcome, but for now we study what we have an understanding of.

A tool which aids our studies is that of the *quiver* Q [6]. The information in many[3] $3d$ $\mathcal{N} = 4$ gauge

[2]Note that there are caveats to this conjecture; there exist $3d$ $\mathcal{N} = 4$ quivers for which the Coulomb branch is not a symplectic singularity. For example, the Coulomb branches of many unitary quivers satisfying gcd(gauge node ranks) > 1. We don't mention these caveats in the main text as we will exclude any quivers whose Coulomb branches are known to not be symplectic singularities from our study.

[3]The first theories realised as quiver theories were those describing D-branes probing orbifolds, but the techniques used have since been generalised to a wider set of theories.

theories can be entirely encoded in a quiver diagram; such theories are called *quiver gauge theories*.[4] In cases where the quiver theory has a Lagrangian $\mathcal{L}$, the quiver is entirely equivalent to $\mathcal{L}$. However there are quivers for which there is no Lagrangian interpretation; they can help us to study classically inaccessible theories. The idea behind using quivers is to simplify problems by translating complex traditional SQFT methods performed on $\mathcal{L}$ to simple graph theory computations performed on Q. Indeed our end goal is to establish simple algorithms to read off any property of the Coulomb branch from the quiver. In recent history many techniques have been developed in aid of this goal, but the three we will employ the most heavily in this note are the *monopole formula* [7], the *magnetic quiver* [8], and the *Hasse diagram* [9]. The methodology and results presented in this thesis in Chapters 3 and 4, based on our works [10] and [11] respectively, hopefully provide additional helpful steps along the way to realising this goal for two particular properties of interest on $\mathcal{C}$: the global symmetry and the symplectic form.

The global symmetry of the Coulomb branch is the product of the $SU(2)_R$ R-symmetry and the topological symmetry GS. In the UV, the topological symmetry of a theory with unitary gauge group containing a unitary factors is $U(1)^a$, but upon flowing to the infrared fixed point, this is often enhanced to some larger group GS for whom this abelian symmetry is the maximal torus. The monopole formula [7] allows us to compute the refined Hilbert series for the Coulomb branch, which counts the operators lying on it graded by their weights under $SU(2)_R$ and GS. The t^2 term of this (possibly after a fugacity map) gives the fundamental weight character of the adjoint representation of GS [12].[5] Whilst this is a reliable method to find GS, it takes time to implement and for quivers of sufficiently high rank it is too computationally intensive to do. We would like to realise GS simply from looking at the quiver. By and large, this can be done by applying an algorithm [14] based on the quiver's balanced gauge nodes [4]. However, there are many quivers known for which this algorithm only gives a strict subgroup of GS. We constructed the bulk of such quivers in [10], building on the few already existing in the literature (see for example [15, 16]). Our findings of the failure of the balance algorithm to always give the full GS group show that there is a need to make alterations to it, and the method we used to construct the quivers for which the algorithm fails naturally leads to one possible amendment. We detail this amended algorithm, which gives the correct GS for all quivers that the previous algorithm worked for, *and* all quivers constructed in [10].[6]

The symplectic form ω defines $\mathcal{C}$ as a symplectic singularity, and naturally induces a Poisson bracket $\{\cdot,\cdot\}_{\mathcal{C}}$. The Poisson brackets between the generators of $\mathcal{C}$ as a symplectic singularity, $\mathcal{G}_{\mathcal{C}}$, fix all Poisson brackets on $\mathcal{C}$ due to the commutative nature of the chiral ring and the Leibniz and antisymmetric properties of the Poisson bracket, and helps us to learn of the symplectic form. In particular, the symplectic form and Poisson brackets degenerate at the same points, and thus $\{\cdot,\cdot\}_{\mathcal{C}}$ provides key information about the singularity structure of $\mathcal{C}$. There has been previous progress with determining Poisson brackets in the literature, see for instance [17, 3, 18, 19, 20]. In [11] we contribute to this by

[4] We will sometimes refer to quiver gauge theories simply as quiver theories or quivers for brevity.

[5] Note that weights only capture the local behaviour of a group; the global form of GS can be obtained from studying the representations which generate the Hilbert series and their charges under the centre of GS (see comments in Appendix A of [13], for example). In the rest of this thesis, we omit the "local form" caveat for brevity; whenever we say global symmetry or GS, we really mean its *local form*. We do not include the global form as it will not be important for our discussions or results.

[6] Note that there are still quivers that this amended algorithm does not cater for, but it is an improvement on what existed previously.

extending the methodology to certain unitary quivers of arbitrarily high rank, using representation theory, conserved charges and the dressed monopole construction of the Coulomb branch.

This thesis is organised as follows. In Chapter 2, we provide a recap of the background material necessary to follow the workings of and results in this note, and a summary of some key terminology and notation used. Topics discussed are supersymmetry, quivers, categorising algebrogeometric objects, $3d$ $\mathcal{N}=4$ Coulomb branches, Hilbert series', magnetic quivers and Hasse diagrams. Chapter 3 is dedicated to the work of [10], constructing infinitely many quivers on which the algorithm for determining GS from the balance fails, and providing an amendment to the algorithm to fix this failing. In Chapter 4 we detail the work of [11], giving the Poisson brackets between Coulomb branch operators for Klein singularities, nilpotent orbits and magnetic quivers of certain five and six dimensional theories at infinite coupling. Finally, we summarise our results and discuss possible future directions in Chapter 5. Appendices A and B cover two techniques needed to understand specific methodologies used in Chapters 3 and 4: discrete projections and tensor, symmetric and antisymmetric products respectively.

In the course of the following discussions, we often omit caveats that apply to all our statements to avoid excessive repetition. For example, we may make a statement about Coulomb branches that *does not hold in general* and is only intended to be taken for the specific quivers we study (which are subject to several conditions, as mentioned in the first paragraph of this introduction), but not explicitly state this. There are several such caveats that we will omit some or all of at different stages in the remainder of this work, and so as to not mislead the reader we make an explicit summary here clarifying the inherent omissions in the terminology used in the following chapters:

- When we talk about a "quiver" or "theory", we mean a good or ugly $3d$ $\mathcal{N}=4$ unitary quiver gauge theory with no mass parameters, such that its Coulomb branch at the IR fixed point is a symplectic singularity.
- When we talk about a "Coulomb branch" for a quiver (see above point), we really mean the IR fixed point of the Coulomb branch for this quiver.
- We rarely mention Higgs branches; unless specified otherwise, all objects that could belong to the Coulomb or Higgs branch should be assumed to be referring to the Coulomb branch case. For example "Hasse diagram" means "Coulomb branch Hasse diagram", "global symmetry" means "Coulomb branch global symmetry" and so on.
- The Coulomb branch global symmetry of a quiver is a product of the $SU(2)_R$ R-symmetry and the topological symmetry GS. However whenever we say global symmetry, unless specified otherwise, we refer solely to the local form of the topological component; the global form will not be important for our discussions or results (and can be determined from the Hilbert series in any case), and the R-symmetry is already established and thus not worth mentioning. That is, "global symmetry" and "GS" both refer to the Coulomb branch topological symmetry.
- We may refer to a quiver Q_1 as being "in the Hasse diagram" of another quiver Q_2. By this, we mean that the Coulomb branch of Q_1 is the closure of some symplectic leaf in the Hasse diagram of the Coulomb branch of Q_2.
- We may refer to an algebraic variety $\mathcal{V}$ either as itself or as the quiver Q whose Coulomb branch is isomorphic to it (the Coulomb quiver). Similarly we may refer to a quiver Q as itself or as the variety $\mathcal{V}$ that is isomorphic to its Coulomb branch.

- For an unframed non-simply-laced quiver, the Coulomb branch we refer to is that obtained from ungauging on a long node (the choice of which long node is irrelevant).

Each of these abbreviations will also be stated in the text at their natural introduction; we summarise them here for the reader's convenience. Chapter 2 should clarify any terminology unfamiliar to the reader appearing in the above list.

Chapter 2

Background Material

As mentioned in Chapter 1, we exclusively study the IR fixed points of Coulomb branches of unitary "good" and "ugly" $3d$ $\mathcal{N} = 4$ quiver gauge theories [4] with no mass parameters, such that said Coulomb branches are symplectic singularities [2].[2] In particular, the new results presented in this thesis in Chapters 3 and 4 pertain to the global symmetry of the Coulomb branch and the Poisson brackets between the vacua at different points on it. This chapter serves as a recap of the necessary prerequisite knowledge and techniques needed to understand our discussions. The author would like to stress that there exist many more techniques to probe $3d$ $\mathcal{N} = 4$ Coulomb branches than those discussed in this section, see for example [21, 22, 23, 24, 25, 26, 27, 28, 29].

Section 2.1 kicks off with some basic supersymmetry, with particular focus to find the allowed representations of the superPoincaré algebra in a $3d$ $\mathcal{N} = 4$ gauge theory [30]. Many such theories are completely encoded by their gauge group, matter content, and how the matter transforms under the gauge group, and this information can be entirely summarised in a diagram called a *quiver* [6]. Section 2.2 is devoted to discussing how this is done. Here we will also introduce the notion of *balance* [4], which will be crucial for Chapter 3. Once we have understood the Lagrangian content of these theories we can then move on to discuss the moduli space, the topic of Section 2.3. Here we see the moduli space in two lights: as the set of vacua of a physical theory, and as an algebrogeometric object. Supersymmetric theories typically have much richer moduli spaces than a generic QFT, and in fact the ones we study are *HyperKähler cones* or *symplectic singularities*. We address some interesting properties of such objects, and see how to categorise them. Section 2.4 then further specialises the discussion of moduli spaces to the type that is the subject of this thesis, the $3d$ $\mathcal{N} = 4$ Coulomb branch, and details how it is described. The moduli space is naturally considered in the IR, where the theories we study are strongly coupled. In Section 2.4.1 we see how the Coulomb branch of the classical UV SCFT defined by the quiver theory receives quantum corrections upon flowing to the IR. It is not known how to implement these corrections in general for a theory, but as we show in Section 2.4.2, we *are* able to describe the quantum Coulomb branch at the IR fixed point using *dressed monopole operators* [31, 32]. In Section 2.5 we discuss how we can use this viewpoint to find properties of the Coulomb branch that are of interest, enabling us to make progress with categorising $\mathcal{C}$ as a symplectic singularity. One tool which enables us to do this is the *Hilbert series* [33] of the Coulomb branch, which can be computed using the monopole formula [7]. How to calculate and interpret this is the topic of Section 2.6. The *Hasse diagram* of Coulomb branches (or of Higgs branches, via their *magnetic quiver* [8]), which explores their singularity structure and gives hints about the global symmetry, can be found using *quiver subtraction* [34]. Hasse diagrams, magnetic quivers and

quiver subtraction are the final tools we'll use in this thesis, and Section 2.7 is dedicated to their review.

2.1 Supersymmetry

In this section we recap the necessary basics of supersymmetry to understand the physics discussed and terminology used in the following chapters; it is aimed at readers already familiar with the topics discussed, and is not intended as a comprehensive overview of the subject. For a thorough discussion of the principles and derivation of supersymmetry, see for example [30].

Recall that the subject of our work is the space of half-BPS Coulomb branch vacua in $3d$ $\mathcal{N} = 4$ gauge theories with no mass parameters. Particles in a theory are excitations of the vacuum and must fit into representations of the global symmetry; the particles we consider lie in supermultiplets, representations of the superPoincaré algebra. Vacua are necessarily Lorentz scalars (we will drop the "Lorentz" from here on in for ease), hence for us it will be sufficient to limit our recap of supersymmetry to the scalars that show up in the $3d$ $\mathcal{N} = 4$ massless supermultiplets that have no component whose absolute value of spin exceeds 1. We will arrive at this in Section 2.1.2.3, but in order to properly understand what we find, we will briefly recap the idea of supersymmetry, the $4d$ $\mathcal{N} = 1$ superPoincaré algebra, and the $4d$ $\mathcal{N} = 1, 2$ multiplets along the way.

2.1.1 The superPoincaré algebra

In a four-dimensional non-supersymmetric theory, Coleman-Mandula states (with a few caveats) that the only non-internal symmetries allowed are that of the Poincaré group: translations and Lorentz transformations, $ISO(1,3)$. These are bosonic symmetries; their generators (P^μ and $M^{\mu\nu}$ respectively) form a purely-even Lie algebra, the Poincaré algebra. All particles in the theory, such as gauge bosons, electrons, the Higgs boson etc. lie in representations of this algebra (for the listed examples these are the vector, fundamental and trivial representation respectively).

When elevating such a theory to be supersymmetric, we want every particle from the non-supersymmetric theory to have a superpartner, which has all the same conserved charges as the particle except for its spin, which differs by a half. The name of the fermionic (bosonic) superpartner of a boson (fermion) is obtained by adding "ino" to the end of the name (adding "s" to the front of the name). For example, the superpartner of the electron is the selectron and the superpartner of the gauge boson is the gaugino.

To successfully implement this symmetry between bosons and fermions, we need to introduce an operator Q which acts on a fermion to give a boson, and vice versa:

$$Q\,|\text{fermion}\rangle = |\text{boson}\rangle\,, \qquad Q\,|\text{boson}\rangle = |\text{fermion}\rangle\,. \tag{2.1.1}$$

Such operators must satisfy certain constraints. They must be spin one-half operators, since they change the spin of the operator on which they act by this amount. Additionally, to live in a Poincaré-invariant space-time, they must additionally be part of a representation of the Poincaré algebra in our four-dimensional theory. Thus the simplest way we can introduce these supersymmetry generators (2.1.1) into our four dimensional theory is as two spinors Q_α and $\bar{Q}^{\dot{\alpha}}$ in the representations $(\frac{1}{2}, 0)$

and $(0, \frac{1}{2})$ of the Lorentz algebra $\mathfrak{so}(1,3) \cong \mathfrak{sl}(2;\mathbb{C}) \cong \mathfrak{su}(2) \oplus \mathfrak{su}(2)$.[1] We use $\mathfrak{su}(2) \oplus \mathfrak{su}(2)$ charges (j_1, j_2) to denote the representations of the Lorentz algebra, and $\mathfrak{sl}(2;\mathbb{C})$ indices α, $\dot{\alpha} = 1, 2$ to denote the left and right (or chiral and anti-chiral) spinors respectively. These indices can be raised and lowered using the $\mathfrak{sl}(2;\mathbb{C})$-invariant tensors $\epsilon_{\alpha\beta}$, $\epsilon_{\dot{\alpha}\dot{\beta}}$.

We call the four combined components of Q_α and $\bar{Q}^{\dot{\alpha}}$ the four *supercharges* of the theory: the degrees of freedom generating the supersymmetry. In four dimensions, a theory with four supercharges is called a $4d$ $\mathcal{N} = 1$ theory.[2] Together with P^μ and $M^{\mu\nu}$ they form a *superPoincaré algebra*, a graded algbera with a Lie bracket which acts on pairs of fermions as an anticommutator, but as a commutator in all other instances. The only non-vanishing Lie bracket between the supercharges is between the conjugates, which pair to give the momentum tensor:

$$\{Q_\alpha, \bar{Q}_{\dot{\alpha}}\} = 2\,(\sigma^\mu)_{\alpha\dot{\alpha}} P_\mu. \tag{2.1.2}$$

The σ^μ that contract the vector indices are the Pauli matrices that generate $\mathfrak{sl}(2;\mathbb{C})$:

$$\sigma^0 = \begin{pmatrix} 1 & 0 \\ 0 & 1 \end{pmatrix}, \quad \sigma^1 = \begin{pmatrix} 0 & 1 \\ 1 & 0 \end{pmatrix}, \quad \sigma^2 = \begin{pmatrix} 0 & -i \\ i & 0 \end{pmatrix}, \quad \sigma^3 = \begin{pmatrix} 1 & 0 \\ 0 & -1 \end{pmatrix}, \tag{2.1.3}$$

whose rows are labelled by spinor indices α, and columns by conjugate spinor indices $\dot{\alpha}$. The factor of two in (2.1.2) is chosen by convention for ease. By matching indices and use of the Jacobi identity, it also follows that the Lie brackets of the supercharges with the Poincaré generators are

$$\begin{aligned} [Q_\alpha, M^{\mu\nu}] &= (\sigma^{\mu\nu})_\alpha{}^\beta Q_\beta, \\ [\bar{Q}_{\dot{\alpha}}, M^{\mu\nu}] &= -(\bar{\sigma}^{\mu\nu})^{\dot{\beta}}{}_{\dot{\alpha}} \bar{Q}_{\dot{\beta}}, \\ [Q_\alpha, P^\mu] &= 0, \\ [\bar{Q}_{\dot{\alpha}}, P^\mu] &= 0, \end{aligned} \tag{2.1.4}$$

where

$$\begin{aligned} (\sigma^{\mu\nu})_\alpha{}^\beta &= \frac{i}{4}(\sigma^\mu \bar{\sigma}^\nu - \sigma^\nu \bar{\sigma}^\mu)_\alpha{}^\beta, \\ (\bar{\sigma}^{\mu\nu})^{\dot{\alpha}}{}_{\dot{\beta}} &= \frac{i}{4}(\bar{\sigma}^\mu \sigma^\nu - \bar{\sigma}^\nu \sigma^\mu)^{\dot{\alpha}}{}_{\dot{\beta}}, \end{aligned} \tag{2.1.5}$$

and

$$(\bar{\sigma}^\mu)^{\dot{\alpha}\alpha} = (1, -\sigma^1, -\sigma^2, -\sigma^3)^{\dot{\alpha}\alpha}. \tag{2.1.6}$$

Much like how a particle in a non-supersymmetric theory lies in a representation of the Poincaré algebra, a particle in a supersymmetric theory lies in a representation of the superPoincaré algebra. These representations are called *supermultiplets*.

---

[1] Our notation here is slightly sloppy: it is not true that $\mathfrak{so}(1,3) \cong \mathfrak{su}(2) \oplus \mathfrak{su}(2)$, as the latter is compact while the former is not. However this issue dissolves under complexification; certain complex linear combinations of $\mathfrak{su}(2) \oplus \mathfrak{su}(2)$ are isomorphic to $\mathfrak{so}(1,3)$, and hence our discussion of Lorentz representations as (j_1, j_2) under $\mathfrak{su}(2) \oplus \mathfrak{su}(2)$ is justified.

[2] This $\mathcal{N}$ refers to the quotient of the number of supercharges by the dimension of the spinor representation in the given number of dimensions. In $4d$ the Lorentz algebra is $\mathfrak{so}(1,3) \cong \mathfrak{so}(4) \cong \mathfrak{su}(2) \oplus \mathfrak{su}(2)$, and here the spinor representation has dimension 4. Hence a four supercharge theory has $\mathcal{N} = 1$. A four-dimensional theory with eight supercharges, say $\{Q_{I,\alpha}, \bar{Q}_I^{\dot{\alpha}}, Q_{II,\alpha}, \bar{Q}_{II}^{\dot{\alpha}}\}$, will have $\mathcal{N} = 2$. In three dimensions the Lorentz algebra is $\mathfrak{so}(1,2) \cong \mathfrak{so}(3) \cong \mathfrak{su}(2)$, the spinor representation of which has dimension 2, hence a three-dimensional theory with four or eight supercharges has $\mathcal{N} = 2$ or $\mathcal{N} = 4$, respectively.

2.1.2 Constructing supermultiplets

To build representations of the superPoincaré algebra we start with projective irreducible representations of the Poincaré algebra, and act on them with supercharges to build supermultiplets containing states of differing spin but identical mass.[3] The details of constructing supermultiplets differs slightly in the massive case to the massless case, and since in our work we study only theories with no mass parameters[4] we will discuss only the massless construction here. We focus first on the multiplets in a $4d$ $\mathcal{N}=1$ theory, before extending our discussion to $4d$ $\mathcal{N}=2$, from which we can dimensionally reduce to arrive at the desired multiplets of a $3d$ $\mathcal{N}=4$ theory.

2.1.2.1 $4d$ $\mathcal{N}=1$

The mass Casimir $m^2 = P_\mu P^\mu$ is used to label irreps of the Poincaré group. Consider a massless particle. Then we can always boost and rotate to a frame in which all motion is in the x^3 direction, i.e. its momentum vector is

$$p_\mu = (E, 0, 0, E). \tag{2.1.7}$$

This clearly gives $m^2 = 0$, but upon fixing this p_μ there is still an $ISO(2)$ symmetry remaining as we can either translate or rotate the x^1 and x^2 dimensions and still leave p_μ invariant. In theory, the translations of this $ISO(2)$ can be labelled by a continuous vector $\boldsymbol{k} = (k_1, k_2)$. If a non-trivial translation is performed, then the $SO(2) \subset ISO(2)$ is no longer a symmetry, and in this case the particle is labelled by $|p_\mu, \boldsymbol{k}\rangle$. However if $\boldsymbol{k} = 0$, the $SO(2)$ rotations of x^2 and x^3, M^{12}, are still a symmetry. Projective irreducible representations of this $SO(2) \cong U(1)$ are labelled by half-integers: the eigenvalues λ of M^{12}. In nature, we do not observe massless particles with continuous spin $\boldsymbol{k}$ but instead with half-integral spin λ, hence we declare that $\boldsymbol{k} = 0$ and see that massless particles must be labelled with their momentum p_μ and *helicity*[5] $\lambda \in \frac{1}{2}\mathbb{Z}$:

$$|p_\mu; \lambda\rangle\,. \tag{2.1.8}$$

Note that (2.1.8) is specified by a single value λ, but we know a massless particle has two polarisations. This is reconciled by completing (2.1.8) with its CPT conjugate $|p_\mu; -\lambda\rangle$. In summary, the representation of a massless particle is comprised of two states:

$$|p_\mu; \lambda\rangle\,, \quad |p_\mu; -\lambda\rangle\,. \tag{2.1.9}$$

In SUSY, spin is no longer a Casimir of the global symmetry algebra, and a representation is built by acting on a Poincaré state $|p_\mu; \lambda\rangle$ with Q and $\bar{Q}$ to find the states with other helicities $|p_\mu; \tilde{\lambda}\rangle$ living in the same mulitplet. We can see that all states in a multiplet will have the same mass (i.e. $P_\mu P^\mu$ is still a Casimir of SUSY) by virtue of the fact that $[Q, P] = 0 = [\bar{Q}, P]$. Since we're considering a frame in which our massless particles have momentum (2.1.7), we can see that for us the supersymmetry algebra is

$$\{Q_\alpha, \bar{Q}_{\dot{\alpha}}\} = \begin{pmatrix} 4E & 0 \\ 0 & 0 \end{pmatrix}, \tag{2.1.10}$$

which immediately tells us

$$Q_2 = \bar{Q}_{\dot{2}} = 0, \quad |Q_1\,|p_\mu; \lambda\rangle\,|^2 = 4E. \tag{2.1.11}$$

[3] Upon including supersymmetry, the mass Casimir $P_\mu P^\mu$ of the Poincarré group is preserved, but the Pauli-Lubański Casimir $W_\mu W^\mu$ is not.

[4] The singularity of the $3d$ $\mathcal{N}=4$ Coulomb branches we study is resolved by the inclusion of mass parameters.

[5] Throughout this note, we often sloppily refer to helicity as spin.

We can also see that Q_1 lowers spin by $\frac{1}{2}$, i.e. $Q_1 |p_\mu; \lambda\rangle \propto |p_\mu; \lambda - \frac{1}{2}\rangle$:

$$\begin{aligned} M^{12} Q_1 |p_\mu; \lambda\rangle &= ([M^{12}, Q_1] + Q_1 M^{12}) |p_\mu; \lambda\rangle \\ &= -\frac{1}{2} Q_1 |p_\mu; \lambda\rangle + Q_1 \lambda |p_\mu; \lambda\rangle \\ &= (\lambda - \frac{1}{2}) |p_\mu; \lambda\rangle . \end{aligned} \tag{2.1.12}$$

We can similarly show that $\bar{Q}_{\dot{1}}$ raises spin by $\frac{1}{2}$. Thus $\bar{Q}_{\dot{1}}, Q_1$ act as raising and lowering operators we can use to build our supermultiplets; if we define

$$\begin{aligned} a &= \frac{1}{2\sqrt{E}} Q_1, \\ a^\dagger &= \frac{1}{2\sqrt{E}} \bar{Q}_{\dot{1}}, \end{aligned} \tag{2.1.13}$$

then $a, a^\dagger$ satisfy the Clifford algebra

$$\{a, a^\dagger\} = 1, \quad a^2 = (a^\dagger)^2 = 0. \tag{2.1.14}$$

Starting from a state $|p_\mu; \lambda\rangle$, all possible states in the supermultiplet are then

$$|A\rangle = |p_\mu; \lambda\rangle , \quad |B\rangle = a^\dagger |p_\mu; \lambda\rangle \propto |p_\mu; \lambda + \frac{1}{2}\rangle . \tag{2.1.15}$$

There is no $|C\rangle = |p_\mu; \lambda - \frac{1}{2}\rangle$, because this would be related to $|B\rangle$ by two actions of a, but this vanishes due to its nilpotency.[6] Since we are interested only in supersymmetric gauge theories (no gravity), we will only be interested in supermultiplets containing spins with absolute value ≤ 1. According to building multiplets as in (2.1.15), this amounts to starting with a Poincaré rep of either spin $\lambda = 0$ or $\lambda = \frac{1}{2}$, giving the *chiral* and *vector* multiplets respectively:

Chiral multiplet:

$$\begin{array}{ccc} \phi & |p_\mu; \lambda = 0\rangle & \xrightarrow{\bar{Q}_{\dot{1}}} & |p_\mu; \lambda = \frac{1}{2}\rangle & \psi \\ & \downarrow + \text{CPT} & & \downarrow + \text{CPT} & \\ & |p_\mu; \lambda = 0\rangle & & |p_\mu; \lambda = -\frac{1}{2}\rangle & \end{array} \tag{2.1.16}$$

Vector multiplet:

$$\begin{array}{ccc} \chi & |p_\mu; \lambda = \frac{1}{2}\rangle & \xrightarrow{\bar{Q}_{\dot{1}}} & |p_\mu; \lambda = 1\rangle & A_\mu \\ & \downarrow + \text{CPT} & & \downarrow + \text{CPT} & \\ & |p_\mu; \lambda = -\frac{1}{2}\rangle & & |p_\mu; \lambda = -1\rangle & \end{array} \tag{2.1.17}$$

The chiral multiplet contains one complex scalar ϕ and one Weyl fermion ψ, made up of the CPT conjugate $|p_\mu; \lambda = 0\rangle$ and $|p_\mu; \lambda = \pm\frac{1}{2}\rangle$ states in (2.1.16), respectively. The vector multiplet contains one Weyl fermion χ and one gauge boson A_μ, made up of the CPT conjugate $|p_\mu; \lambda = \pm\frac{1}{2}\rangle$ and $|p_\mu; \lambda = \pm 1\rangle$ states in (2.1.17), respectively. Clearly each has two fermionic and two bosonic degrees of freedom

[6] Obviously we could have instead chosen $|p_\mu; \lambda\rangle$ and $|p_\mu; \lambda - \frac{1}{2}\rangle$ to live in the same multiplet instead; the Clifford algebra merely restricts to two states, and so the choice between this configuration and (2.1.15) is equivalent to declaring $|p_\mu; \lambda\rangle$ as either the state highest or lowest spin in the multiplet.

(on-shell);[7] indeed the symmetry between bosons and fermions has been realised.

We can see that the gauge degrees of freedom in the theory lie in the vector multiplet, whereas the chiral multiplet encodes the matter content. Gauge symmetries commute with the supercharges; all particles in a supermultiplet transform in the same way under the gauge symmetry G. Hence χ is constrained to be in the adjoint representation of G whereas ϕ, ψ can lie in any representation $\mathcal{R}$.

2.1.2.2 $4d$ $\mathcal{N} = 2$

The starting point for constructing massless $4d$ $\mathcal{N} = 2$ supermultiplets is the same as for $4d$ $\mathcal{N} = 1$: the $4d$ massless Poincaré irreps $|p_\mu; \lambda\rangle$. The only difference now is that we add in *two* pairs of supercharges, logically extending the supersymmetry algebra:

$$\begin{aligned}
\{Q^A_\alpha, \bar{Q}^B_{\dot\alpha}\} &= 2\,(\sigma^\mu)_{\alpha\dot\alpha}\,P_\mu\,\delta^{AB}, \\
\{Q^A_\alpha, Q^B_\beta\} &= \epsilon_{\alpha\beta}\,Z^{AB}, \\
\{\bar{Q}^A_{\dot\alpha}, \bar{Q}^B_{\dot\beta}\} &= \epsilon_{\dot\alpha\dot\beta}\,(Z^\dagger)^{AB}, \\
[Q^A_\alpha, M^{\mu\nu}] &= (\sigma^{\mu\nu})_\alpha{}^\beta\,Q^A_\beta, \\
[\bar{Q}^A_{\dot\alpha}, M^{\mu\nu}] &= (\sigma^{\mu\nu})^{\dot\beta}{}_{\dot\alpha}\,\bar{Q}^A_{\dot\beta}, \\
[Q^A_\alpha, P^\mu] &= 0, \\
[\bar{Q}^A_{\dot\alpha}, P^\mu] &= 0,
\end{aligned} \tag{2.1.18}$$

for $A, B = 1, 2$ and Z^{AB} the so-called central charges of the theory. As in Section 2.1.2.1, a massless Poincaré state is comprised of $|p_\mu; \pm\lambda\rangle$ for $p_\mu = (E, 0, 0, E)$, but now we have

$$\{Q^A_\alpha, \bar{Q}^B_{\dot\alpha}\} = \begin{pmatrix} 4E & 0 \\ 0 & 0 \end{pmatrix} \delta^{AB}. \tag{2.1.19}$$

(2.1.19) tells us that for massless states the central charges vanish, and everything is analogous to the $4d$ $\mathcal{N} = 1$ case except for that we now have two mutually anticommuting sets of ladder operators

$$a^A = \frac{1}{2\sqrt{E}} Q^A_1, \qquad (a^A)^\dagger = \frac{1}{2\sqrt{E}} \bar{Q}^A_{\dot 1} \tag{2.1.20}$$

for $A = 1, 2$, and thus in each multiplet we have four states,

$$|p_\mu; \lambda\rangle\,, \qquad (a^1)^\dagger\,|p_\mu; \lambda\rangle\,, \qquad (a^2)^\dagger\,|p_\mu; \lambda\rangle\,, \qquad (a^1)^\dagger (a^2)^\dagger\,|p_\mu; \lambda\rangle\,, \tag{2.1.21}$$

plus their CPT conjugates. For gauge theories then, there are two such multiplets, the hypermultiplet and vector multiplet, obtained from starting with a state of helicity $\lambda = -\frac{1}{2}$ and $\lambda = 0$ respectively:

Hypermultiplet:

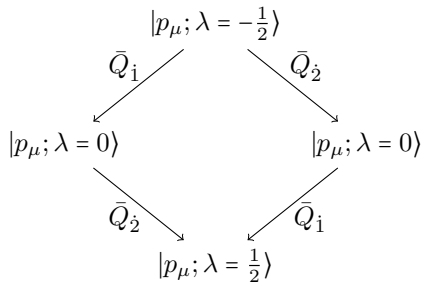

, (2.1.22)

[7] Off-shell, there are additional auxiliary degrees of freedom.

Vector multiplet:

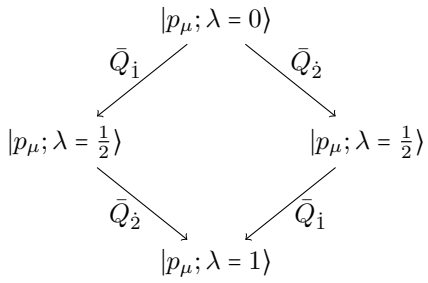

(2.1.23)

plus the CPT conjugate of each state. The hypermultiplet contains two Weyl spinors ψ_1, ψ_2 and two complex scalars φ_1, φ_2. The vectormultiplet contains one gauge boson A_μ, two Weyl spinors χ_1, χ_2 and one complex scalar ϕ. The vector multiplet again encodes the gauge degrees of freedom and is constrained to the adjoint representation of the gauge group G, whereas the hypermultiplet is free to lie in any representation $\mathcal{R}$ of G and encodes the matter content of the theory. We can see that the $4d$ $\mathcal{N}=2$ hypermultiplet is comprised of two $4d$ $\mathcal{N}=1$ chiral multiplets in conjugate representations, and the $4d$ $\mathcal{N}=2$ vector multiplet is comprised of one $4d$ $\mathcal{N}=1$ vector multiplet and one $4d$ $\mathcal{N}=1$ chiral multiplet, each in the adjoint representation of G. As before, the bosonic and fermionic degrees of freedom in each multiplet match, this time taking value 4.

2.1.2.3 $3d$ $\mathcal{N}=4$

Both $4d$ $\mathcal{N}=2$ theories and $3d$ $\mathcal{N}=4$ theories have the same amount of supersymmetry: 8 supercharges. Thus to go from representations in $4d$ $\mathcal{N}=2$ to $3d$ $\mathcal{N}=4$ we simply need to decompose $4d$ Poincaré irreps into $3d$ ones. This amounts to decomposing $\mathfrak{so}(1,3)\cong\mathfrak{su}(2)\oplus\mathfrak{su}(2)$ Lorentz representations into $\mathfrak{so}(1,2)\cong\mathfrak{su}(2)$ representations[8] (the translational component of the Poincaré group plays the same role in three dimensions as in four, giving a conserved mass charge). The $SO(1,3)$ Lorentz irreps that appeared in our $4d$ $\mathcal{N}=2$ theory are those in (2.1.22) and (2.1.23): the vector A_μ in $[1,1]_{\mathfrak{su}(2)\oplus\mathfrak{su}(2)}$; left and right Weyl spinors ψ and $\bar{\psi}$ in $[1,0]_{\mathfrak{su}(2)\oplus\mathfrak{su}(2)}$ and $[0,1]_{\mathfrak{su}(2)\oplus\mathfrak{su}(2)}$ respectively; and complex scalar ϕ in $[0,0]_{\mathfrak{su}(2)\oplus\mathfrak{su}(2)}$. These representations decompose as:

$$\begin{aligned}
[1,1]_{\mathfrak{su}(2)\oplus\mathfrak{su}(2)} &\longrightarrow [2]_{\mathfrak{su}(2)}+[0]_{\mathfrak{su}(2)},\\
[1,0]_{\mathfrak{su}(2)\oplus\mathfrak{su}(2)} &\longrightarrow [1]_{\mathfrak{su}(2)},\\
[0,1]_{\mathfrak{su}(2)\oplus\mathfrak{su}(2)} &\longrightarrow [1]_{\mathfrak{su}(2)},\\
[0,0]_{\mathfrak{su}(2)\oplus\mathfrak{su}(2)} &\longrightarrow [0]_{\mathfrak{su}(2)},
\end{aligned} \tag{2.1.24}$$

and hence the degrees of freedom in the $3d$ $\mathcal{N}=4$ supermultiplets are

Hypermultiplet	Vector multiplet
Two complex scalars φ_1,φ_2	One gauge boson A_μ
Two spinors ψ_1,ψ_2	One real scalar ϕ_1
	One complex scalar $\phi_2+i\phi_3$
	Two spinors χ_1,χ_2

. (2.1.25)

As we will see in Section 2.3 and beyond, in our studies we will be particularly interested in the scalar elements of hypermultiplets and abelian vectormultiplets. The real scalar degrees of freedom in each

[8] Here resurfaces the sloppy notation for isomorphisms of algebras mentioned before[1]; the same caveat applies here.

of these multiplets are as follows:

Hypermultiplet	$U(1)$ Vector multiplet
Four real scalars $\varphi_1, \varphi_2, \varphi_3, \varphi_4$	Three real scalars ϕ_1, ϕ_2, ϕ_3 One dual photon γ

, (2.1.26)

where the *dual photon* γ arises as the 0-form which the Hodge dual of the field strength[9] is the exterior derivative of [35]. It can take any VEV on the circle [36].

2.2 Quivers

Quivers Q[10] are diagrams comprised of nodes and edges which encode and simplify the content of a Lagrangian [6]: traditional Lagrangian SQFT calculations are translated into simple graph theory operations on Q. This section is primarily devoted to seeing how this works for $3d$ $\mathcal{N} = 4$ gauge theories, but also illustrates how the notation decomposes into the 4-supercharge $3d$ $\mathcal{N} = 2$ supermultiplets. We will also address the notions of *excess* and *balance*, which are needed both in Section 2.4.2 to define "good" and "ugly" theories, and in the work of Chapter 3.

2.2.1 $3d$ $\mathcal{N} = 4$ notation

Recall from Section 2.1 that in a $3d$ $\mathcal{N} = 4$ gauge theory there are two types of representations of the superPoincaré algebra, vectormultiplets and hypermultiplets (2.1.25). To build a Lagrangian theory then, all we need to know is what gauge group G (vectormultiplets) we have, what matter (hypermultiplets) we have, and the representation $\mathcal{R}$ of G that the hypermultiplets transform under. To construct a quiver then, we just need a graphical notation for each of these things. We denote the vectormultiplet for a gauge group G_i by a circular node, called a *gauge node*, labelled by its name:

$$\underset{G_i}{\bigcirc} \tag{2.2.1}$$

In our case, since we will only consider unitary groups $G_i = U(n_i)$, we will simplify the label to the rank of the gauge group. That is, a gauge group $G_i = U(n_i)$ is denoted by

$$\underset{n_i}{\bigcirc} \tag{2.2.2}$$

We denote a hypermultiplet with a line, called a *(simply-laced) edge*:[11]

$$\text{——} \tag{2.2.3}$$

Free hypermultiplets do not contribute interestingly to our discussions; we wish to depict hypermultiplets in some representation $\mathcal{R}$ of the gauge group $U(n_i)$. We do this for k hypermultiplets by connecting the edge denoting them to the gauge node $U(n_i)$ in question, possibly with some additional notation (depending on $\mathcal{R}$), and terminating the other end of the edge at a square box called a *flavour node*, labelled by the number of hypermultiplets k. If $\mathcal{R}$ is the fundamental representation

[9] $\star F$ is exact by virtue of the equation of motion for the field strength and the Poincaré lemma, assuming the theory lives on a contractible topological space.

[10] From now on, Q will be used to denote quivers; an algebraic notation for supercharges will no longer be required.

[11] We usually omit the "simply-laced", and instead specify when an edge is *non-simply laced* (see below).

of $U(n_i)$, we leave the edge plain. For example, suppose we have a $U(n)$ gauge node, and wish to add k hypermultiplets in its fundamental representation. Then our quiver is:

(2.2.4)

The quiver theory (2.2.4) has k identical hypermultiplets in the fundamental representation of $U(n)$; there is clearly a symmetry rotating them into each other. Such a symmetry is called a *flavour symmetry*. In order to preserve the norm of the hypermultiplets, this symmetry must be unitary: they are in the anti-fundamental representation of $U(k)$.[12] We can use the $U(n)$ gauge symmetry to scale the determinant of the $U(k)$ matrices acting on the hypermultiplets; on the Higgs branch (see Section 2.3) of this quiver theory there is an $SU(k)$ symmetry. Sometimes flavour nodes are denoted with this Higgs branch flavour symmetry instead of the number of hypermultiplets:

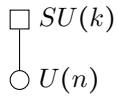

(2.2.5)

(2.2.4) and (2.2.5) are equivalent notation for the same quiver theory. We will stick to the former in this thesis; we mention the latter only to make connection with other work in the literature, for example [37, 38].

If $\mathcal{R}$ is the adjoint representation of a $U(n)$ gauge node, no additional label is needed, but the edge starts and ends on the node with no flavour box. For example, for $k = 1$:

(2.2.6)

If $\mathcal{R}$ is some other representation the edge will need additional notation to specify what $\mathcal{R}$ is. Such edges will not appear in this thesis, so we will not discuss them further. The only other type of edge we will come across is a *non-simply laced edge*, which we will discuss shortly.

Suppose we want to build a theory whose gauge group is a product of two unitary groups, $G = U(n_1) \times U(n_2)$. Then we can start with a $U(n_1)$ gauge group, add n_2 hypermultiplets into its fundamental representation, giving (2.2.4) for $k = n_2$, and then gauge the $U(n_2)$ flavour symmetry:

(2.2.7)

This gauging introduces new dynamical degrees of freedom: we now have $n_1 \times n_2$ hypermultiplets in the *bifundamental representation*[13] of $U(n_1) \times U(n_2)$. We can continue in this way to construct much

[12] Note that for they could have been in the fundamental representation of $U(k)$, but we pick the anti-fundamental so that when we construct bigger quivers, for example (2.2.8), each edge is in a fundamental × antifundamental representation, rather than alternating between fundamental × fundamental and antifundamental × antifundamental.

[13] Note that in general the bifundamental representation of $G_1 \times G_2$ can mean the fundamental or anti-fundamental representation of both groups, or in the fundamental of one and the anti-fundamental of the other. For us, it will always mean the latter.[12]

more complicated unitary quivers,[14] for example

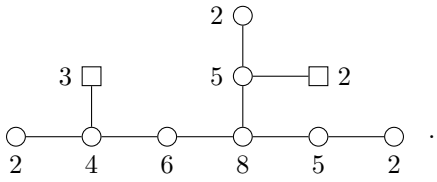

(2.2.8)

Quivers containing one or more flavour nodes (e.g. (2.2.8)) are termed *framed*, while those containing only gauge nodes (e.g. (2.2.7)) are *unframed*.

The final type of quiver notation we will come across in this thesis, as alluded to above, is the *non-simply-laced edge*. This is when two "gauge" nodes are connected by two or more lines with a directional arrow. The nodes on the "greater than" and "less than" side of the directional arrow are known as *long nodes* and *short nodes*, respectively. The number of lines connecting the two nodes is known as the *multiplicity* of the edge. A quiver containing one or more non-simply-laced edges is called a *non-simply-laced quiver*. As an example, consider

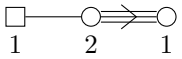

(2.2.9)

The edge connecting the two "gauge" nodes is non-simply-laced with multiplicity 3, represented by the three lines. The direction of the arrow tells us that the $U(2)$ node is the long node and the $U(1)$ node is the short node. Note the air quotes we have used around "gauge". This is because, as we'll see in Section 2.6.4, short nodes have no gauge theoretic interpretation. However despite this, non-simply-laced quivers still define meaningful Coulomb branches, which is why they appear in our discussion.

2.2.2 $3d$ $\mathcal{N} = 2$ notation

Recall that $3d$ $\mathcal{N} = 4$ vectormultiplets and hypermultiplets decompose each into two $\mathcal{N} = 2$ multiplets. The G-vectormultiplet decomposes as a G-vectormultiplet and a chiral multiplet in the adjoint representation of G, and the hypermultipelt in a representation $\mathcal{R}$ of G becomes one chiral and one anti-chiral multiplet in representations $\mathcal{R}$ and $\bar{\mathcal{R}}$ of G, respectively. Quiver notation for a chiral multiplet is a line with a direction indicated by an arrow. An anti-chiral multiplet is denoted in the same way, but with the arrow pointed in the reverse direction. A vectormultiplet is denoted again by a circular node. Hence for the example (2.2.4), the $3d$ $\mathcal{N} = 4$ quiver becomes

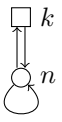

(2.2.10)

in $3d$ $\mathcal{N} = 2$ notation. This notation will not appear in our work, but it is helpful to visualise the decomposition into the 4-supercharge subalgebra.

[14] While we focus purely on unitary quiver theories, it is worth noting that there have been many studies into quivers containing special-unitary or orthosymplectic gauge nodes, see for instance [38, 39, 40, 41, 13, 42, 43, 44, 45, 46, 47, 26].

2.2.3 Balance

The final concepts we address in this section are ones which we will use heavily throughout the thesis: *excess* and *balance* [4]. This notion will enable us to define "good" and "ugly" theories, which are the focus of our work; it is for such theories that the techniques we discuss in Sections 2.3 – 2.7 can be used, as the Coulomb branch flows to its IR fixed point in a protected manner. Balance will also play a major role in Chapter 3, as the balanced nodes in a quiver contribute vital information to simply determine the Coulomb branch global symmetry from surface-level inspection of the quiver.

The concept of the balance of nodes in a quiver originated from quiver theories for which there exists a brane system description [48]. The balance of a unitary node is related to the net charge difference of the two NS5 branes which trap the D3 branes that form the gauge group corresponding to the node. We will not discuss its stringy origin any further; for us, balance is of interest because it leads to extra operators appearing as we flow to the infrared, which elicit more symmetries than seen in the UV theory.

A node is termed balanced if its excess is equal to zero. The definitions of unbalanced nodes, and more specifically overbalanced and underbalanced nodes, all follow naturally. The excess of a node i in a quiver is given by the total number of flavours it sees, minus twice its rank. That is, if f_i is the number of flavours i sees and r_i is its rank, then its excess e_i is given by

$$e_i = f_i - 2r_i. \tag{2.2.11}$$

When we say the number of flavours i sees, we refer to the number of hypermultiplets transforming under the gauge group represented by the node i in a quiver, if no other nodes were gauge nodes. For example, in the quiver for (the closure of)[15] the minimal nilpotent orbit of G_2 [49], given by the balanced affine Dynkin diagram of G_2,

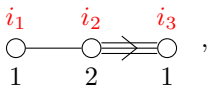

(2.2.12)

the node on the left sees $f_{i_1} = 2$ hypermultiplets in its fundamental representation and thus its excess is $e_{i_1} = 2 - (2 \times 1) = 0$, the node in the centre sees $f_{i_2} = 1 + (3 \times 1) = 4$ hypermultiplets (in its fundamental representation) and thus its excess is $e_{i_2} = 4 - (2 \times 2) = 0$, and the node on the right sees $f_{i_3} = 2$ hypermultiplets in its fundamental representation and thus its excess is $e_{i_3} = 2 - (2 \times 1) = 0$. Because all gauge nodes in this quiver are balanced, we say the quiver is a *balanced quiver*.

2.3 The Moduli Space

As mentioned in Chapter 1, we study a subset of the moduli space of $3d$ $\mathcal{N} = 4$ unitary quiver gauge theories called the *Coulomb branch* $\mathcal{C}$. In particular, we study the IR fixed point of $\mathcal{C}$ for quiver theories Q such that $\mathcal{C}(Q)$ is a HyperKähler space, and thus also a symplectic singularity [2]. The algebrogeometric properties of the Coulomb branch variety correspond to physical properties of the vacua; Coulomb branches can be studied either as affine algebraic symplectic varieties, or as a set of gauge-inequivalent vacua for a physical theory.

[15] We will largely omit this "closure of" when discussing varieties as nilpotent orbits in the future for ease.

This section is devoted to gaining some intuition for these two ways of viewing a moduli space. In order to arrive at symplectic $3d$ $\mathcal{N}=4$ Coulomb branches at low-energies in Section 2.4, we need to first discuss the rough notion of a vacuum in quantum field theory. This is the topic of Section 2.3.1. In Section 2.3.2, we illustrate how a $3d$ $\mathcal{N}=4$ moduli space defines an algebraic variety $\mathcal{V}$, and see how $\mathcal{V}$ can be described by the ring of holomorphic functions over it. We give a brief summary of the important points regarding HyperKähler spaces and symplectic singularities that will be necessary for this thesis.

2.3.1 Vacua in QFT

In a quantum field theory, states (including the particles which can be observed in the world) are excitations of the vacuum $|\Omega\rangle$, a state which has minimal energy $\langle\Omega|\hat{H}|\Omega\rangle$. Any vacuum must be Lorentz invariant; the only non-vanishing operators of a theory in its vacuum state must be Lorentz scalars $\hat{\phi}_i$. Therefore, a vacuum is defined by the set of expectation values ϕ_i that these scalars take upon insisting the energy is minimised: $|\Omega\rangle = |\phi_i\rangle$. The expectation value $\mathcal{O} = \langle\Omega|\hat{\mathcal{O}}|\Omega\rangle$ is called the vacuum expectation value, or VEV, of the operator $\hat{\mathcal{O}}$. The vacuum is naturally considered at low energies (large-length) scales; we study vacua in the IR.

In many QFTs there is often only a finite number of possible sets of VEVs which minimise the energy (noting the physical equivalence of any two vacua whose VEVs are related by a gauge transformation). However, when supersymmetry is included, there are often continuous families of gauge-inequivalent VEVs minimising the energy. These continuous vacua form a manifold, called the moduli space $\mathcal{M}$. Each point on $\mathcal{M}$ corresponds to a vacuum state for the theory.

Suppose in a theory there are n complex scalars, $\hat{\phi}_1, ..., \hat{\phi}_n$. Then a vacuum state is specified by their VEVs, $|\Omega\rangle = |\phi_1 \cdots \phi_n\rangle$. Unrestricted, the expectation values of these fields could take any complex value: $\mathcal{M} \cong \mathbb{C}^n$. However, imposing the vacuum condition restricts these complex variables to the zero set of a collection of equations: that all non-scalars vanish and that $\langle\, \phi_1 \cdots \phi_n \,|\, H \,|\, \phi_1 \cdots \phi_n \,\rangle \Big|_{\psi,\, A_\mu, \ldots = 0}$ is minimised. If there is *enough* supersymmetry – and it transpires that 8 supercharges is indeed enough – these equations turn out to be algebraic. Hence moduli spaces for theories with 8 supercharges are algebraic varieties. Recall that the Coulomb branches we study are actually a certain type of algebraic variety: symplectic singularities. We now explore how to define and describe such objects.

2.3.2 Algebrogeometric objects

In this section, we briefly list some properties of algebraic varieties, HyperKähler spaces and symplectic singularities needed for this thesis. For an introduction to the field of algebraic geometry, see for example [33]. For a review of symplectic singularities in particular, see [50].

2.3.2.1 Algebraic varieties

A major result from algebraic geometry is that any algebraic variety $\mathcal{V}$ is fully described by the ring of algebraic functions over it. In fact, for the varieties we study, this in turn is isomorphic to the ring of *holomorphic* functions over it; our goal is to find the ring of holomorphic functions over the Coulomb branch. In Section 2.4.2.1, we will learn exactly what these holomorphic functions are in

terms of the physical degrees of freedom on $\mathcal{C}$.

The ring of holomorphic functions over a variety is commutative. This means that *an algebraic variety is completely described by the generating holomorphic functions over it, and the relations they satisfy*; to construct the rest of the ring, one just needs to take symmetric products of these (see Appendix B). Therefore, a tool which constructs symmetric products of a function, or conversely tells us the symmetric generators of a given function, would be very useful to us. Luckily, such tools exist: the *plethystic exponential* and *plethystic logarithm*.

2.3.2.2 Plethystics

The functions we want to generate symmetric products of in our studies will always be of the form

$$f(t, z_1, ..., z_n) = \sum_{k=0}^{\infty} \sum_{k_i=-\infty}^{\infty} a_{k_1,...,k_n,k}\, z_1^{k_1} \cdots z_n^{k_n}\, t^k, \tag{2.3.1}$$

where $|t| < 1$ counts the degree and $|z_i| = 1$, and hence it is on such functions that we will define the plethystic exponential and logarithm (PE and PL respectively).

The PE of a function f of the form (2.3.1) is defined as

$$PE[f(t, z_1, ..., z_n)] = \exp\left(\sum_{k=1}^{\infty} \frac{f(t^k, z_1^k, ..., z_n^k) - f(0, ..., 0)}{k}\right) = \prod_{k=0}^{\infty} \prod_{k_i=-\infty}^{\infty} \frac{1}{(1 - z_1^{k_1} \cdots z_n^{k_n}\, t^k)^{a_{k_1,...,k_n,k}}}. \tag{2.3.2}$$

Conversely, given the set of functions in a commutative ring at all degrees $t > 0$, one can compute the generators and relations using the inverse of the plethystic exponential, the plethystic logarithm, defined on functions f of the form (2.3.1) as

$$PL[f(t, z_1, ..., z_n)] = \sum_{k=1}^{\infty} \frac{\mu(k)}{k} \log(f(t^k, z_1^k, ..., z_n^k)), \tag{2.3.3}$$

where $\mu(k)$ is the Möbius function:

$$\mu(k) = \begin{cases} +1 & \text{if } k \text{ is square free with an even number of prime factors,} \\ -1 & \text{if } k \text{ is square free with an odd number of prime factors,} \\ 0 & \text{if } k \text{ has a squared prime factor,} \end{cases} \tag{2.3.4}$$

for any positive integer k.

The first term of PL should always be positive, and will encode the generators of lowest degree. Subsequent positive terms encode higher degree generators. The first minus sign describes a relation that some of the lower degree generators satisfy. Subsequent minus or plus signs encode further generators and relations of higher orders that define the variety: *syzygies*. For complete intersections (where $dim(\mathcal{V})$ = #generators − #relations) this will be a polynomial in t of the form

$$PL[f(t, z_1, ..., z_n)] = \sum_{k=1}^{g} g_k(z_1, ..., z_n) t^k - \sum_{k=1}^{r} r_k(z_1, ..., z_n) t^k, \tag{2.3.5}$$

where g is the polynomial degree of the highest generator, r is the polynomial degree of the highest relation, g_k are the generators at degree t^k, and r_k are the overcounted products of generators at t^k that are equivalent to others due to the relations among the generators. Both g_k and r_k are Laurent polynomials in the z_i. For non-complete intersections, the PL will be an infinite series with syzygies of ever-increasing degree.

Example For example, consider a commutative ring generated by three degree one variables a, b, c, satisfying $ab = c^2$. Then the functions of degree two in the ring are

$$\{a^2, b^2, c^2, ac, bc\} = S^2(\{a, b, c\}). \tag{2.3.6}$$

The *symmetric* product does the job of including only one of ac and ca, or bc and cb. The relation $ab = c^2$ explains the absence of ab or ba in (2.3.6). This is confirmed by the plethystic exponential:

$$PE[(a+b+c)t - abt^2] = \frac{1-abt^2}{(1-at)(1-bt)(1-ct)} = 1+(a+b+c)t+(a^2+b^2+c^2+ac+bc)t^2+\mathcal{O}(t^3). \tag{2.3.7}$$

Alternatively, suppose we have the full list of functions on a variety, graded by their degree:

$$1 + (a+b+c)t + (a^2+b^2+c^2+ac+bc)t^2 + (a^3+b^3+c^3+a^2c+b^2c+c^2b+c^2a+abc)t^3 + \mathcal{O}(t^4). \tag{2.3.8}$$

Then to find the generators and relations, we take the plethystic logarithm:

$$PL((2.3.8)) = (a+b+c)t - abt^2 + \mathcal{O}(t^4). \tag{2.3.9}$$

Note that (2.3.9) doesn't tell us the explicit relation $ab = c^2$: just that ab is related to one of the other degree two polynomials in the generators. □

2.3.2.3 HyperKähler spaces

The Coulomb branches we will study are singular HyperKähler spaces. Essentially, a HyperKähler space is the "quaternionic version" of a Kähler space. A Kähler space has compatible Riemannian, complex and symplectic structures. The symplectic structure is related to the metric, and contributes to defining the Kähler space. A HyperKähler space has a Riemannian metric g and *three* complex structures, satisfying quaternionic relations, each of which are compatible with g and a corresponding symplectic structure (i.e. each complex structure is Kähler with respect to g).

There is a natural $SU(2)$ symmetry on all HyperKähler spaces which rotates the three complex structures. In order to define complex notions such as holomorphicity, one such structure must be chosen. This breaks the $SU(2)$ symmetry, and chooses a particular symplectic form on the remaining Kähler space. That is, all HyperKähler spaces have a symplectic structure, which is explicitly determined upon choosing a complex structure. This choice of structure then enables us to define holomorphicity, find the holomorphic functions[16] over the space, and categorise it as an algebraic variety. The symplectic structure over this algebraic variety defines it as a *symplectic singularity*.

2.3.2.4 Symplectic singularities

Roughly speaking, in the sense of [2], a symplectic singularity is an algebraic variety on which there exists a 2-form ω – the *symplectic form* – which degenerates at zero or more points. The symplectic form defines a pairing on the tangent space at any point on the variety, and points where this pairing degenerates are called *singular*. As stated many times previous, we only study quivers whose Coulomb branches are symplectic singularities. From a physical perspective, moving to a point on such a Coulomb branch where the degeneracy of the symplectic form increases corresponds to more

[16] Note that the functions on the full Coulomb branch – not the "holomorphic portion" selected by this choice of complex structure – are found by applying the $SU(2)$ symmetry to the holomorphic ones on the Kähler subset.

massless states having been integrated out in the corresponding vacuum (see Section 2.7 for further elaboration).

The symplectic form defines a Poisson structure $\{\cdot,\cdot\}$ on a symplectic singularity, as we will see in Section 4.1. Computing the Poisson brackets $\{\cdot,\cdot\}$ therefore helps us to further categorise the singularity by shedding light on ω, and as mentioned in Section 2.3.2.3, in principle this could also be used to find the metric. Chapter 4 is devoted to our work [11], in which we computed the Poisson brackets for several Coulomb branches in aid of this goal.

2.4 The 3d $\mathcal{N}=4$ Coulomb branch

Now that we have seen the physical notion of a moduli space and how we can describe it using techniques of algebraic geometry, we move on to nail down some specific details for the case of the 3d $\mathcal{N}=4$ Coulomb branch.

In Section 2.4.1, we first lay out the construction of the moduli space of any supersymmetric gauge theory with eight supercharges. Such an $\mathcal{M}$ naturally splits into the Coulomb, Higgs and mixed branches, each of whose ring of holomorphic functions is isomorphic to its chiral ring, which we define for a Coulomb branch. We see how these two branches behave under the RG flow, focusing on the Coulomb branch. We discuss its UV and IR fixed points, and the classical Coulomb branch of the UV SCFT. In Section 2.4.2 we discuss the quantum corrections this receives upon flowing to the IR SCFT, arriving finally at our object of study. To explore the quantum-corrected Coulomb branch we will need an alternative description of it, in terms of dressed monopole operators. These operators are labelled by charges under the topological and R global symmetries of the theory. The operators and these symmetries are the topics of Sections 2.4.2.1 and 2.4.2.2 respectively. This will lay the foundations for understanding the properties of $\mathcal{C}$ that we choose to study and the methods we use to do it, which will be discussed in Sections 2.5 and 2.6 – 2.7 respectively.

2.4.1 The classical 3d $\mathcal{N}=4$ moduli space and its RG flow

Classically the allowed vacua are those which minimise the scalar potential. In a supersymmetric theory, this amounts to solving (setting to zero) the so-called *F and D terms*. As previously mentioned, this typically yields a continuous set of gauge-inequivalent vacua. In a 3d $\mathcal{N}=4$ theory, each vacuum will be labelled by a VEV for each scalar field in the theory: the dual photon, real scalar and complex scalar of the vectormultiplet; and the two complex scalars of the hypermultiplet. There are often many physically distinct sets of allowed VEVs in such theories, and we can simplify our study of $\mathcal{M}$ by considering different subsets of it. The subset in which all vectormultiplet scalar VEVs vanish and the subset in which all hypermultiplet scalar VEVs vanish are called the *Higgs branch* $\mathcal{H}$ and *Coulomb branch* $\mathcal{C}$ respectively. They each behave differently, as we'll discuss below. Note that as $\mathcal{H}$, $\mathcal{C}$ are just $\mathcal{M}$ with further algebraic constraints imposed on the coordinates, they are also algebraic varieties. Infact the ones we study are HyperKähler, and thus also symplectic singularities (see Section 2.3.2.4) [3].

In each of these varieties, the ring of holomorphic functions over them is believed to be isomorphic to the *chiral ring* of the theory. We define a chiral operator to be an operator $\mathcal{O}$ which is annihilated by

half of the supercharges.[17] Since we are discussing the moduli space of the theory, we also demand that chiral operators are gauge-invariant and satisfy the vacuum conditions. Any product or linear combination of such chiral operators is also a chiral operator, and they are bosonic; they form a commutative ring. This ring is the so-called chiral ring mentioned above; the Coulomb and Higgs branches are fully specified by their respective chiral rings.

We study quiver theories with enough matter so that the gauge coupling is inversely proportional to the energy scale; they are UV-free, but strongly coupled at low energies, flowing to an SCFT (superconformal field theory) both in the deep UV and deep IR [4]. It is natural to consider moduli spaces at low energies, in the IR. As the gauge coupling increases, the interactions of virtual particles erupting into and out of existence become more important, and quantum corrections need to be introduced. This means our classical discussion thus far in terms of the UV quiver degrees of freedom is insufficient to describe $\mathcal{M}$; we need an IR description of our theory, that accounts for quantum behaviour.

For the Higgs branch, this turns out to be no problem; its UV description holds all along the RG flow[18] due to the non-renormalisation of the superpotential in supersymmetric theories. On $\mathcal{H}$, the vectormultiplet scalars vanish, and so the only remaining vacuum constraints are those involving the superpotential. Since this is not renormalised, the vacuum constraints for the Higgs branch remain the same all along the RG flow.

The Coulomb branch is not so lucky; its metric *does* receive quantum corrections. Suppose the gauge group of a theory is G. Then in the UV picture, the F-terms are automatically satisfied due to the vanishing hypermultiplet scalars, and solving the D-terms amounts to

$$[\phi_a, \phi_b] = 0, \tag{2.4.1}$$

where $a, b = 1, ..., \dim(G)$ labels the vectormultiplets of the theory, and ϕ any scalar in each vectormultiplet (2.1.26). Clearly (2.4.1) says that any vectormultiplet scalar of the theory not lying in the Cartan subalgebra (CSA) of G does not live on the Coulomb branch; only $\text{rank}(G)$ of the $\dim(G)$ vectormultiplets ϕ_a survive on $\mathcal{C}$. Thus a generic VEV on $\mathcal{C}$ is generated by $\text{rank}(G)$ vectormultiplets lying in the CSA of G. Since in each vectormultiplet there are three real scalars and a periodic dual photon [36], the classical Coulomb branch generically takes the form

$$\mathcal{C}_{cl} = (\mathbb{R}^3 \times S^1)^{\text{rank}(G)}/\mathcal{W}_G, \tag{2.4.2}$$

where the quotient by the Weyl group of G ensures gauge invariance. The quaternionic and real dimensions of (2.4.2) are clearly $\dim_{\mathbb{H}} = \text{rank}(G)$ and $\dim_{\mathbb{R}} = 4 \cdot \text{rank}(G)$ respectively. In this thesis we will consider only unitary gauge groups, and for such G any element of the CSA can be diagonalised. Thus a generic VEV of any ϕ on $\mathcal{C}$ will have $\text{rank}(G)$ independent diagonal components: the gauge group is broken to $U(1)^{\text{rank}(G)}$.

In principle, these remaining $\text{rank}(G)$ abelian photons could then be dualised to scalars (see the discussion following (2.1.26)) [35], and the quantum corrected low-energy metric on $\mathcal{C}$ could be found

[17] Note that the precise supercharges annihilating chiral operators differs from $\mathcal{C}$ to $\mathcal{H}$, see for example [19].

[18] Note that in theories in other dimensions this is not the case in general. For example, the Higgs branches of 5 and 6d theories at infinite coupling are not classically exact.

semi-classically by integrating out the massive W-bosons and hypermultiplets which gained a non-zero VEV. However, this process is insufficient in practise for several reasons. Firstly because even for fairly low ranks of gauge group, although it terminates at one-loop, integrating out the massive fields becomes too difficult. Secondly, this semi-classical approach is a perturbative process and is thus only valid in weakly coupled regions which, as discussed at the top of this section, is not the regime of the IR 3d $\mathcal{N}=4$ Coulomb branches we study. Thirdly, certain VEVs taken by the vectormultiplet scalars satisfying (2.4.1) actually preserve a greater, non-abelian subset of the gauge symmetry than $U(1)^{\text{rank}(G)}$, and it is not known how to dualise a non-abelian vector multiplet. While there are other indirect ways to study Coulomb branches, for example via string theory dualities such as mirror symmetry (which relates the Coulomb branch of a quiver to the Higgs branch of its *mirror quiver* [51, 52]), we would like a way to study them directly.

This motivated the search for an alternative method to find the chiral ring of the Coulomb branch, and indeed such a method has been found for $\mathcal{C}$ at the superconformal fixed point. Here, $\mathcal{C}$ can be viewed as the space of *dressed monopole operators*,[19] as opposed to the space of dualised photons in the quantum-corrected metric. This is a viewpoint uniquely valid in three dimensions, and enables great progress to be made with understanding the Coulomb branch. In this thesis, we focus solely on computations for Coulomb branches[20]; we take the discussion of the Higgs branch no further, and move on to further elaborate on the dressed monopole description of $\mathcal{C}$ in the IR SCFT. From now on, any time we mention the Coulomb branch, we will be referring to its IR fixed point.

2.4.2 The quantum Coulomb branch

In this section we aim to give a brief overview of the IR Coulomb branch, where quantum corrections become important as the gauge coupling increases. As mentioned in Section 2.4.1, a description of $\mathcal{C}$ at a generic point along the RG flow is hard to obtain in practise, as loop corrections are non-trivial and are not always valid. However at the IR superconformal fixed point there is an alternative description of the Coulomb branch available to us, as the *space of dressed monopole operators* [32, 53, 54, 4], which allows us to explore $\mathcal{C}$ at this point along the RG flow. This section is devoted to detailing this dressed monopole construction of the IR SCFT Coulomb branch and discussing its global symmetries (the conserved charges of which can be used to label our chiral operators). Please note that this section is not intended as a comprehensive review of 3d $\mathcal{N}=4$ gauge theories and their Coulomb branches at low energies. We cover only the surface-level ideas of this vast topic needed to gain an intuitive understanding of the physics employed in this thesis. For more details on the topics covered in this section, see for example [31, 55, 56, 36, 32, 53, 54, 4].

2.4.2.1 Dressed monopole construction

In Section 2.4.1 we saw that a semi-classical description is not sufficient to describe the physics at all points on the Coulomb branch. However it turns out there is an alternative approach which has validity both in the UV and the IR. In the UV, we can define monopole operators in terms of the

[19] This terminology is common in the literature but is a slight abuse of language; what we really mean is that the Coulomb branch, viewed as an affine algebraic variety, is the spectrum of the Coulomb branch chiral ring, which is generated by dressed monopole operators. The Coulomb branch variety, its chiral ring, and the VEVs of operators on $\mathcal{C}$ can be used interchangably in the literature, so it's important to clarify the distinction.

[20] Note that some of our results will *describe* Higgs branches, but as a virtue of the computations being performed on the Coulomb branch of their magnetic quiver. See Section 2.7.1 for more details.

Coulomb branch degrees of freedom (2.1.26), following [4]. Recall from Section 2.1.2.3 that the $\mathcal{N}=4$ vectormultiplet for a gauge group G splits naturally into an $\mathcal{N}=2$ vectormultiplet and an $\mathcal{N}=2$ chiral multiplet, both of which lie in the adjoint representation of G, whose real scalars are γ, ϕ_1 and ϕ_2, ϕ_3 respectively. The $\mathcal{N}=2$ vectormultiplet degrees of freedom can be encoded in a UV monopole, which is defined at a point via inserting a Dirac monopole singularity

$$F = \frac{m}{2} \star d\frac{1}{r} \tag{2.4.3}$$

in superspace, where r is the distance from the point of insertion and $m \in \mathfrak{g}$ (the Lie algebra of G) is the charge of the monopole. This monopole can then be written explicitly as an operator:

$$v_m = e^{\frac{m}{g^2}(\phi_1 + i\gamma)}, \tag{2.4.4}$$

where g is the gauge coupling of G. The other two Coulomb branch degrees of freedom from the $\mathcal{N}=2$ chiral multiplet can be combined to form a complex scalar:

$$\varphi = \phi_2 + i\phi_3. \tag{2.4.5}$$

It is easy to see that because $\gamma, \phi_1, \phi_2, \phi_3$ are all chiral, linear combinations of products of v and φ are chiral also. Operators formed from the product of only monopoles are called *bare monopoles*. Operators formed from the product of monopoles with at least one complex scalar are called *dressed monopoles*; the complex scalar is the "dressing". Since v_m and φ encode all the UV chiral operators on $\mathcal{C}$, they form the chiral ring.

However, this description no longer accurately describes a monopole when ϕ_1 is small, or as $g \to \infty$. That is, it only works classically in the UV, which seems to be no better than the situation we were in before. However, the difference here is that we can directly define monopole operators in the IR SCFT [32], and this description emerges consistently from the above one under the RG flow.

The gauge fields in the IR SCFT can be defined as spheres centered on Dirac monopole singularities of the gauge field called 't Hooft monopole operators [57]. Suppose the gauge group is G, with Lie algebra $\mathfrak{g}$. Inserting an 't Hooft monopole operator at a point elicits a gauge field surrounding it whose northern and southern patches are described by

$$A_\pm \sim \frac{m}{2}(\pm 1 - \cos\theta)d\phi \tag{2.4.6}$$

where $m \in \mathfrak{g}$, and (r, θ, ϕ) are spherical coordinates around the point of insertion. In order for the transition function between the two patches to be smooth, it can be found that m must satisfy

$$e^{2\pi i m} = \mathbb{1}_G, \tag{2.4.7}$$

which is the criterion for m to belong to the weight lattice of the Langland's dual of the gauge group:

$$m \in \Lambda_{G^\vee}. \tag{2.4.8}$$

The magnetic charge labels the monopole. We denote a bare monopole with charge m as v_m. Recall that we are looking to construct the gauge-invariant chiral operators of $\mathcal{C}$. The gauge group acts on m through the Weyl group of $G^\vee$, $\mathcal{W}_{G^\vee}$; v_m is not be gauge invariant unless the $\mathcal{W}_{G^\vee}$ orbit of m is trivial. Thus gauge invariant bare monopoles V_m are given by

$$V_m = \sum_{\sigma \in \mathcal{W}_{G^\vee}} v_{\sigma(m)}. \tag{2.4.9}$$

Note then that distinct monopoles are labelled by the magnetic charges m in one Weyl-chamber of the magnetic lattice $\Lambda_{G^\vee}$:

$$m \in \Lambda_{G^\vee}/\mathcal{W}_{G^\vee}, \tag{2.4.10}$$

as the V_m for any two m in the same Weyl orbit are gauge equivalent. Furthermore, enforcing chirality (i.e. preserving half of the supersymmetry) amounts to imposing the boundary condition

$$\phi_1 \sim \frac{m}{2r} \tag{2.4.11}$$

on the real scalar in the $\mathcal{N}=2$ vectormultiplet.

We study theories with only unitary gauge groups in this thesis. The magnetic charge for $G=U(n)$, $m \in \mathfrak{g}=\mathfrak{u}(\mathfrak{n})$, subjected to (2.4.10) and (2.4.11) is diagonalisable and integer-valued, hence we denote it as a vector $\boldsymbol{m}=(m_1,...,m_n)$ of its n integer eigenvalues. Since $U(n)$ is Langlands self-dual and has Weyl group S_n, a magnetic charge of $U(n)$ takes the form

$$\boldsymbol{m} \in \{(m_1,...,m_n) \in \mathbb{Z}^n \mid m_1 \geq m_2 \geq \cdots \geq m_n\}. \tag{2.4.12}$$

For a quiver with p unitary gauge nodes $U(n_i)$ $i=1,...,p$, a magnetic charge takes the form

$$\boldsymbol{m}=(\boldsymbol{m_1},...,\boldsymbol{m_p}) \in \left\{ (m_{1,1},...,m_{1,n_1},...,m_{p,1},...,m_{p,n_p}) \in \prod_{i=1}^{p} \mathbb{Z}^{n_i} \;\middle|\; m_{i,1} \geq m_{i,2} \geq m_{i,n_i} \;\forall\, i \right\}. \tag{2.4.13}$$

These bare monopole operators, labelled by magnetic charge $\boldsymbol{m}$, define the $\mathcal{N}=2$ vectormultiplet (gauge) degrees of freedom in the IR SCFT moduli space. As in the UV, we can dress them with a VEV for the complex scalar $\varphi_{\boldsymbol{m}}$ from the $\mathcal{N}=2$ chiral multiplet. However, it must satisfy some conditions. Firstly, in order to preserve the chirality of a bare monopole under dressing, the VEV taken by the complex scalar $\varphi_{\boldsymbol{m}}$ must commute with (i.e. be a Casimir of) the algebra $\mathfrak{h}_{\mathfrak{m}} \subset \mathfrak{g}$ of the residual gauge group $H_{\boldsymbol{m}}$ unbroken by the VEV $\boldsymbol{m} \in \mathfrak{g}$ of the monopole. Secondly, it must be gauge invariant. The former restricts the VEV of $\varphi_{\boldsymbol{m}}$ to the CSA of $\mathfrak{h}_{\mathfrak{m}}$. In the theories we consider, G is a product of unitary groups and therefore the unbroken gauge algebra for any $\boldsymbol{m}$ is of the form

$$\mathfrak{h}_{\mathfrak{m}} = \oplus_{i=1}^{u_{\boldsymbol{m}}} \mathfrak{u}(\mathfrak{l}_{\mathfrak{m},i}), \tag{2.4.14}$$

for some integer ranks $l_{\boldsymbol{m},i}$, $i=1,...,u_{\boldsymbol{m}}$. The CSAs of unitary groups can be diagonalised; let's call the eigenvalues of (2.4.14)

$$\lambda_{1,1}\ ,\ ...\ ,\ \lambda_{1,l_{\boldsymbol{m},1}}\ ,\ ...\ ,\ \lambda_{u_{\boldsymbol{m}},1}\ ,\ ...\ ,\ \lambda_{u_{\boldsymbol{m}},l_{\boldsymbol{m},u_{\boldsymbol{m}}}}. \tag{2.4.15}$$

Then since the gauge group acts on $\varphi_{\boldsymbol{m}}$ via the Weyl group $\prod_{i=1}^{u_{\boldsymbol{m}}} S_{l_{\boldsymbol{m},i}}$ of $H_{\boldsymbol{m}}$ to permute its eigenvalues, imposing gauge invariance restricts the dressing factor to be of the form

$$\varphi_{\boldsymbol{m}} = \prod_{i=1}^{u_{\boldsymbol{m}}} \left(\sum_{j=1}^{l_{\boldsymbol{m},i}} \lambda_{i,j} \right)^{k_{\boldsymbol{m},i}}, \tag{2.4.16}$$

for some non-negative integers $k_{\boldsymbol{m},i}$. Note in particular that when the magnetic charge is zero (i.e. when the adjoint scalar is not dressing a monopole operator), the whole gauge group $U(n_1)\times\cdots\times U(n_p)$ is preserved and the dressing factor is of the form

$$\varphi_{\boldsymbol{0}} = \prod_{i=1}^{p} \left(\sum_{j=1}^{n_i} \lambda_{i,j} \right)^{k_i}. \tag{2.4.17}$$

for some non-negative integers k_i.

In Section 4.2.1, these dressed monopole degrees of freedom and operators are discussed with more precision, and several examples featuring them appear in Sections 4.2 – 4.5. Each VEV (point) on our Coulomb branch describes a vacuum of the IR SCFT. To label the states in this vacuum, we turn to Noether [1], and consider the conserved charges of the vacua under the global symmetries of the Coulomb branch.

2.4.2.2 Global symmetries

The overall global symmetry of the Coulomb branch at the IR fixed point is not generally identical to that present in the UV quiver theory. This is because, although the $SU(2)_R$ R-symmetry is protected against quantum corrections, the *topological* symmetry appearing in the UV is typically enhanced at the IR SCFT. We call this larger IR topological symmetry GS.[21] States in the vacua of the theory are labelled by their conserved charges under these symmetries [1], typically denoted Δ and J respectively. In this section, we will discuss each of these symmetries, and how the operators of Section 2.4.2.1 are charged under them for unitary quiver theories.

R-symmetry The UV Coulomb branch has an $SU(2)_R$ symmetry which the three complex structures form a triplet under: each operator on $\mathcal{C}$ in the UV has some weight under this symmetry. The *chiral* operators however (the bare and dressed monopoles (2.4.4) and (2.4.5)) preserve only half the supersymmetry, forcing the $\mathcal{N}=4$ algebra to break to an $\mathcal{N}=2$ subalgebra and the $SU(2)_R$ symmetry to break to $U(1)_R$. From the "algebraic variety" point of view, picking an $\mathcal{N}=2$ subalgebra corresponds to choosing one of the three complex structures on $\mathcal{C}$, which enables us to define holomorphic functions on the variety. The specific $\mathcal{N}=2$ subalgebra is decided by the choice of monopole construction, and this can be chosen such that the operators with the highest weight in each $SU(2)_R$ representation are the chiral ones:

$$\text{Operators in the chiral ring of } \mathcal{C} \quad \longleftrightarrow \quad \text{highest weights of } SU(2)_R \text{ representations}, \tag{2.4.18}$$

The other operators on $\mathcal{C}$ (whose weights under $SU(2)_R$ are not the highest in the representation they belong to) are not in the chiral ring; they are not needed for our description of $\mathcal{C}$ as an algebraic variety, as they correspond to non-holomorphic functions over it.

The choice of UV monopole operators given by (2.4.4), (2.4.5) are chiral and thus achieve (2.4.18); under this construction, $SU(2)_R$ is broken to $U(1)_R$.[22]

The charge of a bare monopole (2.4.4) in the UV SCFT under this $U(1)_R$ symmetry is given by [4, 58, 59, 7]:

$$\Delta(m) = -\sum_{\alpha\in\Delta_+}|\alpha(m)| + \frac{1}{2}\sum_{i=1}^{H}\sum_{\rho_i\in\mathcal{R}_i}|\rho_i(m)|, \tag{2.4.19}$$

where Δ_+ is the set of positive roots of the gauge group G, H is the number of hypermultiplets, and ρ_i are the weights in the representation $\mathcal{R}_i$ of the i^{th} hypermultiplet. Since all the quiver theories we study are unitary, we will focus on the precise presentation of (2.4.19) for a quiver with p unitary gauge

[21] When reporting results of the global symmetry "GS" and "global symmetry" are used synonymously even though they are not the same, because the other factor of the global symmetry ($SU(2)_R$) is known.

[22] Note that actually the global symmetry group is $SO(2)_R$, of which $U(1)_R$ is the double cover.

nodes $G = U(n_1) \times \cdots \times U(n_p)$. Suppose that there are H hypermultiplets, and that hypermultiplet h is a simply-laced edge between nodes n_{α_h} and n_{β_h}, clearly for $\alpha_h,\ \beta_h = 1, ..., p$ (i.e. h is in the bifundamental representation of $U(n_{\alpha_h}) \times U(n_{\beta_h})$). If we write the magnetic charges for these nodes as $\boldsymbol{m}_{\boldsymbol{\alpha_h}} = (m_{\alpha_h,1}, ..., m_{\alpha_h,n_{\alpha_h}}) \in \mathbb{Z}^{n_{\alpha_h}}$ and $\boldsymbol{m}_{\boldsymbol{\beta_h}} = (m_{\beta_h,1}, ..., m_{\beta_h,n_{\beta_h}}) \in \mathbb{Z}^{n_{\beta_h}}$ respectively, then the R-charge of a monopole operator of magnetic charge $\boldsymbol{m}$ in such a quiver is given by

$$\Delta(\boldsymbol{m}) = -\sum_{a=1}^{p}\sum_{i<j=1}^{n_a}|m_{a,i} - m_{a,j}| + \frac{1}{2}\sum_{h=1}^{H}\sum_{i=1}^{n_{\alpha_h}}\sum_{j=1}^{n_{\beta_h}}|m_{\alpha_h,i} - m_{\beta_h,j}|. \tag{2.4.20}$$

The R-charge of any single dressing factor is protected under the RG flow from the UV theory:

$$\Delta(\text{adjoint scalar}) = 1. \tag{2.4.21}$$

Provided all operators on the low-energy Coulomb branch satisfy

$$\Delta \geq \frac{1}{2}, \tag{2.4.22}$$

then (2.4.19) matches the conformal dimension of the monopole operator with charge m in the IR SCFT [4]. All dressed monopole operators in the chiral ring of $\mathcal{C}$ then acquire a charge Δ under $U(1)_R$.

Quiver theories in which all Coulomb branch operators satisfy $\Delta > \frac{1}{2}$ are termed "good". Those in which all operators satisfy (2.4.22) with at least one meeting the equality are called "ugly". The Coulomb branch of "ugly" theories factorises into a "good" part and a free part which is isomorphic to some number of copies of the quaternionic plane and generated by free twisted hypermultiplets, corresponding to the operators with $\Delta = \frac{1}{2}$. Theories in which at least one operator does not satisfy (2.4.22) are termed "bad"; in these cases, the R-charge of a monopole operator in the UV SCFT (2.4.20) is *not* equal to the one observed in the infrared. Quivers in which all nodes have excess $e > -1$ (see (2.2.11) for the defintion of excess) describe good theories, and those in which one node has $e = -1$ but all other nodes have $e > -1$ describe ugly theories. All quivers studied in this thesis fit into one of these two groups; the conformal dimension of any operator on the low-energy Coulomb branches we consider is given by (2.4.20).

Topological symmetry There is another global symmetry on the Coulomb branch which does *not* remain constant along the RG flow. In the UV theory, for every abelian factor in the gauge group there is an associated conserved current $*F = d\gamma$, and hence a $U(1)$ global symmetry. UV monopoles will be charged under this symmetry, while adjoint scalars will not. This can be seen schematically by the fact that φ is independent of γ, whereas $\partial_\gamma e^{\phi_1 + i\gamma} \propto e^{\phi_1 + i\gamma}$. For the remaining non-abelian factors in the gauge group, the conservation of such a current is prohibited by instantons [35]: for a theory with a unitary gauge groups, the classical UV topological symmetry is

$$U(1)^a. \tag{2.4.23}$$

In the IR, this classical UV symmetry is often enhanced to some group whose maximal torus is (2.4.23). The resultant (generally non-abelian) IR symmetry is the *topological symmetry*[23] of the Coulomb branch at the IR SCFT, and we denote it GS. The charge under this topological symmetry is given the symbol $\boldsymbol{J}$. Consider a unitary gauge theory $G = U(n_1) \times \cdots \times U(n_p)$ with magnetic charges

[23] The name of this symmetry stems from the fact that it arises due to the construction of a gauge field in three dimensional spacetime.

$\boldsymbol{m} = (\boldsymbol{m_1}, ..., \boldsymbol{m_p})$ (2.4.13). Since there are p unitary factors in the gauge group, the topological charge is a vector of length p, and is given by:

$$\boldsymbol{J}(\boldsymbol{m}) = (J_1, ..., J_p) = \left(\sum_{i=1}^{n_1} m_{1,i} \, , \, ... \, , \, \sum_{i=1}^{n_p} m_{p,i} \right). \tag{2.4.24}$$

2.5 Properties of Interest

We have seen that the Coulomb branches we study are fully described by bare and dressed monopole operators, and that such operators which are also gauge invariant and chiral form the chiral ring. Section 2.4 told us that computing the chiral ring of monopole operators explicitly (i.e. the explicit generators and relations they satisfy) would fully describe the Coulomb branch, but generally it is not known how to do this. However, there are other properties of $\mathcal{C}$ that we can learn about which help us to both categorise it as a variety and understand the physics of the theory. Among such properties, that we will refer to much throughout this work, are the following:

1. *Dimension.* Recalling that at a generic point on the Coulomb branch the gauge group is broken to $U(1)^{\text{rank}(G)}$, we can clearly see that there are $\text{rank}(G)$ components labelling each VEV, hence
$$\dim(\mathcal{C}) = \text{rank}(G). \tag{2.5.1}$$
In terms of a unitary quiver, this is equal to the sum of the ranks of the gauge nodes (minus one) for a framed (unframed) quiver.

2. *Operator content graded by charges under global symmetries.* While finding the explicit generators and relations of the Coulomb branch chiral ring is often too challenging, we can compute its **Hilbert series** (for "good" or "ugly" theories [4]), which *counts* the operators on it graded by their charges under the global symmetries of $\mathcal{C}$. This is a helpful step in attempting to categorise the Coulomb branch – two varieties with matching Hilbert series is an indication that they could be the same, although it is by no means a guarantee.[24] Section 2.6 will detail how to compute and analyse the Coulomb branch Hilbert series. These notions will be used extensively throughout this thesis.

3. *Singularity structure.* Analysing the Coulomb phase brane systems of quivers with a string theory construction has lead to a deeper understanding of the singularity structure of $\mathcal{C}$, presented via its **Hasse diagram**. The Hasse diagram indicates transitioning from a generic point on $\mathcal{C}$ to more and more singular (see Section 2.3.2.4) subsets of it. The points regarding Hasse diagrams needed for this thesis will be reviewed in Section 2.7.

4. *Global symmetry.* The Hasse diagram has been conjectured to indicate a subset of the non-abelian global symmetry of a quiver, but often this is a strict subset. A guaranteed method to determine the local form of the full topological global symmetry GS of $\mathcal{C}$ with certainty is to compute its Hilbert series and consult the t^2 term (the global form can be determined from the full Hilbert series), but as gauge group rank increases this quickly becomes too computationally intensive. An easy and efficient algorithm for identifying the Coulomb branch global symmetry directly from the quiver based on the balance of its gauge nodes – the **balance global symmetry (BGS)** algorithm – has been proposed, and until recently was believed to work

[24] For example, subtle differences in the explicit forms of relations do not necessarily show up in the Hilbert series.

unanimously. However, in [10] we were able to construct several families of quivers for which this algorithm failed. This is the topic of Chapter 3: we discuss the construction of the quivers for which the BGS algorithm fails, and provide an amended algorithm which corrects these failings for the quivers listed.

5. *Symplectic form.* Recall that the symplectic form is a key ingredient for defining a symplectic singularity. One can make progress with finding this symplectic form between points on $\mathcal{C}$ by computing Poisson brackets between the corresponding vacua, as a symplectic form automatically induces a Poisson structure. Finding these Poisson brackets (for certain theories) is the topic of Chapter 4, based on [11].

The remaining sections in this chapter are devoted to the methods we will employ in this thesis to analyse the above properties of interest for the quivers we study.

2.6 Hilbert Series

As mentioned in Section 2.5, although computing the exact form of the Coulomb branch chiral ring generators and relations (and thus all other operators) is the optimal description for $\mathcal{C}$ as an algebraic variety, it is not in general known how to achieve this. But something we do know how to do is *count* how many chiral ring operators there are at each charge under the global symmetries [7]. The function that performs this task is called the *Hilbert series*.

The Hilbert series is defined outside of Coulomb branches [33]. Typically, the Hilbert series for an algebraic variety (which is defined by homogeneous equations) counts the holomorphic functions over it, graded by degree. This grading is achieved through a *fugacity* (typically t); the coefficient of t^k is the number of holomorphic functions of degree k on the variety. Using the commutativity of the ring of holomorphic functions, the Hilbert series can be used to find the number of generators and relations at each degree. To see this explicitly, consider the following example.

Example Let's find the Hilbert series for $\mathcal{V} = \mathbb{C}^2/\mathbb{Z}_2$. We need to count the linearly independent holomorphic functions over it at each degree. For $\mathcal{V}$, the ring of such functions is $\mathbb{C}[z_1, z_2]/\mathbb{Z}_2$ for z_1, z_2 complex variables. Under the $\mathbb{Z}_2$ action, $z_1 \to -z_1$, and $z_2 \to -z_2$. The degree k holomorphic functions on $\mathcal{V}$ then are generated by $\mathbb{C}$-linear combinations of $z_1^a\, z_2^b$ with $a + b = k$, such that $z_1^a\, z_2^b$ is invariant under the $\mathbb{Z}_2$ action. Clearly for even and odd k, $z_1^a\, z_2^b \to \pm z_1^a\, z_2^b$ respectively, hence no holomorphic functions of odd degree lie on $\mathcal{V}$ but even ones do. For degree zero, the only linearly independent holomorphic function is clearly just 1. For degree two there are three, z_1^2, z_2^2 and $z_1\, z_2$; for degree four there are five, $z_1^4, z_1^3 z_2, z_1^2 z_2^2, z_1 z_2^3, z_2^4$; and so on:

Degree	Holomorphic functions						
0				1			
2				z_1^2	$z_1\, z_2$	z_2^2	
4			z_1^4	$z_1^3\, z_2$	$z_1^2\, z_2^2$	$z_1\, z_2^3$	z_2^4
6	z_1^6	$z_1^5\, z_2$	$z_1^4\, z_2^2$	$z_1^3\, z_2^3$	$z_1^2\, z_2^4$	$z_1\, z_2^5$	z_2^6
$\vdots$				$\vdots$			

(2.6.1)

The Hilbert series $HS(t)$ for $\mathcal{V} = \mathbb{C}^2/\mathbb{Z}_2$ is a polynomial in a variable t which tells us how many holomorphic functions there are at each degree; the coefficient of t^k counts the number of independent

generating monomials in $\mathcal{V}$ at degree k:

$$\begin{aligned} HS(t) &= 1 + 3t^2 + 5t^4 + 7t^6 + \cdots \\ &= \sum_{n=0}^{\infty} (2n+1)t^{2n} \\ &= \frac{1-t^4}{(1-t^2)^3}. \end{aligned} \tag{2.6.2}$$

It is clear that $\mathbb{C}[z_1, z_2]/\mathbb{Z}_2$ is generated by $a = z_1^2$, $b = z_2^2$ and $c = z_1 z_2$, satisfying the relation $ab = c^2$. However even if it wasn't obvious, the Hilbert series (2.6.2) can tell us the number of generators and relations and their degrees (although not their explicit forms). Recall from Section 2.3.2.1 that the plethystic logarithm (2.3.3) gives the generators and relations of such an input function. The plethystic logarithm of our Hilbert series here is

$$PL(HS(t)) = 3t^2 - t^4. \tag{2.6.3}$$

The positive term tells us there are three generators at degree two, and the subsequent negative terms tells us that these generators satisfy one degree four relation. We could also have seen this from inspection of (2.6.2), using that

$$PE[a\,t^p - b\,t^q] = \frac{(1-t^q)^b}{(1-t^p)^a}. \tag{2.6.4}$$

The expression (2.6.2) has only one fugacity t, counting the degree of the holomorphic functions. One could also note that $\mathcal{V}$ inherits the $SU(2)$ symmetry of $\mathbb{C}^2$, which rotates z_1 and z_2, and grade the holomorphic functions by their charges under this symmetry too, in addition to their degree. Since z_1 and z_2 form a doublet under this $SU(2)$ they have respective charges (weights) ± 1 under it: $z_1^a z_2^b$ has charge $a-b$. We introduce a new fugacity to keep track of the $SU(2)$ charge of each holomorphic function, z. Including this, we see the Hilbert series (2.6.2) becomes

$$\begin{aligned} HS(t) &= 1 + (z^2 + 1 + z^{-2})t^2 + (z^4 + z^2 + 1 + z^{-2} + z^{-4})t^4 \\ &\quad + (z^6 + z^4 + z^2 + 1 + z^{-2} + z^{-4} + z^{-6})t^6 + \cdots \\ &= \frac{1-t^4}{(1-z^2\,t^2)(1-t^2)(1-z^{-2}\,t^2)}, \end{aligned} \tag{2.6.5}$$

and its plethystic logarithm

$$PL(HS(t,z)) = (z^2 + 1 + z^{-2})\,t^2 - t^4. \tag{2.6.6}$$

We can see that the generators of $\mathbb{C}^2/\mathbb{Z}_2$ form the adjoint representation of the $SU(2)$ symmetry with weights $2, 0, -2$ respectively, and that the relation transforms in the trivial representation of $SU(2)$. This Hilbert series, refined with these new fugacities z to keep track of additional information, is what we will call the *refined* Hilbert series. The Hilbert series which is just a function of t, keeping track of degree only, is called the *unrefined* Hilbert series.

Note additionally that this Hilbert series is not unique. Here we had a space generated by three degree two functions, which we called a, b and c, satisfying $ab = c^2$. However a space generated by three degree two functions $\tilde{a}$, $\tilde{b}$ and $\tilde{c}$, satisfying $\tilde{a}\tilde{b} = \tilde{c}(\tilde{c} + \xi)$ for some constant parameter $\xi \neq 0$, will clearly have the same Hilbert series, but describes a different variety; this one has no singularity at

the origin.[25] From the Hilbert series alone, we cannot distinguish between these two varieties. □

Recall from Section 2.4.1 that for $\mathcal{C}$, the ring of holomorphic functions is thought to be isomorphic to the chiral ring. Thus in the context of $3d$ $\mathcal{N}=4$ Coulomb branches, the Hilbert series counts the operators in the chiral ring of the theory, graded this time by their charges under the global symmetries of $\mathcal{C}$. The role of the degree of holomorphic functions – the grading of t – is played by twice the R-charge, as in the theories we study it takes only positive integer values. We can refine the Hilbert series to include fugacities z_i to keep track of topological charges. So, we need a formula to count the bare and dressed monopole operators of a theory, graded by their Δ and J_i. Such a formula, the monopole formula, was found in [7].

2.6.1 Monopole formula

In Section 2.4.2 we saw that the Coulomb branches of interest to us are spaces of dressed monopole operators.[19] That is, a point on $\mathcal{C}$ (equivalently a VEV of the IR SCFT) corresponds to a dressed monopole operator with magnetic charge $\boldsymbol{m} \in \Lambda_{G^\vee}/\mathcal{W}_{G^\vee}$ and a dressing factor $\varphi_{\boldsymbol{m}} \in \mathfrak{h}_{\mathfrak{m}}$ preserved by the gauge group $H_{\boldsymbol{m}}$ unbroken by $\boldsymbol{m}$. This operator has charges $\boldsymbol{J}$ and Δ under the global topological and R-symmetries respectively. Just as the fugacity t graded the degree of holomorphic functions in the example of (2.6.2), here it will grade twice the R-charge of a dressed monopole operator. Since we also want to grade by the topological charges $\boldsymbol{J}=(J_1,...,J_p)$ (2.4.24), we introduce p more fugacities $\boldsymbol{z}=(z_1,...,z_p)$ to keep track of them. The monopole formula then is

$$HS(t;z)=\sum_{\boldsymbol{m}\in\Lambda_{G^\vee}/\mathcal{W}_{G^\vee}} P_G(t,m)\ \boldsymbol{z}^{\boldsymbol{J}(\boldsymbol{m})}\ t^{2\Delta(\boldsymbol{m})} \tag{2.6.7}$$

This sums up over every possible dressed monopole operator. We choose to grade by twice the conformal dimension to avoid fractional powers; 2Δ makes direct analogy with the degree of holomorphic functions. $P_G(t,\boldsymbol{m})$ is known as the *classical dressing factor*, and counts the number of ways a monopole of charge $\boldsymbol{m}$ can be dressed by $\varphi_{\boldsymbol{m}}$: it counts the number of Casimirs of $\mathfrak{h}_{\boldsymbol{m}}$. Such Casimirs are always chargeless under the topological symmetry: no z fugacities appear in P_G. The Casimirs do however acquire an R-charge. To understand this, let's turn to an example.

Example Consider a $U(3)$ gauge theory. We wish to calculate the dressing factor $P_{U(3)}(t,\boldsymbol{m})$ for a generic bare monopole $\boldsymbol{m}$. Here, monopoles can take magnetic charges in

$$\boldsymbol{m}\ \in\ \Lambda_{G^\vee}/\mathcal{W}_{G^\vee}=\{(m_1,m_2,m_3)\in\mathbb{Z}^3\mid m_1\geq m_2\geq m_3\}\ \subset\ \mathfrak{u}(3). \tag{2.6.8}$$

Consider the bare monopole with $\boldsymbol{m}=(3,2,1)$. Embedded in $\mathfrak{g}=\mathfrak{u}(3)$, this is

$$\boldsymbol{m}=\begin{pmatrix}3&0&0\\0&2&0\\0&0&1\end{pmatrix}. \tag{2.6.9}$$

Clearly any element in $\mathfrak{u}(3)$ that commutes with this must be diagonal; the remaining gauge group unbroken by the VEV $\boldsymbol{m}$ is $H_{\boldsymbol{m}}=U(1)^3$, and hence the adjoint scalars allowed to dress $v_{\boldsymbol{m}}$ are the Casimirs of $\mathfrak{u}(1)^3$.

[25] This is clear from the non-zero value of the partial derivative of the defining equation with respect to the generator c at the origin.

A Casimir of an algebra is an invariant of it. Since the adjoint representation of $\mathfrak{u}(1)$ is trivial, any element X transforming in the adjoint representation is an invariant of $\mathfrak{u}(1)$. Thus there is just one independent Casimir one can construct from X: itself. Recall that the R-charge of an adjoint scalar is 1. Since the Casimir for $\mathfrak{u}(1)$ is constructed out of just one group element, its R-charge is just one too; for each $U(1)$ factor in $H_{\boldsymbol{m}}$, there is a single independent Casimir with $\Delta = 1$. In our Hilbert series language each of these translate as $1\,t^2$: for $H_{\boldsymbol{m}} = U(1)^3$, it is $3\,t^2$. All other Casimirs will be symmetric products of these generators; the dressing factors for monopoles with $\boldsymbol{m} = (3,2,1)$ are encapsulated by

$$P_{U(3)}(t,(3,2,1)) = PE[3\,t^2] = \frac{1}{(1-t^2)^3}. \tag{2.6.10}$$

Consider instead the bare monopole with charge $\boldsymbol{m} = (3,3,1)$. Now the unbroken gauge group is $U(2)\times U(1) \cong SU(2)\times U(1)^2$. We get a contribution of $2\,t^2$ inside PE from the two abelian factors, but what about the $SU(2)$? Consider a generic element in $\mathfrak{su}(2)$, X. This transforms under $g \in \mathfrak{su}(2)$ as $X \to gXg^{-1}$. In general, this is not invariant, but we can see that $Tr(X^k)$ is. However, for k odd this vanishes, and for $k > 2$ even it is proportional to the $(\frac{k}{2})^{th}$ power of $Tr(X^2)$: $\mathfrak{su}(2)$ has just one independent Casimir, $Tr(X^2)$, built out of two copies of X, hence $\Delta(Tr(X^2)) = 2$. Thus our dressing factor here is

$$P_{U(3)}(t,(3,3,1)) = PE[2\,t^2 + t^4] = \frac{1}{(1-t^2)^2\,(1-t^4)}. \tag{2.6.11}$$

□

In general, for a unitary gauge group $G = U(n)$, a bare monopole can have $d \le n$ distinct charges. Let the distinctness of these charges be encoded in an ordered partition $\boldsymbol{\lambda}(\boldsymbol{m})$, a vector of length d. That is, $\lambda_1(\boldsymbol{m})$ is the number of times the first entry of $\boldsymbol{m}$ is repeated, $\lambda_i(\boldsymbol{m})$ is the number of times the $(\sum_{j=1}^{i-1}\lambda_j(\boldsymbol{m})+1)^{th}$ entry of $\boldsymbol{m}$ is repeated, $i = 2,\ldots,d$. For example, the charge $\boldsymbol{m} = (3,2,1)$ has one charge with value three, one with value two and one with value one (all distinct), so the ordered partition is $\boldsymbol{\lambda}((3,2,1)) = (1,1,1)$. For $\boldsymbol{m} = (3,3,1)$, there are two with value three and one with value one, so $\boldsymbol{\lambda}((3,3,1)) = (2,1)$. For $\boldsymbol{m} = (3,3,3)$, $\boldsymbol{\lambda}(\boldsymbol{m}) = (3)$. If we call γ_i the number of entries in $\boldsymbol{\lambda}$ that take value i, then the dressing factor for the $U(n)$ monopole with charge $\boldsymbol{m}$ is given by

$$P_{U(n)}(t,\boldsymbol{m}) = \prod_{i=1}^{n}\frac{1}{(1-t^{2i})^{\gamma_i}}. \tag{2.6.12}$$

The dressing factor for a bare monopole with charge $\boldsymbol{m} = (\boldsymbol{m_1},\ldots,\boldsymbol{m_p})$ under a product of unitary gauge groups $G = U(n_1)\times\cdots\times U(n_p)$ is then

$$P_{U(n_1)\times\cdots\times U(n_p)}(t,\boldsymbol{m}) = \prod_{i=1}^{p}\prod_{j=1}^{n_i}\frac{1}{(1-t^{2j})^{\gamma_{i,j}}}, \tag{2.6.13}$$

where $\gamma_{i,j}$ is the number of entries taking value j in the ordered partition $\boldsymbol{\lambda}_i$ for charge $\boldsymbol{m_i} = (m_{i,1},\ldots,m_{i,n_i})$.

Now that we have all the ingredients to the monopole formula (2.6.7), let's illustrate how to use it to compute a simple Coulomb branch Hilbert series.

Example Consider the quiver

$$Q_{A_1} = \begin{array}{c} \square\ 2 \\ |\ \\ \bigcirc\ 1 \end{array} \quad . \tag{2.6.14}$$

We wish to calculate the Hilbert series of $\mathcal{C}(Q_{A_1})$. The ingredients we need are: the magnetic charges to sum over, $m_{i,j}$ for $j = 1, ..., n_i$ and $i = 1, ..., p$; and the conformal dimension Δ, topological charge $\boldsymbol{J}$ and dressing factor $P_{U(1)}$ as functions of these charges.

Here there is just one gauge group, $U(1)$, hence $p = 1$ and $\boldsymbol{m} = m_{1,1} \equiv m$ is a vector of length one containing only one magnetic charge, which can take values in $\mathbb{Z}$ (2.4.12).

The conformal dimension for this node is

$$\Delta(m) = \frac{1}{2}(|m| + |m|) = |m|, \tag{2.6.15}$$

found by using (2.4.20) for the $H = 1$ hypermultiplet connecting the $U(n = 1)$ gauge group to a single rank $n_a = 2$ flavour node (recall flavour nodes have no magnetic charge).

The topological charge for a bare monopole of a single gauge group with magnetic charge m is simply the length one vector

$$J(m) = m, \tag{2.6.16}$$

following (2.4.24) with $p = 1$, $n_1 = 1$, and is graded by a single fugacity z.

The dressing factor counting the adjoint scalars at various R-charges that can dress V_m is simply

$$P_{U(1)}(t, m) = \frac{1}{1 - t^2}, \tag{2.6.17}$$

following (2.6.13) with $p = 1$, $n_1 = 1$.

Thus the Hilbert series is given by

$$\begin{aligned} HS(t, z) &= \frac{1}{1 - t^2} \sum_{m=-\infty}^{\infty} z^m \, t^{2|m|} \\ &= \frac{1 - t^4}{(1 - x^2\, t^2)\,(1 - t^2)\,(1 - x^{-2}\, t^2)} \\ &= 1 + (x^2 + 1 + x^{-2})t^2 + (x^4 + x^2 + 1 + x^{-2} + x^{-4})t^4 \\ &\quad + (x^6 + x^4 + x^2 + 1 + x^{-2} + x^{-4} + x^{-6})t^6 + \mathcal{O}(t^7), \end{aligned} \tag{2.6.18}$$

where the map $z \to x^2$ was used to get from the first line to the second, and the final line is a Taylor expansion of the second about $t = 0$. The $z \to x^2$ mapping is called a *fugacity map*. The reason for the use of such maps is discussed first in Section 2.6.2, then again in 2.6.6 along with details on how to find them. □

Now that we have understood how to use the monopole formula, we'll move on to discuss what exactly the Coulomb branch Hilbert series tells us about the physics of the theory.

2.6.2 Encoded infomation

In Section 2.6.1, we saw a formula (2.6.7) which enables us to calculate Hilbert series, and how to use it. We now want to understand what it can tell us about the Coulomb branch.

Operator content Firstly, it's worth restating the inherent benefit of its design, as this already provides a lot of information: the Hilbert series tells us the number of operators lying in the chiral ring of the Coulomb branch at various charges under the global symmetries of the theory. The powers of t give the charges under the $U(1)_R$ symmetry, and the powers of $\boldsymbol{z}$ give the charges under the enhanced topological symmetry GS. Operators on $\mathcal{C}$ fit into representations of its global symmetries; the coefficient of t^{2k} will be a sum of characters of the representations of GS which have R-charge k (possibly after some fugacity map, see Section 2.6.6).

Global symmetry Secondly, the t^2 coefficient of the Hilbert series tells us the local form of GS: it is the character of the adjoint representation of GS [12], after a possible fugacity map.[26] For example in (2.6.18), after the map $z \to x^2$, the coefficient of t^2 is the fundamental weight character of the adjoint representation of $SU(2)$, hence $GS = SU(2)$ (locally). Indeed, all other t^{2k} coefficients are other characters of $SU(2)$, and this is the local form of our global symmetry. This can help us to write the Hilbert series in an alternative form, as the *highest weight generating function* (HWG) [60], which neatly captures the representations of GS present at each R-charge using notation corresponding to their highest weights. The HWG is found by replacing each fundamental weight character in the Hilbert series with *Dynkin fugacities* $\mu_1, ..., \mu_r$, $r = \text{rank(GS)}$, graded by the character's highest weight. Concretely, to obtain the HWG from the Hilbert series, a character with highest weight $[w_1, ..., w_r]$ is replaced by $\mu_1^{w_1}\mu_2^{w_2}\cdots\mu_r^{w_r}$. For instance, in the example of (2.6.18) the HWG reads:

$$\begin{aligned} HWG(t,\mu) &= 1 + \mu^2 t^2 + \mu^4 t^4 + \mu^6 t^6 + \mathcal{O}(t^7) \\ &= \sum_{i=0}^{\infty} \mu^{2i} t^{2i}. \end{aligned} \tag{2.6.19}$$

where $\mu_1 \equiv \mu$ is the single Dynkin fugacity for our rank one $GS = SU(2)$. Note that from this HWG we can see that no representations with odd highest weights appear on $\mathcal{C}$: the global form of GS is actually $SO(3) \cong SU(2)/\mathbb{Z}_2$. In general the global form will be the local form quotiented by a subgroup of its centre. It can be found from the HWG by analysis of the charges of all generating representations (not just those at t^2) under the centre of the local form of GS (as obtained from the t^2 term), but as previously mentioned this will not be of interest to us in this thesis, and in the remaining chapters we only quote the local forms.

Generators and relations Thirdly, the plethystic logarithm of the Hilbert series can be used to count the generators and relations of $\mathcal{C}$. This is through virtue of the fact that the chiral ring is commutative, and so the Hilbert series is the symmetric product of some set of generating representations subject to relations. As a result, $PL(HS)$ will give us these generating representations and relations, as discussed in Section 2.3.2.1 and at the top of Section 2.6. Recall that the Coulomb branch as an algebraic variety is defined by a set of generators and the relations they satisfy. While $PL(HS)$ does not give us the explicit form of the generators and relations, it does tell us how many there are and in what representations of $U(1)_R \times GS$ they lie. For example, consider the Hilbert series (2.6.18) of the Coulomb branch of (2.6.14). We find that

$$\begin{aligned} PL(HS(\mathcal{C}(Q_{A_1})))(t,z) &= (z^2 + 1 + z^{-2})\, t^2 - t^4 \\ &= [2]\, t^2 - [0]\, t^4, \end{aligned} \tag{2.6.20}$$

[26] Note that in an unrefined Hilbert series, the t^2 coefficient is the dimension of GS. This is often enough to be pretty certain of GS, although without the refinement there is still ambiguity: for example, $3t^2$ could mean $GS = SU(2)$, but could also mean $GS = U(1)^3$, etc.

where in the second line we use highest weight notation for the fundamental weight characters in the first line. This tells us that the Coulomb branch chiral ring is generated by 3 generators which form the adjoint representation of $GS = SU(2)$, each with R-charge $\Delta = 1$, satisfying one relation which transforms trivially under the $SU(2)$ topological symmetry and under the $U(1)_R$ symmetry with charge $\Delta = 2$. Note that this Hilbert series exactly matches that of $\mathbb{C}^2/\mathbb{Z}_2$ (2.6.6). As we saw in the discussion following (2.6.6), on its own, this is not enough to indicate that $\mathcal{C}(Q_{A_1}) \cong \mathbb{C}^2/\mathbb{Z}_2$. In this case, equivalence of the two varieties can actually be proven either directly in the Coulomb branch construction or via mirror symmetry [18, 51], but the details won't be important for us here.

Note that we can also find the generators and relations of the HWG, but that they do not match those of the Hilbert series in general. However, sometimes PL(HWG) is a simpler expression than PL(HS), and so can be used as a nicer way to encapsulate the variety.

2.6.3 Perturbative Hilbert series

While knowing the exact form of the Hilbert series contains all the representation content we could want, often just knowing the first few terms in its Taylor series is sufficient to learn what we would like to. For example, if we are just after the local form of the global symmetry then computing to t^2 is sufficient. We find the Hilbert series to order $t^{2\Lambda}$ by evaluating the monopole formula *perturbatively*; by restricting any infinite sums over the $m_{i,j}$ in (2.6.7) to terminate at $\pm\Lambda$.

Example Consider the example of the monopole formula for (2.6.14), (2.6.18). To obtain the perturbative Hilbert series to order $2\Lambda = 6$, we simply restrict the sum over m to run between $\pm\Lambda = \pm 3$. If we do this, we indeed find

$$HS(t,z) = 1+(z^2+1+z^{-2})t^2+(z^4+z^2+1+z^{-2}+z^{-4})t^4 +(z^6+z^4+z^2+1+z^{-2}+z^{-4}+z^{-6})t^6+\mathcal{O}(t^7), \quad (2.6.21)$$

as we did before when the sum was infinite. We can take the plethystic logarithm of this to find generators and relations as before, again just making sure to terminate both the infinite sum in (2.3.3) *and* the infinite sum in the Taylor expansion of the logarithm at the cut-off order 2Λ. Note that the result will of course only be valid to this order; we will not learn of any generators or relations at R-charges greater than $\Delta = \Lambda$.

2.6.4 Non-simply-laced quivers

Recall from Section 2.2.1 that we sometimes come across $3d$ $\mathcal{N} = 4$ quivers with non-simply-laced edges (for example (2.2.9)). To compute the monopole formula for such quivers, a modification needs to be made to the conformal dimension of the non-simply-laced edge.

A short node is defined to have charges lying in a magnetic lattice scaled by the multiplicity k of its edge; each subdivision of the lattice is split into a further k. In the monopole formula (see Section 2.6.3), this amounts to the following changes [61]:

- In the formula for the conformal dimension of the non-simply-laced edge, the magnetic charges for the long node are scaled by k. That is, for a non-simply-laced edge of multiplicity k connecting a long node $U(n_1)$ to a short node $U(n_2)$, which have magnetic charge $\boldsymbol{m_1}$ and $\boldsymbol{m_2}$ respectively, the conformal dimension Δ is

$$\Delta = \frac{1}{2}\sum_{i=1}^{n_1}\sum_{j=1}^{n_2}|k\,m_{1,i} - m_{2,j}|. \quad (2.6.22)$$

- Ensure any sum over the charges for a short node is running over k times the usual limits (e.g. the upper limit for $m_{i,1}$ in a perturbative calculation would be $k \cdot \Lambda$).

Under this definition, quivers with a short node cannot be interpreted as a supersymmetric gauge theory Lagrangian in the standard way, as the lattice which the short magnetic charges are summed over is not of the form $\Lambda_{G^\vee}/\mathcal{W}_{G^\vee}$ for any semi-simple Lie group G. The reason for defining short nodes in such a way is that it leads to natural extensions of results in simply-laced quivers that reflect simply-laced Dynkin diagrams [61]. Coulomb branches of non-simply-laced quivers can also be seen as folded versions of Coulomb branches of simply-laced Lagrangian quivers [62], although the details of this won't be important for this work. Before we move on, we'll see an explicit calculation of the monopole formula for the non-simply-laced quiver (2.2.9).

Example In (2.2.9), there are two gauge nodes: a $U(2)$ and a $U(1)$. We'll call their magnetic charges $\boldsymbol{m_1} = (m_{1,1}, m_{1,2})$ and $\boldsymbol{m_2} = (m_{2,1})$ respectively. Suppose we wish to compute the monopole formula to order $t^{2\Lambda}$. Then the monopole formula will be:

$$HS(t, z_1, z_2) = \sum_{m_{1,1}=-\Lambda}^{\Lambda} \sum_{m_{1,2}=-\Lambda}^{m_{1,1}} \sum_{m_{2,1}=-3\Lambda}^{3\Lambda} P_{U(2)\times U(1)}(t, m_{1,1}, m_{1,2}, m_{2,1})\, t^{2\Delta(m_{1,1},m_{1,2},m_{2,1})}\, z_1^{m_{1,1}+m_{1,2}}\, z_2^{m_{2,1}}, \tag{2.6.23}$$

where

$$\Delta(m_{1,1}, m_{1,2}, m_{2,1}) = -|m_{1,1} - m_{1,2}| + \frac{1}{2}\left(|m_{1,1}| + |m_{1,2}| + |3m_{1,1} - m_{2,1}| + |3m_{1,2} - m_{2,1}|\right), \tag{2.6.24}$$

and the dressing factors are as given in (2.6.13). For e.g. $\Lambda = 5$, we find HWG

$$HWG(t, \mu_1, \mu_2) = 1 + \mu_2\, t^2 + \mu_2^2\, t^4 + \mu_2^3\, t^6 + \mu_2^4\, t^8 + \mu_2^5\, t^{10} + \mathcal{O}(t^{11}), \tag{2.6.25}$$

where μ_1, μ_2 are the Dynkin fugacities for the topological global symmetry $GS = G_2$.

2.6.5 Ungauging

The two quivers we have computed the monopole formula for so far, (2.6.14) and (2.2.9), both have flavour nodes; they are framed quivers. However recall from Section 2.2.1 that a quiver theory need not have flavours, and in fact virtually all that we study in this thesis do not. To compute the monopole formula for an unframed quiver, one additional action needs to be performed: *ungauging*. This is because there is a diagonal $U(1)_d$ symmetry which acts trivially on the Coulomb branch of unframed quivers, and left untreated this renders infinities in the monopole formula. In order to compute the Hilbert series of the quivers we study, then, it is important we learn how to account for this $U(1)_d$ and only count one operator in each of its orbits. The process of doing this is known as ungauging.

Suppose we have a quiver theory with gauge groups $U(n_i)$ for $i = 1, ..., p$. Denote a generic element in $U(n_i)$ as g_i. Firstly, note that since the center of $U(n_i)$ is $U(1)$, any $U(1)$ transformation leaves the vectormultiplets of the theory invariant. Any hypermultiplet H_{ij} in an unframed quiver is in the bifundamental representation of the two gauge groups it connects $U(n_i) \times U(n_j)$. It transforms as

$$H_{ij} \to g_i H_{ij} g_j^{-1}. \tag{2.6.26}$$

Consider the $U(1)_i$ subgroup of $U(n_i)$, given by $q_i \cdot \mathbb{1}_{n_i}$, for $q_i \in U(1)$ and $\mathbb{1}_{n_i}$ the $n_i \times n_i$ identity matrix. Then a generic bifundamental hypermultiplet transforms as

$$H_{ij} \to q_i\, q_j^{-1}\, H_{ij}. \tag{2.6.27}$$

Clearly if we choose $q_j = q_i$, then H_{ij} is invariant under gauge transformations. Thus, every hypermultiplet is invariant provided all gauge groups act via the same $U(1)$ transformation; this is why $U(1)_d$ is termed *diagonal*. This justifies our claim that $\mathcal{C}$ is completely invariant under $U(1)_d$.

But what does this mean for us? Recall that the monopole formula counts dressed monopole operators on $\mathcal{C}$. This diagonal $U(1)_d$ in the gauge symmetry means that if the magnetic charge $\tilde{\boldsymbol{m}}$ is equal to the magnetic charge $\boldsymbol{m}$ with each entry shifted by the same constant value, then $V_{\tilde{\boldsymbol{m}}}$ is identified with $V_{\boldsymbol{m}}$ under this gauge symmetry. Thus, if we don't ungauge this $U(1)_d$ we will count several gauge equivalent states, overcounting the number of physical monopoles we have. This can be seen directly from the monopole formula, which will give infinitely many operators at each R-charge if nothing is done to mitigate this $U(1)_d$, as $\boldsymbol{m}$ and $\tilde{\boldsymbol{m}}$ give the same Δ and P_G. It is also clear why framed quivers don't face this worry: the flavour contributions to Δ are of the form e.g. $|m_1| + |m_2|$, which are clearly not invariant under shifts.

To sidestep this overcounting for unframed quivers, we ungauge the $U(1)_d$. The way we need to do this, in order to give the correct gauge group,

$$\prod_{i=1}^{p} U(n_i)/U(1)_d, \tag{2.6.28}$$

is to set one of the magnetic charges for one gauge node to zero [13]. Note that this means ungauging on a $U(1)$ gauge node essentially "turns it into" a flavour node of rank 1. For unframed non-simply-laced quivers (see Section 2.2), the Coulomb branch of the quiver is defined as that given by ungauging on a long node. Ungauging on a short node isn't a meaningful notion, as we lack a gauge theoretic interpretation to short nodes (as we saw in Section 2.6.4).[27]

2.6.6 Fugacity maps

We are used to working with characters which are given as fugacities graded by the weights of the representation in question. We will call characters expressed in this way fundamental weight characters, and their fugacities fundamental weight fugacities x_i. However, as mentioned in Sections 2.6.1 and 2.6.2, the coefficients of t appearing in the Hilbert series are not always immediately characters of this form. Often, the z_i of (2.6.7) must undergo some sort of mapping before becoming the fundamental weight fugacities x_i so that the coefficients they form can be readily recognised as some sum of fundamental weight characters of the relevant topological global symmetry group GS. Such a mapping is called a *fugacity map*. Note that in an unframed quiver, the map can change depending on where you ungauge. Recall that the t^2 coefficient of the Hilbert series of a moduli space forms the character for the adjoint representation of its global symmetry. This means that we can isolate just the t^2 term to find the fugacity map.

In the simplest cases, the t^2 coefficient in the Hilbert series comes out as the character of the global symmetry in terms of the simple roots (we will call such characters *simple root characters*[28]) without any manipulation of fugacities. In these cases the fugacity map required is simply given by the

[27] Although note that in [63] it was found that ungauging on a short $U(1)$ node produces an orbifold of the Coulomb branch obtained from ungauging on a long node.

[28] Recall that characters encode a representation. Said representation contains certain weights, written in terms of a linear combination of fundamental weights, and the coefficients in this linear combination are how we grade the fundamental weight fugacities in the fundamental weight character. For the simple root character, the only difference

Cartan matrix. This is the case for example for any affine Dynkin diagram (see Table 3.1.1) when the ungauging is performed on the affine node.

Example Consider the affine A_2 Dynkin diagram, which we know has global symmetry $SU(3)$. The ungauged quiver is

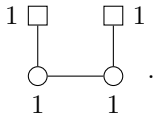

(2.6.29)

If we call the simple roots of $SU(3)$ α_1 and α_2, then the full root system is

$$\{\alpha_1,\ \alpha_2,\ \alpha_1+\alpha_2,\ -\alpha_1,\ -\alpha_2,\ -\alpha_1-\alpha_2\}. \tag{2.6.30}$$

Assigning fugacities z_1 and z_2 to the remaining gauge nodes, the Hilbert series of (2.6.29) can be computed to t^2 as

$$1+(2+z_1+z_2+z_1z_2+\frac{1}{z_1}+\frac{1}{z_2}+\frac{1}{z_1z_2})\,t^2+\mathcal{O}(t^4). \tag{2.6.31}$$

The t^2 term has unrefined dimension 8, and so we expect an $SU(3)$ global symmetry. This can be confirmed by inspecting the refined t^2 coefficient: it is indeed the root decomposition of the algebra of $SU(3)$. The Cartan subalgebra is encoded in the constant term equal to $rank(SU(3)) = 2$, and all positive and negative roots are encoded by the products of z_1, z_2 and their reciprocals: z_1 and z_2 are raised to the powers of the coefficients of the simple roots that are equal to these positive and negative roots. That is, if one uses the identification

$$c_1\,\alpha_1+c_2\,\alpha_2 \ \longleftrightarrow\ z_1^{c_1}\,z_2^{c_2}, \tag{2.6.32}$$

we see that the root system of $SU(3)$ (2.6.30) and the two Cartan elements completely comprises the t^2 coefficient of the Hilbert series (2.6.31). This tells us that (2.6.31) is written in terms of simple root characters of its global symmetry $SU(3)$. To convert to the more familiar fundamental weight characters then, we need to apply the Cartan matrix as our fugacity map:

$$\begin{pmatrix} z_1 \\ z_2 \end{pmatrix} = C \begin{pmatrix} x_1 \\ x_2 \end{pmatrix} \tag{2.6.33}$$

for C the Cartan matrix of $SU(3)$

$$C = \begin{pmatrix} 2 & -1 \\ -1 & 2 \end{pmatrix}. \tag{2.6.34}$$

Note that the matrix multiplication isn't meant in the usual sense here: rather than the entries of the matrix being coefficients of the vector they multiply, they are instead the powers that the vector elements (that they would traditionally multiply) are raised to. Applying this map yields the Hilbert series

$$1+(2+\frac{x_1^2}{x_2}+\frac{x_2^2}{x_1}+x_1x_2+\frac{x_2}{x_1^2}+\frac{x_1}{x_2^2}+\frac{1}{x_1x_2})\,t^2+\mathcal{O}(t^4), \tag{2.6.35}$$

the t^2 coefficient of which we indeed recognise as the usual fundamental weight character of the adjoint representation of $SU(3)$. This confirms the local form of GS as $SU(3)$. □

---

is that the weights are written in terms of a linear combination of the simple roots instead. This linear combination will clearly have different coefficients to the equivalent linear combination of fundamental weights, hence the different character.

In most cases the fugacity maps are a bit trickier to find. However there are some well known tricks that work in a lot of instances, and we will try to illustrate these in the following example, a quiver that will appear in Chapter 3.

Example Consider the quiver:

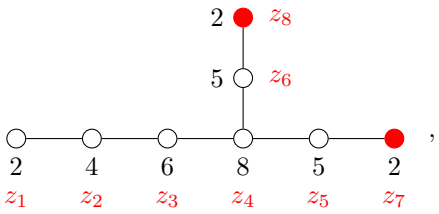

(2.6.36)

and label the topological fugacities for each node as shown in red.[29] The t^2 coefficient in the unrefined Hilbert series is 79, which is the dimension of $SO(13)\times U(1)$.[30] Refined, it has virtually no fractional terms, which means it can't be in the form of the root system of this global symmetry.[31] We have two unbalanced nodes, which we don't expect to contribute to the non-abelian global symmetry. A nice trick that often works is to map a fugacity z_i corresponding to an unbalanced node of rank r_i to the r_i^{th} root of the inverse of the product of all other fugacities raised to the power of their node ranks:

$$z_i \longrightarrow \sqrt[r_i]{\frac{1}{\prod_{j\neq i} z_j^{r_j}}}. \tag{2.6.37}$$

In this case there are two unbalanced nodes: z_7 and z_8. We choose to pick z_8 to be our z_i of (2.6.37), and thus our map here will be

$$z_8 \longrightarrow \sqrt[2]{\frac{1}{z_1^2\, z_2^4\, z_3^6\, z_4^8\, z_5^5\, z_6^5\, z_7^2}}. \tag{2.6.38}$$

After applying this, the z_7 fugacity also drops out of the Hilbert series, and so we have just $z_1, ..., z_6$ left. In the resulting Hilbert series there are terms of the form

$$\sqrt{z_5\, z_6},\ \sqrt{\frac{z_5}{z_6}}$$

appearing, and we don't have fractional powers in root systems. So a natural map to take next is

$$z_5 \longrightarrow \frac{z_9}{z_{10}},\ z_6 \longrightarrow z_9\, z_{10}.$$

In fact we find that then just sending

$$z_9 \longrightarrow z_9\, z_{10}$$

gives us the root decomposition of $SO(13)\times U(1)$,[32] i.e. its simple root character. We can then just note that the simple roots are given by the Cartan matrix acting on the fundamental weights to find

[29] The general intuition for doing this is that there is a balanced D_6 Dynkin diagram, and so we label the nodes in this with index corresponding to the weight that node represents in highest weight notation.

[30] The character of a product group irreducible representation is equal to the sum of the characters of the individual irreducible representations of each group in the product.

[31] The weight system of a real representation is comprised of some set of weights and their inverses, and possibly some trivial elements. The adjoint representation is real, and so here the weights are plus and minus the positive root system, in addition to the Cartan elements. This means the refined t^2 coefficient would have an even number of fractional and non-fractional terms that would be inverses of one another.

[32] Recall the adjoint representation of $U(1)$ is just the trivial representation.

the more recognisable fundamental weight characters. Overall the fugacity map between the z_i in the monopole formula and the fundamental weight fugacities x_i of B_6 is given by

$$\begin{pmatrix} z_1 \\ z_2 \\ z_3 \\ z_4 \\ z_5 \\ z_6 \\ z_7 \\ z_8 \end{pmatrix} = M\,C \begin{pmatrix} x_1 \\ x_2 \\ x_3 \\ x_4 \\ x_5 \\ x_6 \\ f \end{pmatrix} \tag{2.6.39}$$

where f is just some auxhiliary fugacity that disappears in the Hilbert series under this map, and M and C are given by:

$$M = \begin{pmatrix} 1 & 0 & 0 & 0 & 0 & 0 & 0 \\ 0 & 1 & 0 & 0 & 0 & 0 & 0 \\ 0 & 0 & 1 & 0 & 0 & 0 & 0 \\ 0 & 0 & 0 & 1 & 0 & 0 & 0 \\ 0 & 0 & 0 & 0 & 1 & 0 & 0 \\ 0 & 0 & 0 & 0 & 1 & 2 & 0 \\ 0 & 0 & 0 & 0 & 0 & 0 & 1 \\ -1 & -2 & -3 & -4 & -5 & -5 & -1 \end{pmatrix}, \quad C = \begin{pmatrix} 2 & -1 & 0 & 0 & 0 & 0 & 0 \\ -1 & 2 & -1 & 0 & 0 & 0 & 0 \\ 0 & -1 & 2 & -1 & 0 & 0 & 0 \\ 0 & 0 & -1 & 2 & -1 & 0 & 0 \\ 0 & 0 & 0 & -1 & 2 & -2 & 0 \\ 0 & 0 & 0 & 0 & -1 & 2 & 0 \\ 0 & 0 & 0 & 0 & 0 & 0 & 1 \end{pmatrix}. \tag{2.6.40}$$

M is the matrix used to multiply the simple roots to find the z_i, C is the Cartan matrix of B_6 (with an extra trivial row tagged along to respect the auxiliary fugacity), and the fundamental weight fugacities x_i are indexed in the usual order corresponding to the B type Dynkin diagram:

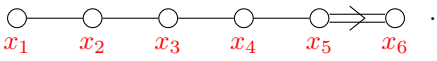

(2.6.41)

□

2.7 Hasse Diagrams

Hasse Diagrams [64, 65, 66] are another tool that have been adapted and developed to help us analyse the moduli space $\mathcal{M}$ of $3d$ $\mathcal{N} = 4$ theories [9, 67, 68]. We can stratify the vacua on $\mathcal{M}$ into sets such that all vacua in each set have the same set of massless states.[33] A *Hasse diagram* for $\mathcal{M}$ is a depiction of this stratification. The more massless states there are at a point, the more the symplectic form degenerates; the variety becomes more singular at that point. From the algebrogeometric perspective then, the Hasse diagram depicts the increasingly singular subsets of the variety. A subset of $\mathcal{M}$ with a particular set of degeneracies of ω (or equivalently a particular set of massless states) is associated to (the closure of) a *symplectic leaf*. The moduli which need to be tuned to move from one symplectic leaf to another are called *transverse slices*. A transverse slice for two adjacent symplectic leaves is called an *elementary slice*.

[33] A massless state in the low-energy vacuum has vanishing vacuum expectation value.

In general, a Hasse diagram is simply a depiction of a partial ordering on a set $(S, \leq)$. For instance, if S is comprised of three distinct elements a, b and c which are related under some partial ordering as $a \leq b \leq c$ (note that these are actually totally ordered), then the Hasse diagram for S would be:

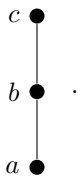

(2.7.1)

For us, S will be the symplectic leaves, and the partial ordering $\leq$ will be an inclusion of closures. That is, if one particular symplectic leaf (i.e. the set of vacua with one particular set of massless states) $\mathcal{L}_1$ lies within the closure of another symplectic leaf $\bar{\mathcal{L}}_2$, then $\mathcal{L}_1 \leq \mathcal{L}_2$:

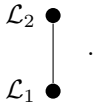

(2.7.2)

The transverse slice from $\mathcal{L}_2$ to $\mathcal{L}_1$ (the line connecting them) is the space inside the closure of $\bar{\mathcal{L}}_2$ that is transverse to $\mathcal{L}_1$. It has dimension equal to the codimension of $\mathcal{L}_1$ inside $\bar{\mathcal{L}}_2$. Note that any transverse slice is also a symplectic singularity, as it defines a set of points inside the closure of the higher symplectic leaf[34] which are singular, via the symplectic form inherited from $\mathcal{C}$.

The classical Higgs branch Hasse diagram can be determined from the bottom up [9], i.e. starting at the most singular point where the gauge group is fully unbroken and all fields are massless. The adjoint Higgs mechanism is then used to determine the massless hypermultiplets at each possible breaking of the gauge group G, all the way up to where G is fully broken (a generic point on the Higgs branch). However when the coupling is taken to infinity, the Higgs branch is non-classical and no Lagrangian description is available, rendering the above technique invalid. To study such Higgs branches, an alternative description is needed. The tool we opt to use to achieve this is called the *magnetic quiver*; a quiver whose $3d$ $\mathcal{N} = 4$ Coulomb branch is equal to the Higgs branch in question. Magnetic quivers feature in this thesis in Section 4.7 to describe the Higgs branches of certain 5 and $6d$ theories with UV/IR fixed points at infinite coupling (i.e. at their UV [69] and IR [70] fixed points, respectively).

2.7.1 Magnetic Quivers

Suppose we are concerned with the Higgs branch of a quiver theory Q which we are unable to compute classically. We'll call Q the *electric quiver*. Then its *magnetic quiver*, Q', is defined such that[35]

$$\mathcal{H}(Q) = \mathcal{C}(Q'). \tag{2.7.3}$$

When the electric theory is a $5d$ quiver Q at infinite coupling, since the coupling is a parameter of the theory and not a modulus or inherently specified by Q, we write

$$\mathcal{H}_\infty(Q) = \mathcal{C}(Q'). \tag{2.7.4}$$

[34] The "higher leaf" is the leaf inside the closure of which the "lower leaf" lies. Here, the higher and lower leaves are $\mathcal{L}_2$ and $\mathcal{L}_1$ respectively.

[35] The pair are called electric and magnetic quivers to reflect this duality between the Higgs and Coulomb branches of their moduli spaces.

One can find the magnetic quiver for an electric theory via analysis of its brane system [69, 48, 71, 72, 73, 40, 16, 74, 75, 76, 77, 78]. How this is done will not be important for understanding the results we present; when we employ a magnetic quiver to help us calculate the non-classical Higgs branch of an electric theory, it will simply be stated without proof.

We pause briefly to make a quick comment on terminology. The two phrases *magnetic quiver* and *Coulomb quiver* are used many times during this thesis, and seem to mean the same thing: they describe the quiver whose Coulomb branch is the object in question. The distinction in terminology is important for context of the object. We use the term *magnetic quiver* when we are studying the Higgs branch of some electric theory via the Coulomb branch of the magnetic quiver, whereas we use the term *Coulomb quiver* when we are studying an algebraic variety of unspecified origin via a quiver whose Coulomb branch is known to match it. Analogously to a Coulomb quiver, a *Higgs quiver* for a variety $\mathcal{V}$ is a quiver whose Higgs branch is known to match $\mathcal{V}$.

2.7.2 Quiver Subtraction

In this thesis, while we do study some Higgs branches (for example in Section 4.7), it is always via the Coulomb branch of their magnetic quivers; we only need to learn of the techniques we use in relation to Coulomb branches. In the context of Hasse diagrams, this means we only need to learn how to explore the singularity structure of the Coulomb branch.

Recall that to explore a classical Higgs branch Hasse diagram, one starts from the origin of $\mathcal{H}$ where the gauge group is fully unbroken and everything is massless, before Higgsing to climb up the Hasse diagram to the most generic (and least singular) points of $\mathcal{H}$. The technique developed to produce the Coulomb branch Hasse diagram takes an opposing approach: top down. We start from the most generic points on $\mathcal{C}$ (the least singular) and work down to find the singularities, using a method called *quiver subtraction* [34].

Quiver subtraction was conceived by the authors based on their work with Kraft-Procesi transitions [79] in the brane system [80, 39]. It was found that for brane systems of maximal nilpotent orbits, one could reproduce the known Hasse diagram of the orbits for a specified algebra by aligning branes in the Coulomb phase of the brane system and "un-Higgsing". This corresponds to tuning moduli to move from a leaf[36] in $\mathcal{C}$ to another leaf with additional massless states. When a minimal number of branes are aligned (or equivalently a minimal number of moduli are tuned) to move from one leaf to another, the transverse slice corresponding to these moduli is called an elementary slice, and the two leaves are adjacent (there exist no other intermittent leaves between them). From these minimal transitions, all composite ones can be obtained. The process of aligning branes was translated into quiver subtraction, a graph theoretic algorithm to be performed on a given quiver [34]. Here it was conjectured that subtracting Coulomb quivers of elementary slices from the quiver of a theory constructs its Coulomb branch Hasse diagram. This conjecture has not been proven generically, but there are many cases for which it has been (for example through use of mirror symmetry [51] and Higgsing), and no counterexamples have yet been found.[37]

[36] Here, as in many places throughout the thesis, we use "leaf" in place of "symplectic leaf" for the sake of brevity.

[37] Note that the precise form of the quiver subtraction algorithm has received updates along the way (for example in [16]), and we anticipate it will continue to do so.

Quiver subtraction starts from the quiver Q for a theory, which represents the top leaf $\mathcal{L}$ of the Coulomb branch Hasse diagram. Each known elementary slice (note that this list is incomplete) has a corresponding Coulomb quiver σ (or possibly several). One identifies all σ_i that "lie within" Q, and for each one, subtracts $Q - \sigma_i$ to give another quiver $Q_{1,i}$ which corresponds to a leaf $\mathcal{L}_{1,i}$ on the next level down from $\mathcal{L}$ in the Hasse diagram. If $Q_{1,i}$ is non-trivial, the process is repeated again for each leaf $\mathcal{L}_{1,i}$, until no non-trivial quivers representing leaves are left. The Hasse diagram then takes the form:

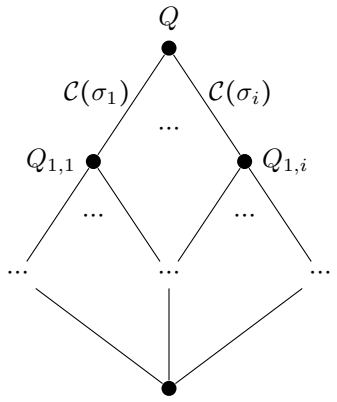

(2.7.5)

where the closure of a leaf is the Coulomb branch of the quiver associated to the leaf, and each edge is labelled by the symplectic singularity that the moduli in the transverse slice form.

Importantly for us, it is conjectured that the product of the symmetries of the bottom-most elementary slices in a Hasse diagram is a subgroup of the non-abelian part of the topological global symmetry GS. In Chapter 3, quiver subtraction and its reverse process, quiver addition [10], are exploited to find quivers with enhanced Coulomb branch global symmetry. Although quiver subtraction was derived from brane systems, in the absence of a brane picture the rules for subtracting quivers can often still be implemented, although a physical motivation for doing so is absent and the Hasse diagram derived cannot be verified. Whilst this is the case for many quivers studied in Chapter 3, in all cases we find evidence supporting the validity of using quiver subtraction. In particular, for all Coulomb branches studied in Chapter 3, the symmetries of the bottom-most elementary slices of the Hasse diagram agree with the non-abelian part of the correct GS as computed using the monopole formula.

It's now time to make the above discussion concrete and explicitly state the quiver subtraction algorithm, presented so as to be of greatest use for our purposes. In particular, we state the algorithm for unframed quivers only, as it is only such quivers whose Coulomb branch Hasse diagram we explore (we are not concerned with the Hasse diagrams of the select few framed quivers appearing in this thesis). The steps in the algorithm we are about to outline are all detailed in other papers [34, 9, 16], but we compile them here for the readers convenience. It will be necessary to consider the Coulomb quivers for all known elementary slices, and the complete up-to-date collection can be found by compiling Table 1 of [81], and Table 3.1.2 of this note.

Quiver subtraction algorithm Consider an unframed unitary $3d$ $\mathcal{N} = 4$ quiver Q. A valid elementary slice that can be subtracted from Q is one whose Coulomb quiver σ has nodes that "lie

within" Q. By this, we mean that a connected subset of the nodes in Q, Q_σ, is in the shape of σ,[38] and that the rank of each node in Q_σ is greater than or equal to that of its corresponding nodes in σ. Note that there may be many possible choices for Q_σ for a given σ, and many choices of σ for a given elementary slice: all such choices lead to different transverse slices in the Hasse diagram. The following steps then show us how to perform the subtraction $Q - \sigma$ for a particular Q_σ.

1. **Subtract**. For each node in Q_σ, subtract the rank of the corresponding node in σ.

2. **Rebalance**. Identify the nodes which have undergone a change in excess, as defined in (2.2.11), due to the subtraction. Call the set of such nodes E, and define E_l as the subset of E that are long nodes and E_s as the subset of E that are short nodes. The nodes in E must be "rebalanced" so that they have the same excess as before. This is done differently depending on the scenario:

   a) If the subtraction performed was *not* identical to the previous subtraction (i.e the same slice σ being taken from exactly the same subset Q_σ of Q), then add a $U(1)$ node u to the quiver, and connect it to the nodes in E in the following way:

      i) Connect all nodes in E_l to u with sufficiently many simply laced edges such that the excess of the nodes in E_l is restored to the values they took before the subtraction.

      ii) Connect all nodes in E_s to u with sufficiently many *non*-simply laced edges whose multiplicity is equal to the "shortness" of the node in E_s in question, such that u is the long node and the excess of the nodes in E_s is restored to the values they took before the subtraction.

   Note that the added $U(1)$ node u need not be balanced; it may have excess $e_u \neq 0$. However if a subsequent distinct subtraction[39] is performed, the excess of u after this subtraction will have to be restored to its value before the subtraction, e_u.

   b) If the subtraction performed was the n^{th} $(n \geq 2)$ in a string of identical subtractions (i.e. subtracting the same slice σ from precisely the same subset Q_σ of Q multiple times in a row), then, calling the $U(1)$ node added to rebalance after the *first* such subtraction u, apply the following:[40]

      i) If $n = 2$, add an adjoint hypermultiplet to u, and increase the rank of this node to two.

      ii) If $n \geq 3$, u will already have an adjoint hypermultiplet from the $n = 2$ subtraction, so simply raise the rank of u by one (this will mean its rank is n).

Example Consider the quiver

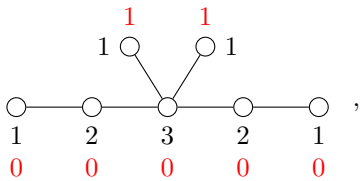

(2.7.6)

[38] More precisely, Q_σ being in the shape of σ means that, up to some permutations of rows, the Cartan matrix describing the links between nodes in Q_σ contains the Cartan matrix describing the links between nodes in σ.

[39] By distinct subtraction, we mean any subtraction which is not subtracting σ from the exact same set of nodes Q_σ.

[40] Note that the concept of *decorated quivers* has been introduced to keep track of multiple same slice subtractions [16, 68, 82].

where the ranks of the gauge nodes are given in black, and we've noted the excess of each node in red. We can see that the central five nodes form the shape of the magnetic quiver for the d_4 slice and have appropriately large ranks, so this slice can be subtracted. No other slice is a subset of the nodes of this quiver, so this is the only possible subtraction. Performing Step 1 gives

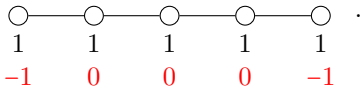

(2.7.7)

Here, the nodes which have changed excess are the two end nodes. They are both long nodes, and so $E = E_l$ (E_s is empty). This means that in Step 2, we must follow option $a)i)$.[41] The nodes in E both need just one extra flavour to restore their balance, and so we connect the new $U(1)$ to either end node with just a single simply laced edge:

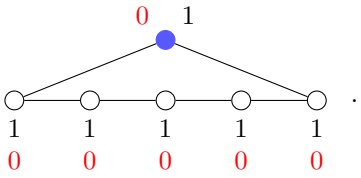

(2.7.8)

We have coloured the rebalancing node u in blue for clarity. (2.7.8) is precisely the Coulomb quiver of the elementary slice $\sigma = a_5$, and so clearly this is all that can be subtracted. Doing so leaves nothing left, and so this concludes the exploration of the foliation of the Coulomb branch of (2.7.6); its Hasse diagram is

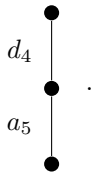

(2.7.9)

The interpretation here is if you pick a point on the Coulomb branch moduli space, it will lie on one of the closures of the three leaves in the Hasse diagram (2.7.9), each of which correspond to a certain set of massless states. The Coulomb branch of the quiver theory of (2.7.6) is obviously the closure of the top leaf (the whole Hasse diagram), as this is the moduli space we're studying. A generic point on this Coulomb branch will have the maximal number of massless states: 10 massless vectormultiplets,[42] and no massless hypermultiplets (by the BPS formula). All such points live on the top leaf, associated to the quiver (2.7.6). There are then certain points on the Coulomb branch which have fewer massless states: just 5 massless vectormultiplets now, plus a massless hypermultiplet.[43] Such points lie on the middle leaf of (2.7.9), and are associated to the quiver (2.7.8). The Coulomb branch of (2.7.8) is then the closure of this middle leaf (i.e all points on this leaf and the bottom leaf). At one particular point on the Coulomb branch all 20 vectormultiplets and 22 hypermultiplets are massless. This is the origin of the Coulomb branch, and is the sole point which lives on the bottom leaf of (2.7.9). The

[41] An example of a quiver where one must instead follow Step 2)b) during the quiver subtraction process is (3.2.4).

[42] The number of massless vectormultiplets can be read from the quiver. The quaternionic dimension of the Coulomb branch will be the number of monople operators we have, which is equal to the rank of the gauge group. The complex or real dimension then is twice or four times this respectively.

[43] This massless hypermultiplet opens up Higgs branch directions in the Hasse diagram for the full moduli space as it may now acquire a VEV [67]. That is, there is a set of moduli associated to this hypermultiplet which can be tuned away from zero to explore the Higgs branch. It can be seen from the brane picture that these moduli correspond to the d_4 variety. Such a set of moduli is called a transverse slice, as discussed later in this paragraph.

whole Hasse diagram obviously contains its bottom half, and so the Coulomb branch moduli space of (2.7.6) contains that of (2.7.8). The transverse slice between these two Coulomb branches is d_4, and between the origin and the (2.7.8) Coulomb branch is a_5. The transverse slices connecting two leaves tell us the moduli that need tuning to or away from zero to move between the two corresponding leaves. The lowest elementary slice is a_5, and thus $SU(6)$ must be at least a subgroup of the global symmetry. Indeed this is confirmed upon computation of the Hilbert series, which tells us that the global symmetry is $SU(6) \times U(1)$. □

Chapter 3

Global Symmetry

In this chapter we present the work of [10], where we constructed many infinite families of quivers for which the previously accepted algorithm for identifying GS from a quiver based on the balance of its gauge nodes fails, giving only a subgroup,[1] and provide a suggested amendment to this algorithm to fix this. The content of this chapter relies heavily on the concepts of balance, the Coulomb branch topological symmetry GS, fugacity maps, Hasse diagrams, quiver subtraction and discrete projections. For a recap of these topics, see Sections 2.2.3, 2.4.2.2, 2.6.6, 2.7, 2.7.2, and Appendix A respectively.

As discussed in Section 2.6.2, the GS for a quiver (recall we don't concern ourselves with the global form, although the generators of the Hilbert series can be used to determine this) can be determined explicitly by computing the monopole formula and consulting the t^2 term, after a possibly fugacity map. However for quivers of sufficiently high rank, this method becomes too computationally intensive to carry out, driving the want for an algorithm to determine GS from simple inspection of a quiver. By and large, this can be done (for quivers containing only regular matter[2]) by applying an algorithm [14] based on the quiver's balanced gauge nodes [4]. We call the symmetry predicted by this algorithm the **balance global symmetry** (BGS), and the algorithm itself the BGS algorithm. However, there have been examples found in the past where the BGS algorithm only produces a strict subgroup of GS, see for example [15, 16]. For these quivers, the true GS is an enhancement of the BGS; we call the GS of such quivers the **enhanced global symmetry** (EGS). The failure of the BGS algorithm to give the correct GS for all quivers indicates a need to improve it. In order to decipher what the needed amendments are, we must first understand *why* it fails on the set of examples found. This is precisely the concern of this chapter.

We make progress with this by considering the Coulomb branch Hasse diagrams of quivers with an EGS. Recall from Section 2.7.2 that the symmetries of the bottom elementary slices in the Coulomb branch Hasse diagram are conjectured to form a subgroup of GS. It turns out that the Hasse diagrams

[1] When we say the BGS fails, we mean that it fails to give the *full* global symmetry. This is not technically a failure of the BGS as it only claims to give a subgroup of the full global symmetry, but it is a failure of the BGS as an algorithm to always give us the full global symmetry of a quiver, hence our use of the terminology.

[2] Regular matter is used to refer to that contained in quivers for which the Cartan matrix of any two connected nodes, n_i and n_j, has either the ij or ji entry as -1. This is extended from the definition of just having bifundamental matter to include non-simply laced edges.

of quivers experiencing an EGS contain a symplectic leaf whose corresponding quiver[3] has an adjoint hypermultiplet(s). In this chapter, we show that the presence in the Hasse diagram of balanced quivers with adjoint matter,[4] which we call Q_a, induce lowest elementary slices and thus (under the above conjecture) a GS of greater dimension than expected.[5] In order to do this we start with these quivers Q_a, many of whom's Coulomb branches appear in the Kostant Brylinski classification [12], and reverse-engineer the process of quiver subtraction to obtain infinitely many quivers with an EGS. This process that undoes quiver subtraction is called *quiver addition*, and has been introduced before in [81]. We amend the method given there to include how to perform quiver addition to remove the adjoint matter in Q_a. We then use the logic implemented to construct these quivers with an EGS to give a modification to the BGS algorithm which corrects its previous failings for all quivers presented in this chapter.

As far as we checked, using quiver addition on many non-balanced quivers with adjoint matter also gives an EGS.[6] We restrict ourselves to the balanced subset Q_a in this paper as we cannot list all quivers with an EGS (there are infinitely many of them), and this is a natural and fairly small subset to focus on to illustrate the idea.

The chapter is organised as follows. In Section 3.1 we review the BGS algorithm, and see an example for which it fails. In Section 3.2, we conjecture an amendment to the BGS for balanced quivers with adjoint matter Q_a, provide a full list of such quivers, and give the method we use to perform quiver addition on them. In Sections 3.3, 3.4, 3.5 and 3.6, the quivers with EGS which arise as the result of performing quiver addition on the respective Q_a (given in Table 3.2.1 of Section 3.2.1) are listed. The global symmetries predicted by the BGS algorithm in these sections contain a factor that is enhanced to B_n, G_2, D_n and A_2 respectively.[7] Finally, in Section 3.7 we give a modified BGS algorithm which works not only on all quivers for which the previous BGS algorithm worked, but also on all those constructed in Sections 3.3 – 3.6.

3.1 Balance Global Symmetry

We start by reviewing the algorithm previously established for determining (a subgroup of) the Coulomb branch topological symmetry from a quiver. The concept of framing and balance both feature; for a recap, see Sections 2.2.1 and 2.2.3 respectively. The other potentially unfamiliar terminology used is the phrase *sub-Dynkin diagram*. If a quiver contains unbalanced gauge nodes, the balanced nodes naturally split into connected subsets which each take the form of a Dynkin diagram of some simple Lie algebra. We call these balanced sub-quivers sub-Dynkin diagrams.

[3] By the quiver corresponding to a symplectic leaf, we mean the quiver whose Coulomb branch is equal to the closure of the symplectic leaf.

[4] See the bullet points at the end of Chapter 1 for clarification of this statement.

[5] We do not rule out the possibility to find more quivers with an EGS whose Hasse diagrams do not contain a leaf corresponding to one of the Q_a.

[6] Although note that we may need to use an adaptation of the quiver addition algorithm presented in Section 3.2.2 if the quiver with adjoint matter in question does not satisfy the necessary conditions stated.

[7] The algebraic and Dynkin names for Lie groups, for example B_n and $SO(2n+1)$, will be used synonymously throughout this paper.

BGS algorithm

The balance global symmetry for a good quiver containing only regular matter,[2] Q_r, is computed as follows:

1. If Q_r is framed, and the gauge nodes in it comprise s balanced sub-Dynkin diagrams D_i of the simple Lie groups G_i, and k unbalanced nodes, then the BGS is given by

$$BGS_{Q_r}^{\text{framed}} = \prod_{i=1}^{s} G_i \times U(1)^k. \tag{3.1.1}$$

2. If Q_r is unframed, there are two scenarios:

   a) If Q_r is balanced, then it must be either the affine or twisted affine quiver for some simple Lie group G (these quivers are given in Tables 3.1.1 and 3.1.2 respectively), in which case

$$BGS_{Q_r} = G. \tag{3.1.2}$$

   b) If Q_r is unbalanced, and the gauge nodes in it comprise s balanced sub-Dynkin diagrams D_i of the simple Lie groups G_i, and k unbalanced nodes, then the BGS is given by

$$BGS_{Q_r}^{\text{unframed}} = \prod_{i=1}^{s} G_i \times U(1)^{k-1}. \tag{3.1.3}$$

   where the definitions of s, G_i and k are as in Step 1.

As noted in the introduction however, this algorithm does not always yield the full global symmetry. To see this explicitly, consider the following example.

Example Consider the quiver

$Q =$ 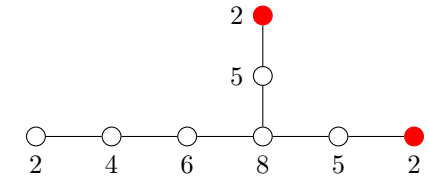

(3.1.4)

where the red indicates that the corresponding node is unbalanced. Here, there are two unbalanced nodes and one balanced sub-D_6 Dynkin diagram. Thus we read off the BGS

$$BGS_Q = SO(12) \times U(1). \tag{3.1.5}$$

However if we compute the refined Hilbert series perturbatively (see Section 2.6.3) to order t^2 for Q we find that, after the appropriate fugacity map (see Section 2.6.6),

$$HS_Q = 1 + (1 + [0,1,0,0,0,0]_{B_6})t^2 + \mathcal{O}(t^4), \tag{3.1.6}$$

which means that the global symmetry is actually enhanced to

$$EGS_Q = SO(13) \times U(1). \tag{3.1.7}$$

Blue is used to highlight the factor of the global symmetry that is enhanced. Here we see explicitly the failure of the BGS to give the full global symmetry. □

Coulomb branch	Affine Quiver
a_k	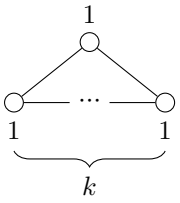
b_k $k \geq 3$	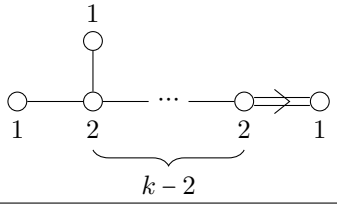
c_k $k \geq 2$	
d_k $k \geq 4$	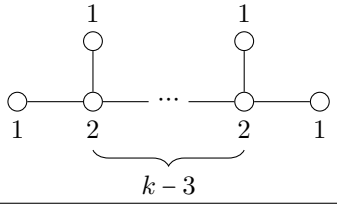
e_6	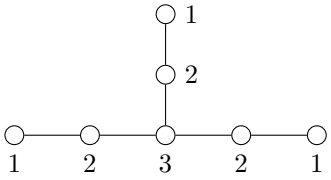
e_7	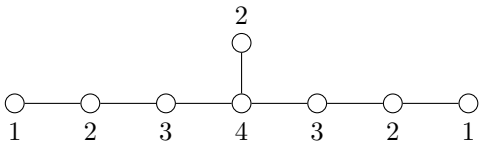
e_8	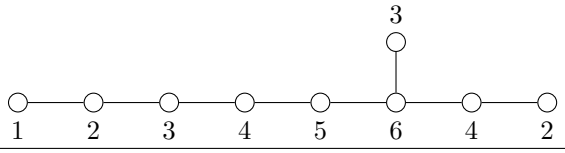
f_4	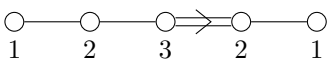
g_2	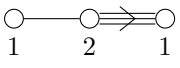

Table 3.1.1: Quivers of the affine Dynkin diagrams. The first column lists the Coulomb branch varieties, which are all the minimal nilpotent orbits g_k of the simple Lie groups G_k, of the quivers in the second column when ungauged on a long node. These quivers will be referred to as "affine g_k".

Coulomb Branch	Twisted Affine Quiver
a_2	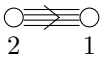
a_{2k-1}	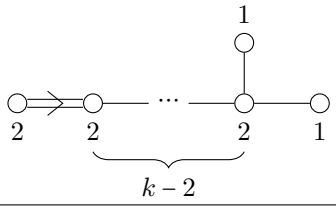
a_{2k} $k \geq 2$	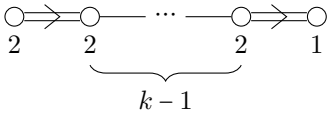
d_4	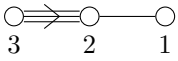
d_{k+1} $k \geq 4$	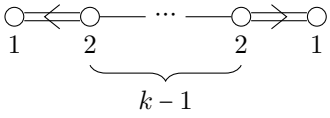
e_6 $k \geq 2$	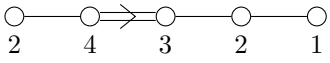

Table 3.1.2: Quivers of the twisted affine Dynkin diagrams. The first column lists the Coulomb branch varieties, which are all the minimal nilpotent orbits g_k of the simple Lie groups G_k, of the quivers in the second column when ungauged on a long node. These quivers will be referred to as "twisted affine g_k".

Now that we have seen the BGS algorithm and seen an example quiver on which it fails (i.e. a quiver that has an EGS), we are ready to move on to describe the method by which we construct infinitely many quivers with an EGS. In Section 3.7, we will present a modified BGS algorithm which *does* work on Q (and all other quivers constructed with an EGS which appear in Sections 3.3 – 3.6), and see its success with Q illustrated explicitly in an example.

3.2 Constructing Quivers with Enhanced Global Symmetry

The gauging of discrete symmetries in supersymmetric quiver gauge theories has received much attention in recent years. The notion of gauging continuous symmetries is a familiar one: introducing fabricated degrees of freedom to elicit mathematical trickery in order to simplify problems. Many theories also have global discrete symmetries, such as time reversal or charge conjugation, and so exploring the potential to gauge these symmetries should be of equal interest. In the context of the moduli spaces of supersymmetric quiver gauge theories, this has been explored in [71, 83, 84, 62], for example. The outer automorphisms of the quiver itself are obvious discrete global symmetries of the theory, and thus we could choose to gauge them. In the string theory picture, this corresponds to moving branes on top of one another, inducing extra massless strings stretching between them. A

result of this is the following conjecture:

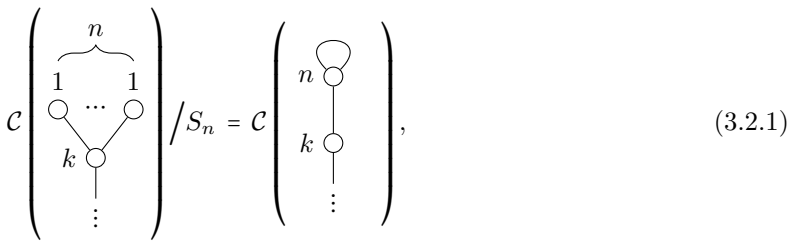

(3.2.1)

where $\mathcal{C}(Q)$ is used to denote the Coulomb branch of the quiver Q. This conjecture has been proven on the level of the Hilbert series [83], but this is not sufficient to prove for good that the two Coulomb branches are the same.

Let's be explicit about what this tells us. The quiver on the left hand side, which we'll call A, has an S_n outer automorphism permuting the bouquet of n identical $U(1)$ nodes, and so this S_n is a discrete global symmetry of the theory described by A. Upon gauging this symmetry, we add further constraining relations to the ring of gauge invariant chiral operators on the Coulomb branch, and thus the Coulomb branch of this gauged theory will be an S_n quotient of that of A. Moreover, the Coulomb quiver for this discretely gauged theory is found by compiling the bouquet in A together into one single $U(n)$ node with a hypermultiplet in the adjoint representation, as shown in the quiver on the right hand side of (3.2.1), which we'll call B. The intuition for this comes from the brane picture discussed above. From here on out, we refer to such a hypermultiplet (i.e. one that is in the adjoint representation of some gauge group) as an adjoint hypermultiplet, or more vaguely as adjoint matter. Adjoint matter is represented in the quiver by a loop going to and from the node that it is in the adjoint representation of. The conjecture (3.2.1) has been shown to be true in many cases, and a counterexample has not yet been found, so it is believed to be true in general. For details on how to find an S_n quotient of a moduli space in terms of its Hilbert series, see Appendix A in which an example for $n = 2$ is illustrated.

In Section 3.2.1 we look at quivers with adjoint matter (whose Coulomb branches, by the above, can be seen as discrete quotients of quivers containing only regular matter[2]) and see how to read their BGS, before constructing the full set of balanced quivers for which each node has at most one adjoint hypermultiplet. It is these quivers from which in the following sections we will construct, via quiver addition, quivers with only regular matter that enjoy an EGS. The process of this construction is outlined in Section 3.2.2.

3.2.1 Quivers with Adjoint Matter

The main result of this work is as follows: there are balanced quivers with adjoint matter which we call Q_a, listed in Table 3.2.1,[8] that induce an EGS. By this, we mean that we have found many quivers, derived by performing quiver addition on Q_a to "absorb" the adjoint hypermultiplet (we will see what this means more concretely in Section 3.2.2), which experience a symmetry that is enhanced from that predicted by the BGS. Since the adjoint matter is absorbed in this process, the resulting quivers are of type Q_r.[2] The Hasse diagram of such a quiver Q_r will contain the Hasse

[8] Note that, as explained in the bullet points at the end of Section 3.2.1, the quiver with global symmetry $SU(2n+1)$ in Table 3.2.1 is not part of the set of quivers Q_a which we study in this note, as it is unclear how to perform quiver addition in this case.

diagram of the quiver Q_a it was derived from, and so the global symmetry of Q_a will be a subgroup of the global symmetry of Q_r, as explained in Section 2.7. This motivates us to study the quivers Q_a, and in particular their global symmetry. However, the above prescription for reading the BGS does not specify what happens when there are gauge nodes with adjoint matter in the quiver. We will call such gauge nodes a_i, $i = 1, ..., L$, where $L \in \mathbb{N}$ is the number of nodes with adjoint matter. One might naively think to just "ignore" the adjoint hypermultiplets (other than their contribution to the balance of a_i), and proceed with the algorithm given in Section 3.1. However, as the example below shows, this leads to us identifying incorrect global symmetries. To correct this, we propose the following extension to the BGS algorithm for balanced quivers containing an adjoint hypermultiplet.

Claim: Q_a BGS algorithm

Let Q_a be a balanced[9] quiver which has L nodes that each have a single adjoint hypermultiplet, and no nodes with more than one. Label these nodes a_i and their ranks r_{a_i}, for $i = 1, ..., L$. Furthermore, impose that the nodes a_i are only connected to other gauge nodes in Q_a via simply laced edges. Then the global symmetry of Q_a can be determined by performing the following steps:

1. Replace the simply laced connections of the a_i to other gauge node(s) of Q_a by a non-simply laced edge of multiplicity r_{a_i} such that a_i are the short nodes.
2. Remove the adjoint hypermultiplets attached to all nodes a_i.
3. Set all $r_{a_i} = 1$.
4. Call the resulting quiver after performing steps $1 - 3$ $\tilde{Q}_a$. The global symmetry of Q_a is then given by implementing the previous BGS algorithm listed in Section 3.1 on $\tilde{Q}_a$.

The justification for this claim is found in examining the Hilbert series. For Q_a, under the topological-to-simple-root fugacity map, the topological fugacities for the nodes with adjoint matter a_i correspond to the simple root fugacities for the short nodes in $\tilde{Q}_a$. This motivates the above algorithm, and indeed gives the correct global symmetry for all quivers in Table 3.2.1. We illustrate the need for and implementation of this claim below with the following example.

Example Consider the quiver

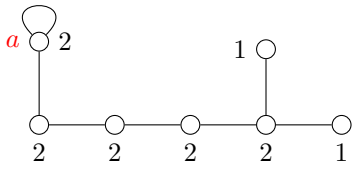

(3.2.2)

This is a Coulomb quiver of the Kostant Brylinski classification [12], as its Coulomb branch is the $\mathbb{Z}_2$ quotient of the minimal nilpotent orbit of D_7 [84]: the next to minimal nilpotent orbit of B_6 [62], $\mathcal{O}_{(3,1^{10})}$. Thus the global symmetry of (3.2.2) is B_6. Let's check this against the initial BGS algorithm we gave in Section 3.1, if we were to treat a as we would any other node. Since there are no unbalanced nodes, and among the gauge nodes there is just one balanced sub-Dynkin diagram which is in the shape of A_6, we would conclude that the global symmetry is $SU(7)$, which is incorrect.

[9] This algorithm does also work for some unbalanced quivers with hypermultiplets as specified here. However it does not work for all such quivers, and hence we restrict the validity of the algorithm to only the balanced subset.

However, under the Q_a BGS algorithm above, to correctly read the global symmetry, the connection of a to its adjacent node is replaced by a non-simply laced edge of multiplicity two such that a is the short node, its adjoint hypermultiplet is removed, and its rank is set to one:

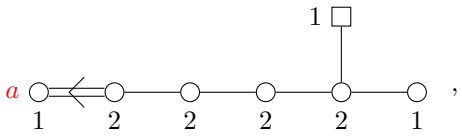

(3.2.3)

We then proceed with the original BGS algorithm. Since (3.2.3) is unframed and forms the affine Dynkin diagram of B_6, hence we conclude that this is the global symmetry, which is indeed correct. Note that although the quiver (3.2.3) has the same global symmetry as (3.2.2), it does not have the same Coulomb branch. This algorithm should only be used to determine the global symmetry. □

It is worth noting that while this extension to the BGS algorithm is nice, it does not fulfill the requirement of an all encompassing method for determining the global symmetry, as it still fails in many cases. See for instance the example of (3.1.4), which is a quiver of type Q_r and therefore has no adjoint hypermultiplet, so the previous BGS failure is not fixed by the above ammendment.

The reason we are interested in these quivers with adjoint matter is because, as is explained in Section 3.2.2, when quiver addition is performed on them to absorb the node(s) with the adjoint hypermultiplet, the resulting quiver experiences an enhanced global symmetry.

There are many quivers with adjoint hypermultiplets which will elicit an EGS in quivers derived from them via quiver addition, but in this work we restrict ourselves to just a subset: the family of balanced quivers whose nodes each have at most one adjoint hypermultiplet. These are the quivers we refer to as Q_a. They can be completely classified, and the full classification is listed in Table 3.2.1, along with the Coulomb branch variety, enhanced global symmetry and HWG (see Section 2.6.2). It is sufficient to, for now, restrict our study to these quivers, as they can be used to construct a healthy range of examples for which the BGS fails. We proceed with proving the classification of these Q_a.

Theorem. *The set of 3d $\mathcal{N}=4$ balanced unframed unitary quivers with $L \in \mathbb{N}\setminus\{0\}$ nodes a_i, $i=1,...,L$ that each have a single adjoint hypermultiplet but which otherwise only contain regular matter can be completely classified, and the classification is given by Table 3.2.1.*

Proof. First start by considering a single node a of rank r_a with a single adjoint hypermultiplet, which all such quivers in the theroem must contain. Note that $r_a > 1$ because the adjoint representation of $U(1)$ is trivial. To be balanced, a must be attached to exactly two flavours. This limits us to: (i) one rank two node attached via a simply laced edge; (ii) one rank two node with an adjoint hypermultiplet attached via a simply laced edge; (iii) two rank one nodes, each attached via a simply laced edge; (iv) one short rank one node attached by a non-simply laced edge of multiplicity two; or (v) one long rank two node attached by a non-simply laced edge of multiplicity two. Note that we cannot have one rank one node connected to a via two simply laced hypermultiplets because for this node to be balanced it would force $r_a = 1$. In the cases (ii), (iii), (iv) and (v), for these new nodes added to be balanced, and because $r_a \neq 1$,[10] it must be that $r_a = 2$. Furthermore, this must be the end of the

[10] This constraint is relevant to mention because if $r_a = 1$ were allowed, the new node could have been balanced by attaching further nodes to it.

chain, as these final nodes added are already balanced so we cannot possibly add anything more to them. In case (i) we have three possibilities, as $r_a \leq 4$ otherwise the new node will be overbalanced, and we know $r_a \neq 1$. Call this new rank two node attached to a in (i) node T. If $r_a = 4$, the chain ends here as T is already balanced. If $r_a = 3$, then T must be connected to one flavour to be balanced, and this ends the chain. If $r_a = 2$, then in order for T to be balanced, it must connect to two flavours also. This will again have the same options (i),(ii), (iii), (iv) and (v) as above, and again if option (i) is chosen the chain will continue, until at some point it must end by choosing one of the other options. Running through all these possibilities gives the full list of quivers in Table 3.2.1. ∎

The balanced quivers with adjoint hypermultiplets in Table 3.2.1, except for the $n = 2$ cases of $b_n/\mathbb{Z}_2$ and $a_{2n-1}/\mathbb{Z}_2$, could also be derived in an alternative way. Readers who are confident in the material may wish to skip this paragraph and proceed to the bullet-pointed remarks on Table 3.2.1 below, as its main use is to clarify ideas already introduced. Recall that the lowest elementary slices of the Hasse diagram reveal a subgroup of the global symmetry. We therefore try to construct the most basic building block quivers with adjoint matter which induce an EGS.[11] This can be done by finding the quivers Q_a for whom $\tilde{Q}_a$, as named in the Q_a BGS alogrithm given at the top of this section, is an elementary slice. More complicated quivers with adjoint matter that induce an EGS can then be derived from these. At the time of writing, the full list of Coulomb quivers of the known elementary slices is comprised of Table 1 in [81] and Table 3.1.2 in this paper. Thus our building block quivers Q_a are found by identifying these quivers that have short rank one nodes a_i each connected to a single rank two node b_i via a non-simply laced edge of multiplicity r_{a_i}, or to two rank one nodes b_{i_1} and b_{i_2} both via non simply laced edges both of multiplicity r_{a_i}, and replacing these short nodes by rank r_{a_i} nodes with an adjoint hypermultiplet, connected to b_i (or b_{i_1} and b_{i_2}) via a simply laced edge. Looking at the elementary slices, the only ones whose Coulomb quivers satisfy these criteria are the affine quivers b_n, c_2 and g_2, and the twisted affine quivers a_{2k} (for all $k \geq 1$) and d_{k+1} (for $k \geq 4$).

There are several things worth noting regarding the quivers Q_a in Table 3.2.1:

- The quivers are ordered in such a way to best aid an illustration of the results in this paper. In particular the first quiver yields the best illustration of the most basic quiver addition needed, and the final quiver will not appear at all (it is unclear if it is possible to use quiver addition to absorb the adjoint hypermultiplet on this node).
- We have been unable to find the fully refined Hilbert series and HWG for the $b_n/\mathbb{Z}_2$, $d_{n+1}/(\mathbb{Z}_2 \times \mathbb{Z}_2)$, d_4/S_4 and $a_{2n-1}/\mathbb{Z}_2$ quivers in Table 3.2.1. The reason is that in these cases, there are not sufficient topological fugacities to apply the normal tricks we use to find fugacity maps. However the *partially refined* Hilbert series can be found, which is the Hilbert series in terms of the characters of some subgroup of the global symmetry. These partially refined Hilbert series have been computed for all the quivers under discussion in this bullet point, but are not listed as we were able to find the fully refined HWGs via other methods. We discuss these in turn, labelling the quiver we're addressing in each case by its Coulomb branch variety:
  - $b_n/\mathbb{Z}_2$: Here the HWG can be obtained by noticing that the variety of $b_n/\mathbb{Z}_2$ is the next to minimal nilpotent orbit of D_n [12], and so the Coulomb branch HWG can be computed by applying the monopole formula to the unitary Coulomb quiver for this variety, given in [38].

[11] Note that the Coulomb branches of these building block quivers are not elementary slices themselves, rather they are derived from them.

- $d_{n+1}/(\mathbb{Z}_2 \times \mathbb{Z}_2)$: Here we have found the HWG in two different ways. Firstly, we use conjecture (3.2.1) to realise the Coulomb branch of this quiver as the $\mathbb{Z}_2$ projection of the next to minimal nilpotent orbit of B_n. The fully refined HWG for n.min B_n can be computed exactly by applying the monopole formula to the top quiver in Table 3.2.1. The $\mathbb{Z}_2$ projection of this can then be computed: see Appendix A for an example of how to do this. We then (a) unrefined and (b) partially refined the HWG that resulted from this projection, and confirmed that it agreed exactly with the unrefined and partially-refined Hilbert series for the Coulomb quiver of $d_{n+1}/(\mathbb{Z}_2 \times \mathbb{Z}_2)$ given in Table 3.2.1. The second way we checked this HWG was by computing the Higgs branch of the Higgs quiver for $d_{n+1}/(\mathbb{Z}_2 \times \mathbb{Z}_2)$, given in Figure 17 of [84]. This has been done for several n, and the result matches that obtained by the first method, providing as much evidence for the validity of this result as is possible using the monopole formula.
- d_4/S_4: Again using conjecture (3.2.1), the HWG for this variety can be found by applying an S_4 projection to the minimal nilpotent orbit of D_4. This has been done by Siyul Lee and does indeed have a closed form, but it is rather lengthy and not particularly illuminating to give here, so we list it to order 6. Again, the result of (3.2.1) in this case has been checked by unrefining and partially refining the HWG computed for d_4/S_4 and comparing with the unrefined and partially refined Hilbert series for the Coulomb quiver of d_4/S_4 given in Table 3.2.1.
- $a_{2n-1}/\mathbb{Z}_2$: Here (3.2.1) tells us that this quiver is the $\mathbb{Z}_2$ quotient of the twisted affine Dynkin diagram for A_{2n-1} (see Table 3.1.2). However this cannot be fully refined, so we instead exploit the fact that the Coulomb branches of the twisted affine and affine quiver for the same Lie algebra match: we perform the $\mathbb{Z}_2$ projection on the HWG computed from the affine quiver (which does fully refine). When unrefined, this result matches the unrefined Hilbert series for the Coulomb quiver for $a_{2n-1}/\mathbb{Z}_2$ given in Table 3.2.1.

• This is not an exhaustive list of quivers with adjoint matter that induce an EGS, but it is an exhaustive list of all *balanced* quivers with adjoint matter that induce EGS, and as such is rich enough to provide us with many examples for which the BGS algorithm of Section 3.1 fails.

We now move on to discussing how to use quiver addition on the quivers in Table 3.2.1 to construct quivers with only regular matter Q_r (remember that among other things this means with*out* adjoint matter) whose global symmetry is enhanced from that predicted by the BGS.

3.2.2 Quiver Addition

Recall that our goal is to find all possible quivers whose Hasse diagram[12] has as the closure of one of its lowest leaves the Coulomb branch of one of the quivers in Table 3.2.1, because this leads to an enhancement of the BGS predicted by the algorithm outlined in Section 3.1. In order to do this, quiver subtraction must be reverse engineered to "absorb" the nodes with adjoint hypermultiplets appearing in Table 3.1. One notion of quiver addition is discussed in [81], but here we will develop a new algorithm for the case when we add to absorb nodes with adjoint hypermultiplets from a quiver. This will be done based on the quiver subtraction rule conjectured in Appendix C of [16]. For a review of this rule, and all other necessary information on quiver subtraction for the present work, see Section

[12] In most cases that we will see in this chapter, the Hasse diagram we find will only be a conjecture. This is because, as mentioned in Section 2.7.2, since we are unaware of a brane system, we have no way to physically motivate this process of quiver subtraction or addition.

Quiver with Adjoint Matter	Coulomb Branch Variety	Global Symmetry	PL(HWG)
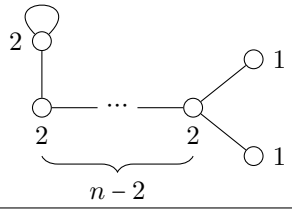	$d_{n+1}/\mathbb{Z}_2$ = n.min B_n	$SO(2n+1)$	$\mu_2^2 t^2 + \mu_1^2 t^4, \quad n = 2$ $\mu_2 t^2 + \mu_1^2 t^4, \quad n \geq 3$
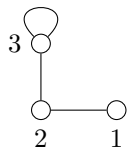	d_4/S_3 = sub-regular G_2	G_2	$\mu_1 t^2 + \mu_2^2 t^4 + \mu_2^3 t^6 + \mu_1^2 t^8 + \mu_1 \mu_2^3 t^{10} - \mu_1^2 \mu_2^6 t^{20}$
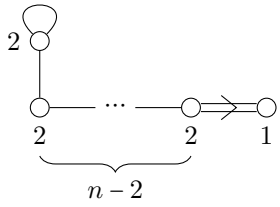	$b_n/\mathbb{Z}_2$ = n.min D_n	$SO(2n)$	$(\mu_1^2 + \mu_2^2) t^2, \quad n = 2$ $\mu_2 \mu_3 t^2 + \mu_1^2 t^4, \quad n = 3$ $\mu_2 t^2 + \mu_1^2 t^4, \quad n \geq 4$
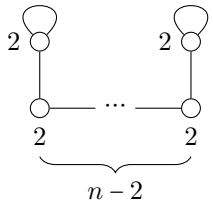	$d_{n+1}/(\mathbb{Z}_2 \times \mathbb{Z}_2)$	$SO(2n)$	$(\mu_1^2 + \mu_2^2) t^2 + (1 + \mu_1^2 \mu_2^2) t^4 + \mu_1^2 \mu_2^2 t^6 - \mu_1^4 \mu_2^4 t^{12}, \quad n = 2$ $\mu_2 \mu_3 t^2 + (1 + 2\mu_1^2) t^4 + \mu_1^2 t^6 - \mu_1^4 t^{12}, \quad n = 3$ $\mu_2 t^2 + (1 + 2\mu_1^2) t^4 + \mu_1^2 t^6 - \mu_1^4 t^{12}, \quad n \geq 4$
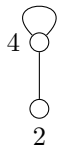	d_4/S_4	$SU(3)$	$\mu_1 \mu_2 t^2 + (1 + \mu_1^2 + \mu_1 \mu_2 + \mu_2^2) t^4 +$ $(1 + \mu_1^3 + \mu_2^2 + \mu_1 \mu_2^2 + \mu_2^3 + \mu_1^2 + \mu_1^2 \mu_2) t^6 + \mathcal{O}(t^8)$
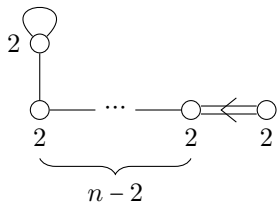	$a_{2n-1}/\mathbb{Z}_2$	$SU(2n-1)$ × $U(1)$	$(1 + \mu_1 \mu_{2n-2}) t^2 + (q^{4n} \mu_1^2 + q^{-4n} \mu_{2n-2}^2) t^4 - \mu_1^2 \mu_{2n-2}^2 t^8$

Table 3.2.1: The full list of balanced unframed unitary $3d$ $\mathcal{N} = 4$ quivers with $L \in \mathbb{N} \setminus \{0\}$ nodes that each have a single adjoint hypermultiplet but which otherwise contain only regular matter. Upon performing quiver addition to remove the adjoint hypermultiplet(s), the resulting quiver will elicit an enhanced global symmetry. For all quivers that depend on the parameter n the quiver is valid for $n \geq 2$. N.min is shorthand for the (closure of the) next to minimal nilpotent orbit of the corresponding algebra. The μ_i, q in the PL(HWG) column are the Dynkin label fugacities of the corresponding Lie group and abelian factors of the global symmetry group respectively.

2.7.2. To illustrate how the process of quiver addition was developed by reverse engineering quiver subtraction, we use the example of the quiver Q of (3.1.4) which was used to highlight the inadequacy of the BGS algorithm in Section 3.1. Performing double e_6 quiver subtraction[13] on Q gives

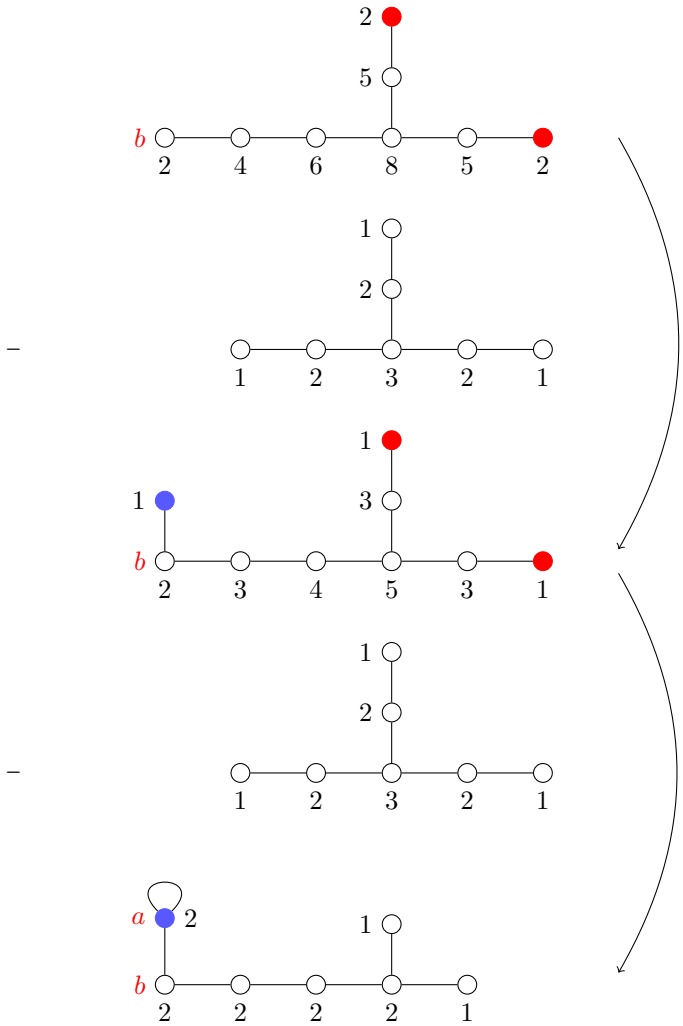

(3.2.4)

Blue nodes indicate those that were introduced in the rebalancing stage of quiver subtraction, red nodes indicate unbalanced nodes, b is the node being rebalanced as a result of the subtractions (the reason for this labelling is to make contact with the notation we introduce shortly in (3.2.6)), and as before a is the name of the node with the adjoint hypermultiplet (that has arisen through multiple same slice subtractions). From Table 3.2.1, we see that this quiver has the next to minimal nilpotent orbit of B_6 as a leaf in its Hasse diagram. The Hasse diagram of this orbit is

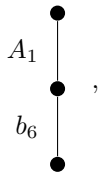

(3.2.5)

[13] Generally, when we say a g_k quiver subtraction, we mean the act of subtracting the Coulomb quiver for the g_k variety (the minimal nilpotent orbit of G_k). In this particular example, we are taking $G_k = E_6$.

which can be derived using quiver subtraction on the Coulomb quiver for n.min B_6, found in [38]. As explained in Section 3.1, the BGS of Q is $SO(12) \times U(1)$, but the Hilbert series shows the true global symmetry, the EGS, to be $SO(13) \times U(1)$. The quiver subtraction above illustrates why this enhancement occurs: the Hasse diagram of Q contains b_6 among its bottom-most elementary slices, and so this must be a subset of the global symmetry. The lowest slice is b_6 and not d_6 (which is what was expected from the BGS) because of the appearance of the adjoint hypermultiplet in quiver subtraction as opposed to an additional rebalancing $U(1)$ node.

Note that although in this case these e_6 subtractions are the only possible ones that could be performed, in other quivers that we find in this work multiple subtractions will be possible, leading to bifurcations in the Hasse diagram. However, it is only subtracting the same slice twice in a row from the same set of nodes in the quiver that leads to the arisal of a node with an adjoint hypermultiplet and thus an EGS, and so it is only the "same slice twice" subtractions and additions we focus on, as the other factors can be read accurately from the BGS algorithm.

From this example, we can see that the quiver subtraction algorithm which brings about these adjoint hypermultiplets can be reverse engineered to find quivers with only regular matter which have an EGS. In order to explain how this works, we will refer to the node with the adjoint hypermultiplet as a of rank r_a, the node adjacent to it b of rank r_b, and any generic node adjacent to *this* c of rank r_c:

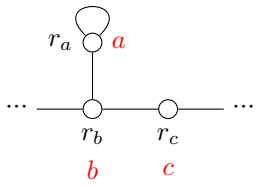

. (3.2.6)

These will be the names of the nodes *after* quiver additions also: note in particular that this means that after the penultimate quiver addition, a will not have an adjoint hypermultiplet attached, and after the final addition a will no longer exist, as explained below.

In the "forward" process of quiver subtraction, an example of which was shown in (3.2.4), the adjoint hypermultiplet arose as a result of rebalancing node b after multiple subsequent same slice subtractions. Thus to "absorb" the adjoint hypermultiplet in the reverse process, we will have to add the same elementary slice mutliple subsequent times to node c such that node b becomes overbalanced, and thus the rebalancing process will involve removing a rank from a. With all this in mind, we are ready to construct the algorithm for quiver addition.

Quiver addition algorithm

Let Q_a be a quiver with a single node a that has a single adjoint hypermultiplet, such that a is connected to the remainder of the quiver via a single simply laced edge to node b, and with all other nodes being linked by regular matter[2] only. Let Q_σ be a Coulomb quiver for a generic elementary slice σ.[14] Then adding some Q_σ to Q_a *that is going to be added multiple subsequent times* can be performed as follows:

1. First ensure that Q_σ is balanced and contains as a subset the run of nodes connecting to and including c but excluding a and b (i.e. c and the "$\cdots$" next to it in (3.2.6)) in Q_a.

[14] Recall that the full list of these to date can be found by comprising Table 1 of [81] and Table 2 of this note.

2. Line up Q_σ with Q_a so that one of the long rank 1 nodes of Q_σ is superimposed upon c, and the subset of the rest of the nodes of Q_σ which is of the same form as the nodes connecting to and including c of Q_a (as described in Step 1) is aligned with these nodes.

3. Add the ranks of the nodes in Q_σ to those in Q_a that they line up with.

4. Reduce the rank of a by one. Note that if this reduces the rank of a to one, the adjoint hypermultiplet can be eliminated as the adjoint representation of $U(1)$ is trivial, and if it reduces the rank of a to zero, a itself can just be eliminated as it is now an "empty node".

There are a few things to note here with regards to this algorithm:

- Firstly, the condition on Q_σ of balance and needing a long rank one node restricts the possible slices we can add to be just the affine quivers displayed in Table 3.1.1.

- Secondly, c can be an existing node, as pictured in (3.2.6), or it could be an "empty node". By taking c as an empty node, we mean that the quiver being added is superimposed on top of currently non-existent nodes, but such that it is linked to node b. If we take c to be an existing node, we call such an addition *adding to existing nodes*. If we take c to be an empty node, we call such an addition *adding to empty nodes*. We call all possible options for the node c the *c-nodes* of the quiver.

- Thirdly, during such a process of quiver addition, extra unbalanced nodes that were not in the original quiver may appear, but this is not a problem as long as throughout both additions no nodes undergo a *change* in balance.

- Fourthly, this algorithm is modified for the $d_3/\mathbb{Z}_2$, $b_2/\mathbb{Z}_2$ and $d_{n+1}/(\mathbb{Z}_2 \times \mathbb{Z}_2)$ quivers in Table 3.2.1. In the $d_3/\mathbb{Z}_2$ case this is because we have two possible "b-nodes" which each need a c-node, and so, among other modifications, any added slice must have *two* rank one long nodes. In the $b_n/\mathbb{Z}_2$ case it is because a is attached to b via a non-simply laced edge of multiplicity two. In the $d_{n+1}/(\mathbb{Z}_2 \times \mathbb{Z}_2)$ case it is due to the fact that there are two nodes with adjoint hypermultiplets, and so we need to be careful where we can add. These modifications will be explained within the relevant sections of the paper: Section 3.3.1, Section 3.5.1 and Section 3.5.2 respectively.

- Finally, this is only the quiver addition process for the specific purpose outlined in this paper, and not a general algorithm. When not adding the same slice twice to the same node, there are often many possible ways to add a slice to a quiver. In Section 3.3.2 "single additions" will be performed (just adding one slice once), so an example of the general algorithm for this type of addition will be illustrated here.

For complete clarity regarding the execution of this algorithm, we provide here an example of an *incorrect* addition (i.e. adding a slice σ to a quiver Q_1 to give a quiver Q_2 from which performing the reverse processs of subtraction does not give back Q_1: $Q_2 - \sigma \neq Q_1$), followed by the correct way to execute it.

Example Consider trying to add d_4 to the *existing node* in n.min B_5.[15] The Coulomb quiver for n.min B_5 is

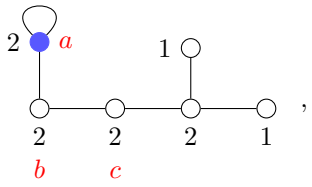

(3.2.7)

where c has been labelled as such as it is the only possible existing node we could add to.[16] This addition fits in with Step 1 in the algorithm, as d_4 contains as a subset the nodes to the right of and including c in (3.2.7). So adding this slice *could* be valid, but we will perform the addition in a way that violates step 2:

[15] To clarify the terminology one last time, here what we are actually saying is "consider trying to add the quiver whose Coulomb branch is the closure of the minimal nilpotent orbit of D_4, which we call d_4, to the existing node of the quiver whose Coulomb branch is the closure of the next to minimal nilpotent orbit of B_5, which we call n.min B_5.

[16] Note that we could have taken c to be the empty nodes: the space to the left of b in (3.2.7), but for this case we wouldn't have been able to demonstrate this type of incorrect addition.

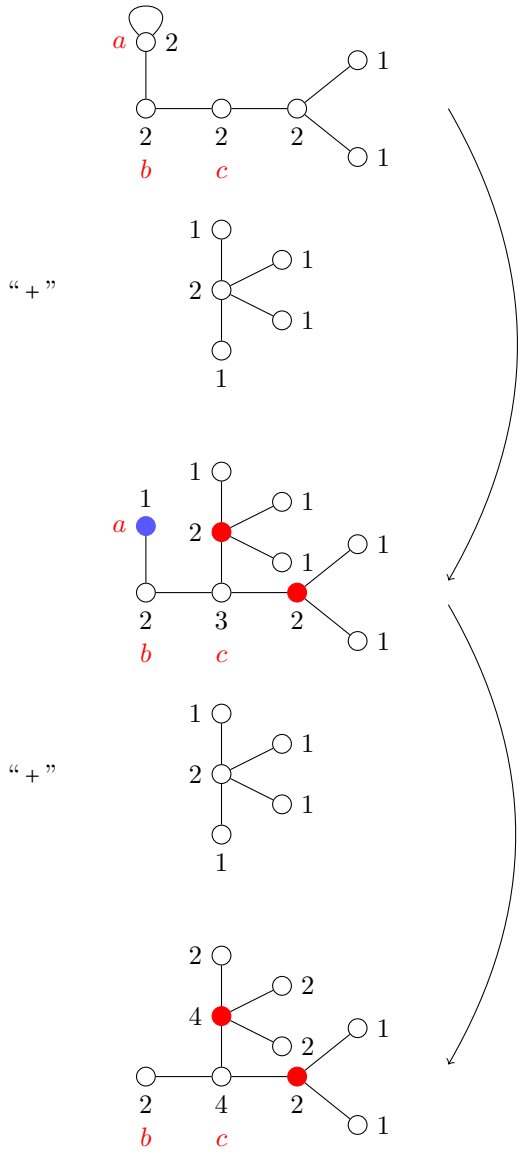

(3.2.8)

Here the d_4 slice that was added was not superimposed correctly on top of the nodes next to and including c in n.min B_5 that it "matched to" (i.e. that formed a subset of the d_4's nodes). We can immediately see why this is an incorrect addition, because the final rank two node in n.min B_5 has changed balance during this process, and we know quiver subtraction always preserves the balance of nodes. Thus if we subtract d_4 from our result here, we see that both a and this node undergo a change in balance, and so the rank one node added to rebalance must be attached to both. When the subtraction is performed again, this node will then become a rank two node with an adjoint hypermultiplet, and we will not have the quiver n.min B_5, but instead

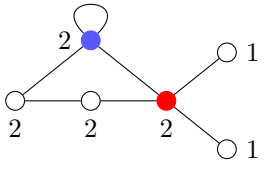

(3.2.9)

and so the subtraction is invalid. The *correct* way to add d_4 on to n.min B_5 would be as follows:

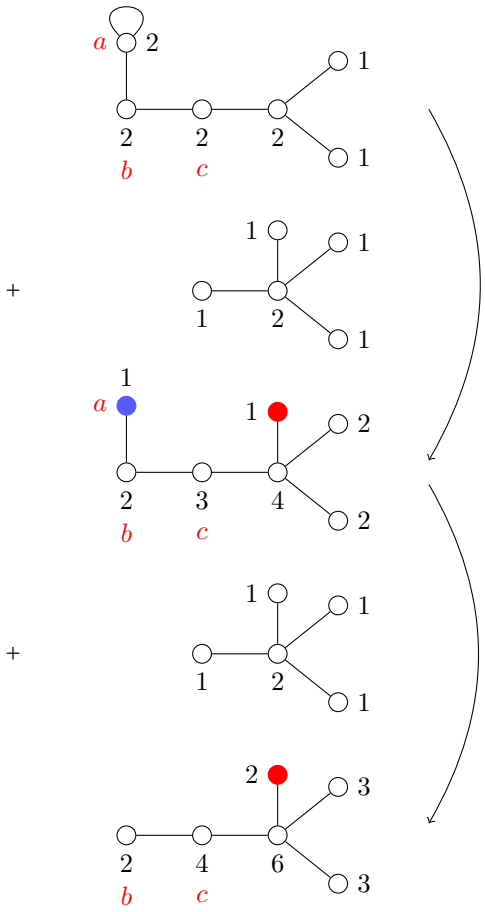

(3.2.10)

One can check that subtracting d_4 twice from the final quiver in (3.2.10) will indeed give n.min B_5 (3.2.7) as desired. The final quiver in (3.2.10), following the algorithm in Section 3.1, has BGS $SO(10)$. However, we have seen that the Hasse diagram contains $SO(11)$, and thus this must be a subgroup of the global symmetry. Indeed, upon Hilbert series computation, $SO(11)$ is the confirmed EGS. □

This concludes the methodology needed for the results of this chapter. Throughout the paper the results of quiver additions will be labelled with two parameters, n and k, pertaining to the Coulomb branch variety of the base quiver from Table 3.2.1 we add to (or equivalently the rank of the global symmetry factor experiencing enhancement) and the rank of the Coulomb branch variety of the slice which we are adding twice, respectively. In some cases, the only valid way to add a slice restricts the allowed values of n and/or k. Where relevant, these constraints will be indicated. We now proceed to performing the quiver addition method discussed in this section one by one on the quivers from Table 3.2.1,[17] to derive quivers with an EGS, before we use these results to propose a modification to the BGS algorithm.

[17] Excluding the $a_{2n-1}/\mathbb{Z}_2$ case, as discussed in the bullet points following Table 3.2.1.

3.3 Enhancement to $SO(2n+1)$

In this section, we focus on deriving quivers with EGS from the first quiver in Table 3.2.1, the next to minimal nilpotent orbit of B_n:

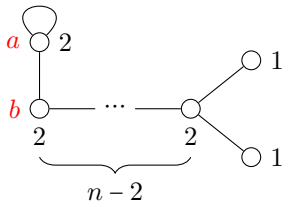

(3.3.1)

Using the Q_a BGS algorithm given in Section 3.2.1, one can see that the BGS of (3.3.1) is $SO(2n+1)$. Indeed, the Hasse diagram of (3.3.1) is

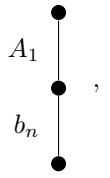

(3.3.2)

which agrees with this, and this global symmetry is confirmed upon Hilbert series computation. The quivers derived from using quiver addition on (3.3.1) to absorb a will therefore experience a symmetry enhancement of this type. After considering all possible additions following the addition algorithm listed in Section 3.2.2, two types of enhancement are found: $SO(2n) \to SO(2n+1)$ and $SU(n)\times U(1) \to SO(2n+1)$. In all cases listed, except those where an e_8 is added twice, the EGS has been verified via Hilbert series computation. In the cases where adding a slice gives a family of quivers depending on one or two parameters, this EGS has been verified via Hilbert series computation for several low values of the parameters. The results for all quivers not depending on parameters have been confirmed too, except the e_8 cases which have proved too computationally complex to verify, so the EGS in these cases remain as conjectures. Brane systems for a selection of the e_8 cases listed both in this section and in subsequent sections are known and the construction is discussed in [73]. The result of the e_8 enhancement shown in Table 3.3.1 has been previously found in [85] through an F-theory construction, and in [86] using $5d$ brane webs. Several of the quivers appearing in this work also appear in the construction of so-called minimally unbalanced quivers in [14].

3.3.1 Enhancement from $SO(2n)$ to $SO(2n+1)$

In this section, we see quivers whose BGS has as one of its factors a D_n type symmetry which undergoes enhancements to B_n. That is,

$$\prod_i G_i \times SO(2n) \to \prod_i G_i \times SO(2n+1) \tag{3.3.3}$$

for some simple Lie groups G_i. Here we use blue to highlight the symmetry factor which experiences enhancement, and this will continue to be used throughout the paper. There are two possible ways we can construct these quivers by using quiver addition to absorb a of (3.3.1): by adding to its existing nodes or its empty nodes (as discussed in the bullet points following the quiver addition algorithm of Section 3.2.2). We explore each of these in turn now.

3.3.1.1 Adding to existing nodes of n.min B_n

Let's first investigate adding on to the existing nodes in (3.3.1). The case of $n = 3$ will be treated separately. For the case of $n = 2$, there are two b-nodes and no possible existing option for the node c (taking b and c nodes as defined in the quiver addition algorithm of Section 3.2.2), so we cannot add on to existing nodes here. Note however that we can add on to empty nodes, and this will be discussed in Section 3.3.1.2.

For adding to the existing nodes of (3.3.1) for $n \geq 4$, our c-node will be given by

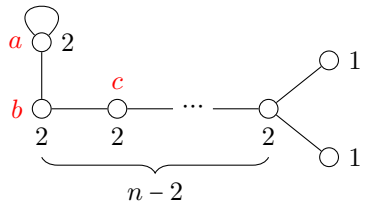

(3.3.4)

The only slices that can be validly added to (3.3.4) according to the quiver addition algorithm in Section 3.2.2 are a_k, d_k, e_6, e_7 and e_8. The method of addition for all slices can be easily extended from the d_4 example shown in (3.2.10). Adding each of these slices (a_k, d_k, e_6, e_7 and e_8) will fix n in (3.3.1) to be a particular value, in order for the addition to obey Step 2 of our quiver addition algorithm. The results of these additions are listed in Table 3.3.1. The second column gives the quiver arrived at after twice adding the affine quiver corresponding to the slice listed in the first column of (3.3.1) to the quiver (3.3.1) for the values of n listed. The third column shows the enhancement of the BGS to the EGS, with the factor(s) that experience enhancement shown in blue. This will also be the format of all future tables documenting results in this chapter.

For the case of $n = 3$, there are two possible c-nodes

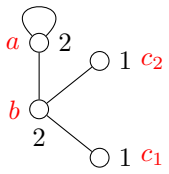

(3.3.5)

which we call c_1 and c_2. However due to the $\mathbb{Z}_2$ outer automorphism of (3.3.5), adding to either c-node gives the same result, and so only one need be considered. Here there are more allowed quivers that we can add to the c-node of (3.3.5) than there were for (3.3.4), because (3.3.5) has no nodes connected to the c-node that we have to ensure the added slice contains as a subset. As a result, we may add any affine quiver to the existing nodes of n.min B_3. The resulting quivers are listed in Tables 3.3.2 and 3.3.3.

Added Slice	Quiver	Global Symmetry
a_3 $n = 4$	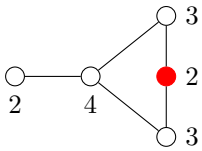	$SO(8)$ $\downarrow$ $SO(9)$
a_k $k \geq 4,\ n = 4$	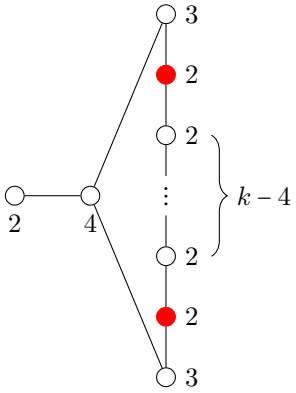	$SO(8) \times U(k-3)$ $\downarrow$ $SO(9) \times U(k-3)$
d_k $k \geq 4,\ n = k+1$	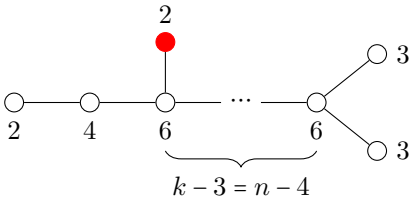	$SO(2n)$ $\downarrow$ $SO(2n+1)$
e_6 $n = 6$	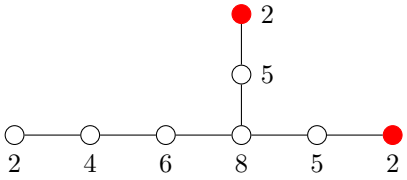	$SO(12) \times U(1)$ $\downarrow$ $SO(13) \times U(1)$
e_7 $n = 7$	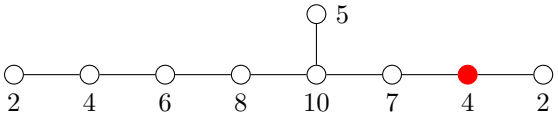	$SO(14) \times SU(2)$ $\downarrow$ $SO(15) \times SU(2)$
e_8 $n = 9$	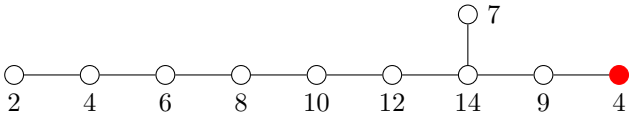	$SO(18)$ $\downarrow$ $SO(19)$

Table 3.3.1: Quivers resulting from adding all possible elementary slices to the existing nodes of n.min B_n (3.3.1) to absorb a, $n \geq 4$.

Added Slice	Quiver	Global Symmetry
a_1	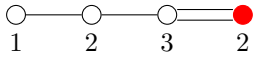	$SU(4)$ ↓ $SO(7)$
a_k $k \geq 2$	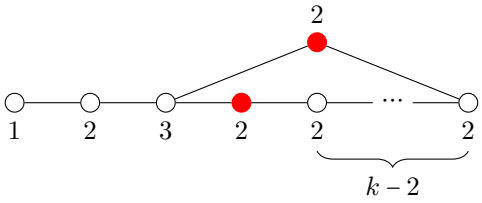	$SU(4) \times U(k-1)$ ↓ $SO(7) \times U(k-1)$
d_k $k \geq 4$	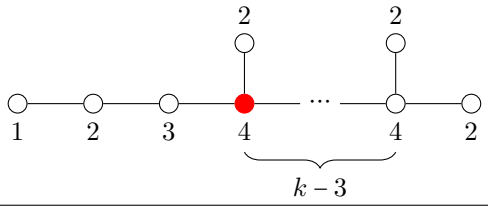	$SU(4) \times SU(2) \times SO(2k-4)$ ↓ $SO(7) \times SU(2) \times SO(2k-4)$
e_6	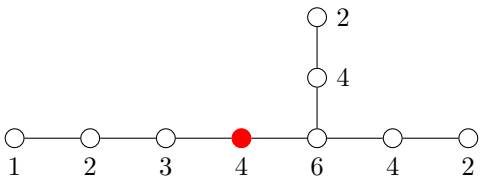	$SU(4) \times SU(6)$ ↓ $SO(7) \times SU(6)$
e_7	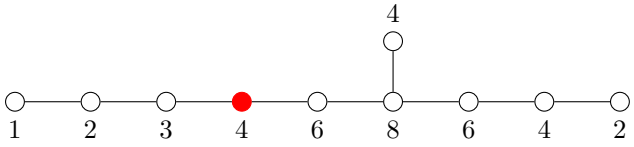	$SU(4) \times SO(12)$ ↓ $SO(7) \times SO(12)$
e_8	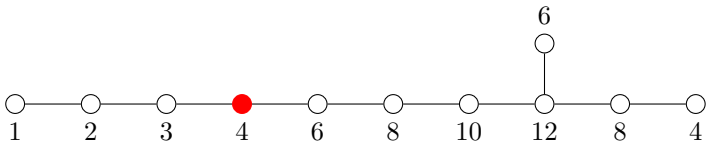	$SU(4) \times E_7$ ↓ $SO(7) \times E_7$

Table 3.3.2: Quivers resulting from adding the possible simply laced elementary slices to n.min B_3 (3.3.5) to absorb a.

Added Slice	Quiver	Global Symmetry
b_k $k \geq 3$	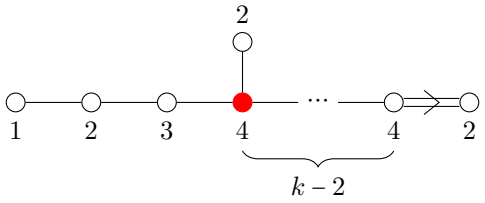	$SU(4) \times SU(2) \times SO(2k-3)$ ↓ $SO(7) \times SU(2) \times SO(2k-3)$
c_k $k \geq 2$	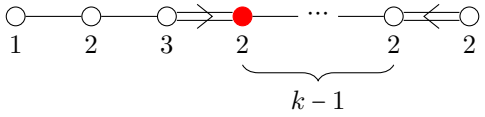	$SU(4) \times Sp(k-1)$ ↓ $SO(7) \times Sp(k-1)$
f_4	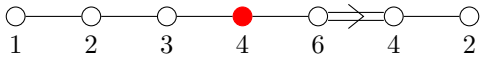	$SU(4) \times Sp(3)$ ↓ $SO(7) \times Sp(3)$
g_2	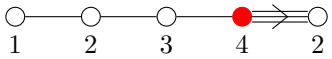	$SU(4) \times SU(2)$ ↓ $SO(7) \times SU(2)$

Table 3.3.3: Quivers resulting from adding the possible non-simply laced elementary slices to n.min B_3 (3.3.5) to absorb a.

3.3.1.2 Adding to empty nodes of n.min B_n

We now turn our attention to adding on to the empty nodes (as defined in the quiver addition algorithm of Section 3.2.2) of (3.3.1). That is, we take the c-node to be empty:

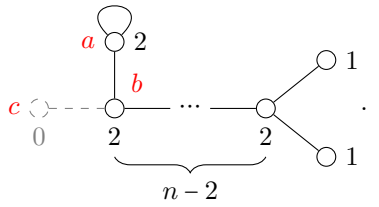

(3.3.6)

The dashed grey line indicates that c is not really there, reinforced by its vanishing rank. Note that in the $n = 2$ case there are two possible b-nodes, which we call b_1 and b_2, and their corresponding empty c-nodes will be called c_1 and c_2:

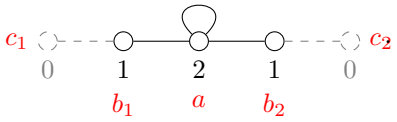

(3.3.7)

In order for the adjoint hypermultiplet to appear on the node a, which is connected to both b_1 and b_2, during quiver subtraction, c-nodes c_1 and c_2 must coincide so that an added slice is being "attached" on to both b_1 and b_2. As a result, because the quiver addition algorithm of Section 3.2.2 requires any slice which is added to have two long rank one nodes, the allowed slices which can be validly added to 3.3.7 to absorb a are restricted to a_k, b_k, c_k, d_k, e_6 and e_7. The results of these additions are given in Table 3.3.4.

In the case of $n \geq 3$ there is only one b-node, so the above problem does not arise. Here c is still an empty node, and so the requirement in Step 1 of the quiver addition algorithm in Section 3.2.2 that the added slice must contain the nodes in (3.3.6) connected to and including c becomes trivial, and so we may add any affine slice. The results of adding these slices are given in Tables 3.3.5 and 3.3.6.

Added Slice	Quiver	Global Symmetry
a_k $k \geq 1$	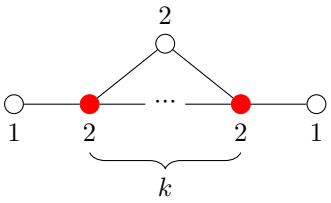	$SU(2)^2 \times SU(2) \times U(k-1)$ ↓ $SO(5) \times SU(2) \times U(k-1)$
b_k $k \geq 3$	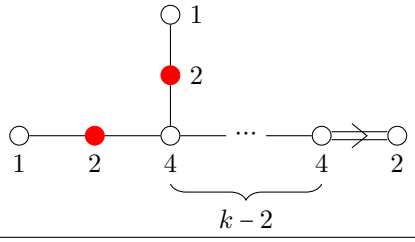	$SU(2)^2 \times SO(2k-1) \times U(1)$ ↓ $SO(5) \times SO(2k-1) \times U(1)$
c_k $k \geq 2$	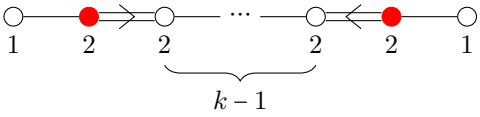	$SU(2)^2 \times U(k)$ ↓ $SO(5) \times U(k)$
d_k $k \geq 4$	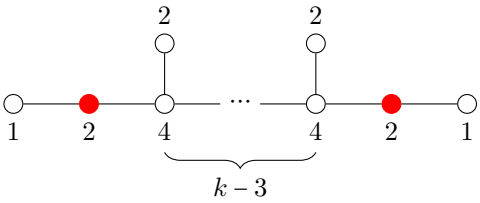	$SU(2)^2 \times U(k)$ ↓ $SO(5) \times U(k)$
e_6	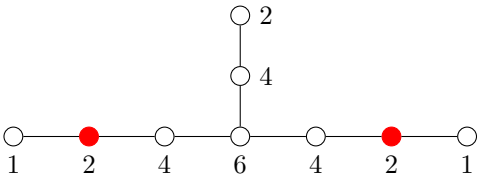	$SU(2)^2 \times SO(10) \times U(1)$ ↓ $SO(5) \times SO(10) \times U(1)$
e_7	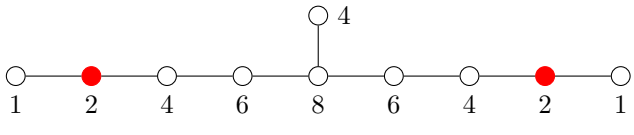	$SU(2)^2 \times E_6 \times U(1)$ ↓ $SO(5) \times E_6 \times U(1)$

Table 3.3.4: Quivers resulting from adding all possible elementary slices to n.min B_2 (3.3.7) to absorb a.

Added Slice	Quiver	Global Symmetry
a_k $k \geq 1, n \geq 3$	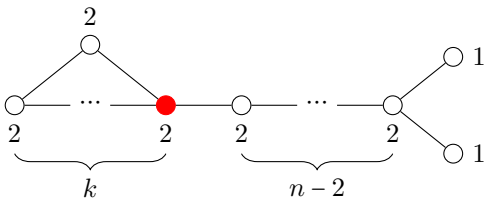	$SU(k+1) \times SO(2n)$ ↓ $SU(k+1) \times SO(2n+1)$
d_k $k \geq 4, n = k+1$	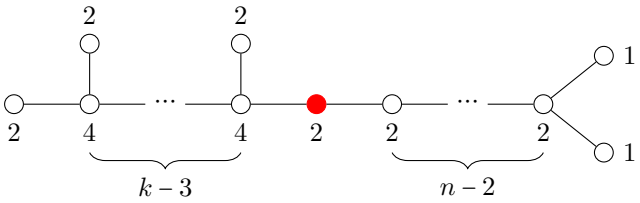	$SO(2k) \times SO(2n)$ ↓ $SO(2k) \times SO(2n+1)$
e_6 $n \geq 3$	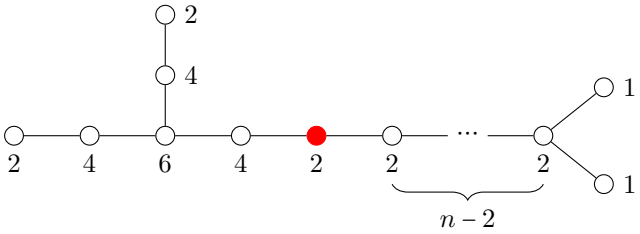	$E_6 \times SO(2n)$ ↓ $E_6 \times SO(2n+1)$
e_7 $n \geq 3$	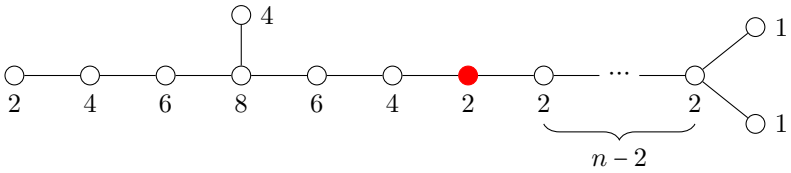	$E_7 \times SO(2n)$ ↓ $E_7 \times SO(2n+1)$
e_8 $n \geq 3$	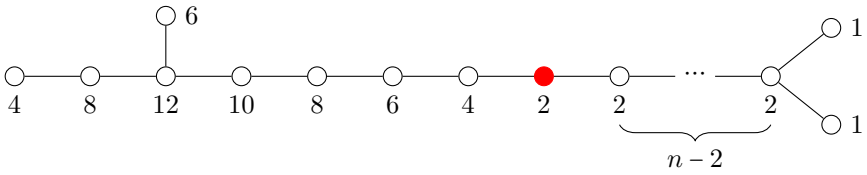	$E_8 \times SO(2n)$ ↓ $E_8 \times SO(2n+1)$

Table 3.3.5: Quivers resulting from adding all possible simply laced elementary slices to the empty nodes of n.min B_n (3.3.1) to absorb a, $n \geq 3$.

Added Slice	Quiver	Global Symmetry
b_k $k \geq 3, n \geq 3$	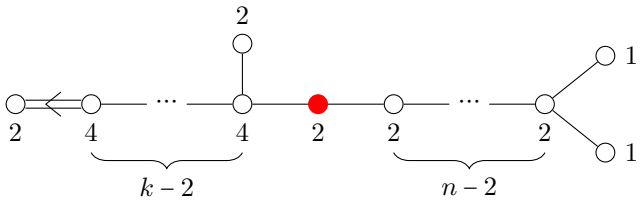	$SO(2k+1) \times SO(2n)$ $\downarrow$ $SO(2k+1) \times SO(2n+1)$
c_k $k \geq 2, n \geq 3$	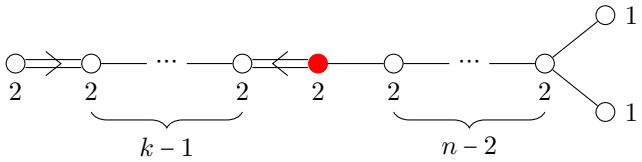	$Sp(k) \times SO(2n)$ $\downarrow$ $Sp(k) \times SO(2n+1)$
f_4 $n \geq 3$	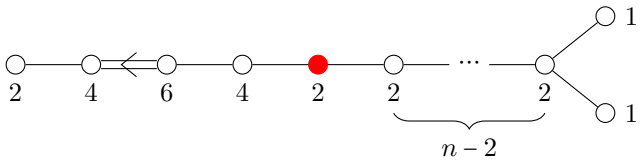	$F_4 \times SO(2n)$ $\downarrow$ $F_4 \times SO(2n+1)$
g_2 $n \geq 3$	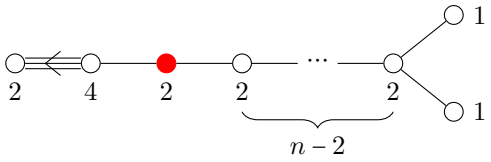	$G_2 \times SO(2n)$ $\downarrow$ $G_2 \times SO(2n+1)$

Table 3.3.6: Quivers resulting from adding all possible non-simply laced elementary slices to the empty nodes of n.min B_n (3.3.1) to absorb a, $n \geq 3$.

3.3.2 Enhancement from $SU(n)\times U(1)$ to $SO(2n+1)$

The results of Section 3.3.1 exhaust all possibilities of adding to (3.3.1) to immediately absorb a. However we could also have first performed a "different sort" of quiver addition to absorb one of the two rank one nodes of (3.3.1), and *then* have added to the resulting quiver from this to absorb a. This "different" type of quiver addition does not quite follow the algorithm of Section 3.2.2: it is actually a little simpler. Here, instead of "undoing" multiple same slice quiver subtractions that result in an adjoint hypermultiplet of increasing rank, we instead "undo" just a single quiver subtraction. We will not list this slightly different algorithm here, but for those interested it is derivable from reverse engineering the basic quiver subtraction process that is given in following Steps 1 and 2)a) of Section 2.7.2 with E_s being empty. An example of the result of such an addition will also be given below. A key feature of this quiver addition worth mentioning is that, as before, in order for it to work we must be adding a balanced elementary slice via a long rank one node, restricting us to adding only the affine slices (whose Coulomb quivers live in Table 3.1.1). Such an addition is of interest because, if the quiver addition algorithm of Section 3.2.2 is then used to absorb their remaining adjoint hypermultiplet, we find quivers which experience a different type of BGS enhancement:

$$\prod_i G_i \times SU(n)\times U(1) \to \prod_i G_i \times SO(2n+1) \tag{3.3.8}$$

for some simple Lie groups G_i.

Let's see an example of how this works. We choose to take the case of adding an $A_1 = a_1$ slice to absorb one of the rank one nodes of (3.3.1). The resulting quiver will be

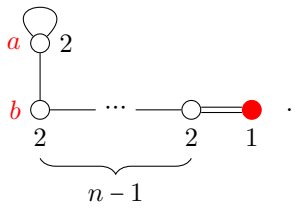

(3.3.9)

One can verify this is a valid addition by subtracting A_1 (see Section 2.7.2 for the quiver subtraction algorithm) from the two rightmost nodes of (3.3.9) to find (3.3.1).

Working from (3.3.9) we can then perform the adjoint-hypermultiplet-absorbing quiver addition of Section 3.2.2, as we did before on (3.3.1) in Section 3.3.1, to absorb a. At first glance, it seems as though we can add to either existing or empty nodes to absorb a, but actually doing the former doesn't yield the enhancement above. The reason for this is that the additions possible on the existing nodes are restricted to the $n = 3$ case, to which we may only add an A_1 to unbalance the node b in the necessary way to absorb a:

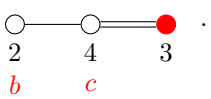

(3.3.10)

But if we perform quiver subtraction on this quiver to find the Hasse diagram, we will find ourselves performing three A_1 subtractions before arriving at the Coulomb quiver for the sub-regular nilpotent orbit of G_2, the second quiver in Table 3.2.1. As a result, here we actually expect a factor of the BGS to be enhanced to G_2, rather than $SO(2n+1)$. This is indeed confirmed upon computation of the Hilbert series, and actually this quiver appears later in our classification, in Table 3.4.1 of Section

3.4. This result is actually more general: if Q_{g_k} is obtained by adding some affine slice g_k to (3.3.1) to absorb one of the rank one nodes, as shown above for $g_k = A_1$, then any quiver derived from this by using quiver addition on its existing nodes to absorb a will exhibit an EGS of type G_2 as opposed to $SO(2n+1)$. This is because the only way to add to the existing nodes of Q_{g_k} to absorb a is by adding g_k when $n = 3$, so upon subtraction, we will be subtracting g_k *three* times, rather than two, and so an adjoint hypermultiplet of rank three will arise from rebalancing. This explains why we are left with the sub-regular nilpotent orbit of G_2, and why we have enhancement to G_2 symmetry from an apparent $SU(3)$.

Although adding to existing nodes gives us nothing new, adding to the empty nodes on the left hand side of b in (3.3.9) does yield quivers who experience the enhancement (3.3.8). Again the slices that can be validly added are affine slices via a rank one long node. The resulting quivers for this process are listed in Tables 3.3.7 and 3.3.8.

Recall that this was just one example of performing a single addition on (3.3.1) (that of adding an A_1) to find quivers with a new type of symmetry enhancement. This enhancement is actually exhibited by infinitely many quivers: those obtained by performing further additions on the quiver (3.3.9), or those constructed by adding a single slice other than A_1 to (3.3.1), and then adding to this and so on. We restrict the list of examples provided to just the A_1 case, as we (obviously!) cannot list them all, and these illustrate the enhancement. In conclusion, these infinitely many quivers, combined with those in Tables 3.3.1, 3.3.2, 3.3.3, 3.3.4, 3.3.5, 3.3.6, 3.3.7 and 3.3.8 concludes the families of quivers derived from quiver addition on the next to minimal nilpotent orbit of B_n (3.3.1) whose global symmetry contains a factor which is enhanced to $SO(2n+1)$ from that predicted by the BGS.

Added Slice	Quiver	Global Symmetry
a_k $k \geq 1$	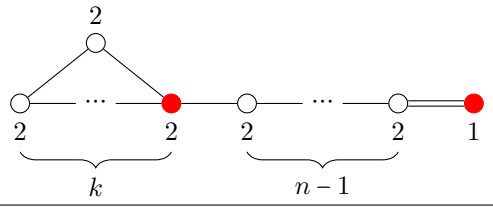	$SU(k+1) \times SU(n) \times U(1)$ $\downarrow$ $SU(k+1) \times SO(2n+1)$
d_k $k \geq 4$	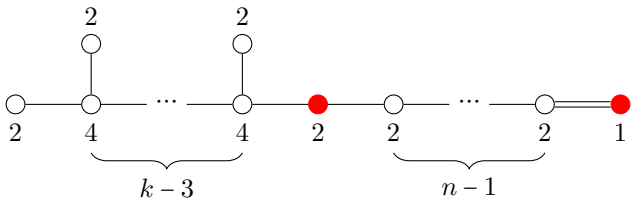	$SO(2k) \times SU(n) \times U(1)$ $\downarrow$ $SO(2k) \times SO(2n+1)$
e_6	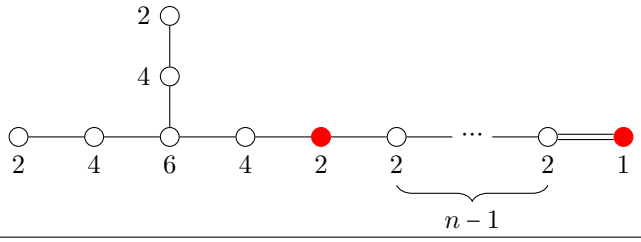	$E_6 \times SU(n) \times U(1)$ $\downarrow$ $E_6 \times SO(2n+1)$
e_7	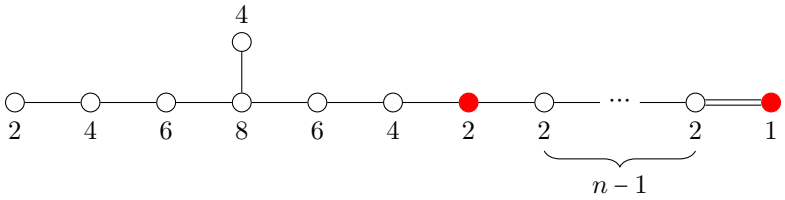	$E_7 \times SU(n) \times U(1)$ $\downarrow$ $E_7 \times SO(2n+1)$
e_8	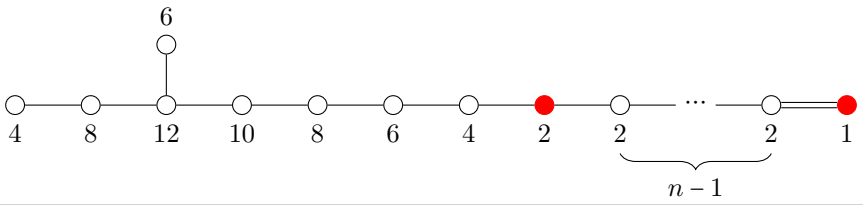	$E_8 \times SU(n) \times U(1)$ $\downarrow$ $E_8 \times SO(2n+1)$

Table 3.3.7: Quivers resulting from adding all possible simply laced elementary slices to the empty nodes of (3.3.9) to absorb a.

Added Slice	Quiver	Global Symmetry
b_k $k \geq 3$	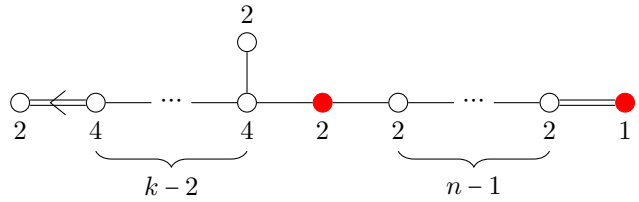	$SO(2k+1) \times SU(n) \times U(1)$ ↓ $SO(2k+1) \times SO(2n+1)$
c_k $k \geq 2$	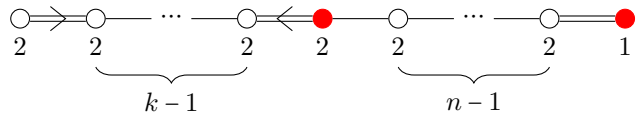	$Sp(k) \times SU(n) \times U(1)$ ↓ $Sp(k) \times SO(2n+1)$
f_4	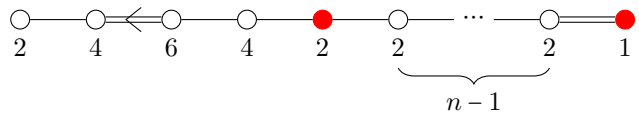	$F_4 \times SU(n) \times U(1)$ ↓ $F_4 \times SO(2n+1)$
g_2	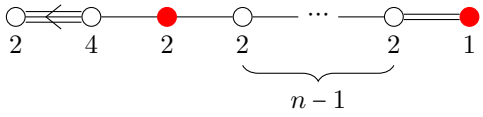	$G_2 \times SU(n) \times U(1)$ ↓ $G_2 \times SO(2n+1)$

Table 3.3.8: Quivers resulting from adding all possible non-simply laced elementary slice to the empty nodes of (3.3.9) to absorb a.

3.4 Enhancement to G_2

We move on to focus on the second quiver in Table 3.2.1, the sub-regular nilpotent orbit of G_2

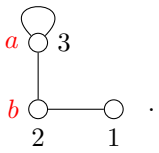

(3.4.1)

The Hasse diagram of this quiver can be inferred from the Hasse diagram of the G_2 nilpotent cone:

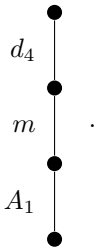

(3.4.2)

It involves a non-normal slice m, which we make no further comment on here. In all quivers listed in this section, which are a result of adding the same elementary slice three subsequent times to the same node of (3.4.1), the BGS enhances as

$$\prod_i G_i \times SU(3) \to \prod_i G_i \times G_2, \tag{3.4.3}$$

for some simple Lie groups G_i. The enhancements in global symmetry of the quivers in this section were also found via a different approach in [15]. Note that here, the conjecture that the lowermost leaves of the Hasse diagram forming a subgroup of the global symmetry does not force the enhancement (but of course do not contradict it).

As before, following the quiver addition algorithm from Section 3.2.2, the only possible slices we can add to the node c are the affine quivers via a rank one long node. Here, we can see that c could either be the existing rank one node to the right of b in (3.4.1)

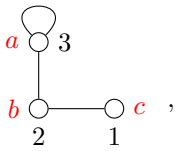

(3.4.4)

or the empty node to its left

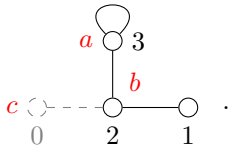

(3.4.5)

As before in Section 3.3, we call these ways to absorb a in (3.4.1) "adding to existing nodes" or "adding to empty nodes" respectively. In these cases, since the set of nodes connected to c is either $\{b\}$ or the empty set, the condition that the affine quivers we add must contain c and its connected nodes as a subset is trivial, and so all affine quivers are allowed. The results for these additions are

given in Tables 3.4.1 and 3.4.2 in the case where c is taken to be an existing node, as in (3.4.4), and Tables 3.4.3 and 3.4.4 in the case where c is taken to be an empty node, as in (3.4.5). As in Section 3.3, in the cases where the quivers listed depend on a parameter, the EGS has been verified via Hilbert series computation for small values of the parameter. In the cases with no parameter dependence, every case except for that of e_8 has been verified.

Added Slice	Quiver	Global Symmetry
a_k $k \geq 1$	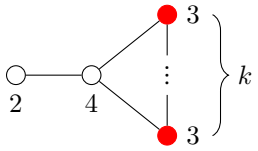	$SU(3) \times U(1)^l \times SU(k-1)$ $\downarrow$ $G_2 \times U(1)^l \times SU(k-1)$, $l = \begin{cases} 1, & k \geq 2 \\ 0, & k = 1 \end{cases}$
d_k $k \geq 4$	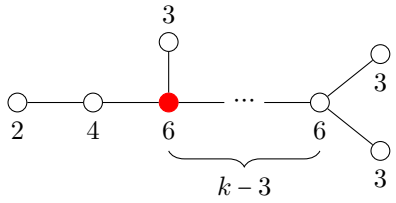	$SU(3) \times SU(2) \times SO(2k-4)$ $\downarrow$ $G_2 \times SU(2) \times SO(2k-4)$
e_6	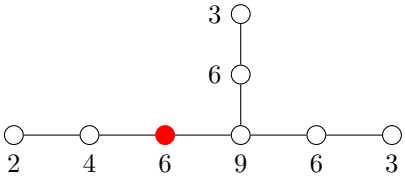	$SU(3) \times SU(6)$ $\downarrow$ $G_2 \times SU(6)$
e_7	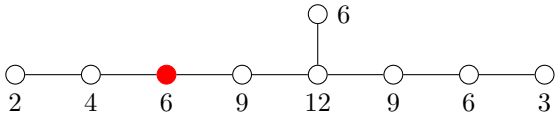	$SU(3) \times SO(12)$ $\downarrow$ $G_2 \times SO(12)$
e_8	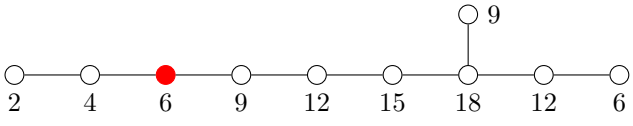	$SU(3) \times E_7$ $\downarrow$ $G_2 \times E_7$

Table 3.4.1: Quivers resulting from adding all possible simply laced elementary slices to the existing nodes of sub-regular G_2 (3.4.1) to absorb a.

Added Slice	Quiver	Global Symmetry
b_k $k \geq 3$	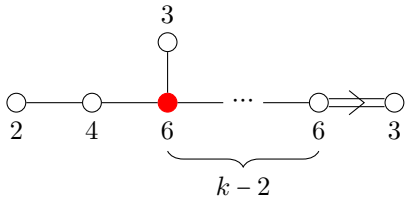	$SU(3) \times SU(2) \times SO(2k-3)$ ↓ $G_2 \times SU(2) \times SO(2k-3)$
c_k $k \geq 2$	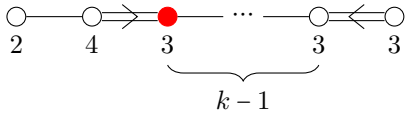	$SU(3) \times Sp(k-1)$ ↓ $G_2 \times Sp(k-1)$
f_4	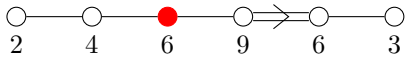	$SU(3) \times Sp(3)$ ↓ $G_2 \times Sp(3)$
g_2	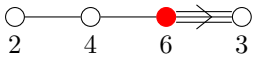	$SU(3) \times SU(2)$ ↓ $G_2 \times SU(2)$

Table 3.4.2: Quivers resulting from adding all possible non-simply laced elementary slices to the existing nodes of sub-regular G_2 (3.4.1) to absorb a.

Added Slice	Quiver	Global Symmetry
a_k $k \geq 1$	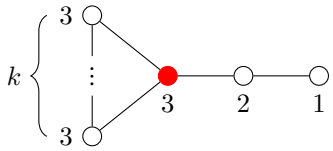	$SU(k+1) \times SU(3)$ $\downarrow$ $SU(k+1) \times G_2$
d_k $k \geq 4$	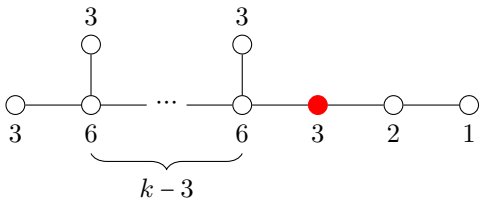	$SO(2k) \times SU(3)$ $\downarrow$ $SO(2k) \times G_2$
e_6	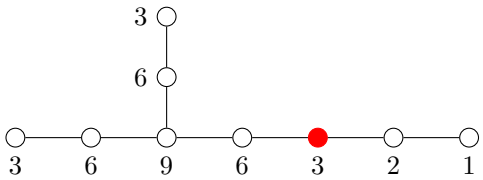	$E_6 \times SU(3)$ $\downarrow$ $E_6 \times G_2$
e_7	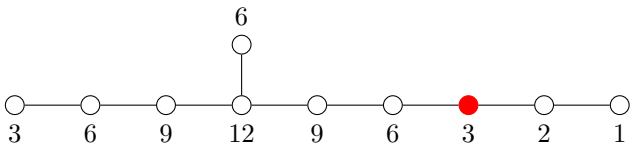	$E_7 \times SU(3)$ $\downarrow$ $E_7 \times G_2$
e_8	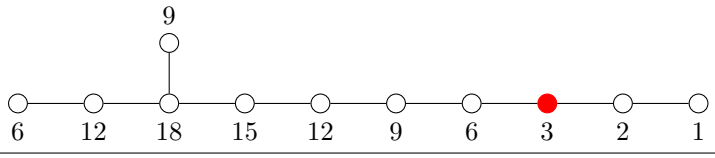	$E_8 \times SU(3)$ $\downarrow$ $E_8 \times G_2$

Table 3.4.3: Quivers resulting from adding all possible simply laced elementary slices to the empty nodes of sub-regular G_2 (3.4.1) to absorb a.

Added Slice	Quiver	Global Symmetry
b_k $k \geq 3$	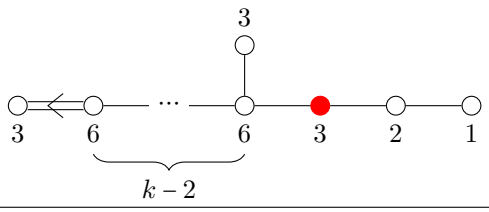	$SO(2k+1) \times SU(3)$ $\downarrow$ $SO(2k+1) \times G_2$
c_k $k \geq 2$	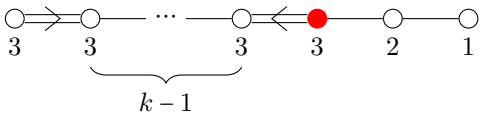	$Sp(k) \times SU(3)$ $\downarrow$ $Sp(k) \times G_2$
f_4	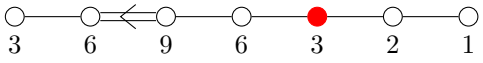	$F_4 \times SU(3)$ $\downarrow$ $F_4 \times G_2$
g_2	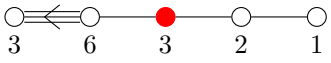	$G_2 \times SU(3)$ $\downarrow$ $G_2 \times G_2$

Table 3.4.4: Quivers resulting from adding all possible non-simply laced elementary slices to the empty nodes of sub-regular G_2 (3.4.1) to absorb a.

As in the previous section, because of the rank one node in (3.4.1), we can also perform a single quiver addition to absorb this node before absorbing a and find yet more quivers whose Hasse diagrams contain (3.4.1) and therefore experience the $SU(3) \to G_2$ enhancement. Again, there are infinitely many such quivers one could construct. However, unlike in the case of Section 3.3.2, here the actual enhancement won't be of a different type to that of the above quivers, and so won't be of particular interest to us. To illustrate this, consider the quiver after adding an A_1:

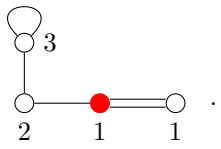

(3.4.6)

The reason that (3.4.6) gives us no new quivers of interest can be made explicit if we ungauge on the rank one unbalanced node,[18] in which case it becomes

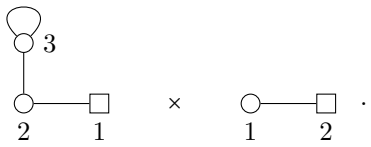

(3.4.7)

The Coulomb branch moduli space of this quiver theory is then the product of A_1 and the sub-regular nilpotent orbit of G_2. We don't worry about product moduli spaces, because if we understand individual ones then we can construct and know everything about the products too. Indeed, if we for example add a_2 thrice on to the empty nodes of (3.4.6) and again ungauge on the unbalanced rank one node, we get

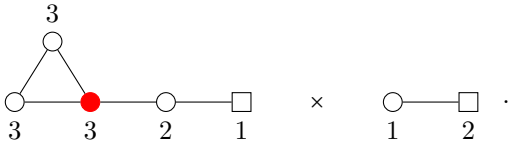

(3.4.8)

The Coulomb branch of the quiver on the left is in the top row of Table 3.4.3, and the Coulomb branch of the quiver on the right is the minimal nilpotent orbit of A_1, so we do indeed have nothing new. Thus Tables 3.4.1 through to 3.4.4 conclude the list of quivers with a global symmetry factor experiencing enhancement to G_2 that can be found as a result of performing quiver addition on the sub-regular nilpotent orbit of G_2 (3.4.1).

3.5 Enhancement to $SO(2n)$

There are two quivers in Table 3.2.1 with $SO(2n)$ global symmetry, and so both can be used as a base to construct quivers with a global symmetry factor which enhances to $SO(2n)$. It is the BGS factor that enhances which distinguishes the results from adding to the third or fourth quiver in Table 3.2.1. Section 3.5.1 addresses quivers derived from adding to the former, and Section 3.5.2 addresses quivers derived from adding to the latter.

[18] Recall we always choose to ungauge on a long node, and ungauging on any long node is equivalent to ungauging on any other.

3.5.1 Enhancement from $SO(2n-1)$ to $SO(2n)$

The next to minimal nilpotent orbit of D_n for $n \geq 2$ is given by the third quiver in Table 3.2.1 [12, 84, 62],

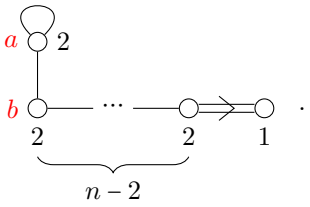

(3.5.1)

Following the BGS algorithm for quivers with adjoint matter in Section 3.2.1, the global symmetry of (3.5.1) is $SO(2n)$. The Hasse diagram is

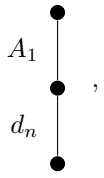

(3.5.2)

The bottom leaf of (3.5.2) matches the prediction of the global symmetry of (3.5.1) given by the Q_a BGS algorithm in Section 3.2.1, and this is confirmed by computing the Hilbert series. The quivers which can be constructed by adding to (3.5.1) to absorb a experience an enhancement of their BGS given by

$$\prod_i G_i \times SO(2n-1) \to \prod_i G_i \times SO(2n), \tag{3.5.3}$$

for some simple Lie groups G_i. The $n = 2$ case needs to be treated separately from $n \geq 3$ because for $n = 2$, a is a short node.

For $n \geq 4$ and using the algorithm from Section 3.2.2, we can again either add to the existing nodes of (3.5.1) by taking c as the node to the right of b

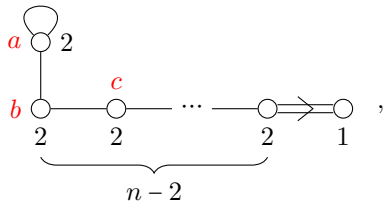

(3.5.4)

or add to the empty nodes of (3.5.1) by taking c to be some non-existent node to the left of b

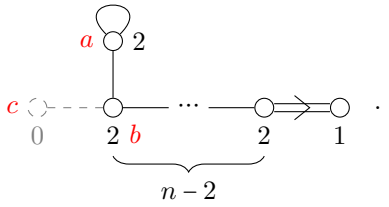

(3.5.5)

As previously, when adding to the empty nodes, there will be no restriction on the affine slices we can add. Adding to the existing nodes requires that all nodes to the right of b in (3.5.1) be a subset of the slice that is added. Thus we can only add b_k, c_k and f_4 to the existing nodes, and doing so

will fix the value of n for these cases. The results of all these additions may be found in Table 3.5.1 for the existing nodes addition, and Tables 3.5.2 and 3.5.3 for the empty nodes addition.

For $n = 3$, we can only add to the empty nodes due to absence of an existing long c-node. The results of these additions are simply the $n = 3$ case of Table 3.5.2. In the case where $n = 2$, we are considering the next to minimal nilpotent orbit of D_2,

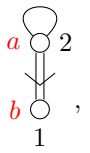

(3.5.6)

the global symmetry of which can be computed to be $SU(2)^2$ using the Hilbert series. This quiver is different to the previous cases from Table 3.2.1 that we've looked at thus far, in that here a is connected to the other nodes in the quiver via a non-simply laced edge. Because of this, the BGS algorithm given in Section 3.2.1 and the quiver addition algorithm given in Section 3.2.2 do not apply. Because a is connected to b via a non-simply laced edge, if we view the adjoint hypermultiplet as having arisen from a double same slice subtraction, b must have been becoming unbalanced by one more each time and must have been a short node, in line with the rules for rebalancing on a short node in Step 2)a)ii) in Section 2.7.2. Thus the only quivers we can add to this are those for which there is a rank one node which is on the short end of a non-simply laced edge of multiplicity two. The only quivers for elementary slices for which this is the case are affine b_k, c_k and f_4 and twisted affine a_k, d_k, and e_6. They all experience an enhancement from their BGS as

$$\prod_i G_i \times SU(2) \to \prod_i G_i \times SU(2)^2, \tag{3.5.7}$$

for some simple Lie groups G_i. The quivers derived from these additions are displayed in Table 3.5.4.

For all cases $n \geq 2$ listed across this section, unlike before in Section 3.3.2, we cannot find more quivers with such an enhancement by performing a different quiver addition on (3.5.1) prior to absorbing the adjoint hypermultiplet as there are no long rank one nodes present.

Added Slice	Quiver	Global Symmetry
b_k $k = n-2$	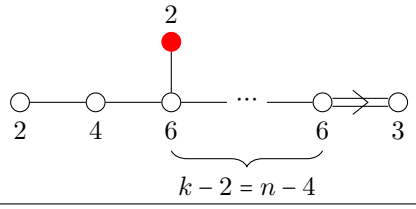	$SO(2n-1)$ ↓ $SO(2n)$
c_k $n = 4$	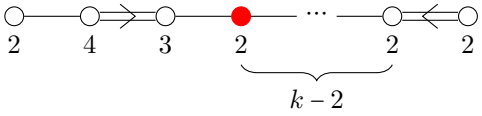	$SO(7)\times Sp(k-2)$ ↓ $SO(8)\times Sp(k-2)$
f_4 $n = 6$	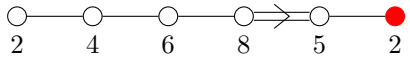	$SO(11)$ ↓ $SO(12)$

Table 3.5.1: Quivers resulting from adding all possible elementary slices to the existing nodes of n.min D_n (3.5.1) to absorb a for $n \geq 4$.

Added Slice	Quiver	Global Symmetry
a_k $k \geq 1, n \geq 3$	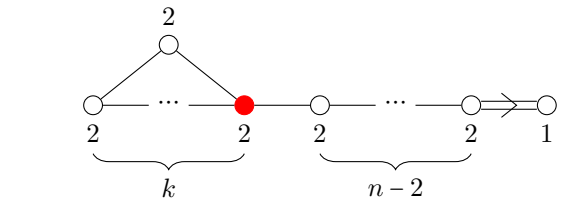	$SU(k+1) \times SO(2n-1)$ ↓ $SU(k+1) \times SO(2n)$
d_k $k \geq 4, n = k+1$	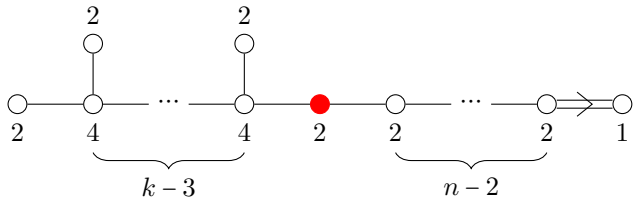	$SO(2k) \times SO(2n-1)$ ↓ $SO(2k) \times SO(2n)$
e_6 $n \geq 3$	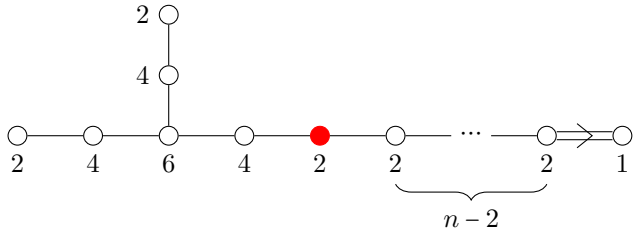	$E_6 \times SO(2n-1)$ ↓ $E_6 \times SO(2n)$
e_7 $n \geq 3$	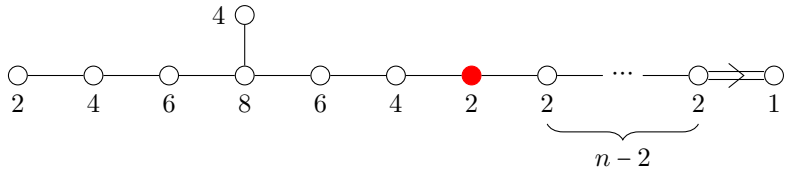	$E_7 \times SO(2n-1)$ ↓ $E_7 \times SO(2n)$
e_8 $n \geq 3$	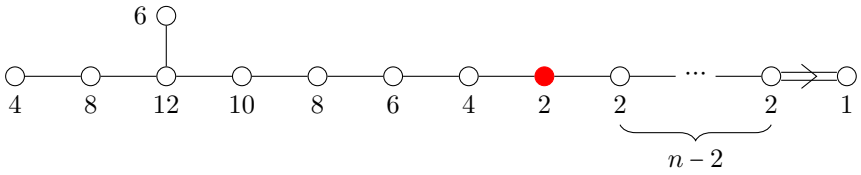	$E_8 \times SO(2n-1)$ ↓ $E_8 \times SO(2n)$

Table 3.5.2: Quivers resulting from adding all possible simply laced slices to the empty nodes of n.min D_n (3.5.1) to absorb a for $n \geq 3$.

Added Slice	Quiver	Global Symmetry
b_k $k \geq 3, n \geq 3$	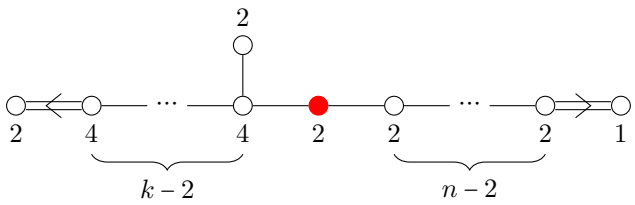	$SO(2k+1) \times SO(2n-1)$ ↓ $SO(2k+1) \times SO(2n)$
c_k $k \geq 2, n \geq 3$	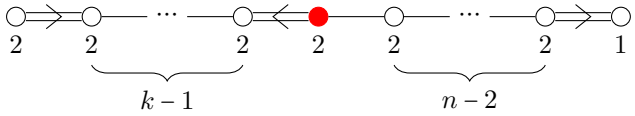	$Sp(k) \times SO(2n-1)$ ↓ $Sp(k) \times SO(2n)$
f_4 $n \geq 3$	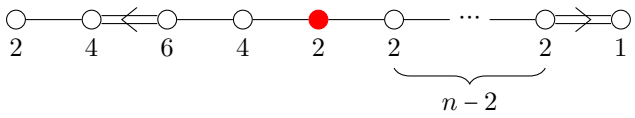	$F_4 \times SO(2n-1)$ ↓ $F_4 \times SO(2n)$
g_2 $n \geq 3$	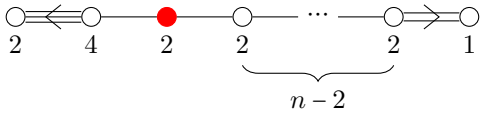	$G_2 \times SO(2n-1)$ ↓ $G_2 \times SO(2n)$

Table 3.5.3: Quivers resulting from adding all possible non-simply laced slice to the empty nodes of n.min D_n (3.5.1) to absorb a for $n \geq 3$

Added Slice	Quiver	Global Symmetry
b_k $k \geq 3$	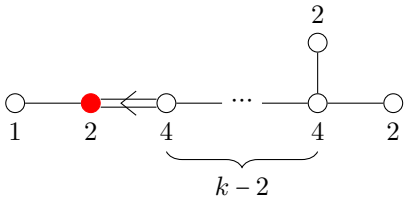	$SU(2) \times SO(2k)$ ↓ $SU(2)^2 \times SO(2k)$
c_k $k \geq 2$	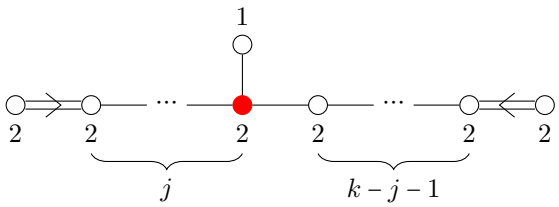	$SU(2) \times Sp(j) \times Sp(k-j)$ ↓ $SU(2)^2 \times Sp(j) \times Sp(k-j)$
f_4	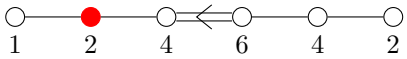	$SU(2) \times SO(9)$ ↓ $SU(2)^2 \times SO(9)$
a_{2k-1} $k \geq 3$	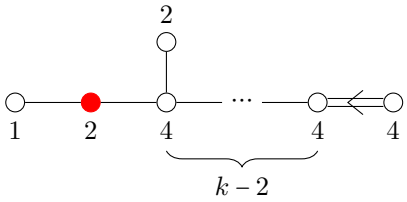	$SU(2) \times Sp(k)$ ↓ $SU(2)^2 \times Sp(k)$
d_{k+1} $k \geq 2$	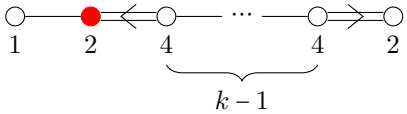	$SU(2) \times SO(2k+1)$ ↓ $SU(2)^2 \times SO(2k+1)$
e_6	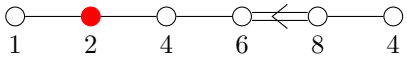	$SU(2) \times F_4$ ↓ $SU(2)^2 \times F_4$

Table 3.5.4: Quivers resulting from adding all possible elementary slices to n.min D_2 (3.5.6) to absorb a.

3.5.2 Enhancement from $SU(n)\times U(1)$ to $SO(2n)$

The final quiver we consider for enhancement to D-type symmetry is that of (3.3.1) with a further $\mathbb{Z}_2$ quotient taken, to combine the two spinor nodes into another rank two node with an adjoint hypermultiplet [62]:

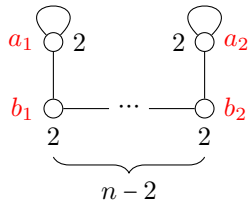

(3.5.8)

This quiver has $SO(2n)$ global symmetry because under the modified BGS algorithm of Section 3.2.1 we see the shape of the twisted affine d_n quiver. As mentioned in Section 3.2.2, a modification on the quiver addition algorithm is needed in this case. This is because if we take c_1 and c_2 to be the existing nodes the right and left of b_1 and b_2 respectively, then one can check that it is impossible to absorb a_1 and a_2 by adding on to these nodes. Thus the only legitimate additions one can perform here are by taking c_1 and c_2 to be the empty nodes to the left and right of b_1 and b_2 respectively,

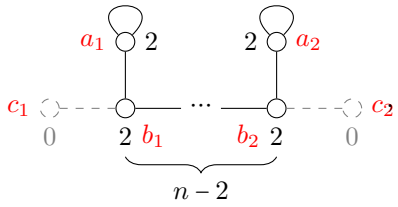

(3.5.9)

and adding some affine quiver g_k to c_1 and another affine quiver $\tilde{g}_l$ to c_2, so that upon double subtraction of both g_k and $\tilde{g}_l$, both a_1 and a_2 must appear in order to rebalance. There will be 45 such quivers so we shall not list them all here, but they take the form

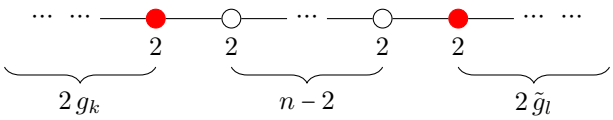

(3.5.10)

and will exhibit the enhancement from the BGS as

$$G_k \times SU(n-1)\times U(1)\times \tilde{G}_l \to G_k \times SO(2n)\times \tilde{G}_l. \tag{3.5.11}$$

To be explicit, we show an example of adding b_3 to the left of node a_1, and d_4 to the right of node a_2. That is, $g_k = b_3$ and $\tilde{g}_l = d_4$:

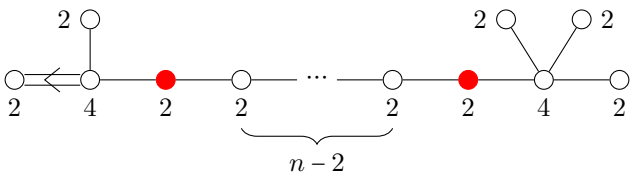

(3.5.12)

The enhancements for several of these cases have been checked and confirmed via the Hilbert series.

Again, due to the lack of long rank one nodes present, a different addition prior to absorbing a_1 or a_2 cannot happen as it did in Section 3.3.2, and so the quivers given in Tables 3.5.1, 3.5.2, 3.5.3,

3.5.4 and those encapsulated by the general form of (3.5.10) comprise the full list of quivers derived from quiver addition on the next to minimal nilpotent orbit of D_n (3.5.1) and (3.5.8) whose global symmetry contains a factor which is enhanced to $SO(2n)$ from that predicted by the BGS.

3.6 Enhancement to $SU(3)$

The final quiver from Table 3.2.1 that we know how to perform quiver addition on is

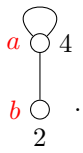

(3.6.1)

Note that although the greatest common divisor of the ranks of the gauge nodes here is greater than one, the Coulomb branch of this quiver is still a symplectic singularity. The Hasse diagram for (3.6.1) is a question for future work. The amended BGS algorithm in Section 3.2.1 tells us that the global symmetry of this quiver is $SU(3)$, and indeed this is confirmed upon Hilbert series computation. As a result, the quivers presented in this section all experience the enhancement in a factor of their BGS to $SU(3)$:

$$\prod_i G_i \times SU(2) \to \prod_i G_i \times SU(3), \tag{3.6.2}$$

for some simple Lie groups G_i.

Following the terminology of the quiver addition algorithm in Section 3.2.2, there are no possible existing c-nodes in (3.6.1), so the only available c-nodes here are empty:

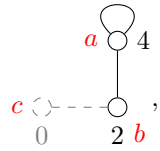

(3.6.3)

A result of this is that, as before, we may add any affine slice. Since the node a is of rank four, to absorb it the slice that we add g_k must be added four times. The results of performing these quiver additions are given in Tables 3.6.1 and 3.6.2. For those quivers in these tables which depend on the parameter k, for low values of k Hilbert series computations have confirmed this enhancement. The e_6 and g_2 cases have also been confirmed, but we have been unable to compute the Hilbert series for the e_7, e_8 and f_4 cases, and so these enhancements remain as conjectures. Also, note that the greatest common divisor of the node ranks of the quivers in Tables 3.6.1 and 3.6.2 is greater than one. As mentioned in Chapter 1,[2] this is often an indication of a diverging Hilbert series. Here the quivers are too complex to confirm or deny this by computation, but since they are derived from (3.6.1) which we know does not suffer this divergence, there is a strong possibility that these quivers are also exempt.

Again as with (3.5.1) and (3.5.8) of Section 3.5, since (3.6.1) has no long rank one nodes we cannot add onto this quiver other than to absorb a, and so do not get further constructions as in Section 3.3.2. As a result, Tables 3.6.1 and 3.6.2 conclude all possible quivers derived from performing quiver addition on (3.6.1) to absorb a whose global symmetry contains a factor which is enhanced to $SU(3)$.

Added Slice	Quiver	Global Symmetry
a_k $k \geq 1$	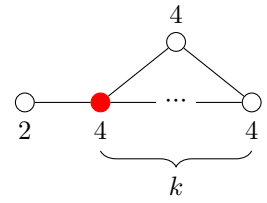	$SU(2) \times SU(k+1)$ $\downarrow$ $SU(3) \times SU(k+1)$
d_k $k \geq 4$	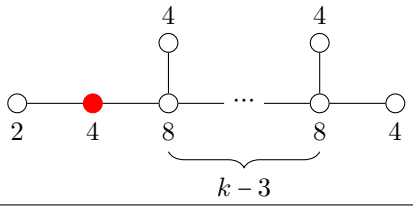	$SU(2) \times SO(2k)$ $\downarrow$ $SU(3) \times SO(2k)$
e_6	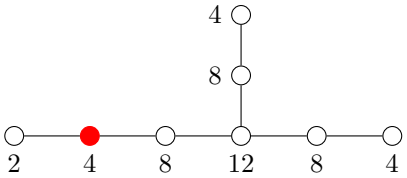	$SU(2) \times E_6$ $\downarrow$ $SU(3) \times E_6$
e_7	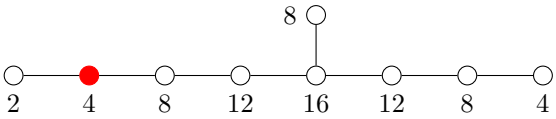	$SU(2) \times E_7$ $\downarrow$ $SU(3) \times E_7$
e_8	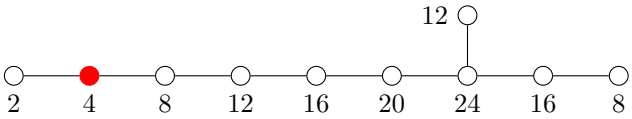	$SU(2) \times E_8$ $\downarrow$ $SU(3) \times E_8$

Table 3.6.1: Quivers resulting from adding all possible simply laced elementary slices to (3.6.1) to absorb a.

Added Slice	Quiver	Global Symmetry
b_k $k \geq 3$	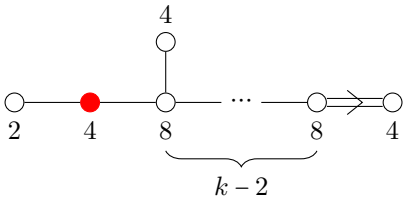	$SU(2) \times SO(2k+1)$ $\downarrow$ $SU(3) \times SO(2k+1)$
c_k $k \geq 2$	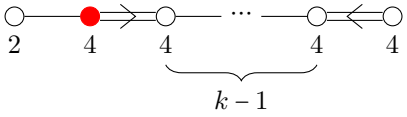	$SU(2) \times Sp(k)$ $\downarrow$ $SU(3) \times Sp(k)$
f_4	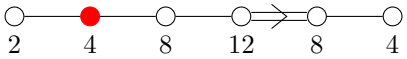	$SU(2) \times F_4$ $\downarrow$ $SU(3) \times F_4$
g_2	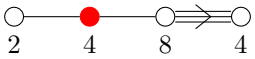	$SU(2) \times G_2$ $\downarrow$ $SU(3) \times G_2$

Table 3.6.2: Quivers resulting from adding all possible non-simply laced elementary slices to (3.6.1) to absorb a.

3.7 Modified Global Symmetry Algorithm

In this chapter, we have seen a huge range of quivers for which the BGS algorithm of Section 3.1 fails to give the full GS, and identified that this failure was due to the appearance of a quiver Q_a in the Hasse diagram. As a result, we are now ready to present a modified version of the algorithm which correctly gives the full GS for all quivers that the previous algorithm did in addition to all quivers in this chapter. Note that it *is not sufficient to compute GS for all quivers containing regular matter*; for example, it does not cater for the quivers whose Hasse diagrams contain quivers with adjoint matter that do not appear in Table 3.2.1. We present it here as a stepping-stone algorithm that we hope can be built upon in aid of the goal to find an algorithm which works in all cases.

Modified BGS algorithm for quivers in this chapter

We say that a quiver Q contains c copies of an elementary slice[19] whose Coulomb quiver is σ if Q has a set of connected nodes Q^c_σ in the shape of the nodes in σ, such that the ranks of all nodes in Q^c_σ are at least c times the ranks of the corresponding nodes in σ, but at least one node of Q^c_σ is less than $c+1$ times its corresponding node rank in σ. We use Q_r to denote quivers which contain regular matter only and appear either in this chapter, or in the set of quivers for which the BGS algorithm of Section 3.1 works. Suppose a quiver Q_r contains E Coulomb quivers for elementary slices, σ_i, $i = 1, ..., E$, and moreover contains c_i copies of each. Then the GS for Q_r is given as follows:

1. If $c_i = 1$ for all i, then follow the BGS algorithm of Section 3.1:

   a) If Q_r is framed, and the gauge nodes in it comprise s balanced sub-Dynkin diagrams D_i of the simple Lie groups G_i, and k unbalanced nodes, then the BGS is given by

   $$GS^{\text{framed}}_{Q_r} = \prod_{i=1}^{s} G_i \times U(1)^k. \tag{3.7.1}$$

   b) If Q_r is unframed, there are two scenarios:

      i) If Q_r is balanced, then it must be either the affine or twisted affine quiver for some simple Lie group G (these quivers are given in Tables 3.1.1 and 3.1.2 respectively), in which case

      $$GS_{Q_r} = G. \tag{3.7.2}$$

      ii) If Q_r is unbalanced, and the gauge nodes in it comprise s balanced sub-Dynkin diagrams D_i of the simple Lie groups G_i, and k unbalanced nodes, then the BGS is given by

      $$BGS^{\text{unframed}}_{Q_r} = \prod_{i=1}^{s} G_i \times U(1)^{k-1}. \tag{3.7.3}$$

      where the definitions of s, G_i and k are as in Step 1.

2. If $c_i > 1$ for at least one $i = 1, ..., E$, then:[20]

   a) Colour in any unbalanced nodes.

[19] Recall the known elementary slices to date can be found in Table 1 of [81] and Table 3.1.2 of this note.

[20] Note that there is no appearance of the affine Dynkin diagram in this case. This is because the only way this could happen is if there was several copies of a single affine diagram, and we do not consider such quivers as they do not fall under the collection of those whose Coulomb branches are symplectic singularities.

b) For each $i = 1, ..., E$, perform c_i identical subtractions of σ_i from Q_r. For each i, this will give a quiver Q_i containing a node $U(c_i)$ with an adjoint hypermultiplet.

c) In each Q_i, label the adjoint node $U(c_i)$ by a_i, and the nodes of Q_i connected to a_i as $b_{i,j}$.

d) Each $b_{i,j}$ is also present in the quiver Q_r. Label these nodes in Q_r as $b_{i,j}$ also.

e) Attach each node a_i (from Q_i, uncoloured) to all nodes $b_{i,j}$ in Q_r, giving quiver $\tilde{Q}_r$.

f) Ignoring current node ranks and excess (adhere to the colouring of unbalanced nodes in Step 2*a* to dictate which nodes are considered balanced), if the gauge nodes of $\tilde{Q}_r$ comprise s balanced sub-Dynkin diagrams D_i of the simple Lie groups G_i, t quivers $Q_{a,i}$ appearing in Table 3.2.1 with global symmetries $\tilde{G}_i$, and k unbalanced nodes, then GS is given by:

$$GS_{Q_r} = \begin{cases} \prod_{i=1}^{s} G_i \times \prod_{j=1}^{t} \tilde{G}_j \times U(1)^k & \text{if } Q_r \text{ framed} \\ \prod_{i=1}^{s} G_i \times \prod_{j=1}^{t} \tilde{G}_j \times U(1)^{k-1} & \text{if } Q_r \text{ unframed} \end{cases} . \tag{3.7.4}$$

Example We'll illustrate this algorithm with the example Q of (3.1.4), for which we saw the BGS algorithm of Section 3.1 fail:

$Q =$ 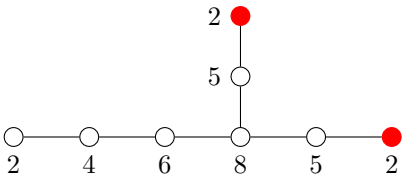

. (3.7.5)

We can see that the only elementary slice whose Coulomb quiver lies within Q is e_6, and there are two copies of it: $E = 1$, $\sigma_1 = e_6$ and $c_1 = 2$. Since $c_1 = 2$, we use Step 2 of the above modified algorithm:

(a) The unbalanced nodes are already coloured in red in (3.7.5).

(b) There is just $E = 1$ subtraction to perform: taking $\sigma_1 = e_6$ away from Q $c_1 = 2$ times. This gives the quiver Q_1:

$Q_1 =$ 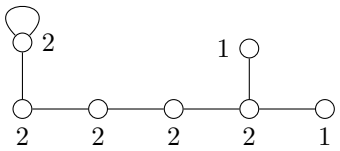

. (3.7.6)

(c) We can see the adjoint node $U(c_1 = 2)$ is connected to just a single node in Q_1. This means there is just one $b_{1,j}$, $b_{1,1}$, and we label this and the adjoint node a_1:

$Q_1 =$ 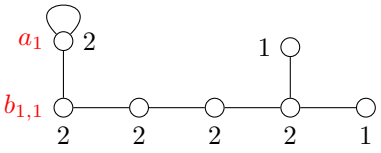

. (3.7.7)

(d) We see that the corresponding node in Q is the left-hand rank two node, and label it as such:

$Q =$ 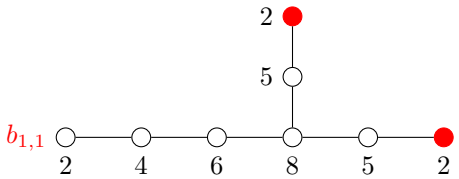

. (3.7.8)

(e) We construct $\tilde{Q}$ by attaching a_1 (uncoloured) to $b_{1,1}$:

$\tilde{Q} =$ 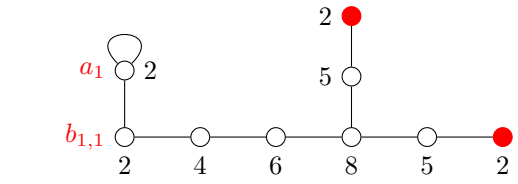

. (3.7.9)

(f) $\tilde{Q}$ has only one balanced subsets of nodes (where remember the balance is indicated by the colouring in Step (a); white nodes are balanced, red nodes are unbalanced) which form the first quiver in Table 3.2.1 for $n = 6$, and two unbalanced nodes: $s = 0$, $t = 1$, $Q_{a_1,1} = \text{n.min } B_6$, $\tilde{G}_1 = SO(13)$, and $k = 2$. Thus, since Q is unframed, we find the Coulomb branch topological symmetry to be:

$$GS_Q = SO(13) \times U(1). \tag{3.7.10}$$

□

Chapter 4

Poisson Brackets

In this chapter, we present the work of [11] where we used various methods to determine the unordered Poisson brackets $\{\cdot,\cdot\}_{\mathcal{C}}$ on $\mathcal{C}$ between its generators $\mathcal{G}_{\mathcal{C}}$, $\{\mathcal{G}_{\mathcal{C}},\mathcal{G}_{\mathcal{C}}\}_{\mathcal{C}}$. The antisymmetry and Leibniz properties of the Poisson bracket and the ring structure of the Coulomb branch then fully fix the Poisson brackets between any two operators on $\mathcal{C}$. They are of interest as the Poisson structure on the Coulomb branch relates its symplectic one, as briefly mentioned in Section 2.3.2.4 (and will be further elaborated on in Section 4.1). In particular, the Poisson bracket and symplectic form degenerate at the same points. There has been previous progress on determining Poisson brackets for Coulomb branches in the literature (see for instance [17, 18, 3, 19, 20]); in this note we add to this by providing explicit computations for a selected set of examples, including quivers with many unitary gauge nodes of high rank.

So, given a quiver, how does one compute the Poisson brackets between the generators of its Coulomb branch? We can answer this question in two ways, depending on how we choose to view $\mathcal{C}$. The first way will be the topic of Sections 4.2 – 4.5: we view the Coulomb branch as the space of dressed monopole operators (see Section 2.4.2.1), and study the Poisson brackets between those that generate the variety. This method gives more explicit information, but has the drawbacks of being more computationally intensive or requiring the exact description of the Coulomb branch as an algebraic variety to be known[1] (e.g. via mirror symmetry [51, 48]). The second viewpoint we can take, if the representation content of $\mathcal{C}$ at low orders is known, is slightly more reductionist: we can characterise the Coulomb branch simply as a space of representations of its topological global symmetry GS, isolate those which generate the space and then conjecture the Poisson brackets between them based on representation theoretic and operator content constraints. This viewpoint is discussed in Sections 4.6 – 4.7; it is a more abstract approach, but allows us to say something about the Poisson structure of a wider set of Coulomb branches.

The outline of this chapter is as follows. Section 4.1 makes concrete our definition of a symplectic singularity, and shows how the symplectic form induces a Poisson structure. In Sections 4.2 – 4.5 we detail the computation of $\{\mathcal{G}_{\mathcal{C}},\mathcal{G}_{\mathcal{C}}\}_{\mathcal{C}}$ for $\mathcal{G}_{\mathcal{C}}$ the explicit dressed monopole operators of the physical theory: Section 4.2 explains the method used to do this for the cases where either the explicit variety

[1] Here, by "an exact description" we mean an explicit realisation of the Coulomb branch as the space traced out by some known set of generators which are expressed as holomorphic polynomials in some complex coordinates, and any relations they are subject to.

$\mathcal{C} = \mathcal{V}$ is known, or the dimension of the Coulomb branch is sufficiently small; and Sections 4.3, 4.4 and 4.5 report the results for the examples of Coulomb branches which are free spaces, A and D Klein singularities and small dimension nilpotent orbits respectively. Sections 4.6 – 4.7 cover the alternative method of computing $\{\mathcal{G}_{\mathcal{C}}, \mathcal{G}_{\mathcal{C}}\}_{\mathcal{C}}$ for generators $\mathcal{G}_{\mathcal{C}}$ viewed abstractly as representations of the global symmetry: Section 4.6 details the method, and Section 4.7 details the results for several families of magnetic quivers for the Higgs branch of 5 or $6d$ theories at infinite coupling.

Before we begin by discussing the monopole construction of the Coulomb branch, we briefly list some notation that will be used throughout:

- $\mathcal{G}_{\mathcal{C}}$, $\mathcal{G}_{\mathcal{V}}$ and $\mathcal{G}_{\mathcal{H}}$ are used to denote the generators for a Coulomb branch $\mathcal{C}$, variety $\mathcal{V}$ and Higgs branch $\mathcal{H}$ respectively.
- $\{\cdot,\cdot\}_{\mathcal{C}}$ and $\{\cdot,\cdot\}_{\mathcal{V}}$ denote the Poisson bracket between any two Coulomb branch operators written in terms of the Coulomb branch degrees of freedom and written in terms of the holomorphic functions on the abstract variety we know the Coulomb branch to be respectively. When the chosen degrees of freedom are clear, the subscripts will be dropped.
- Throughout, $\{\cdots\}$ is used to denote both a set and a Poisson bracket (the latter is only applicable when there are two arguments), but the context should make clear in which sense it is being used.
- We use $\boldsymbol{m}(\cdot)$, $\boldsymbol{J}(\cdot)$ and $\Delta(\cdot)$ to denote the magnetic, topological and conformal dimension of an operator respectively.
- In Sections 4.6 and 4.7, μ, ν and μ_i will be used both as an index labelling representation generators that takes on certain specified values, and as the highest weight fugacities to denote a representation. Its meaning in a given situation should be clear from context (i.e. whether it lies in an exponent/subscript or not).

4.1 Symplectic Singularities and the Poisson Bracket

Recall from Chapter 1 that all Coulomb branches $\mathcal{C}$ of quivers we consider are symplectic singularities, in the sense of Beauville [2]. In Section 2.3.2.4 we saw that in our languauge, this essentially means they are algebraic varieties on which there exists a 2-form which degenerates at zero or more points. This 2-form is called the symplectic form ω, and defines a pairing on the tangent space at any point on the variety. We see now how the symplectic form induces a Poisson structure on the Coulomb branch.

Recall from Sections 2.3 and 2.4 that the Coulomb branch chiral ring is thought to be isomorphic to the ring of holomorphic functions over it, and hence completely captures $\mathcal{C}$ as an algebrogeometric object. Since ω maps two tangent vectors at a point p on $\mathcal{C}$ to $\mathbb{C}$, it can be thought of as a map from a tangent space at p to the cotangent space at p,

$$\omega : T_p\mathcal{C} \to T_p^*\mathcal{C}. \tag{4.1.1}$$

This induces a correspondence between one-forms and vector fields on $\mathcal{C}$. Consider any holomorphic function f (chiral operator) on $\mathcal{C}$. Since it is differentiable, we can consider its differential df. Since this is a one-form, the symplectic form then says that away from singularities (where the correspondence (4.1.1) ceases to be bijective) this is equivalent to a vector field X_f. Thus we can define the Poisson

bracket of two chiral operators on the Coulomb branch isomorphic to holomorphic functions f and g as

$$\{f, g\} \equiv \omega(X_f, X_g). \tag{4.1.2}$$

Example Take the concrete example of $\mathbb{C}^2 \cong \mathbb{C}[z_1, z_2]$. The holomorphic functions on this variety are generated by the two complex coordinates over which it is formed, z_1 and z_2. As a result, we can find the Poisson bracket between any two functions on $\mathbb{C}^2$ by postulating a relation between z_1 and z_2 and then invoking the Leibniz behviour, bilinearity and antisymmetry of $\{\cdot, \cdot\}$. We postulate that z_1 and z_2 satisfy

$$\{z_1, z_2\} = 1, \tag{4.1.3}$$

a direct analogue of that of phase space coordinates in classical mechanics. Leibniz can then be used to see that the Poisson bracket between any two functions f and g on $\mathbb{C}^2$ is

$$\{f(z_1, z_2), g(z_1, z_2)\} = \frac{\partial f}{\partial z_1}\frac{\partial g}{\partial z_2} - \frac{\partial f}{\partial z_2}\frac{\partial g}{\partial z_1}. \tag{4.1.4}$$

Note that the properties of the Poisson bracket – a bilinear map which obeys anticommutativity, Leibniz and the Jacobi identity – match those of a Lie bracket, and this fact can be exploited in both directions. For example, consider the generators $\mathcal{G}_{\mathcal{C}}$ of a given Coulomb branch $\mathcal{C}$. They lie in the adjoint representation of the topological global symmetry algebra $\mathfrak{g}_{\mathfrak{s}}$. If the structure constants of this algebra are known, we can use them to conclude the Poisson brackets. If the structure constants are unknown and we can compute the Poisson brackets, then we can use these to conclude the structure constants. More generally, the form of the Poisson brackets between two operators can be inferred by combining the imposition of conserved charges with constraints from other available information. Two different approaches to doing this will be discussed in Sections 4.2 and 4.6 respectively. We start with the approach which considers the Coulomb branch as the space of dressed monopole operators $\mathcal{O}_{\mathcal{C}}$, and use the Hilbert series or the known variety $\mathcal{C} = \mathcal{V}$ to fix the Poisson brackets between $\mathcal{O}_{\mathcal{C}}$.

4.2 Poisson Brackets for Dressed Monopole Operators

In this section, we write down the chiral operators on $\mathcal{C}$ as bare and dressed monopoles (as in Section 2.4.2), and compute the Poisson brackets between them. The method we present to do this is fairly simple in principle:

Method

1. Explicitly write down the generators of the Coulomb branch in terms of its basic degrees of freedom (bare monopoles and adjoint scalars).

2. Constrain the Poisson brackets by demanding the result have the expected conserved charges under the global symmetries of the Coulomb branch. This will fix the results up to constant factors.

3. *a*) If the Coulomb branch is known as a variety with coordinates on which there exists a canonical Poisson bracket,[2] use the results of Step 2 to identify which dressed monopoles correspond to which holomorphic functions on this variety, and declare that their Poisson brackets are equal.

[2] We use the term canonical Poisson bracket to mean the one associated to a known algebraic symplectic variety.

b) Otherwise, fix the constant factors by demanding that the Poisson bracket of the Cartan elements of the Coulomb branch generators with any operator on the Coulomb branch yield the correct weight under the global symmetry of the Coulomb branch.

As already alluded to, these steps are easier said than done: the number of quivers whose Coulomb branch satisfies the condition of 3.*a*) is rather small; and even for quivers with fairly low-dimension Coulomb branches there quickly become too many variables to actually find an explicit solution following the idea of 3.*b*) (at least using the methods we have so far). Essentially, there are many quivers for which Step 3 becomes too hard to do and we cannot ascertain the Poisson relations between the explicit dressed monopole operators of $\mathcal{C}$. It is in these cases that we turn to an alternate viewpoint, as discussed in Section 4.6 and executed in Section 4.7. In Sections 4.2.1, 4.2.2, 4.2.3.1 and 4.2.3.2 respectively we elaborate on each of the steps 1, 2, 3.*a*) and 3.*b*) in the method above (assuming that the Coulomb branches we consider satisfy the above conditions of being either known exactly as a variety or of low enough dimension), detailing exactly how to perform the relevant computations and illustrating them in our favourite example of SQED with 2 electrons (2.6.14).

4.2.1 Writing down Coulomb branch generators

Recall from Section 2.4.2 that the Coulomb branch is the space of gauge invariant bare and dressed monopole operators[19] labelled by magnetic charges in the weight lattice of the GNO dual of the gauge group. Before we see explicitly how to construct these, we make a brief remark on terminology. We refer to gauge-invariant monopole operators which are not dressed by any adjoint scalars as physical bare monopoles, and the gauge-invariant supersymmetry-preserving dressing factors as physical adjoint scalars or Casimirs. Together these form the physical Coulomb branch degrees of freedom $\mathcal{D}_{\mathcal{C}}$. These degrees of freedom can then be used to construct the Coulomb branch operators $\mathcal{O}_{\mathcal{C}}$, the dressed monopole operators, which we define as linear combinations of products of $\mathcal{D}_{\mathcal{C}}$ that have matching conserved charges (topological charge and conformal dimension).

Physical bare monopoles Recall from Section 2.4.2.1 that a bare monopole operator for a gauge group G with $\text{rank}(G) = n$ has magnetic charge $\boldsymbol{m} = (m_1, ..., m_n) \in \Lambda_{G^\vee}$. We denote this bare monopole operator $v_{\boldsymbol{m}} = v_{m_1 \cdots m_n}$. However $v_{\boldsymbol{m}}$ is not necessarily a physical degree of freedom $\mathcal{D}_{\mathcal{C}}$, as it may not be gauge-invariant. The gauge group acts on the weights of $G^\vee$ via its Weyl group $\mathcal{W}_{G^\vee}$, and if $\boldsymbol{m}$ is not invariant under $\mathcal{W}_{G^\vee}$ then this bare monopole operator $v_{\boldsymbol{m}}$ is not physical. To rectify this, for a given magnetic charge $\boldsymbol{m}$ we need to sum up the unphysical bare monopole operators with magnetic charges in the $\mathcal{W}_{G^\vee}$ orbit of $\boldsymbol{m}$. We will call the physical bare monopole corresponding to $v_{\boldsymbol{m}}$ by the name $V_{\boldsymbol{m}}$:

$$V_{\boldsymbol{m}} = \sum_{\sigma \in \mathcal{W}_{G^\vee}} v_{\sigma(\boldsymbol{m})}. \tag{4.2.1}$$

Note that in this notation we clearly have $V_{\boldsymbol{m}} = V_{\sigma(\boldsymbol{m})}$ for any $\sigma \in \mathcal{W}_{G^\vee}$, and so if we write down all the $V_{\boldsymbol{m}}$ for every $\boldsymbol{m} \in \Lambda_{G^\vee}$, many will be identical and the duplicates will need deleting so as not to overcount. To avoid these duplicates, we can just compute (4.2.1) for each $\boldsymbol{m}$ in a single Weyl chamber of $\Lambda_{G^\vee}$ to find the set of all physical bare monopole degrees of freedom $\mathcal{D}_{\mathcal{C}}^V$:

$$\mathcal{D}_{\mathcal{C}}^V = \{V_{\boldsymbol{m}} \;\big|\; \boldsymbol{m} \in \Lambda_{G^\vee}/\mathcal{W}_{G^\vee}\} = \left\{ \sum_{\sigma \in \mathcal{W}_{G^\vee}} v_{\sigma(\boldsymbol{m})} \;\middle|\; \boldsymbol{m} \in \Lambda_{G^\vee}/\mathcal{W}_{G^\vee} \right\}. \tag{4.2.2}$$

Recall for a single unitary gauge group $G = U(n)$ that $\Lambda_{G^\vee}/\mathcal{W}_{G^\vee} \cong \mathbb{Z}^n/S_n$. Then the physical bare monopoles in this case are

$$\mathcal{D}_{\mathcal{C}}^{V} = \{V_{\boldsymbol{m}} \;\big|\; \boldsymbol{m} \in \mathbb{Z}^n/S_n\} = \left\{ \sum_{\sigma\in S_n} v_{\sigma(\boldsymbol{m})} \;\middle|\; \boldsymbol{m} \in \mathbb{Z}^n/S_n \right\}, \tag{4.2.3}$$

We could pick the Weyl chamber $\mathbb{Z}^n/S_n$ to be

$$\boldsymbol{m} = (m_1, ..., m_n) \in \mathbb{Z}^n \text{ such that } m_1 \geq m_2 \geq \cdots \geq m_n. \tag{4.2.4}$$

By extension, the unphysical bare monopoles in a quiver with p unitary gauge nodes $U(n_i)$ $i = 1, ..., p$ are labelled by vectors $\boldsymbol{m} = (\boldsymbol{m_1}, ..., \boldsymbol{m_p}) = (m_{1,1}, ..., m_{1,n_1}, ..., m_{p,1}, ..., m_{p,n_p})$ of length $\sum_{i=1}^{p} n_i$ with integer entries: $\{v_{\boldsymbol{m}} \mid \boldsymbol{m} \in \prod_{i=1}^{p} \mathbb{Z}^{n_i}\}$. The set of all physical bare monopole degrees of freedom is then

$$\mathcal{D}_{\mathcal{C}}^{V} = \left\{ V_{\boldsymbol{m}} \;\middle|\; \boldsymbol{m} \in \prod_{i=1}^{p} \mathbb{Z}^{n_i}/S_{n_i} \right\} = \left\{ \sum_{\sigma \in \prod_{i=1}^{p} S_{n_i}} v_{\sigma(\boldsymbol{m})} \;\middle|\; \boldsymbol{m} \in \prod_{i=1}^{p} \mathbb{Z}^{n_i}/S_{n_i} \right\}. \tag{4.2.5}$$

Again, we could pick the Weyl chambers $\mathbb{Z}^{n_i}/S_{n_i}$ to be (4.2.4) for each $\boldsymbol{m_i}$, $i = 1, ..., p$.

Adjoint valued complex scalars Recall from Section 2.4.2.1 that a physical adjoint scalar dressing factor $\varphi_{\boldsymbol{m}}$ for a bare monopole $V_{\boldsymbol{m}}$ is a gauge-invariant linear combination of the eigenvalues of the residual gauge algebra $\mathfrak{h}_{\mathfrak{m}}$ unbroken by the monopole VEV $\boldsymbol{m} \in \mathfrak{g}$. In particular, we saw that for an unbroken gauge algebra $\mathfrak{h}_{\mathfrak{m}} = \oplus_{i=1}^{u_{\boldsymbol{m}}} \mathfrak{u}(\mathfrak{l}_{\mathfrak{m},i})$ with eigenvalues $\lambda_{1,1}$, ... , $\lambda_{1,l_{\boldsymbol{m},1}}$, ... , $\lambda_{u_{\boldsymbol{m}},1}$, ... , $\lambda_{u_{\boldsymbol{m}},l_{\boldsymbol{m},u_{\boldsymbol{m}}}}$, the dressing factor is (2.4.16). So the set of adjoint scalar *degrees of freedom* $\mathcal{D}_{\mathcal{C}}^{\varphi}$ for a quiver with p unitary gauge nodes $U(n_i)$ $i = 1, ..., p$ is

$$\mathcal{D}_{\mathcal{C}}^{\varphi} = \left\{ \sum_{j=1}^{l_{\boldsymbol{m},i}} \lambda_{i,j} \;\middle|\; i = 1, ..., u_{\boldsymbol{m}},\ \boldsymbol{m} \in \prod_{i=1}^{p} \mathbb{Z}^{n_i}/S_{n_i} \right\} \equiv \left\{ \varphi_{\boldsymbol{m},i} \;\middle|\; i = 1, ..., u_{\boldsymbol{m}},\ \boldsymbol{m} \in \prod_{i=1}^{p} \mathbb{Z}^{n_i}/S_{n_i} \right\}. \tag{4.2.6}$$

All physical degrees of freedom and operators We have seen that the complete list of physical Coulomb branch degrees of freedom for a quiver with p unitary gauge nodes of ranks n_i for $i = 1, ..., p$ is comprised of (4.2.5) and (4.2.6):

$$\begin{aligned} \mathcal{D}_{\mathcal{C}} &= \mathcal{D}_{\mathcal{C}}^{V} \cup \mathcal{D}_{\mathcal{C}}^{\varphi} \\ &= \left\{ V_{\boldsymbol{m}} \;\middle|\; \boldsymbol{m} \in \prod_{i=1}^{p} \mathbb{Z}^{n_i}/S_{n_i} \right\} \cup \left\{ \varphi_{\boldsymbol{m},i} \;\middle|\; i = 1, ..., u_{\boldsymbol{m}},\ \boldsymbol{m} \in \prod_{i=1}^{p} \mathbb{Z}^{n_i}/S_{n_i} \right\}, \end{aligned} \tag{4.2.7}$$

and so any Coulomb branch operator is some product of bare monopoles (4.2.5) and adjoint scalars (2.4.16),

$$\mathcal{O}_{\mathcal{C}} = \left\{ \prod_{\boldsymbol{m} \in \prod_{i=1}^{p} \mathbb{Z}^{n_i}/S_{n_i}} \left((V_{\boldsymbol{m}})^{\tilde{k}_{\boldsymbol{m}}} \prod_{i=1}^{u_{\boldsymbol{m}}} (\varphi_{\boldsymbol{m},i})^{k_{\boldsymbol{m},i}} \right) \;\middle|\; \tilde{k}_{\boldsymbol{m}}, k_{\boldsymbol{m},i} \in \mathbb{Z}_{\geq 0} \right\}, \tag{4.2.8}$$

and linear combinations thereof, for any choice of non-negative integers $\tilde{k}_{\boldsymbol{m}}$ and $k_{\boldsymbol{m},i}$ such that each term in the linear combination has the same values for the conserved charges (from here on out we will refer to such linear combinations as "consistent").

Generators To find which linear combinations of (4.2.8) have the correct charges to be generators of the Coulomb branch in question, we first consult the plethystic logarithm of its Hilbert series. This tells us the conformal dimension(s) at which the generators lie, which we'll call Δ_i^{gen} for $i = 1, ..., d$ where d is the number of distinct conformal dimensions of generators (note that clearly d must be less than or equal to the number of generators). We then solve the d equations

$$\Delta_i^{\text{gen}} = \Delta(\mathcal{G}_{\mathcal{C}}), \tag{4.2.9}$$

to find which of the Coulomb branch operators $\mathcal{O}_{\mathcal{C}}$ (4.2.8) are the generators of the Coulomb branch, $\mathcal{G}_{\mathcal{C}}$. To do this we need to know how to compute the conformal dimension of any Coulomb branch operator. From (4.2.8) we see that any $\mathcal{O}_{\mathcal{C}}$ is some product of physical Coulomb branch degrees of freedom (4.2.7). Its conformal dimension is then simply the sum of the conformal dimensions of each of these degrees of freedom in the product, (2.4.20) and (2.4.21) for the bare monopoles and adjoint scalars respectively.

Example Consider a $U(1)$ gauge theory with 2 electrons, described by the quiver Q_{A_1} (2.6.14). Since there is just one gauge group and it is Abelian, here $\boldsymbol{m} = m \in \mathbb{Z}$ is just a vector of length one, and its Weyl group is trivial. The residual gauge group is always $U(1)$, so for any value of m there is just one adjoint scalar dressing $\varphi_m = \lambda \in \mathbb{C}$. The physical degrees of freedom on the Coulomb branch here are then[3]

$$\mathcal{D}_{\mathcal{C}} = \{V_m,\ \lambda\}. \tag{4.2.10}$$

The Coulomb branch operators then are

$$\mathcal{O}_{\mathcal{C}} = \{ \prod_{m \in \mathbb{Z}} (V_m)^{\tilde{k}_m} \lambda^{k_m} \} \tag{4.2.11}$$

for non-negative integers $\tilde{k}_m$ and k_m, and consistent linear combinations thereof.

Now let's find the operators among $\mathcal{O}_{\mathcal{C}}$ which are generators. The plethystic logarithm of the Hilbert series is

$$PL(HS(\mathcal{C}(Q_{A_1}))) = [2]_{SU(2)} t^2 - t^4, \tag{4.2.12}$$

hence every generator has $\Delta^{\text{gen}} = 1$. This means that the Coulomb branch generators $\mathcal{G}_{\mathcal{C}}$ are the operators $\mathcal{O}_{\mathcal{C}}$ (4.2.11) which have $\Delta(\mathcal{O}_{\mathcal{C}}) = 1$. For this quiver theory, using (2.4.20) we see that the conformal dimension of a bare monopole is

$$\Delta_{Q_{A_1}}(m) = |m|, \tag{4.2.13}$$

and we know from (2.4.21) that

$$\Delta_{Q_{A_1}}(\lambda) = 1, \tag{4.2.14}$$

thus the generators of $\mathcal{C}(Q_{A_1})$ are the bare monopoles $V_{\pm 1}$ and the complex-valued adjoint scalar λ:

$$\mathcal{G}_{\mathcal{C}} = \{\lambda,\ V_{+1},\ V_{-1}\}, \tag{4.2.15}$$

up to constants. More complex linear combinations are not allowed because (4.2.15) all have distinct topological charges: 0, +1 and −1 respectively. All other physical Coulomb branch operators $\mathcal{O}_{\mathcal{C}}$ (4.2.11) can be formed from products of (4.2.15) and consistent linear combinations thereof. □

[3] Note that since here the only Weyl group is the trivial group S_1, the V_m are equal to the v_m, as v_m are already physical.

4.2.2 Fixing the form of Poisson bracket relations using charge conservation

In the refined Hilbert series we grade the Coulomb branch operators by their charges under two global symmetries of the Coulomb branch: the conformal dimension Δ under $SU(2)_R$ ((2.4.20), (2.4.21)), and the topological charge $\boldsymbol{J}$ under the topological symmetry (2.4.24). These charges must be logically conserved under action with the Poisson bracket.

We know the Poisson bracket of a variety acts like two derivatives with respect to the variety's coordinates (4.2.24): it has "weight" -2 with respect to the degree of any function in these coordinates (see [20] for an intuitive physical reasoning for this). The Hilbert series counts the holomorphic functions (chiral operators) on the Coulomb branch, graded by a power of t equal to twice their conformal dimension, so the conformal dimension of the Poisson bracket between two Coulomb branch operators $\mathcal{O}_1$ and $\mathcal{O}_2$ should be

$$\Delta(\{\mathcal{O}_1,\mathcal{O}_2\}) = \Delta(\mathcal{O}_1) + \Delta(\mathcal{O}_2) - 1. \tag{4.2.16}$$

The Poisson bracket is a structure defined on the variety, independent of any gauge theory construction, and thus the magnetic charge $\boldsymbol{m}$ of the Poisson bracket itself should be zero. The magnetic charge of the result of a Poisson bracket between two Coulomb branch operators $\mathcal{O}_1$ and $\mathcal{O}_2$ should therefore be

$$\boldsymbol{J}(\{\mathcal{O}_1,\mathcal{O}_2\}) = \boldsymbol{J}(\mathcal{O}_1) + \boldsymbol{J}(\mathcal{O}_2). \tag{4.2.17}$$

Using (4.2.16) and (4.2.17), we can constrain which operators can lie in the result of our Poisson bracket, up to linear combinations.

Example As in Section 4.2.1, consider the example of the Coulomb branch of Q_{A_1} (2.6.14). Recall that here all the generators have conformal dimension 1

$$\begin{aligned}\Delta(\lambda) &= 1,\\ \Delta(V_{+1}) &= 1,\\ \Delta(V_{-1}) &= 1,\end{aligned} \tag{4.2.18}$$

and therefore, using (4.2.16), the Poisson bracket between any two generators from (4.2.15) must have conformal dimension

$$\Delta(\{\mathcal{G}_C,\mathcal{G}_C\}) = 1. \tag{4.2.19}$$

The topological charges of the generators (4.2.15) are

$$\begin{aligned}J(\lambda) &= 0,\\ J(V_{+1}) &= +1,\\ J(V_{-1}) &= -1,\end{aligned} \tag{4.2.20}$$

and so, using (4.2.17), the topological charges for all possible Poisson brackets between them are[4]

$$\begin{aligned} J(\{\lambda, V_{+1}\}) &= +1, \\ J(\{\lambda, V_{-1}\}) &= -1, \\ J(\{V_{+1}, V_{-1}\}) &= 0. \end{aligned} \tag{4.2.21}$$

Hence, using the constraints of (4.2.19) and (4.2.21), the Poisson brackets themselves must take the form

$$\begin{aligned} \{\lambda, V_{+1}\} &= c_1\, V_{+1}, \\ \{\lambda, V_{-1}\} &= c_2\, V_{-1}, \\ \{V_{+1}, V_{-1}\} &= c_3\, \lambda, \end{aligned} \tag{4.2.22}$$

for some constants c_1, c_2, c_3.[5] □

4.2.3 Fixing the remaining constants

Thus far we've discussed how to fix the general form of the Poisson brackets between generators using charge conservation, but now we'd like to find the explicit constants of proportionality (e.g. the c_1, c_2, c_3 in (4.2.22)). We can do this in one of two ways depending on the situation, as detailed in the Method at the start of Section 4.2: using the Poisson relations of the exact variety (if known), or demanding that each operator has the correct weight under the global symmetry.

4.2.3.1 Using the Poisson relations of the variety

We start with determining the Poisson brackets in the situation where the Coulomb branch of the quiver in question is a known variety $\mathcal{V}$ (i.e. $\mathcal{C}(Q) \equiv \mathcal{V}$) that is equipped with a canonical Poisson bracket. To establish the Poisson brackets between the generating monopoles in this case, we adhere to the following steps:

1. Explicitly write down the generators $\mathcal{G}_{\mathcal{V}}$ of $\mathcal{V}$ as holomorphic polynomials in its coordinates.

2. Calculate the Poisson bracket between these generators using the canonical Poisson bracket on the coordinates of $\mathcal{V}$.

3. Compare these with the "rough form" of the Poisson brackets between the generating monopoles found using the constraints of Section 4.2.2: identify which monopoles in $\mathcal{G}_{\mathcal{C}}$ correspond to which holomorphic polynomials in $\mathcal{G}_{\mathcal{V}}$, and declare their Poisson brackets to be those found in Step 2 above.

[4] Remember that by antisymmetry, the Poisson bracket of anything with itself is zero and the only relevant Poisson brackets to consider are those between all non-ordered pairs of distinct generators.

[5] These Poisson brackets indeed form a closed algebra as we would expect: $\{\cdot,\cdot\}$ acts as the Lie bracket of the global symmetry.

Example Recall that for the Coulomb branch of Q_{A_1} (2.6.14), $\mathcal{G}_{\mathcal{C}}$ were simply (4.2.15) or mulitples thereof. In this case however, we also know (via mirror symmetry and the Higgs branch construction [51, 48]) that

$$\mathcal{C}(Q_{A_1}) = \mathbb{C}^2/\mathbb{Z}_2, \tag{4.2.23}$$

i.e. here $\mathcal{V} = \mathbb{C}^2/\mathbb{Z}_2$. The coordinates on this variety are just inherited from those on $\mathbb{C}^2$, z_1 and z_2, as is the canonical Poisson bracket

$$\{z_1, z_2\} = 1. \tag{4.2.24}$$

Let's proceed with the steps above to find the Poisson brackets between $\mathcal{G}_{\mathcal{C}}$ by finding those between $\mathcal{G}_{\mathcal{V}}$:

1. The variety $\mathcal{V} = \mathbb{C}^2/\mathbb{Z}_2$ is simply comprised of the elements of $\mathbb{C}^2 = \mathbb{C}[z_1, z_2]$ which are invariant under the $\mathbb{Z}_2$ action

$$\begin{aligned} \mathbb{Z}_2 : z_1 &\to -z_1 \\ : z_2 &\to -z_2 \end{aligned} \tag{4.2.25}$$

   Thus we can clearly see that $\mathcal{V}$ is generated by

$$\mathcal{G}_{\mathcal{V}} = \{A = z_1 z_2\,,\ B = z_2^2\,,\ C = z_1^2\} \tag{4.2.26}$$

   up to constant factors.

2. We can then use the Leibniz property of the Poisson bracket and the canonical relation (4.2.24) to find the Poisson brackets between any pair of generators:

$$\begin{aligned} \{A, B\} &= 2\,B, \\ \{A, C\} &= -2\,C, \\ \{B, C\} &= -4\,A. \end{aligned} \tag{4.2.27}$$

3. Comparing (4.2.27) with (4.2.22), we can match the members of $\mathcal{G}_{\mathcal{V}}$ and $\mathcal{G}_{\mathcal{C}}$ as follows:

$$\begin{aligned} A &= \lambda, \\ B &= V_{+1}, \\ C &= V_{-1}, \end{aligned} \tag{4.2.28}$$

   and therefore we could conclude that

$$\begin{aligned} \{\lambda, V_{+1}\} &= 2\,V_{+1}, \\ \{\lambda, V_{-1}\} &= -2\,V_{-1}, \\ \{V_{+1}, V_{-1}\} &= -4\,\lambda. \end{aligned} \tag{4.2.29}$$

   Note that the constant factors here can be rescaled by redefining the generators by multiplication by a constant: we will do this in Section 4.2.3.2 to make the equivalence between the methods presented in that section and this one clear.

□

4.2.3.2 Demanding correct global symmetry weights

We now turn to Coulomb branches for which the exact variety $\mathcal{V}$, and canonical Poisson bracket thereof, is not known. In these cases we make headway with constructing the Poisson brackets between $\mathcal{G}_{\mathcal{C}}$ by inspecting the Hilbert series. We exploit the fact that the Poisson bracket acts on representations of the global symmetry as the Lie bracket: a Cartan element of the global symmetry is an eigenoperator of the Poisson bracket, with eigenvalue equal to the weight under the global symmetry of the operator it acts on.[6] Note that since it's an eigenoperator of $\{\cdot,\cdot\}$, a Cartan element must have $\Delta = 1$ and $\boldsymbol{J} = 0$.

Suppose that after completing Step 2 of the Method (as explained in Section 4.2.2), we found that a Poisson bracket between two generators was proportional to the Coulomb branch operator $\mathcal{O}$ (for example, in the case of $U(1)$ with 2 flavours we found that $\{\lambda, V_{+1}\}$ was proportional to $\mathcal{O} = V_{+1}$). Then the method to constrain the constant of proportionality is as follows:

1. First, find which monomial in the refined Hilbert series corresponds to $\mathcal{O}$.
2. Using an appropriate fugacity map (see Section 2.6.6), find which monomial in the character of the Coulomb branch global topological symmetry GS that this corresponds to, and hence deduce the weight of $\mathcal{O}$ under GS.
3. Define $r = \text{rank(GS)}$ Cartan elements, $C_1, ..., C_r$, as linear combinations of all possible Coulomb branch operators with $\Delta = 1$ and $\boldsymbol{J} = \boldsymbol{0}$.
4. Demand that the Poisson brackets $\{C_1, \mathcal{O}\}, \ldots, \{C_{rank(GS)}, \mathcal{O}\}$ yield the correct weight of $\mathcal{O}$ under GS (as found in Step 2), and solve for the constants in the problem (the constants of proportionality in the postulated Poisson brackets based on charge conservation, and the constants appearing in the linear combinations in $C_1, ..., C_r$).

Example Recall the "rough" (i.e. up to constants) Poisson relations (4.2.22) for the Coulomb branch generators (4.2.15) of Q_{A_1} (2.6.14) considered in the previous two subsections. To fix the constants of proportionality c_1, c_2, c_3 here, let's follow the steps above.

1. First, we find the monomials in the refined Hilbert series corresponding to each of λ, V_{+1}, V_{-1}, which all had $\Delta = 1$. Recall the monopole formula (2.6.7); for this quiver theory, the $\Delta = 1$ contribution to the Hilbert series is $(1 + z + z^{-1})\, t^2$. Matching the topological charges, it is clear that λ, V_{+1}, V_{-1} correspond to (up to constants) the monomials $1, z, z^{-1}$ in the refined Hilbert series.
2. The fugacity map
$$z \to x^2, \tag{4.2.30}$$
takes $(1 + z + z^{-1})\, t^2$ to the more familiar character of $[2]_{SU(2)}$ in the fundamental weight basis: $(1 + x^2 + x^{-2})\, t^2$. Recall from Section 2.6.2 that the t^2 term gives the adjoint character of the topological global symmetry: here $GS = SU(2)$. Note that $SU(2)$ is actually the local form of GS; its global form is actually $SU(2)/\mathbb{Z}_2$, as can be seen from the fact that no fermionic representations show up in the Hilbert series (4.2.12). As we do not make use of this global

[6] We thank the referee for pointing out that this also follows from the fact that the Casimir elements are the complex moment maps for the topological symmetry.

form, we refer to GS simply as its local form $SU(2)$ in the subsequent discussion.[7] Under such a map (4.2.30), the physical Coulomb branch generators λ, V_{+1} and V_{-1} have charges 0, +2 and −2 respectively under GS.

3. The rank of the global symmetry here is $\text{rank}(SU(2)) = 1$, and so we need to just define one Cartan element C_1 in the Lie algebra of GS, $\mathfrak{su}(2)$. Only one Coulomb branch operator satisfies $\Delta = 1$ and $m = 0$: λ. So the Cartan operator here must be

$$C_1 = \alpha\,\lambda \tag{4.2.31}$$

for some constant $\alpha \in \mathbb{C}$.

4. Finally we need to demand that the Poisson bracket, which takes the role of the Lie bracket of the complexification of the Lie algebra of the $SU(2)$ global symmetry on the Coulomb branch $\mathfrak{su}(2)_{\mathbb{C}} = \mathfrak{sl}(2;\mathbb{C})$, yields the correct charges of our Coulomb branch generators under this global symmetry (as determined in Step 2):

$$\begin{aligned} \{C_1, \lambda\} &\equiv 0, \\ \{C_1, V_{+1}\} &\equiv +2\,V_{+1}, \\ \{C_1, V_{-1}\} &\equiv -2\,V_{-1}. \end{aligned} \tag{4.2.32}$$

Substituting in our expression for the Cartan element (4.2.31) and using the solved Poisson bracket results fixed up to constants found in Section 4.2.2 (4.2.22), we find that the first of (4.2.32) is automatically satisfied, and solving the second two amounts to

$$\begin{aligned} \alpha\,\{\lambda, V_{+1}\} &= +2\,V_{+1} = \alpha\,c_1\,V_{+1}, \\ \alpha\,\{\lambda, V_{-1}\} &= -2\,V_{-1} = \alpha\,c_2\,V_{-1}, \end{aligned} \tag{4.2.33}$$

i.e.

$$c_1 = -c_2. \tag{4.2.34}$$

Several α, c_1, c_2, c_3 satisfy this, but we will pick values so that we can make the following identification of λ, V_{+1}, V_{-1} with the canonical symmetric generators of $\mathfrak{sl}(2;\mathbb{C})$:

$$\lambda = \begin{pmatrix} 0 & 1 \\ 1 & 0 \end{pmatrix}, \quad V_{+1} = \begin{pmatrix} 0 & 0 \\ 0 & 1 \end{pmatrix}, \quad V_{-1} = \begin{pmatrix} 1 & 0 \\ 0 & 0 \end{pmatrix}. \tag{4.2.35}$$

The Poisson bracket acts on these 2×2 matrices as a commutator (see the discussion preceeding (4.2.39) for more details), and so we can compute:

$$\begin{aligned} \{\lambda, V_{+1}\} &= 2\,V_{+1}, \\ \{\lambda, V_{-1}\} &= -2\,V_{-1}, \\ \{V_{+1}, V_{-1}\} &= -\lambda. \end{aligned} \tag{4.2.36}$$

[7] Throughout the rest of this chapter, continuing the form of the whole thesis, we will not specify the global form of the global symmetry $GS \times SU(2)_R$. We provide the terminating PL(HS) or PL(HWG) of all quivers we study, and this inherently contains the information of the global form of $GS \times SU(2)_R$, as it tells us exactly what representations show up. To write down the global form from this does not take much work, and since it will not be of use to us in our study of Poisson brackets we opt not to include it.

Thus we pick α, c_1, c_2, c_3 to be

$$\alpha = 1,\ c_1 = +2,\ c_2 = -2,\ c_3 = -1, \tag{4.2.37}$$

so that the Poisson brackets between the generators of our Coulomb branch (4.2.22) match those between the generating symmetric matrices of $\mathfrak{sl}(2;\mathbb{C})$ (4.2.36).

□

The Poisson brackets we have computed in this section (4.2.36) may look different from those in Section 4.2.3.1 (4.2.29), but infact they are equivalent by a redefinition of generators: if in (4.2.29) we rescale the generators as

$$\begin{aligned} \lambda &\to \lambda, \\ V_{+1} &\to \frac{1}{2} V_{+1}, \\ V_{-1} &\to \frac{1}{2} V_{-1}, \end{aligned} \tag{4.2.38}$$

then we recover the relations (4.2.36).

The form of the generators of $\mathfrak{sl}(2;\mathbb{C})$ used in (4.2.35) is worth a comment. Often $\mathfrak{sl}(2;\mathbb{C})$ is viewed as the $n = 2$ version of $\mathfrak{sl}(n;\mathbb{C})$; generated by traceless $n \times n$ matrices, which (4.2.35) obviously are not. However, since the fundamental of $\mathfrak{sl}(2;\mathbb{C})$ is pseudo-real, not complex, and the adjoint is the second rank symmetric of the fundamental, not the product of the fundamental with the anti-fundamental minus the trace (in $\mathfrak{sl}(2;\mathbb{C})$ there is no concept of anti-fundamental, or "up vs down" indices), it is more natural to think of $\mathfrak{sl}(2;\mathbb{C})$ matrices as being 2×2 symmetric matrices instead. The obvious generators for such matrices are (4.2.35). The only invariant of $\mathfrak{sl}(2;\mathbb{C})$ when viewed in this way is $\epsilon_{\alpha\beta}$ (the δ invariant that exists for all $\mathfrak{sl}(n;\mathbb{C})$ can be expressed in terms of the ϵ for $n = 2$), and so matrix multiplication is done with contraction by ϵ. For example, the Poisson bracket between the $\mathfrak{sl}(2;\mathbb{C})$ matrices identified with λ and V_{+1} is:

$$\{\lambda, V_{+1}\}_{\alpha\beta} = [\lambda, V_{+1}]_{\alpha\beta} = \lambda_{\alpha\gamma}\epsilon_{\gamma\delta}(V_{+1})_{\delta\beta} - (V_{+1})_{\alpha\gamma}\epsilon_{\gamma\delta}\lambda_{\delta\beta}. \tag{4.2.39}$$

We now move on to detail the results of such calculations for Coulomb branches that are free, Klein singularities and nilpotent orbits in Sections 4.3, 4.4 and 4.5 respectively. The former two use Step 3.*a*) in the Method at the top of Section 4.2 (the topic of Section 4.2.3.1), while the latter uses Step 3.*b*) (the topic of this section).

4.3 Free Spaces

The first type of Coulomb branches we consider are those which are free, in the sense that they are some number of copies of the quaternionic plane: $\mathcal{C} = \mathbb{H}^k$. These are the simplest cases to consider, as the generators of $\mathbb{H}^k = (\mathbb{C}^2)^k$ are in the fundamental representation of the global symmetry $Sp(k)$, and the Poisson brackets between them are trivially inherited from those on each copy of $\mathbb{C}^2$ (4.1.3). We can logically extend this structure for the $k = 1$ case to $k > 1$ by fixing a complex structure,

$$\mathbb{H}^k \cong (\mathbb{C}^2)^k \cong \prod_{i=1}^{d} \mathbb{C}[z_{i,1}, z_{i,2}], \tag{4.3.1}$$

and equipping its $2k$ complex generators $z_{i,a}$ for $i = 1, ..., k$ and $a = 1, 2$ with Poisson brackets

$$\{z_{i,a}, z_{j,b}\} = \delta_{ij}\epsilon_{ab}. \tag{4.3.2}$$

This notation is less useful however, as the i and j indices are not antisymmetrised. It is more convenient to label the $2k$ generators in the standard way for the fundamental representation of $Sp(k)$: with a single index taking values from $1, ..., 2k$. The Poisson bracket between two such generators z_α and z_β is then just

$$\{z_\alpha, z_\beta\} = \Omega_{\alpha\beta}, \tag{4.3.3}$$

where $\alpha, \beta = 1, ..., 2k$, and the $2k \times 2k$ matrix $\Omega_{\alpha\beta}$ is the invariant skew-symmetric two-form of $Sp(k)$, which we take to be

$$\Omega_{\alpha\beta} = \begin{pmatrix} \mathbf{0} & \mathbb{1} \\ -\mathbb{1} & \mathbf{0} \end{pmatrix}, \tag{4.3.4}$$

where each entry is a $k \times k$ block matrix.

4.3.1 Coulomb quivers for free spaces

A family of simple unframed quivers whose Coulomb branches are $\mathbb{H}^k$ can be formed by removing the affine node from the balanced affine Dynkin quiver of any Lie group G for which $h^\vee_G = k + 2$.[8] We call such quivers *Dynkin quivers of finite type*, and denote the one corresponding to G with D_G. They are drawn explicitly in Table 4.3.1.

The method to compute the Poisson brackets for the dressed monopole operators generating the Coulomb branch $\mathcal{G}_\mathcal{C}$ is the same for all quivers in Table 4.3.1 and is fairly trivial. We illustrate the process with one example, D_{D_5}, to introduce and walk through some of the notions discussed in Section 4.2.

4.3.2 Example: $\mathbb{H}^6 = \mathcal{C}(\mathsf{D}_{D_5})$

The D_{D_5} quiver is given by[9]

D_{D_5} = 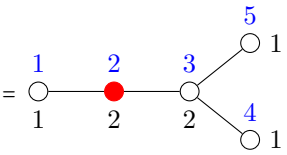

, (4.3.5)

where the black labels are the ranks of the unitary gauge nodes and the blue labels are names to distinguish between the nodes (we will make use of these shortly). The Coulomb branch here is entirely free ($\mathbb{H}^6$), as showcased by its Hilbert series,

$$HS(\mathcal{C}(\mathsf{D}_{D_5})) = PE[\,[1,0,0,0,0,0]_{Sp(6)}\,t\,]. \tag{4.3.6}$$

In particular, its only generators lie in the fundamental representation of $Sp(6)$. The global symmetry group expected from the balance of the quiver (the BGS [10]) is embedded inside the observed

[8] If G is a Lie group, $h^\vee_G$ is called the dual coxeter number of G. It is equal to the sum of the entries of the vector whose dot product with the simple roots of the corresponding Lie algebra $\mathfrak{g}$ gives the highest root of $\mathfrak{g}$. Equivalently $h^\vee_G$ is the sum of the node ranks on the affine quiver of G. The affine quiver of G is the quiver in the shape of the affine Dynkin diagram of G, with node ranks equal to the smallest possible positive integers which render it balanced. The affine quivers are listed for example in Table 1 of [10], where also the notion of balance is explained in Section 2.1.

[9] A red node indicates an unabalanced node. Here the excess is -1.

Lie Group G	Dynkin Quiver D_G	Coulomb Branch
A_k	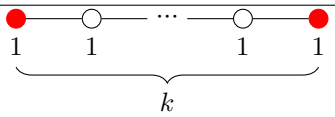	$\mathbb{H}^{k-1}$
B_k $k \geq 3$	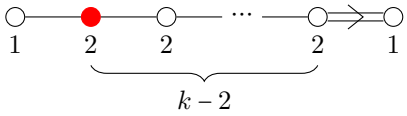	$\mathbb{H}^{2k-3}$
C_k $k \geq 2$	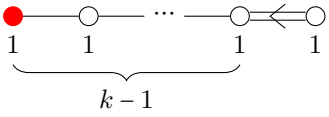	$\mathbb{H}^{k-1}$
D_k $k \geq 4$	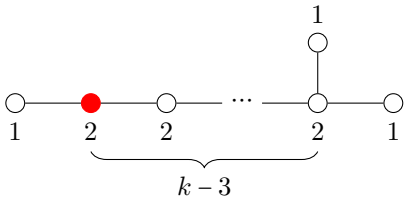	$\mathbb{H}^{2k-4}$
E_6	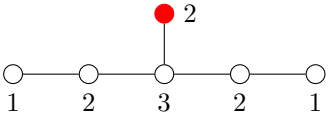	$\mathbb{H}^{10}$
E_7	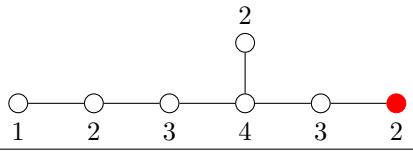	$\mathbb{H}^{16}$
E_8	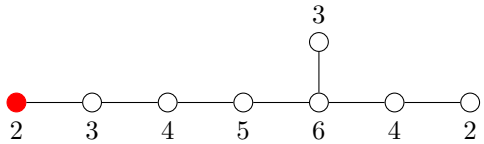	$\mathbb{H}^{28}$
F_4	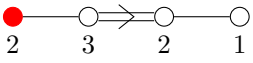	$\mathbb{H}^{7}$
G_2	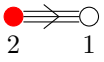	$\mathbb{H}^{2}$

Table 4.3.1: Dynkin quivers of finite type. The quiver in the central column is the Dynkin quiver for the Lie group in the left-hand column. The Coulomb branch variety of this quiver, after ungauging the diagonal $U(1)_d$ (see Section 2.6.5), is listed in the right hand column. Red nodes are those which are unbalanced. All unbalanced nodes in this table have an excess of −1; they are all ugly quivers [4].

global symmetry $SU(2)\times SU(4) \hookrightarrow Sp(6)$. More generally, for D_{D_k} (shown in the fourth row of Table 4.3.1), there is an embedding of the BGS $SU(2)\times SO(2k-4)$ inside the observed global symmetry $Sp(2k-4)$. The Coulomb branch of D_{D_k} is $\mathbb{H}^{2k-4}$; we can deduce this quaternionic dimension $2k-4$ as half the complex dimension, given by the degrees of freedom in the unbalanced node. This node is connected to the only node of the balanced $SU(2)$ Dynkin diagram to its left and the vector node of the balanced $SO(2k-4)$ Dynkin diagram to its right; it lies in the representation formed from the product of the fundamental of $SU(2)$ and the vector of $SO(2k-4)$, and thus has $2\cdot(2k-4)=4k-8$ complex degrees of freedom. The quaternionic dimension of the corresponding space is then half of this: $2k-4$. In this case, $k=5$ and we see from the above that the quaternionic dimension of the Coulomb branch is $2\cdot 5-4=6$, which matches that of $\mathbb{H}^6$ as expected.

We will concretely demonstrate how to compute the Poisson brackets for the generating Coulomb branch operators of these theories, following steps $1,2,3.a)$ of the Method, as outlined in Sections 4.2.1 - 4.2.3.1.

4.3.2.1 Writing down $\mathcal{G}_{\mathcal{C}}$

We start with Step 1 of the Method: writing down the dressed monopole operators that generate the Coulomb branch explicitly.

Recall from (4.3.6) that the generators all lie at order t in the Hilbert series; they have conformal dimension $\Delta=\frac{1}{2}$. This means no adjoint scalars can be generators as they have $\Delta=1$; physical bare monopoles V generate $\mathcal{C}$ and the adjoint scalars are formed as bilinears in these V. Thus we need to find which operators on the Coulomb branch of the quiver theory (4.3.5) have $\Delta=\frac{1}{2}$. The magnetic charge of a monopole operator takes the form of (2.4.13) for $p=5$, $\{n_1,...,n_5\}=\{1,2,2,1,1\}$: $\boldsymbol{m}=(\boldsymbol{m_1},\boldsymbol{m_2},\boldsymbol{m_3},\boldsymbol{m_4},\boldsymbol{m_5})=(m_{1,1},m_{2,1},m_{2,2},m_{3,1},m_{3,2},m_{4,1},m_{5,1})$. Demanding the correct conformal dimension of the generating bare monopole operators in this theory amounts to setting:

$$\begin{aligned}\frac{1}{2}=\Delta=&-|m_{2,1}-m_{2,2}|-|m_{3,1}-m_{3,2}|+\frac{1}{2}(|m_{1,1}-m_{2,1}|+|m_{1,1}-m_{2,2}|+|m_{2,1}-m_{3,1}|\\&+|m_{2,1}-m_{3,2}|+|m_{2,2}-m_{3,1}|+|m_{2,2}-m_{3,2}|+|m_{3,1}-m_{4,1}|+|m_{3,2}-m_{4,1}|\\&+|m_{3,1}-m_{5,1}|+|m_{3,2}-m_{5,1}|),\end{aligned}\tag{4.3.7}$$

and so we need to find the $\boldsymbol{m}$ which solve (4.3.7). The number of solutions can be reduced by the restrictions we impose on $\boldsymbol{m}$: recall that we need to (a) ungauge (see Section 2.6.5), and (b) only find solutions to (4.3.7) in one Weyl chamber, as physical bare monopole operators $V_{\boldsymbol{m}}$ are the sum of all unphysical bare monopoles $v_{\tilde{\boldsymbol{m}}}$ with magnetic charge $\tilde{\boldsymbol{m}}$ in the Weyl orbit of $\boldsymbol{m}$ (4.2.1). Explicitly, the constraints these conditions impose on $\boldsymbol{m}$ are

$$\begin{aligned}&(a)\ m_{1,1}=0,\\&(b)\ m_{1,1}\geq 0,\\&\quad m_{2,1}\geq m_{2,2}\geq 0,\\&\quad m_{3,1}\geq m_{3,2}\geq 0,\\&\quad m_{4,1}\geq 0,\\&\quad m_{5,1}\geq 0,\end{aligned}\tag{4.3.8}$$

respectively. The solutions to (4.3.7) satisfying (4.3.8) are

$$(m_{2,1}, m_{2,2}, m_{3,1}, m_{3,2}, m_{4,1}, m_{5,1}) = \begin{cases} (0,-1,-1,-1,-1,-1) \\ (0,-1,0,-1,-1,-1) \\ (0,-1,0,-1,-1,0) \\ (0,-1,0,-1,0,-1) \\ (0,-1,0,-1,0,0) \\ (0,-1,0,0,0,0) \\ (1,0,0,0,0,0) \\ (1,0,1,0,0,0) \\ (1,0,1,0,0,1) \\ (1,0,1,0,1,0) \\ (1,0,1,0,1,1) \\ (1,0,1,1,1,1) \end{cases} . \tag{4.3.9}$$

This gives us twelve unphysical bare monopoles $v_{\boldsymbol{m}}$ each in distinct Weyl orbits, and hence acting with the Weyl group $S_2 \times S_2 \times S_1 \times S_1$ (where S_n is the finite symmetric group of order n) on each of these will give us the twelve physical bare monopoles that generate the Coulomb branch. That is, our twelve generators for $\mathcal{C}(\mathsf{D}_{D_5})$ are:[10]

$$\mathcal{G}_{\mathcal{C}} = \begin{cases} V_{\pm 100000} = v_{\pm 100000} + v_{0 \pm 10000} \\ V_{\pm 10 \pm 1000} = v_{\pm 10 \pm 1000} + v_{0 \pm 1 \pm 1000} + v_{\pm 100 \pm 100} + v_{0 \pm 10 \pm 100} \\ V_{\pm 10 \pm 100 \pm 1} = v_{\pm 10 \pm 100 \pm 1} + v_{0 \pm 1 \pm 100 \pm 1} + v_{\pm 100 \pm 10 \pm 1} + v_{0 \pm 10 \pm 10 \pm 1} \\ V_{\pm 10 \pm 10 \pm 10} = v_{\pm 10 \pm 10 \pm 10} + v_{0 \pm 1 \pm 100 \pm 10} + v_{\pm 100 \pm 1 \pm 10} + v_{0 \pm 10 \pm 1 \pm 10} \\ V_{\pm 10 \pm 10 \pm 1 \pm 1} = v_{\pm 10 \pm 10 \pm 1 \pm 1} + v_{0 \pm 1 \pm 10 \pm 1 \pm 1} + v_{\pm 100 \pm 1 \pm 1 \pm 1} + v_{0 \pm 10 \pm 1 \pm 1 \pm 1} \\ V_{\pm 10 \pm 1 \pm 1 \pm 1 \pm 1} = v_{\pm 10 \pm 1 \pm 1 \pm 1 \pm 1} + v_{0 \pm 1 \pm 1 \pm 1 \pm 1 \pm 1} \end{cases} , \tag{4.3.10}$$

up to constants.[11]

4.3.2.2 Constraining Poisson brackets by charge conservation

Next we will constrain the results of the Poisson brackets between unordered pairs of these generators using conservation of conformal dimension and magnetic charge, as discussed in Section 4.2.2.

Using (4.2.16), we see that imposing Δ-conservation tells us that for any $V_1, V_2 \in \mathcal{G}_{\mathcal{C}}$,

$$\Delta(\{V_1, V_2\}) = 0. \tag{4.3.11}$$

This tells us that the Poisson brackets between any two of the $\mathcal{G}_{\mathcal{C}}$ must be proportional to operators with charge $\Delta = 0$ under the R-symmetry. The Hilbert series tells us that there is only one such

[10] In this case, ungauging on node 1, there are the exact same number of solutions to (4.3.7) as there are generators (the coefficient of t in the unrefined HS is indeed twelve), and so no two solutions (4.3.9) will give the same $V_{\boldsymbol{m}}$: there are no duplicate solutions to delete. If we had chosen to ungauge on a different node however, there would have been more than twelve solutions to (4.3.7) satisfying (4.3.8), yielding duplicates upon action by the Weyl group, all but one of which we would then need to delete. Hence ungauging on node 1 is computationally simplest.

[11] No two operators in (4.3.10) have matching topological chargers, so the only valid linear combinations are multiples of (4.3.10) by a constant.

operator: the identity. So $\{V_1, V_2\}$ must be proportional to the identity. This agrees with (4.3.3) which says that the brackets should have value either ± 1 or 0.

To determine which Poisson brackets vanish and which do not, we invoke the conservation of topological charge. Recalling the topological charge for a physical monopole operator (2.4.24), we can see that the topological charges of our $\mathcal{G}_{\mathcal{C}}$ are

$$\begin{aligned} \boldsymbol{J}(V_{\pm 100000}) &= (\pm 1, 0, 0, 0), \\ \boldsymbol{J}(V_{\pm 10 \pm 1000}) &= (\pm 1, \pm 1, 0, 0), \\ \boldsymbol{J}(V_{\pm 10 \pm 100 \pm 1}) &= (\pm 1, \pm 1, 0, \pm 1), \\ \boldsymbol{J}(V_{\pm 10 \pm 10 \pm 10}) &= (\pm 1, \pm 1, \pm 1, 0), \\ \boldsymbol{J}(V_{\pm 10 \pm 10 \pm 1 \pm 1}) &= (\pm 1, \pm 1, \pm 1, \pm 1), \\ \boldsymbol{J}(V_{\pm 10 \pm 1 \pm 1 \pm 1 \pm 1}) &= (\pm 1, \pm 2, \pm 1, \pm 1). \end{aligned} \tag{4.3.12}$$

Above, we saw that any non-zero result result of a Poisson bracket between two generators V_1 and V_2 should be proportional to the identity operator and thus have zero topological charge. Thus we can see from (4.2.17) that the only pairs of operators that can have non-zero Poisson pairing are those with equal and opposite magnetic charges. That is

$$\{V_{\boldsymbol{m}}, V_{\tilde{\boldsymbol{m}}}\} = \begin{cases} c_{\boldsymbol{m},\tilde{\boldsymbol{m}}} = -c_{\tilde{\boldsymbol{m}},\boldsymbol{m}} & \text{if } \boldsymbol{m} = -\tilde{\boldsymbol{m}} \\ 0 & \text{if } \boldsymbol{m} \neq -\tilde{\boldsymbol{m}} \end{cases} \tag{4.3.13}$$

for some antisymmetric constant $c_{\boldsymbol{m},\tilde{\boldsymbol{m}}}$.

4.3.2.3 Fixing the constants using the Poisson brackets of $(\mathbb{C}^2)^6$

We now compare the relations (4.3.13) to those we expect of $\mathbb{H}^6$, which recall are (4.3.3) for $k = 6$. It is clear that $|c_{\boldsymbol{m},-\boldsymbol{m}}| = 1$, but it is up to us which operator of $V_{\boldsymbol{m}}$ and $V_{-\boldsymbol{m}}$ to associate to with z_α for some $\alpha = 1, ..., 6$, and which to associate with the corresponding $z_{\alpha+6}$. We'll choose to assign each $\boldsymbol{m} \in \mathbb{Z}^6_{\geq 0}$ in (4.3.9) a different $\alpha = 1, ..., 6$. This fixes the corresponding $-\boldsymbol{m} \in \mathbb{Z}^6_{\leq 0}$ to be assigned to $z_{\alpha+6}$, and gives the following Poisson brackets for the generating dressed monopoles $V_{\boldsymbol{m}}$ of D_{D_5}:

$$\{V_{\boldsymbol{m}}, V_{\tilde{\boldsymbol{m}}}\} = \begin{cases} 1 & \text{if } \boldsymbol{m} = -\tilde{\boldsymbol{m}} \in \mathbb{Z}^6_{\geq 0} \\ -1 & \text{if } \boldsymbol{m} = -\tilde{\boldsymbol{m}} \in \mathbb{Z}^6_{\leq 0} \\ 0 & \text{otherwise} \end{cases}, \tag{4.3.14}$$

recovering the exact structure of $\mathbb{H}^6$ given in (4.3.3).

4.4 Klein Singularities

We now turn our heads to Klein singularities. The results we arrive at here have previously been deduced with alternative methods, see for example [87, 88, 89]. We rederive them here from our perspective, using the method of Section 4.2.

Klein singularities are varieties $\mathcal{V} = \mathbb{C}^2/\Gamma$; they are quotients of $\mathbb{C}^2$ by a finite subgroup of its global symmetry $\Gamma \subset SU(2)$. An exhaustive list of such subgroups are in one to one correspondence with

the affine ADE Dynkin diagrams [90, 91] and as such we often denote $\mathbb{C}^2/\Gamma$ instead by the capital letter of the ADE diagram it corresponds to, with its rank as subscript. In particular, the full list of Klein singularities can be denoted as follows:

$$A_k, \quad D_k, \quad E_6, \quad E_7, \quad E_8. \tag{4.4.1}$$

The generators $\mathcal{G}_\Gamma$ of the subgroups $\Gamma \subset SU(2)$ are listed on page 14 of [92] as 2×2 matrices, which we can think of as acting on the vector containing the complex coordinates of $\mathbb{C}^2$:

$$\begin{pmatrix} z_1 \\ z_2 \end{pmatrix}. \tag{4.4.2}$$

The elements of the corresponding Klein singualrity $\mathbb{C}^2/\Gamma$ (4.4.1) will then just be the elements of $\mathbb{C}^2$ (i.e. polynomials in z_1, z_2) which are invariant under action by any product of these Γ generators.

The Hilbert series of these Klein singularities is also listed in [92]; the degree of their generators can be found by taking the plethystic logarithm. We can then explicitly construct these generators $\mathcal{G}_\mathcal{V}$ by finding the monomials of $\mathbb{C}^2$ which are: invariant under the action of Γ; of the correct polynomial degree; and irreducible (i.e. not generated by a product of elements of $\mathbb{C}^2/\Gamma$ of lower degrees). Each Klein singularity has 3 such generators

$$|\mathcal{G}_\mathcal{V}| = 3, \tag{4.4.3}$$

and they satisfy a relation which is termed the *defining relation* of the singularity, also given in [92].[12] The Poisson brackets between these generators can be computed using $\{\cdot,\cdot\}_{\mathbb{C}^2}$, the inherited canonical Poisson bracket of $\mathbb{C}^2$ (4.2.24). This can then be used to identify the Poisson brackets between the dressed monopole generators $\mathcal{G}_\mathcal{C}$ for the Coulomb quiver of $\mathcal{V} = \mathbb{C}^2/\Gamma$, as in Step 3.$a$) of the Method.

We found that the Poisson brackets of $\mathcal{G}_\mathcal{V}$ for all Klein singularities (4.4.1), including the $E_{6,7,8}$ cases, can be summed up by the same succinct formula: if we call g_1, g_2, g_3 the generators and $E(g_1, g_2, g_3)$ the defining equation for $\mathbb{C}^2/\Gamma$, then

$$\{g_i, g_j\} = \epsilon_{ijk} \frac{\partial E}{\partial g_k}. \tag{4.4.4}$$

It is worth noting that the explicit form of a defining relation is not fixed inherently: a change of variables would alter it. However, imposing the Poisson brackets (4.4.4) fully fixes the defining equation and vice versa.

Since it is only the cases of A_k and D_k for which Coulomb quivers are known, it is just these that we will restrict our study to in the remainder of this chapter. The Higgs quivers for $E_{6,7,8}$ are known, and the Poisson brackets of the generators of the Higgs branch of these quivers can be found, but we do not cover this here as our goal is to focus on the Poisson brackets of Coulomb branch generators. In Section 4.4.1, we spell out the full steps of this process and derive the $\mathcal{G}_\mathcal{C}$ Poisson brackets for the Coulomb quiver of A_k. In Section 4.4.2, we jump straight to the result for the Coulomb quiver of D_k.

4.4.1 A type

The cyclic subgroup $\Gamma = \mathbb{Z}_{k+1} \subset SU(2)$ corresponds to the affine A_k Dynkin diagram, and hence $\mathbb{C}^2/\mathbb{Z}_{k+1} = A_k$ is referred to as the A type Klein singularity. Analogously to how the Coulomb quiver

[12] Note that by a change of variables the precise form of this equation can be modified.

for $\mathbb{C}^2/\mathbb{Z}_2 = A_1$ was Q_{A_1} (2.6.14), the Coulomb quiver of A_k ($k \geq 1$) is given by SQED with $k+1$ electrons, Q_{A_k}:[13]

$$Q_{A_k} = \underset{1}{\bigcirc}\!\!-\!\!\!-\!\!\underset{k+1}{\square} \quad . \tag{4.4.5}$$

We will first derive the Poisson brackets of the generators $\mathcal{G}_\mathcal{V}$ of the abstract variety $\mathcal{V} = A_k$ as described at the top of Section 4.4, before using this to do the same for the generating dressed monopoles $\mathcal{G}_\mathcal{C}$ of the Coulomb quiver (4.4.5).

4.4.1.1 Poisson brackets for the abstract variety

Here we simply view A_k as the set of polynomials in two complex variables invariant under action by $\mathbb{Z}_{k+1}$.

The first step is to find the generators of A_k. By taking the plethystic logarithm of the Hilbert series listed in [92], we can see that the three generators are of degrees 2, $k+1$ and $k+1$:

$$PL(HS(A_k)) = t^2 + (q + \frac{1}{q})t^{k+1} - t^{2k+2}. \tag{4.4.6}$$

In general to find the holomorphic functions corresponding to the degree d generators of $\mathbb{C}^2/\Gamma$, we take all monomials in our complex coordinates z_1, z_2 of degree d, and for each one we total the results of the action on them by each Γ group element. This construct invariants of Γ in $\mathbb{C}^2$, and thus of $\mathbb{C}^2/\Gamma$. A vanishing result tells us the starting monomial was not an invariant.

To find the holomorphic functions corresponding to the degree d generators of A_k, we construct the degree d monomials in z_1, z_2 which are invariant under $\mathbb{Z}_{k+1}$. The generator of $\mathbb{Z}_{k+1}$ is

$$C = \begin{pmatrix} \omega_{k+1} & 0 \\ 0 & \omega_{k+1}^{-1} \end{pmatrix}, \tag{4.4.7}$$

where $\omega_k = e^{\frac{2\pi i}{k}}$, and thus under the $\mathbb{Z}_{k+1}$ action,

$$\begin{aligned} z_1 &\to e^{\frac{2\pi i}{k+1}} z_1, \\ z_2 &\to e^{-\frac{2\pi i}{k+1}} z_2. \end{aligned} \tag{4.4.8}$$

The irreducible invariants under this action at degree 2 and $k+1$ are

$$\begin{aligned} \mathcal{G}_\mathcal{V} &= \{z_1\, z_2,\ z_1^{k+1},\ z_2^{k+1}\} \\ &\equiv \{g_1',\ g_2',\ g_3'\}, \end{aligned} \tag{4.4.9}$$

and so these are our generators.[14] The generators g_1', g_2', g_3' clearly satisfy the equation

$$E'(g_1', g_2', g_3') = {g_1'}^{k+1} - g_2'\, g_3' = 0. \tag{4.4.10}$$

[13] You may also see this quiver with the flavour node labelled as $SU(k+1)$: recall from Section 2.2 that this is because there is an $SU(k+1)$ symmetry rotating the $k+1$ identical hypermultiplets. This is a symmetry of the Higgs branch, so it does not play a part in our discussion.

[14] We use primed variables here as we will have to redefine them by a constant to achieve the relation (4.4.4), and we will use the corresponding unprimed variable for these to match with those used in that relation.

The Poisson brackets between these generators can easily be calculated using (4.2.24):

$$\begin{aligned}\{g_1', g_2'\} &= -(k+1)\, g_2',\\ \{g_1', g_3'\} &= (k+1)\, g_3',\\ \{g_2', g_3'\} &= (k+1)^2\, {g_1'}^k.\end{aligned} \tag{4.4.11}$$

We can see that if we rescale our generators to the following g_1, g_2, g_3

$$\begin{aligned}g_1 &= \frac{1}{k+1}\, g_1' = \frac{1}{k+1}\, z_1\, z_2,\\ g_2 &= \frac{1}{(k+1)^{\frac{k+1}{2}}} g_2' = \frac{1}{(k+1)^{\frac{k+1}{2}}} z_1^{k+1},\\ g_3 &= \frac{1}{(k+1)^{\frac{k+1}{2}}} g_3' = \frac{1}{(k+1)^{\frac{k+1}{2}}} z_2^{k+1},\end{aligned} \tag{4.4.12}$$

then we find they satisfy the same defining equation as the g_i':

$$E(g_1, g_2, g_3) = E'(g_1, g_2, g_3) = g_1^{k+1} - g_2 g_3 = 0, \tag{4.4.13}$$

and indeed that

$$\{g_i, g_j\} = \epsilon_{ijk} \frac{\partial}{\partial g_k} E(g_1, g_2, g_3) \tag{4.4.14}$$

as claimed in (4.4.4).

4.4.1.2 Poisson brackets for the dressed monopoles of the Coulomb quiver

We now make a connection with physics: we view A_k as the Coulomb branch of Q_{A_k} (4.4.5) and find the Poisson brackets $\{\cdot,\cdot\}_{\mathcal{C}}$ of $\mathcal{G}_{\mathcal{C}}$ following Steps $1-3.a)$ of the Method.

For Step 1, we need the generating dressed monopoles $\mathcal{G}_{\mathcal{C}}$. Recall that the Hilbert series for $\mathcal{C}(Q_{A_k})$ has plethystic logarithm given by (4.4.6). In particular, the generating dressed monopoles $\mathcal{G}_{\mathcal{C}}$ have conformal dimensions 1, $\frac{k+1}{2}$ and $\frac{k+1}{2}$. Following the same method as in Section 4.2.1, we find that the gauge invariant dressed monopoles generating the Coulomb branch are

$$\mathcal{G}_{\mathcal{C}} = \{\lambda,\ V_{+1},\ V_{-1}\}, \tag{4.4.15}$$

up to constant multiples.

Step 2 then tells us to constrain the $\{\mathcal{G}_{\mathcal{C}}, \mathcal{G}_{\mathcal{C}}\}_{\mathcal{C}}$ via charge conservation. Following the same ideas as illustrated in previous examples, this tells us

$$\begin{aligned}\{\lambda, V_{+1}\} &\propto V_{+1},\\ \{\lambda, V_{-1}\} &\propto V_{-1},\\ \{V_{+1}, V_{-1}\} &\propto \lambda^k.\end{aligned} \tag{4.4.16}$$

Finally, we fix $\{\cdot,\cdot\}_{\mathcal{C}}$ by comparing $\mathcal{G}_{\mathcal{C}}$ (4.4.15) with the generators of the abstract variety $\mathcal{G}_{\mathcal{V}}$ (4.4.12). We can see that if we declare that

$$\begin{aligned}\{\lambda, V_{+1}\} &= V_{+1},\\ \{\lambda, V_{-1}\} &= -V_{-1},\\ \{V_{+1}, V_{-1}\} &= \lambda^k,\\ V_{+1}V_{-1} &= -\frac{\lambda^{k+1}}{k+1}\end{aligned} \tag{4.4.17}$$

(which are consistent with (4.2.16) and (4.2.17)), then the following linear combinations of $\mathcal{G}_{\mathcal{C}}$

$$\begin{aligned}g_1 &= -\lambda,\\ g_2 &= (-1)^{\frac{k}{2}}\sqrt{k+1}V_{+1},\\ g_3 &= (-1)^{\frac{k}{2}}\sqrt{k+1}V_{-1},\end{aligned} \tag{4.4.18}$$

satisfy the same defining equation (4.4.13) and Poisson bracket relations (4.4.4) as $\mathcal{G}_{\mathcal{V}}$: our declaration of the Poisson brackets between generators (4.4.17) for this Coulomb branch is valid. The Poisson bracket between any two operators on $\mathcal{C}(Q_{A_k})$ can then be deduced from (4.4.17).

4.4.2 D type

The Coulomb quiver for the D type Klein singularity D_k is:[15]

$$Q_{D_k} = \quad \underset{SU(2)}{\bigcirc}\!\!-\!\!\!-\underset{k}{\square}\ , \tag{4.4.19}$$

for $k \geq 4$. Note that this is not a unitary quiver, so many formulae given in Chapter 2 and elsewhere do not apply here. For example, there is no UV $U(1)$ topological symmetry (2.4.23), and one must use (2.4.19) as opposed to (2.4.20) for computing the conformal dimension. Since this is the only non-unitary quiver upon which we perform Coulomb branch computations and its Hilbert series is given in [92], we do not detail how to compute the monopole formula for this quiver and instead just report the result, but the details are not hard to work out. The plethystic logarithm of the Hilbert series of $\mathcal{C}(Q_{D_k}) \cong D_k$ is given by

$$PL(HS(\mathcal{C}(Q_{D_k}))) = t^4 + t^{2k-4} + t^{2k-2} - t^{4k-4}. \tag{4.4.20}$$

The lack of UV $U(1)$ topological symmetry means that in Step 2 of the Method, the only conservation of charge we need to impose under the Poisson bracket is that of the conformal dimension (4.2.16).

We won't go through the details here as they are very similar to those of Section 4.4.1, but the generators of the Klein D type singularity $\mathcal{V} = D_k$ are

$$\begin{aligned}\mathcal{G}_{\mathcal{V}} = \{&-\frac{z_1^2 z_2^2}{(2k-4)^2}\ ,\ \frac{1}{2(2k-4)^{k-2}}(z_1^{2k-4} + (-1)^k z_2^{2k-4})\ ,\\ &\frac{z_1 z_2}{2(2k-4)^{k-1}}(z_1^{2k-4} + (-1)^{k-1} z_2^{2k-4})\}\\ \equiv \{&g_1,\ g_2,\ g_3\},\end{aligned} \tag{4.4.21}$$

[15] You may also see this quiver with the flavour node labelled as $SO(2k)$: here the k identical hypermultiplets are in a pseudo-real representation, and so there is an $SO(2k)$ symmetry rotating them. This is a symmetry of the Higgs branch, so it does not play a part in our discussion.

and they satisfy the defining equation

$$E(g_1, g_2, g_3) = g_1\, g_2^2 + g_3^2 - g_1^{k-1} = 0, \tag{4.4.22}$$

with Poisson bracket relations as stated before in (4.4.4).

As in the case of the A_k Coulomb quiver, since there is just one gauge group of rank one, a (un)physical bare monopole is labelled by a single integer (v_m) V_m. There is also a single adjoint valued complex scalar λ everywhere, as the residual gauge group is always rank one. This time the Weyl group $\mathcal{W}(SU(2)) = \mathbb{Z}_2$ is non-trivial; it acts on m and λ as

$$\begin{aligned} \mathbb{Z}_2 :\ & m \to -m, \\ & \lambda \to -\lambda, \end{aligned} \tag{4.4.23}$$

meaning that unlike before the basic degrees of freedom v_m and λ are not physical. From the Hilbert series (4.4.20), we see that the Coulomb branch generators have conformal dimensions $\Delta_1 = 2$, $\Delta_2 = k-2$ and $\Delta_3 = k-1$. One can check that the physical Coulomb branch operators with these dimensions are

$$\lambda^2, \quad V_1^+, \quad \lambda\, V_1^- \tag{4.4.24}$$

respectively, where

$$\begin{aligned} V_1^+ &= v_{+1} + v_{-1}, \\ V_1^- &= v_{+1} - v_{-1}. \end{aligned} \tag{4.4.25}$$

Note that under action by the Weyl group, V_1^+ is invariant and $V_1^- \to -V_1^-$.

Step 2 of the Method tells us that

$$\begin{aligned} \{\lambda^2, V_1^+\} &\propto \lambda\, V_1^-, \\ \{\lambda^2, \lambda\, V_1^-\} &\propto \lambda\, V_-, \\ \{V_1^+, \lambda\, V_1^-\} &= c_1\, \lambda^{2k-4} + c_2\, (V_1^+)^2 + c_3\, (V_1^-)^2, \end{aligned} \tag{4.4.26}$$

for some constants c_i. If we declare that the constants of proportionality are as follows

$$\begin{aligned} \{\lambda^2, V_1^+\} &= 2\lambda\, V_1^-, \\ \{\lambda^2, \lambda\, V_1^-\} &= -2\lambda^2\, V_1^+, \\ \{V_1^+, \lambda\, V_1^-\} &= (V_1^+)^2 - (k-1)\, \lambda^{2k-4} \end{aligned} \tag{4.4.27}$$

and demand that the three generators (4.4.24) satisfy

$$(V_1^-)^2 = \lambda^{2k-4} - (V_1^+)^2, \tag{4.4.28}$$

then can we can see that if we identify

$$\begin{aligned} g_1 &= \lambda^2, \\ g_2 &= V_1^+, \\ g_3 &= \lambda\, V_1^-, \end{aligned} \tag{4.4.29}$$

then the declared brackets (4.4.27) and defining equation (4.4.28) between the generators reproduce the brackets and defining equation for the D_k Klein singularity (4.4.4) and (4.4.22) respectively.

4.5 Nilpotent Orbits

Closures of nilpotent orbits of Lie algebras $\mathfrak{g}$ as moduli spaces of quiver gauge theories [38, 49] have been studied intensively (see for example [80, 39, 93]) due to their nice properties: they are classifiable, and entirely generated by the adjoint representation of $\mathfrak{g}$. Since the explicit construction of these moduli spaces is fully known in the math literature, it makes their Higgs and Coulomb quivers (see Section 2.7.1) good candidates on which to explore new techniques or properties of interest. This is precisely our intention here. Since all generators in these moduli spaces are at order t^2 in the Hilbert series, and since operators at weight 2 form a closed algebra under the symplectic form [12], we know a-priori that the results of the Poisson brackets between generators must be the structure constants of the global symmetry algebra, as mentioned in Section 4.1. This has been previously discussed, see for example [17].

Actually computing these constants in practise however can be quite tricky. Since there is no $\mathbb{C}^2$ (or equivalent) Poisson bracket to be inherited on these spaces, like there was in the cases of free spaces and Klein singularities (as shown in Sections 4.3 and 4.4 respectively), we must turn to Step 3.*b*) in the Method and use the refined Coulomb branch Hilbert series to find the Poisson brackets between $\mathcal{G}_{\mathcal{C}}$, as outlined in Section 4.2.3.2. We demonstrate our successful execution of this method in the case of the closure of the minimal nilpotent orbit of A_2, denoted a_2, below. We have not provided Poisson brackets for closures of other nilpotent orbits in this way because the excess of unconstrained constants quickly becomes too many variables to deal with when the complexity[16] of the quiver is increased.

4.5.1 Minimal A_2

The Coulomb quiver for a_2 is

$Q_{a_2} =$ 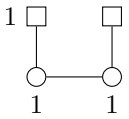

. (4.5.1)

To find the Poisson brackets we'll follow Steps 1, 2 and 3.*b*) of the Method.

Step 1 The global symmetry of $\mathcal{C}(Q_{a_2})$ is $SU(3)$ and all generators lie in the adjoint representation, at $\Delta = 1$. The adjoint of $SU(3)$ has dimension 8, and thus we have 8 generators:[17]

$$\mathcal{G}_{\mathcal{C}} = \{c^1{}_1\,\lambda_1 + c^2{}_1\,\lambda_2\ ,\ c^1{}_2\,\lambda_1 + c^2{}_2\,\lambda_2\ ,\ V_{-1-1}\ ,\ V_{-10}\ ,\ V_{0-1}\ ,\ V_{01}\ ,\ V_{10}\ ,\ V_{11}\},\tag{4.5.2}$$

where $V_{m_1 m_2}$ are the bare monopole operators with magnetic charge[18] $m_1 \in \mathbb{Z}$ under the first $U(1)$ gauge group and $m_2 \in \mathbb{Z}$ under the second; $\lambda_1, \lambda_2 \in \mathbb{C}$ are the adjoint scalars of the first and second gauged $U(1)$ groups respectively; and $c^i{}_j \in \mathbb{C}$ are constants.

[16] Here we consider a quiver more complex if its Coulomb branch has higher dimension (which scales with the sum of the gauge group ranks).

[17] As with previous cases where the only gauge groups were Abelian (e.g. Section 4.4.1), the Coulomb branch degrees of freedom v are automatically gauge invariant, and so the v and V of Section 4.2.1 are interchangeable.

[18] For monopole operators in an abelian theory, the magnetic charge coincides with the topological charge.

Step 2 (4.2.16) then tells us that the Poisson brackets between $\mathcal{G}_\mathcal{C}$ will give another operator with $\Delta = 1$; another element in the adjoint of $SU(3)$. This is what we expect, as the Poisson bracket acts on representations of the global symmetry $SU(3)$ as the Lie bracket of $SU(3)$, under the action of which the adjoint representation is closed. Schematically,

$$\{\mathcal{G}_\mathcal{C}, \mathcal{G}_\mathcal{C}\} = \mathcal{G}_\mathcal{C}. \tag{4.5.3}$$

On top of this, the conservation of topological charge (4.2.17) implies that the Poisson bracket between any two $\mathcal{G}_\mathcal{C}$, for which the componentwise sum of the vectors of their magnetic charges is not the magnetic charge of any other $\mathcal{G}_\mathcal{C}$, must vanish:

$$\begin{gathered}\{V_{-1-1}, V_{10}\} = 0,\\ \{V_{-1-1}, V_{0-1}\} = 0,\\ \{V_{11}, V_{10}\} = 0,\\ \{V_{11}, V_{01}\} = 0,\\ \{V_{10}, V_{0-1}\} = 0,\\ \{V_{01}, V_{-10}\} = 0,\end{gathered} \tag{4.5.4}$$

and fully fixes the others up to constants. For example,[19]

$$\begin{gathered}\{V_{-1-1}, V_{10}\} = \alpha_{-1-1001000}\, V_{0-1},\\ \{V_{01}, V_{0-1}\} = \alpha^1{}_{01000-100}\, \lambda_1 + \alpha^2{}_{01000-100}\, \lambda_2.\end{gathered} \tag{4.5.5}$$

Step 3 We then fix the constants of proportionality $\alpha^{(i)}{}_{abcdefgh}$ in the relations found in Step 2 by demanding consistency with global symmetry charges. To do this, we first find what global symmetry charge each generator $\mathcal{G}_\mathcal{C}$ has. We can see that the topological charges $\boldsymbol{J}(\boldsymbol{m}) = (m_1, m_2)$ of $\mathcal{G}_\mathcal{C}$ (4.5.2) respectively are:

$$\{(0,0)\ ,\ (0,0)\ ,\ (-1,-1)\ ,\ (-1,0)\ ,\ (0,-1)\ ,\ (0,1)\ ,\ (1,0)\ ,\ (1,1)\}. \tag{4.5.6}$$

Under the appropriate fugacity map (see Section 2.6.6), which one can find to be

$$\boldsymbol{J}(\boldsymbol{m}) = \begin{pmatrix} m_1 \\ m_2 \end{pmatrix} \to \tilde{\boldsymbol{J}}(\tilde{\boldsymbol{m}}) = \begin{pmatrix} \tilde{m}_1 \\ \tilde{m}_2 \end{pmatrix} = \begin{pmatrix} 2 & -1 \\ -1 & 2 \end{pmatrix} \cdot \begin{pmatrix} m_1 \\ m_2 \end{pmatrix}, \tag{4.5.7}$$

we see that (4.5.2) have charges $\tilde{\boldsymbol{J}}$ under the global symmetry given respectively by:

$$\{(0,0)\ ,\ (0,0)\ ,\ (-1,-1)\ ,\ (-2,1)\ ,\ (1,-2)\ ,\ (-1,2)\ ,\ (2,-1)\ ,\ (1,1)\}. \tag{4.5.8}$$

Since $\{\cdot,\cdot\}$ acts as the Lie bracket of $SU(3)$, which has rank 2, there are 2 Cartan elements C_1 and C_2 which act as eigenoperators of the Poisson bracket with eigenvalue equal to the weight under $SU(3)$ of the adjoint operator it acts on. For $\mathcal{G}_\mathcal{C}$, the weights are $\tilde{\boldsymbol{J}}$:

$$\{C_i, \mathcal{G}_\mathcal{C}\} = \tilde{J}_i\, \mathcal{G}_\mathcal{C} \tag{4.5.9}$$

[19] The horrible looking subscript on the constants of proportionality $\alpha^{(i)}{}_{abcdefgh} = -\alpha^{(i)}{}_{efghabcd} \in \mathbb{C}$ (the bracket around the upper index is to indicate that it is not always present) was chosen to reflect the arguments in the Poisson bracket in question: with no upper index, it is the constant of proportionality for $\{V_{ab}\, \lambda_1^c\, \lambda_2^d\ ,\ V_{ef}\, \lambda_1^g\, \lambda_2^h\}$. Upper indices 1 and 2 are included in the cases where the result must have topological charge zero, because there are two operators (λ_1 and λ_2) which have this charge and they do not necessarily have the same coefficient.

for $i = 1, 2$. Thus we must ensure the brackets between each generator and the Cartan elements give the correct global symmetry charges (4.5.8). The Cartan elements must lie in the adjoint representation of the $SU(3)$ global symmetry and have charge $(0, 0)$ under it, and thus they are precisely our two chargeless generators from (4.5.2):

$$\begin{aligned} C_1 &= c^1{}_1\lambda_1 + c^2{}_1\lambda_2, \\ C_2 &= c^1{}_2\lambda_1 + c^2{}_2\lambda_2. \end{aligned} \tag{4.5.10}$$

We can then demand that (4.5.9) holds and substitute in (4.5.10) for C_i, and implement the results of the Poisson brackets we derived in Step 2 (for example (4.5.4) and (4.5.5)). Then using the bilinearity, antisymmetry and Jacobi identity of the Poisson bracket, we can solve for the constants $\alpha^{(i)}{}_{abcdefgh}$ and $c^i{}_j$. This is where the computational difficulty comes in: for higher dimensional Coulomb branches, there are simply too many unknown constants of proportionality α, c introduced to solve for. However in this case we can do it, and find that the Cartans are

$$\begin{aligned} C_1 &= \lambda_1, \\ C_2 &= \lambda_1 + \lambda_2, \end{aligned} \tag{4.5.11}$$

with Poisson brackets between the generators given by

	C_1	C_2	V_{-1-1}	V_{-10}	V_{0-1}	V_{01}	V_{10}	V_{11}
C_1	0	0	$-V_{-1-1}$	$-2V_{-10}$	V_{0-1}	$-V_{01}$	$2V_{10}$	V_{11}
C_2	·	0	$-V_{-1-1}$	V_{-10}	$-2V_{0-1}$	$2V_{01}$	$-V_{10}$	V_{11}
V_{-1-1}	·	·	0	0	0	V_{-10}	V_{0-1}	$C_1 + C_2$
V_{-10}	·	·	·	0	V_{-1-1}	0	C_1	V_{01}
V_{0-1}	·	·	·	·	0	$-C_2$	0	V_{10}
V_{01}	·	·	·	·	·	0	V_{11}	0
V_{10}	·	·	·	·	·	·	0	0
V_{11}	·	·	·	·	·	·	·	0

. (4.5.12)

All dots in the table (4.5.12) are fixed by the negative of their transpose entries due to antisymmetry of the Poisson bracket.

4.6 Poisson Brackets for Generating Representations

In Sections 4.3 – 4.5 we used the Method of Section 4.2 to explicitly compute Poisson bracket relations for Coulomb branch monopole operators, but noted that this method cannot be performed on most quivers. While we do not by any means rule out the existence of more effective methods to perform computations and find the Poisson brackets explicitly for a generic quiver, we would like to conjecture the results in the cases that are currently too difficult to find using the Method of Section 4.2. In this section, we illustrate how this is possible for families of quivers for which the representation content of the Coulomb branch is known (from the HWG) to low orders: we forget about the monopole construction of the Coulomb branch, viewing it simply as a space of representations, and then conjecture the Poisson bracket relations between the generating representations using purely the known HWG, the antisymmetric property of the Poisson bracket, and representation theory. Section 4.7 will see us detail the results for a small number of families of quivers derived from 5 and 6 dimensional physics, which have just one or two generating representations other than the adjoint.

The explicit outline of the approach to conjecture the relevant Poisson brackets is as follows:

1. Identify the generating representations by taking the plethystic logarithm of the Hilbert series.
2. Use the tensor/antisymmetric product of the generating representations to constrain the possible result of the Poisson brackets between generators.
3. Use the representations appearing at the appropriate degree in the HWG (according to (4.2.16)) to constrain the possible result of the Poisson brackets between generators.
4. Find the simplest representation common to the constraints from Step 2 and Step 3, and find constants to contract relevant indices.
5. Insert appropriate flavour symmetry invariants to ensure consistency in conformal dimension.

The reason for Step 2 is that the Poisson bracket is antisymmetric, hence when taking the Poisson bracket of a representation with itself, the result will lie in the second rank antisymmetric product of this representation. For the Poisson bracket of two different representations, the result will lie in the tensor product of these two representations (see Appendix B for a more thorough discussion of tensor and antisymmetric products of representations). Step 3 is there to ensure that the result of the Poisson bracket between two generators actually lies on the particular Coulomb branch variety we are studying. To clarify any uncertainties in Steps 2, 3, 4 and 5, we turn to an example.

Example We will use the same example Q_{A_1} (2.6.14) as in Sections 4.2.1 – 4.2.3.2 to illustrate the success of this more representation-theoretic and less monopole-focused approach. We follow the steps above:

1. We have already seen before in (4.2.12) that the generators of this Coulomb branch are simply in the adjoint representation μ_1^2 of $SU(2)$ with conformal dimension $\Delta = 1$. The 3 generators lie in the complexification of the global symmetry algebra $\mathfrak{su}(2)_{\mathbb{C}} = \mathfrak{sl}(2;\mathbb{C})$: a^i for $i = 1,2,3$. Since the adjoint of $\mathfrak{sl}(2;\mathbb{C})$ is the second rank symmetric of the fundamental, these three generators can be encapsulated in a symmetric 2×2 "matrix of generators" $a_{\alpha\beta}$ for $\alpha,\beta = 1,2$ symmetric indices labelling which generator is which. The only Poisson bracket we need to determine is then
$$\{a_{\alpha\beta}\,,\, a_{\gamma\delta}\}. \tag{4.6.1}$$
2. Then we can ask what possible representations (4.6.1) could actually be in. Here it is trivial as we know the adjoint representation is closed under the Lie (and hence Poisson) bracket and so the result must also lie in the adjoint representation. This can also be seen by noting that the second rank antisymmetric product of the adjoint representation is just itself:[20]
$$\Lambda^2(\mu_1^2) = \mu_1^2, \tag{4.6.2}$$
and since the Poisson structure antisymmetrises comparable arguments, the result of (4.6.1) must lie in (4.6.2).
3. If (4.6.2) had contained multiple representations, we could have further constrained the representations that (4.6.1) could lie in by examining the HWG. Using (4.2.16), the result must have conformal dimension $1+1-1=1$, i.e. lie at t^2 in the Hilbert series. For $\mathcal{C}(Q_{A_1})$, the HWG is
$$HWG(\mathcal{C}(Q_{A_1})) = PE[\mu_1^2 t^2]. \tag{4.6.3}$$

[20]Note that we will use μ or μ_i both as an index labelling generators that takes on certain specified values, and as the highest weight fugacities to denote a representation. Its meaning in a given situation should be clear from context (i.e. whether it lies in an exponent/subscript or not).

We can therefore see easily that the only representation at t^2 on this Coulomb branch is indeed the adjoint, and so this enforces that the Poisson bracket of the adjoint generators lies again in the adjoint:

$$\{a\,,\,a\} \propto a. \tag{4.6.4}$$

We see that in this case either the available Coulomb branch operators or possible representations would be sufficient to deduce (4.6.4), but in more complicated cases they will work in tandem to help postulate the brackets.

4. Finally, we aim to get rid of the proportionality sign in (4.6.4) and make an explicit conjecture. To do this, we note that on the left-hand side of (4.6.4) there will be indices labelling the generators (say for instance $\alpha, \beta, \gamma, \delta$ as in (4.6.1)) which must be matched on the right hand side. Two of these indices will be held by the "a" on the right-hand side, which leaves two remaining indices for the equation to be consistent. In the algebra of $\mathfrak{sl}(2;\mathbb{C})$, the only thing that makes sense to go here is the epsilon invariant (the delta invariant of $\mathfrak{sl}(n;\mathbb{C})$ can be constructed from the epsilon invariant in the $n = 2$ case). So we expect (4.6.4) to take form along the lines of $\{a_{\alpha\beta}\,,\,a_{\gamma\delta}\} \sim A\,(\epsilon_{\alpha\delta}a_{\gamma\beta} + \epsilon_{\beta\delta}a_{\gamma\alpha} + \epsilon_{\alpha\gamma}a_{\delta\beta} + \epsilon_{\beta\gamma}a_{\delta\alpha})$; the relative signs chosen to ensure the result is antisymmetric upon simultaneously exchanging $\alpha \leftrightarrow \gamma$ and $\beta \leftrightarrow \delta$, and symmetric upon exchanging $\alpha \leftrightarrow \beta$ or $\gamma \leftrightarrow \delta$. The overall constant A is fixed by the way in which we identify the $a_{\alpha\beta}$ with the symmetric generators of $\mathfrak{sl}(2;\mathbb{C})$. For example, we could use the representation of the generators of $\mathfrak{sl}(2;\mathbb{C})$ given in (4.2.35). Then if we identify $a_{12} = \lambda$, $a_{11} = 2\,V_{-1}$ and $a_{22} = 2\,V_{+1}$, a positive overall sign:

$$\{a_{\alpha\beta}\,,\,a_{\gamma\delta}\} = \epsilon_{\alpha\delta}a_{\gamma\beta} + \epsilon_{\beta\delta}a_{\gamma\alpha} + \epsilon_{\alpha\gamma}a_{\delta\beta} + \epsilon_{\beta\gamma}a_{\delta\alpha} \tag{4.6.5}$$

for $\alpha, \beta, \gamma, \delta = 1, 2$ would recover the appropriate Poisson brackets (4.2.36) of (4.2.35).

5. Our result (4.6.5) is already consistent with conformal dimension: the left hand side has $\Delta = 1 + 1 - 1 = 1$, which matches the $\Delta = 1$ of the right hand side.

Although the example above did not illustrate it, non-trivial ammendments can be made in Step 5, causing the need for a scale to be introduced in the form of some invariant of the global symmetry. In such cases, there is an operator which spontaneously breaks the conformal and R-symmetry but preserves the flavour symmetry. We will see this explicitly in the examples of Section 4.7, where we will discuss its physical significance in more detail.

Structure constants for $\mathfrak{sl}(n > 2;\mathbb{C})$ Note that, as mentioned in the discussion preceeding (4.2.39), in $\mathfrak{sl}(2;\mathbb{C})$ the fundamental representation is pseudo-real, not complex, and all non-trivial representations are symmetric products of this. Hence all indices are lowered and we can write the structure constants in the special form of (4.6.5). For $\mathfrak{sl}(n > 2;\mathbb{C})$ the fundamental representation is complex, so the structure constants here must be written in a more general form; we cannot generalise (4.6.5) to all $\mathfrak{sl}(n > 2;\mathbb{C})$. The adjoint of $\mathfrak{sl}(n > 2;\mathbb{C})$ lies in the tensor product of the fundamental and anti-fundamental (the complex conjugate and dual of the fundamental) representations, hence the matrix of generators is given by one upper and one lower index $a^{\mu}{}_{\nu}$ for $\mu, \nu = 1, ..., n$ traceless labelling which generator is which. In this case, taking into account the upper and lower indices that appear on the left and right side of (4.6.4), we have two spare indices on the right hand side that do not accompany "a": one upper and one lower. The only invariant of $\mathfrak{sl}(n > 2;\mathbb{C})$ with this structure is $\delta^{\mu}{}_{\nu}$, and so

we find that the structure constants of $\mathfrak{sl}(\mathfrak{n};\mathbb{C})$ are

$$\{a^{\mu}{}_{\nu}\,,\, a^{\rho}{}_{\sigma}\} = \delta^{\mu}{}_{\sigma}a^{\rho}{}_{\nu} - \delta^{\rho}{}_{\nu}a^{\mu}{}_{\sigma}, \tag{4.6.6}$$

where analogously to Step 5 above, the overall sign was determined by ensuring that the result matched the expected result for the $n = 2$ case, if we took the generators to be $\mathfrak{sl}(\mathfrak{n} = 2;\mathbb{C})$ matrices. Because here we are viewing $\mathfrak{sl}(\mathfrak{n} = 2;\mathbb{C})$ as the $n = 2$ case of $\mathfrak{sl}(\mathfrak{n};\mathbb{C})$, we take the generators to be the canonical generators for 2×2 traceless complex matrices (unlike in Step 1 above, or in (4.2.35), where it was more natural to view them as symmetric complex matrices):

$$\tilde{\lambda} = \begin{pmatrix} 1 & 0 \\ 0 & -1 \end{pmatrix}, \quad \tilde{V}_{+1} = \begin{pmatrix} 0 & 1 \\ 0 & 0 \end{pmatrix}, \quad \tilde{V}_{-1} = \begin{pmatrix} 0 & 0 \\ 1 & 0 \end{pmatrix}. \tag{4.6.7}$$

The Poisson bracket acts on two such generators by matrix multiplication, using contraction with δ (rather than ϵ as we did when we were treating $\mathfrak{sl}(2;\mathbb{C})$ separately from $\mathfrak{sl}(\mathfrak{n};\mathbb{C})$, for example in the discussion preceeding (4.2.39)). We see that this gives

$$\begin{aligned} \{\tilde{\lambda}, \tilde{V}_{+1}\} &= 2\,\tilde{V}_{+1}, \\ \{\tilde{\lambda}, \tilde{V}_{-1}\} &= -2\,\tilde{V}_{-1}, \\ \{\tilde{V}_{+1}, \tilde{V}_{-1}\} &= \tilde{\lambda}. \end{aligned} \tag{4.6.8}$$

If we identify our $a^{\mu}{}_{\nu}$ generators as

$$\begin{aligned} a^{1}{}_{1} - a^{2}{}_{2} &= \tilde{\lambda}, \\ a^{1}{}_{2} &= \tilde{V}_{+1}, \\ a^{2}{}_{1} &= \tilde{V}_{-1}, \end{aligned} \tag{4.6.9}$$

for the $\tilde{\lambda}$, $\tilde{V}_{+1}$, $\tilde{V}_{-1}$ of (4.6.7), then we see that (4.6.6) with its positive overall sign matches (4.6.8). With this identification, we can see that (4.6.6) are the structure constants for $\mathfrak{sl}(\mathfrak{n} > 2;\mathbb{C})$.

We can see that the approach to determine Poisson brackets outlined in this section is slightly more abstract than that detailed in the previous three sections, and in the case of this example is actually somewhat redundant; since the moduli space is solely generated by the adjoint representation at $\Delta = 1$ – a closed algebra – we could have said without any calculations or thought that the Poisson brackets had to be given by the structure constants. The method outlined in Sections 4.2.1 – 4.2.3.2 uncovered additional information that we did not know a-priori: in particular, the Poisson bracket relations for the specific monopole operators on the Coulomb branch. That explicit construction is clearly preferable, but is not accessible for many of the quivers for which the approach in this section can be used, hence the utility of this more abstract method. We will now move on to illustrate examples of such cases.

4.7 Higgs Branches of Certain $5d$ and $6d$ Theories at Infinite Coupling

It is in this section that we finally study Higgs branches at infinite coupling. As explained in Section 2.7.1, up until recently it was not known how to make progress with these Higgs branches as they

could not be computed classically. This was overcome for wide families of such theories with the discovery of their magnetic quivers, and the study of their Coulomb branches. In this section we exploit this; we find the Poisson brackets between the Higgs branch generators $\{\mathcal{G}_\mathcal{H}, \mathcal{G}_\mathcal{H}\}_\mathcal{H}$ of certain 5 and 6 dimensional theories at infinite coupling by computing $\{\mathcal{G}_\mathcal{C}, \mathcal{G}_\mathcal{C}\}_\mathcal{C}$ for their magnetic quivers.

This task sees the utility of the method outlined in Section 4.6; the families we study have one or two generating representations other than the adjoint, hence the Poisson brackets cannot be trivially concluded to be the structure constants a-priori (as they could have been in the example of Section 4.6). In some cases, Step 4 of Section 4.6 finds many representations, the set of which we call R_{mult}, that are common to both the tensor/antisymmetric product of the input representations for a given Poisson bracket and the operators on the Coulomb branch at the appropriate conformal dimension. With these constraints alone, we can only say for certain that the Poisson bracket in question would be some undetermined linear combination of R_{mult}, but we *conjecture* that the principle of Occam's razor applies: the coefficients of all representations *other than the simplest* vanish. We call this simplest representation $R_{\text{simp}} \in R_{\text{mult}}$, and in all cases studied it turns out to be either the trivial or the adjoint representation of the global symmetry. The motivation for such a conjecture is that the moduli spaces we study are fairly simple spaces; there is no reason to expect that the symplectic form should take unecessarily elaborate values. To check this conjecture and verify the exact coefficients would require further analysis of the 5 and 6 dimensional physics, a task we leave for future work.

The breaking of conformality In all the 5 and 6 dimensional theories studied, we find that the Higgs branch Poisson brackets between representations other than the adjoint include a Casimir to some non-zero power to ensure consistency of conformal dimension. This Casimir takes some numerical value: it is a scale. This tells us that on the Higgs branch of these theories, the conformal symmetry at infinite coupling is spontaneously broken. This sounds like nothing new; any VEV will break the conformal symmetry in the vacuum. However the difference between this scale and other VEVs is that other VEVs also break the Coulomb branch flavour symmetry, whereas this Casimir scale preserves it. This is a powerful statement and is worth unpacking a little, but we should be careful to distinguish between 5 and 6 dimensions. In $5d$, the gauge coupling is a parameter of the theory, and so the Poisson brackets we find below in Section 4.7.5 tell us that while conformal symmetry is spontaneously broken in SQCD theories taken at infinite coupling, the flavour symmetry is preserved. In $6d$, the inverse gauge coupling $\frac{1}{g^2}$ is a modulus, not a parameter. If we look at the Higgs branch at finite coupling (i.e. the Higgs branch over a generic point of the tensor branch), $\frac{1}{g^2}$ is an obvious scale and so conformal symmetry is broken. If we look at the Higgs branch at infinite coupling (i.e. the Higgs branch over the origin of the tensor branch), the scale $\frac{1}{g^2}$ disappears, but the Poisson brackets we find in Sections 4.7.1 tell us that another one emerges, C_2. That is, as we move towards the origin of the tensor branch the scale which breaks conformal symmetry transitions from $\frac{1}{g^2}$, a scalar in the tensormultiplet, to C_2, a scalar in the hypermultiplet which preserves the flavour symmetry. It would be interesting to see how observables (e.g. correlation functions) in the $6d$ theory lying close to the origin of the tensor branch (i.e. when the gauge coupling is very large but not infinite) vary as a function of these two scales, $\frac{1}{g^2}$ and C_2.

For the first family of theories we consider (the subject of Section 4.7.1), we go through in detail the method used to obtain the Coulomb branch Poisson brackets $\{\mathcal{G}_\mathcal{C}, \mathcal{G}_\mathcal{C}\}_\mathcal{C}$ of the magnetic quiver. One Poisson bracket on this Coulomb branch – the bracket of the generating spinor representation with itself – fits into the categories of brackets discussed above for which the methods of Section 4.6 do not

constrain the result to lie in a single representation. We detail the full list of representations it could lie in (R_{mult}), and then end with the conjecture that it actually lies in the simplest (R_{simp}). For the remaining families (the subjects of Sections 4.7.2 - 4.7.5.4) we simply state the conjectured results (and in particular give only R_{simp} and not the full list R_{mult} for any brackets which the methods of Section 4.6 fail to constrain to a single representation), skipping the method. The quivers in Sections 4.7.1 – 4.7.4 are taken from [69], and those in Section 4.7.5 from [72] and an unpublished work by Hanany and Zhong.

4.7.1 $E_{8,n}$ family

The first family we discuss is that arising from the Higgs branch of the $6d$ theory of $Sp(n)$ gauge group and $2n+8$ flavours at infinite coupling [70, 76], or equivalently the Higgs branch of the $5d$ theory of $SU(n+2)$ gauge group with Chern Simons level $k = \pm\frac{1}{2}$ and $2n+7$ flavours at infinite coupling [69] for $n \geq 0$. The magnetic quiver in question for these theories is [69, 76, 94]

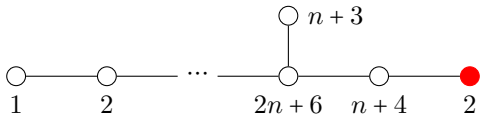

(4.7.1)

The right hand rank 2 node is coloured red to indicate that it is unbalanced (for $n \neq 0$). Generically, we can read off that this quiver has global symmetry $SO(4n+16)$ [10]. For $n = -1$ however, (4.7.1) is the Dynkin quiver of E_7 (D_{E_7}, as discussed in Section 4.3.1) hence the global symmetry is enhanced to $Sp(16) \supset SO(12)$ and the Poisson brackets are those given in Section 4.3. For $n = 0$, (4.7.1) is the affine E_8 quiver; the global symmetry is enhanced to $E_8 \supset SO(16)$, and the Poisson brackets are the structure constants of E_8. For all $n \geq 1$ the global symmetry of the Coulomb branch is $SO(4n+16)$ and there are 2 generating representations, as can be found from the HWG:[21]

$$HWG = \frac{1}{(1-t^4)(1-\mu_{2n+8}\,t^{n+2})(1-\mu_{2n+8}\,t^{n+4})\prod_{i=1}^{n+3}(1-\mu_{2i}\,t^{2i})}, \tag{4.7.2}$$

where $\mu_1, ..., \mu_{2n+8}$ are highest weight fugacities of the global symmetry $D_{2n+8} = SO(4n+16)$. The Poisson brackets in the $n \geq 1$ case are thus not so trivial; we must proceed with Steps 1 – 4 of Section 4.6 to determine them. To illustrate these steps we start by carrying them out for the simplest case of $n = 0$, viewing the representations of the global symmetry E_8 in terms of the $SO(16)$ subalgebra, and then use this to help us find the Poisson brackets for general $n \geq 1$.

4.7.1.1 $n = 0$

In this case, (4.7.1) morphs into the affine Dynkin diagram of E_8 and hence its Coulomb branch is the corresponding minimal nilpotent orbit closure, e_8. Since here the global symmetry enhances to E_8, we could write the HWG in terms of representations of E_8 as $PE[\tilde{\mu}_7\,t^2]$ (for $\tilde{\mu}_1, ..., \tilde{\mu}_8$ highest weight fugacities of E_8), however it will be more useful to write it as the $n = 0$ case of (4.7.2) – i.e. in terms of $SO(16) \subset E_8$ representations – so that we can use our results to generalise to higher n:

$$HWG = PE[(\mu_2+\mu_8)t^2 + (1+\mu_4+\mu_8)t^4 + \mu_6 t^6]. \tag{4.7.3}$$

[21] Recall from Section 2.6.2 that the HWG and Hilbert series are different objects. In particular, their generators are not the same. This is clear here: the HWG has more than two generating representations, it is the Hilbert series which has two. But the HWG can be used to help us see this; from the HWG we can find the Hilbert series, and then take the plethystic logarithm to find the generators.

Recall from Section 4.6 that the first step to finding $\{\mathcal{G}_\mathcal{C}, \mathcal{G}_\mathcal{C}\}$ is to write down the generating representations $\mathcal{G}_\mathcal{C}$ themselves. This can be done by converting (4.7.3) into a Hilbert series and taking the plethystic logarithm [95]. It turns out that all generators here lie at order t^2 (i.e. have $\Delta = 1$), and fall into the adjoint $a_{\mu\nu}$[22] (μ_2 in Dynkin labels) and spinor s_α[23] (μ_8 in Dynkin labels) representations of the $SO(16) \subset E_8$ global symmetry. We collect this information on the generators in the following table:

Generator	Δ	$SO(16)$ representation
$a_{\mu\nu}$	1	adjoint
s_α	1	spinor

. (4.7.4)

Note that both of these representations are real; we don't need to worry about raising or lowering indices. This is Step 1 of the method in Section 4.6 accomplished. We then carry out Steps 2 – 4 for each of the Poisson brackets we need to calculate:

$$\{a_{\mu\nu}, a_{\rho\sigma}\}\,, \quad \{a_{\mu\nu}, s_\alpha\}\,, \quad \{s_\alpha, s_\beta\}\,. \tag{4.7.5}$$

Adjoint with adjoint, $\{\mathbf{a}, \mathbf{a}\}$

2. $\{a, a\}$ generates a representation in the second rank antisymmetric product of the adjoint. One can calculate this to be
$$\Lambda^2(\mu_2) = \mu_2 + \mu_1\mu_3, \tag{4.7.6}$$
and thus conclude that the Poisson bracket of two a's must lie in one of the following representations of $SO(16)$:
$$\mu_2\,,\ \mu_1\mu_3\,. \tag{4.7.7}$$

3. Using (4.2.16) and (4.7.4), we see that $\{a, a\}$ must have conformal dimension $\Delta = 1$, and therefore lie in a representation in the Hilbert series appearing at t^2. This constrains $\{a, a\}$ to lie in one of the following representations:
$$\mu_2\,,\ \mu_8\,. \tag{4.7.8}$$

4. The only overlap between (4.7.7) and (4.7.8) is μ_2. That is, under the Poisson bracket the adjoint representation is closed. Schematically, this means
$$\{a, a\} \sim a. \tag{4.7.9}$$
To make this rigorous, we need to put the indices in and contract appropriately. Suppose on the left hand side we choose indices as follows:
$$\{a_{\mu\nu}, a_{\rho\sigma}\}, \tag{4.7.10}$$
On the right hand side all these indices must remain, and since the Poisson bracket is just the Lie bracket on the $SO(16)$ algebra, the result is determined by the structure constants:
$$\{a_{\mu\nu}, a_{\rho\sigma}\} = \delta_{\nu\rho}a_{\mu\sigma} - \delta_{\mu\rho}a_{\nu\sigma} + \delta_{\mu\sigma}a_{\nu\rho} - \delta_{\nu\sigma}a_{\mu\rho}. \tag{4.7.11}$$

5. Our result (4.7.11) is already consistent with conformal dimension: the left hand side has $\Delta = 1 + 1 - 1 = 1$, which matches the $\Delta = 1$ of the right hand side.

[22] In the $16d$ analogy to the Lorentz transformations, $\mu, \nu = 1, \ldots, 16$ are antisymmetrised.

[23] Each spinor s_α is a 128 dimensional representation, and $\alpha = 1, \ldots, 2^{\frac{16}{2}-1} = 128$ is a spinor index.

Note the use of $\delta_{\mu\nu}$ as apposed to $\eta_{\mu\nu}$: we are not using representations of Minkowski $SO(1,15)$ spacetime, but rather representations of $SO(16)$ whose indices are Euclidean in nature. (4.7.11) are the structure constants for all $SO(2k)$, with all indices ranging from $1,...,2k$. Note how the result is antisymmetric under the three index permutations (a) $\mu \leftrightarrow \nu$, (b) $\rho \leftrightarrow \sigma$, and (c) $\mu \leftrightarrow \rho$, $\nu \leftrightarrow \sigma$, as expected.

Adjoint with spinor, $\{a, s\}$

2. The tensor product of μ_2 with μ_8 restricts this Poisson bracket to lie in the following representations:
$$\mu_8\,,\ \mu_1\mu_7\,,\ \mu_2\mu_8\,. \tag{4.7.12}$$
3. Since $\Delta = 1$ for the spinor representation also, again $\{a, s\}$ must lie at t^2 in the Hilbert series, and so must lie among (4.7.8).
4. This time the only overlap between (4.7.12) and (4.7.8) is μ_8, and so schematically we have
$$\{a, s\} \sim s \tag{4.7.13}$$
Again we could have known this a-priori as any representation is an "eigenrepresentation" of the adjoint under action by the Lie bracket, with eigenvalue equal to its weight. To put in the indices, we need something on the right hand side to contract the two vector indices of a, leaving just the spinor index of s, which transforms compatibly under $SO(16)$. A natural candidate is the generator of the spinor representation: $\gamma_{\mu\nu} = \frac{1}{4}[\gamma_\mu, \gamma_\nu]$,[24] where γ_μ are the Euclidean gamma matrices, satisfying the Clifford algebra $\{\gamma_\mu, \gamma_\nu\} = 2\delta_{\mu\nu}$.[25] Concretely,[26]
$$\{a_{\mu\nu}, s_\alpha\} = (\gamma_{\mu\nu})_{\alpha\beta}\, s_\beta. \tag{4.7.14}$$
5. Our result (4.7.14) is already consistent with conformal dimension: the left hand side has $\Delta = 1 + 1 - 1 = 1$, which matches the $\Delta = 1$ of the right hand side.

Spinor with spinor, $\{s, s\}$

2. The Poisson bracket lying in the second rank antisymmetric of the spinor representation s constrains $\{s, s\}$ to lie among
$$\mu_6\,,\ \mu_2\,. \tag{4.7.15}$$
3. Again, the conformal dimension of $\{s, s\}$ must be 1, meaning that again it must lie among the representations of (4.7.8).
4. The only representation common to (4.7.15) and (4.7.8) is μ_2, so schematically
$$\{s, s\} \sim a. \tag{4.7.16}$$

[24] This factor of $\frac{1}{4}$ is typical in the literature, to ensure the $\gamma_{\mu\nu}$ satisfy the structure constants of the SO algebra (4.7.11). Here it is also convenient to use as it results in no factors of $\frac{1}{4}$ in the results of the Poisson brackets (4.7.32).

[25] Note that confusingly, unlike in the rest of the paper, here in the Clifford algebra $\{\cdot,\cdot\}$ denotes the anticommutator.

[26] Note that the indices μ and ν are labelling which gamma matrix we are referring to of the possible $120 = \dim(SO(16))$, and the spinor indices α and β label the matrix components of $\gamma_{\mu\nu}$ (spinor indices remind us that s_α transforms as a spinor, not a vector, and that the $(\gamma_{\mu\nu})_{\alpha\beta}$ act on spinors and satisfy the Clifford algebra).

On the left hand side there are two spinor indices, on the right hand side there are two antisymmetrised vector indices. A constant with matching spinor indices must contract these vector indices. Again $\gamma_{\mu\nu}$ is the natural candidate:

$$\{s_\alpha, s_\beta\} = (\gamma_{\mu\nu})_{\alpha\beta}\, a_{\mu\nu}. \tag{4.7.17}$$

5. As in the previous two cases, our result (4.7.17) is already consistent with conformal dimension.

4.7.1.2 $n \geq 0$

Now that we have seen the explicit working for the $n = 0$ case, it is easy to follow the same logic and arrive at a postulate of the Poisson brackets for the generating operators of the $\mathcal{C}$(4.7.1) for general $n \geq 0$.

For generic n, the generators are a slightly non-trivial generalisation of (4.7.4), found in the same way as described in Section 4.7.1.1:

Generator	Δ	$SO(4n+16)$ representation
$a_{\mu\nu}$	1	adjoint
s_α	$\frac{n+2}{2}$	spinor

. (4.7.18)

Note that both of these representations are real (or pseudo-real in the case of the spinor representation for odd n); we don't need to worry about raising or lowering indices. The form of the $\{a, a\}$ and $\{a, s\}$ Poisson brackets do not change from those discussed in the $n = 0$ case of Section 4.7.1.1: (4.7.11) and (4.7.14) hold for all $n \geq 0$, with μ, ν and ρ, σ pairs of antisymmetrised vector indices going from $1, ..., 4n+16$ and α, β spinor indices going from $1, ..., 2^{\frac{4n+16}{2}-1}$. However, the Poisson bracket between two spinors depends on whether n is odd or even.

Even n

2. In the case of even n, the second rank antisymmetric of the spinor is (see Appendix B for more details)[27]

$$\Lambda^2(\mu_{2n+8}) = \mu_{2n+6} + \mu_{2n+2} + \cdots + \mu_2, \tag{4.7.19}$$

and so $\{s, s\}$ must lie in some combination of the following representations of $SO(4n+16)$:

$$\mu_{2n+6}\,,\ \mu_{2n+2}\,,\ \cdots\ ,\ \mu_2. \tag{4.7.20}$$

3–4. The spinor appears at t^{n+2} in the Hilbert series, i.e. has $\Delta = \frac{n}{2} + 1$, hence (4.2.16) tells us that $\{s, s\}$ must have $\Delta = n+1$. The representations with this conformal dimension on the Coulomb branch in question are those which appear at order t^{2n+2} in the HWG. The only overlap between such representations and (4.7.20) are

$$R_{mult} = \{\mu_{2n+2}\,,\ \mu_{2n-2}\,, \ldots\,,\ \mu_2\}, \tag{4.7.21}$$

and so the Poisson brackets must take the form

$$\{s_\alpha, s_\beta\} \sim (\gamma_{\mu\nu})_{\alpha\beta}\, a_{\mu\nu} + \sum_{i=1}^{\frac{n}{2}} (\gamma_{\mu_1\cdots\mu_{4i+2}})_{\alpha\beta}\, b_{\mu_1\cdots\mu_{4i+2}}, \tag{4.7.22}$$

[27] Note that this shows that the spinor representation of $SO(4n+16)$ is real for even n, because the lack of the singlet in $\Lambda^2(s)$ means it must lie in the second rank symmetric product $S^2(s)$.

where the indices on b are completely antisymmetrised to reflect the $(4i{-}2)^{th}$ rank antisymmetric of the vector representation of $SO(4n+16)$, and each term has some coefficient preceeding it. As stated at the start of Section 4.7, to explicitly determine these coefficients would require analysis of the physics in the $6d$ theory from which these states originate. We leave this as a challenge for future work, but we conjecture that the solution should be the simplest: that the coefficients of all terms other than the first of (4.7.22) are zero (i.e. $R_{\text{simp}} = \mu_2$),

$$\{s_\alpha, s_\beta\} \sim (\gamma_{\mu\nu})_{\alpha\beta}\, a_{\mu\nu}. \tag{4.7.23}$$

5. As it stands in (4.7.23), the conformal dimension of the right hand side does not match what it should do: the left hand side has $\Delta = \frac{n+2}{2} + \frac{n+2}{2} - 1 = n+1$, but the right hand side only has $\Delta = 1$. The right hand side *should* be in the adjoint representation of $SO(4n+16)$ with $\Delta = n+1$: an additional factor which is an $SO(4n+16)$ invariant with $\Delta = n$ must be included.

   The HWG tells us that, on this Coulomb branch, the only generating singlet of $SO(4n+16)$ lies at t^4 (or equivalently $\Delta = 2$). The only invariant with this dimension is the second Casimir:[28]

$$C_2 = Tr(a^2), \tag{4.7.24}$$

   and hence we see that all other $SO(4n+16)$ invariants are powers of C_2.[29] Consequently, the only candidate to include in (4.7.23) to rectify the current inconsistency in conformal dimension is the $\left(\frac{n}{2}\right)^{\text{th}}$ power of C_2:

$$\{s_\alpha, s_\beta\} = C_2{}^{\frac{n}{2}}\, (\gamma_{\mu\nu})_{\alpha\beta}\, a_{\mu\nu}. \tag{4.7.25}$$

Odd n

2. For odd n, the second rank antisymmetric of the spinor is[30]

$$\Lambda^2(\mu_{2n+8}) = \mu_{2n+6} + \mu_{2n+2} + \cdots + \mu_4 + 1, \tag{4.7.26}$$

   hence $\{s, s\}$ must transform in some combination of the following representations of $SO(4n+16)$:

$$\mu_{2n+6}\,,\ \mu_{2n+2}\,,\ \ldots\ ,\ 1\,. \tag{4.7.27}$$

3–4. As in the even case, the result lies at t^{2n+2} in the Hilbert series. The representations under the $SO(4n+16)$ global symmetry at this order which overlap with (4.7.27) are

$$R_{\text{mult}} = \{\mu_{2n+2}\,,\ \mu_{2n-2}\,,\ \ldots\ ,\ 1\,\}, \tag{4.7.28}$$

   and so we find that the Poisson bracket must take the form

$$\{s_\alpha, s_\beta\} \sim \Omega_{\alpha\beta} + \sum_{i=1}^{\frac{n+1}{2}} (\gamma_{\mu_1\cdots\mu_{4i}})_{\alpha\beta}\, b_{\mu_1\cdots\mu_{4i}}, \tag{4.7.29}$$

   for $\Omega_{\alpha\beta}$ the skew-symmetric form of $Sp(k = 2^{2n+6})$ as in (4.3.4). As above the indices of b are antisymmetrised and each term has some coefficient preceeding it, but we conjecture that the coefficients of all terms other than the first of (4.7.29) are zero (i.e. that $R_{\text{simp}} = 1$):

$$\{s_\alpha, s_\beta\} \sim \Omega_{\alpha\beta} \tag{4.7.30}$$

[28] Here, as above, a schematically represents any matrix in the adjoint of the $SO(4n+16)$ algebra in question.

[29] This is another indicator, along with the Hasse diagram, that this Coulomb branch is "very close" to being a nilpotent orbit.

[30] Note that this shows that the spinor representation of $SO(4n+16)$ is pseudo-real for odd n, as the singlet lies in the second rank antisymmetric product.

5. As above, in (4.7.30) the right hand side should have $\Delta = n+1$, but it currently has $\Delta = 0$. To rectify this, an $SO(4n+16)$ invariant factor with $\Delta = n+1$ must be included. Following the same logic as above, the only possibility is ${C_2}^{\frac{n+1}{2}}$. The Poisson brackets are

$$\{s_\alpha, s_\beta\} = {C_2}^{\frac{n+1}{2}}\,\Omega_{\alpha\beta}. \tag{4.7.31}$$

4.7.1.3 Summary of conjectured brackets

We collect the results derived in this section. We conjecture that the Poisson bracket relations for the Coulomb branch generators of the $E_{8,n}$ family (4.7.1) for $n \geq 0$ are given by:

$$\begin{aligned}
\{a_{\mu\nu}, a_{\rho\sigma}\} &= \delta_{\nu\rho}a_{\mu\sigma} - \delta_{\mu\rho}a_{\nu\sigma} + \delta_{\mu\sigma}a_{\nu\rho} - \delta_{\nu\sigma}a_{\mu\rho} \quad \forall\ n,\\
\{a_{\mu\nu}, s_\alpha\} &= (\gamma_{\mu\nu})_{\alpha\beta}\, s_\beta \quad \forall\ n,\\
\{s_\alpha, s_\beta\} &= \begin{cases} {C_2}^{\frac{n}{2}}(\gamma_{\mu\nu})_{\alpha\beta}\, a_{\mu\nu}, & \text{if } n \text{ even} \\ {C_2}^{\frac{n+1}{2}}\,\Omega_{\alpha\beta} & \text{if } n \text{ odd} \end{cases}
\end{aligned} \tag{4.7.32}$$

where α and β spinor indices going from $1, ..., 2^{\frac{4n+16}{2}-1}$; any other indices are vector indices going from $1, ..., 4n+16$, antisymmetrised with those appearing with them in a given subscript; $\Omega_{\alpha\beta}$ is the skew-symmetric two form of $Sp(k = 2^{2n+6})$ (4.3.4); and $C_2 = Tr(a^2)$ is the second Casimir of $SO(4n+16)$, which is normalised to give no numerical coefficient in the final bracket of (4.7.32).

4.7.2 $E_{7,n}$ family

The Higgs branch of a $5d$ $SU(n)$ gauge theory with Chern Simons level 0 and $2n+2$ flavours at infinite coupling (i.e. at its UV fixed point) has magnetic quiver [69, 94]

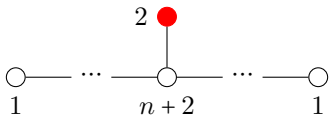

(4.7.33)

for $n \geq 1$. The rank 2 node is coloured red to indicate that it is unbalanced (for $n \neq 2$). Generically, we can read off that this quiver has global symmetry $SU(2n+4)$. For $n = 1$ however, (4.7.33) is the Dynkin quiver of E_6 (D_{E_6}, as discussed in Section 4.3.1) hence the global symmetry is enhanced to $Sp(10) \supset SU(6)$ and the Poisson brackets are those given in Section 4.3. For $n = 2$, (4.7.33) is the affine E_7 quiver; the global symmetry is enhanced to $E_7 \supset SU(8)$, and the Poisson brackets are the structure constants of E_7. For all $n \geq 3$ the global symmetry of the Coulomb branch is $SU(2n+4)$ and there are 2 generating representations, as can be found from the HWG:

$$HWG = \frac{1}{(1-t^4)(1-\mu_{n+2}\,t^n)(1-\mu_{n+2}\,t^{n+2})\prod_{i=1}^{n+1}(1-\mu_i\,\mu_{2n+4-i}\,t^{2i})}. \tag{4.7.34}$$

where $\mu_1, ..., \mu_{2n+3}$ are the highest weight fugacities for the $SU(2n+4)$ global symmetry. Explicitly, the generators are:

Generator	Δ	$SU(2n+4)$ representation
${a^\mu}_\nu$	1	adjoint
$b^{\mu_1\cdots\mu_{n+2}}$	$\frac{n}{2}$	$(n+2)^{th}$ rank antisymmetric

, (4.7.35)

where all indices involving μ and ν range from $1,...,2n+4$, and any indices on b are completely antisymmetrised. We conjecture that the Poisson brackets of (4.7.35) are given by:

$$\begin{aligned}
\{a^{\mu}{}_{\nu}, a^{\rho}{}_{\sigma}\} &= \delta^{\mu}{}_{\sigma} a^{\rho}{}_{\nu} - \delta^{\rho}{}_{\nu} a^{\mu}{}_{\sigma}, \\
\{a^{\mu}{}_{\nu}, b^{\mu_1\cdots\mu_{n+2}}\} &= \delta^{[\mu_1}{}_{\nu}\, b^{\mu_2\cdots\mu_{n+2}]\mu}, \\
\{b^{\mu_1\cdots\mu_{n+2}}, b^{\nu_1\cdots\nu_{n+2}}\} &= \begin{cases} C_2{}^{\frac{n-2}{2}} \left(\epsilon^{\rho\mu_1\cdots\mu_{n+2}[\nu_2\cdots\nu_{n+2}}\, a^{\nu_1]}{}_{\rho} + \epsilon^{\rho\nu_1\cdots\nu_{n+2}[\mu_2\cdots\mu_{n+2}}\, a^{\mu_1]}{}_{\rho}\right) & \text{if } n \text{ even}, \\ C_2{}^{\frac{n-1}{2}}\, \epsilon^{\mu_1\cdots\mu_{n+2}\nu_1\cdots\nu_{n+2}} & \text{if } n \text{ odd}, \end{cases}
\end{aligned} \tag{4.7.36}$$

where $C_2 = Tr(a^2)$ is the only non-zero $SU(2n+4)$ Casimir invariant of this moduli space, which is normalised to give no numerical coefficient in the final bracket of (4.7.36).

4.7.3 $E^I_{6,n}$ family

The Higgs branch UV fixed point of a $5d$ $SU(n)$ gauge theory with Chern Simons level $\pm\frac{1}{2}$ and $2n+1$ flavours has magnetic quiver [94, 69]

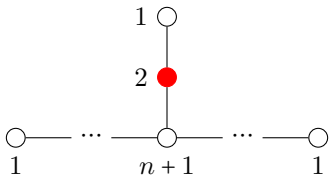

(4.7.37)

for $n \geq 1$. The rank 2 node is coloured red to indicate that it is unbalanced (for $n \neq 2$). Generically, we can read off that this quiver has global symmetry $SU(2n+2)\times SU(2)$. For $n = 1$, (4.7.37) is the Dynkin quiver of D_5 (D_{D_5}, as discussed in Section 4.3.1) and so the global symmetry is enhanced to $Sp(6)$ and the Poisson brackets are those given in Section 4.3. For $n = 2$, (4.7.37) is the affine E_6 quiver; the global symmetry is enhanced to $E_6 \supset SU(6) \times SU(2)$, and the Poisson brackets are the structure constants of E_6. For all $n \geq 3$ the global symmetry of the Coulomb branch is $SU(2n+2) \times SU(2)$ and there are 3 generating representations, as can be found from the HWG:

$$HWG = \frac{1 - \nu^2\, \mu_{n+1}^2\, t^{2n+4}}{(1-\nu^2\, t^2)(1-t^4)(1-\nu\, \mu_{n+1}\, t^n)(1-\nu\, \mu_{n+1}\, t^{n+2}) \prod_{i=1}^{n+1}(1-\mu_i\, \mu_{2n+2-i}\, t^{2i})}, \tag{4.7.38}$$

where $\mu_1,...,\mu_{2n+1}$ and ν are the highest weight fugacities for the $SU(2n+2)$ and $SU(2)$ factors in the global symmetry respectively. Explicitly, the generators are:

Generator	Δ	$SU(2n+2) \times SU(2)$ representation
$A^{\mu}{}_{\nu}$	1	adjoint $\times$ trivial
$a_{\alpha\beta}$	1	trivial $\times$ adjoint
$B^{\mu_1\cdots\mu_{n+1}}{}_{\alpha}$	$\frac{n}{2}$	$(n+1)^{th}$ rank antisymmetric $\times$ fundamental

, (4.7.39)

where all indices involving μ and ν are $SU(2n+2)$ indices ranging from $1,...,2n+2$ and those that appear in exponent of B are antisymmetrised among themselves; and indices involving α and β are $SU(2)$ indices ranging from $1,2$. We conjecture that the non-zero Poisson brackets of (4.7.39) are

given by:

$$\{A^{\mu_1}{}_{\nu_1}, A^{\mu_2}{}_{\nu_2}\} = \delta^{\mu_1}{}_{\nu_2} A^{\mu_2}{}_{\nu_1} - \delta^{\mu_2}{}_{\nu_1} A^{\mu_1}{}_{\nu_2},$$

$$\{a_{\alpha_1\beta_1}, a_{\alpha_2\beta_2}\} = \epsilon_{\alpha_1\beta_2} a_{\alpha_2\beta_1} + \epsilon_{\beta_1\beta_2} a_{\alpha_2\alpha_1} + \epsilon_{\alpha_1\alpha_2} a_{\beta_2\beta_1} + \epsilon_{\beta_1\alpha_2} a_{\beta_2\alpha_1},$$

$$\{A^{\mu}{}_{\nu}, B^{\mu_1\cdots\mu_{n+1}}{}_{\alpha}\} = \delta^{[\mu_1}{}_{\nu} B^{\mu_2\cdots\mu_{n+1}]\mu}{}_{\alpha},$$

$$\{a_{\alpha\beta}, B^{\mu_1\cdots\mu_{n+1}}{}_{\alpha_1}\} = B^{\mu_1\cdots\mu_{n+1}}{}_{(\beta}\, \epsilon_{\alpha)\alpha_1},$$

$$\{B^{\mu_1\cdots\mu_{n+1}}{}_{\alpha}, B^{\nu_1\cdots\nu_{n+1}}{}_{\beta}\} = \begin{cases} C_2{}^{\frac{n-2}{2}} \Big(\epsilon^{\mu_1\cdots\mu_{n+1}\nu_1\cdots\nu_{n+1}}\, \epsilon_{\alpha_1[\alpha}\, a_{\beta]\alpha_1} + \epsilon_{\alpha\beta} \\ \quad \Big(\epsilon^{\nu\nu_1\cdots\nu_{n+1}[\mu_2\cdots\mu_{n+1}}\, A^{\mu_1]}{}_{\nu} + \epsilon^{\nu\mu_1\cdots\mu_{n+1}[\nu_2\cdots\nu_{n+1}}\, A^{\nu_1]}{}_{\nu} \Big) \Big) & \text{if } n \text{ even}, \\ C_2{}^{\frac{n-1}{2}}\, \epsilon_{\alpha\beta}\, \epsilon^{\mu_1\cdots\mu_{n+1}\nu_1\cdots\nu_{n+1}} & \text{if } n \text{ odd}, \end{cases} \tag{4.7.40}$$

where $(\cdot)/[\cdot]$ indicates a symmetrisation/antisymmetrisation over the enclosed indices with no numerical prefactor; and C_2 is the second and only non-zero Casimir for $SU(2n+2) \times SU(2)$ on this Coulomb branch, which is normalised to give no numerical coefficient in the final bracket of (4.7.40). The second Casimir C_2 of the product group $SU(2n+2) \times SU(2)$ is proportional to the second Casimir of each individual group ($SU(2n+2)$ and $SU(2)$ respectively).[31] All other Poisson brackets between (4.7.39) that are not listed in (4.7.40) vanish.

4.7.4 $E_{6,n}^{II}$ family

The Higgs branch UV fixed point of a $5d$ $SU(n)$ gauge theory with Chern Simons level $\pm\frac{3}{2}$ and $2n+1$ flavours has magnetic quiver [94, 69]

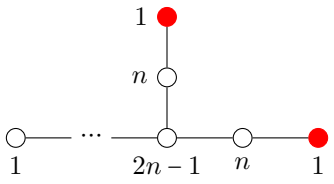

(4.7.41)

for $n \geq 1$. The two rank 1 nodes are coloured red to indicate that they are unbalanced (for $n \neq 2$). Generically, we can read off that this quiver has global symmetry $SO(4n+2) \times U(1)$. For $n = 1$, (4.7.41) is Dynkin quiver of A_5 (D_{A_5}, as discussed in Section 4.3.1) and hence the global symmetry is enhanced to $Sp(4) \supset SO(6) \times U(1)$, and the Poisson brackets are given in Section 4.3. For $n = 2$, (4.7.41) is the affine E_6 quiver; the global symmetry is enhanced to $E_6 \supset SO(10) \times U(1)$, and the Poisson brackets are the structure constants of E_6. For all $n \geq 3$ the global symmetry of the Coulomb

[31] The 2nd Casimirs of $SU(2n+2)$ and $SU(2)$, $C_{2,SU(2n+2)} = Tr(A^2)$ and $C_{2,SU(2)} = Tr(a^2)$ respectively, both have conformal dimension 2. The HWG tells us that there is just a single invariant of the Coulomb branch global symmetry, and that it has $\Delta = 2$. This means that some linear combination of the individual Casimirs $C_{2,SU(2n+2)}$ and $C_{2,SU(2)}$, say $\beta_1 C_{2,SU(2n+2)} + \beta_2 C_{2,SU(2)}$, must vanish, and all Casimirs of the flavour symmetry $SU(2n+2) \times SU(2)$ on this Coulomb branch must be proportional to an orthogonal linear combination, say $C_2 = \alpha_1 C_{2,SU(2n+2)} + \alpha_2 C_{2,SU(2)}$. The vanishing linear combination tells us that $C_{2,SU(2n+2)}$ and $C_{2,SU(2)}$ are proportional, and so we can see that the second Casimir of the product group C_2 is proportional to either of the second Casimirs of the individual groups.

branch is $SO(4n+2)\times U(1)$ and there are 4 generating representations, as can be found from the HWG:

$$HWG = \frac{1}{(1-t^2)(1-\frac{\mu_{2n+1}\,t^n}{q})(1-q\,\mu_{2n}\,t^n)\prod_{i=1}^{n-1}(1-\mu_{2i}\,t^{2i})}, \tag{4.7.42}$$

where $\mu_1,...,\mu_{2n+1}$ are the highest weight fugacities for $SO(4n+2)$ and q is the fugacity for the $U(1)$ charge. Explicitly, the generators are:

Generator	Δ	$SO(4n+2)\times U(1)$ representation
$a_{\mu\nu}$	1	adjoint $\times(0)$
C_1	1	trivial $\times(0)$
s^α	$\frac{n}{2}$	left spinor $\times(+1)$
s_α	$\frac{n}{2}$	right spinor $\times(-1)$

, (4.7.43)

where α and β are spinor indices going from $1,...,2^{2n}$; and any other indices are vector indices going from $1,...,4n+2$, antisymmetrised with those appearing alongside them in a given subscript. C_1 is the invariant of the $U(1)$ factor in the flavour symmetry, so-called to make connection with the notation for the flavour symmetry invariants in the Coulomb branches of Sections 4.7.1 – 4.7.3. This $U(1)$ is formed from a linear combination of the two $U(1)$ symmetries in the classical (finite coupling) Higgs branch of the $5d$ theory in question: the $U(1)_B\subset U(2n+1)$ baryon symmetry associated to the trace of the meson matrix M, and the $U(1)_I$ instanton symmetry associated to the gaugino bilinear S one can construct.[32] The orthogonal linear combination of these $U(1)$ symmetries is combined with the $SU(2n+1)$ factor in the classical flavour symmetry, enhancing it to the $SO(4n+2)$ we see at infinite coupling. The left and right spinors of $SO(4n+2)$ are complex representations which are conjugate to one another, hence the raised and lowered indices respectively. This makes matching the indices in the Poisson brackets (Step 4 of Section 4.6) slightly more complicated in this case. The matrices δ and $\gamma_{\mu\nu}$ are spinor valued (i.e. their entries are labelled by two spinor indices α and β), and lie in the trivial (1) and adjoint (μ_2) representations of $SO(4n+2)$ respectively. To see what form their spinor indices take, it is therefore important to ascertain whether these representations lie in the second rank symmetric/antisymmetric of one of the spinors or in the tensor product of the two conjugate spinors. It turns out that both 1 and μ_2 lie in the tensor product $\mu_{2n}\otimes\mu_{2n+1}$, and hence have one upper and one lower spinor index labelling their matrix entries: $\delta^\alpha{}_\beta$ and $(\gamma_{\mu\nu})^\alpha{}_\beta$.

We conjecture that the non-zero Poisson brackets of (4.7.43) are given by:

$$\begin{aligned}
\{a_{\mu\nu},a_{\rho\sigma}\} &= \delta_{\nu\rho}a_{\mu\sigma}-\delta_{\mu\rho}a_{\nu\sigma}+\delta_{\mu\sigma}a_{\nu\rho}-\delta_{\nu\sigma}a_{\mu\rho},\\
\{a_{\mu\nu},s^\alpha\} &= (\gamma_{\mu\nu})^\alpha{}_\beta\, s^\beta,\\
\{a_{\mu\nu},s_\alpha\} &= s_\beta\,(\gamma_{\mu\nu})^\beta{}_\alpha,\\
\{C_1,s^\alpha\} &= +s^\alpha\\
\{C_1,s_\alpha\} &= -s_\alpha\\
\{s^\alpha,s_\beta\} &= {C_1}^{n-1}\,\delta^\alpha{}_\beta,
\end{aligned} \tag{4.7.44}$$

[32] By "associated", we mean that M and S are the scalar superpartners of the conserved currents associated to these symmetries. We use this association because, for study of the moduli space, it is the scalars which we are interested in.

where C_1 is normalised such that there are no additional numerical coefficients in (4.7.44). All other Poisson brackets between (4.7.43) that are not listed in (4.7.44) vanish.

4.7.5 Magnetic quivers for $5d$ $\mathcal{N} = 1$ SQCD

The following four sections are based on magnetic quivers [73] found for certain cones of the Higgs branch at infinite coupling of $5d$ $\mathcal{N} = 1$ special unitary SQCD theories with UV fixed points [72]. Such a $5d$ theory is specified by three parameters: the number of colours N_c of the gauge group; the number of flavours N_f transforming in its fundamental representation; and the Chern-Simons level k;

$$SU(N_c)_{\pm|k|} \text{ ○——□ } N_f \ . \tag{4.7.45}$$

To have a UV fixed point, these three parameters must satisfy the following inequality [96]:

$$|k| \leq N_c - \frac{N_f}{2} + 2. \tag{4.7.46}$$

In these instances, we can investigate the case of infinite coupling.

In [72], the authors split (4.7.46) into four regions and computed the magnetic quivers – plural as each Higgs branch is the union of various cones – for the various Higgs branches in each region. In an unpublished work by Zhenghao Zhong and Amihay Hanany, the HWG for each of these magnetic quivers was computed. We will use these HWGs to derive the Poisson brackets for the Coulomb branch generators of these magnetic quivers. Many of the quivers appearing in [72] either only have generators in the adjoint representation or have already appeared in Sections 4.7.1 – 4.7.4. We will omit the Poisson brackets for these quivers as they have been covered in previous sections, but will give a brief comment noting the relevant ones in each of Sections 4.7.5.1 – 4.7.5.4. The remaining quivers (bar certain exceptional cases of the Chern Simons coupling in regions 2 and 4) fall into four families: the so-called trapezium, pyramid, kite and truck families. The first two such families are specified by three parameters, $N_f - 1$, n and σ, and the latter two families by just n and σ. Each of these parameters is a function of the parameters of the $5d$ theory, N_f, N_c and k, and one can check the original paper [72] for the specific relationship (the new parameters n and σ have been introduced to encapsulate multiple cones by the same quiver: the only difference between cones being the dependence of n and σ on N_f, N_c and k). The structure of each family of quivers restricts the values that n and σ can take (for example, for the Trapezium family (4.7.48) can only have $n = 1$ for $N_f = 2$ or 3). In Sections 4.7.5.1 – 4.7.5.4 we will explore the Poisson brackets for the Coulomb branch generators of each of these four families in turn.

4.7.5.1 Trapezium family

The trapezium family encapsulates the magnetic quivers for two cones which make up the Higgs branch of $5d$ $\mathcal{N} = 1$ SQCD with parameters satisfying the following subsets of (4.7.46), "region 1" and "region 3" of [72] respectively:

$$|k| < N_c - \frac{N_f}{2} \qquad \text{and} \qquad |k| = N_c - \frac{N_f}{2} + 1. \tag{4.7.47}$$

Note that there is an additional cone comprising the Higgs branch of each of these regions (4.7.47) with a magnetic quiver that does not conform to the structure of (4.7.48), but they are closures

nilpotent orbits.[33] The family is given by

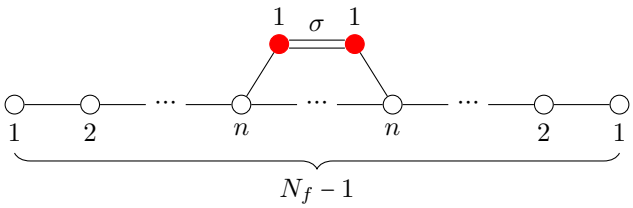

(4.7.48)

for $N_f \geq 2$, where a red node indicates that it is unbalanced, and σ indicates the multiplicity of the hypermultiplet linking the two unbalanced $U(1)$ nodes. Generically, we can read off that this quiver has global symmetry $SU(N_f) \times U(1)$. Note that this is less than in the classical case. In the case where $n = \sigma = 1$ however, the two red nodes are actually balanced and this quiver becomes the affine A_{N_f} quiver; the global symmetry is enhanced to $SU(N_f + 1) \supset SU(N_f) \times U(1)$, and the Poisson brackets are the structure constants of $SU(N_f + 1)$. From the structure of the quiver, one can see that we must necessarily have $1 \leq n \leq \lfloor \frac{N_f}{2} \rfloor$. When we don't have $n = \sigma = 1$, there are 4 generating representations, as can be found from the HWG:

$$HWG = \frac{1 - \mu_n \, \mu_{N_f - n} \, t^{2(n+\sigma)}}{(1-t^2)(1-\mu_n \, q \, t^{n+\sigma})(1 - \frac{\mu_n}{q} \, t^{n+\sigma}) \prod_{i=1}^{n} (1 - \mu_i \, \mu_{N_f - i} \, t^{2i})}. \tag{4.7.49}$$

where $\mu_1, ..., \mu_{N_f - 1}$ are the highest weight fugacities for $SU(N_f)$, and q is the fugacity for the $U(1)$ charge. Explicitly, the generators are:[34]

Generator	Δ	$SU(N_f) \times U(1)$ representation
$a^{\mu}{}_{\nu}$	1	adjoint $\times (0)$
C_1	1	trivial $\times (0)$
$b^{\mu_1 \cdots \mu_n}$	$\frac{n+\sigma}{2}$	n^{th} rank antisymmetric $\times (+1)$
$d_{\mu_1 \cdots \mu_n}$	$\frac{n+\sigma}{2}$	$(N_f - n)^{th}$ rank antisymmetric $\times (-1)$

, (4.7.50)

where all indices involving μ and ν range from $1, ..., N_f$; those on b are completely antisymmetrised; and C_1 is the invariant of the $U(1)$ factor in the flavour symmetry (see Section 4.7.4 for more details). The parameter n takes different values with regards to the parameters N_c, N_f and k on each of the Higgs branch cones whose magnetic quiver is encapsulated by (4.7.48). The specific expression for n will dictate the physical states of b and d, hence their generic names.

[33] For the exceptional cases of $k = \frac{1}{2}$ and $k = 0$ in region 3, the magnetic quiver does not take the form of (4.7.48), and instead takes the form of (4.7.37) for $N_f = 2n + 1$ and (4.7.33) for $N_f = 2n + 2$ respectively (where this n is that used in (4.7.37) and (4.7.33) respectively, not to be confused with the n of (4.7.48)).

[34] The $(N_f - n)^{\text{th}}$ rank antisymmetric could be written with $N_f - n$ upper antisymmetrised indices, but the invariance of $\epsilon^{\mu_1 \cdots \mu_{N_f}}$ means we can also write it with n lower antisymmetrised indices instead. This choice of notation makes clear the fact that it is the conjugate to the n^{th} rank antisymmetric representation.

We conjecture that the non-zero Poisson brackets of (4.7.50) are given by:

$$\begin{aligned}
\{a^{\mu}{}_{\nu}, a^{\rho}{}_{\sigma}\} &= \delta^{\mu}{}_{\sigma} a^{\rho}{}_{\nu} - \delta^{\rho}{}_{\nu} a^{\mu}{}_{\sigma}, \\
\{a^{\mu}{}_{\nu}, b^{\mu_1\cdots\mu_n}\} &= \delta^{[\mu_1}{}_{\nu}\, b^{\mu_2\cdots\mu_n]\mu} \\
\{a^{\mu}{}_{\nu}, d_{\mu_1\cdots\mu_n}\} &= \delta^{\mu}{}_{[\mu_1}\, d_{\mu_2\cdots\mu_n]\nu}, \\
\{C_1, b^{\mu_1\cdots\mu_n}\} &= +\, b^{\mu_1\cdots\mu_n}, \\
\{C_1, d_{\mu_1\cdots\mu_n}\} &= -\, d_{\mu_1\cdots\mu_n}, \\
\{b^{\mu_1\cdots\mu_n}, d_{\nu_1\cdots\nu_n}\} &= C_1{}^{n+\sigma-1}\, \delta^{[\mu_1}{}_{[\nu_1}\cdots\delta^{\mu_n]}{}_{\nu_n]}.
\end{aligned} \tag{4.7.51}$$

where C_1 is normalised such that there are no additional numerical coefficients in (4.7.51). In one of the cones $n = N_f - N_c$, meaning b and d are the baryons that we would expect to show up (due to C_1 acting as the baryon number: the $U(1)_B$ baryon symmetry is preserved). In the other cone, we expect b and d to be instanton operators. All other Poisson brackets between (4.7.50) that are not listed in (4.7.51) vanish.

4.7.5.2 Pyramid family

The pyramid family are magnetic quivers for one cone which makes up the Higgs branch of $5d$ $\mathcal{N} = 1$ SQCD with parameters satisfying the following subset of (4.7.46), "region 2" of [72]:

$$|k| = N_c - \frac{N_f}{2}. \tag{4.7.52}$$

Note that there is an additional Higgs branch cone with a magnetic quiver that does not conform to the structure of (4.7.53), but it is the closure of a nilpotent orbit or a product thereof (depending on the values of the parameters).[35] The family is given by

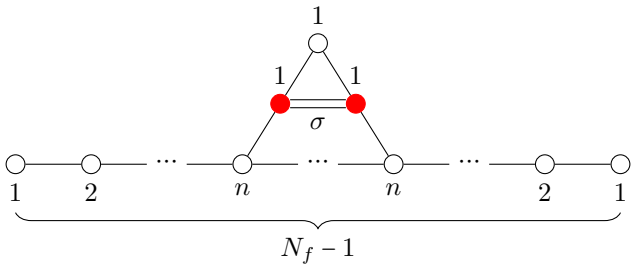

(4.7.53)

for $N_f \geq 2$, where a red node indicates that it is unbalanced, and σ indicates the multiplicity of the hypermultiplet stretching between the two unbalanced $U(1)$ nodes. Generically, we can read off that this quiver has global symmetry $SU(N_f) \times SU(2) \times U(1)$. The structure of the quiver means that we must necessarily have $1 \leq n \leq \lfloor \frac{N_f}{2} \rfloor$. There are 5 generating representations, as can be found from the HWG:

$$HWG = \frac{1 - \nu^2\, \mu_n\, \mu_{N_f-n}\, t^{2(n+\sigma+1)}}{(1-t^2)(1-\nu^2 t^2)(1-\nu\, \mu_n\, q\, t^{n+\sigma+1})(1-\frac{\nu\, \mu_n}{q}\, t^{n+\sigma+1}) \prod_{i=1}^{n}(1-\mu_i\, \mu_{N_f-i}\, t^{2i})}, \tag{4.7.54}$$

[35] Note also that for the exceptional case of $k = 0$ in (4.7.52), the magnetic quiver does not take the form of (4.7.53).

where ν and $\mu_1, ..., \mu_{N_f-1}$ are the highest weight fugacities for $SU(2)$ and $SU(N_f)$ respectively, and q is the fugacity for the $U(1)$ charge. Explicitly, the generators are:

Generator	Δ	$SU(N_f) \times SU(2) \times U(1)$ representation
$A^{\mu}{}_{\nu}$	1	adjoint $\times$ trivial $\times$ (0)
$a_{\alpha\beta}$	1	trivial $\times$ adjoint $\times$ (0)
C_1	1	trivial $\times$ trivial $\times$ (0)
$B^{\mu_1\cdots\mu_n}{}_{\alpha}$	$\frac{n+\sigma+1}{2}$	n^{th} rank antisymmetric $\times$ fundamental $\times$ (+1)
$D_{\mu_1\cdots\mu_n\,\alpha}$	$\frac{n+\sigma+1}{2}$	$(N_f-n)^{th}$ rank antisymmetric $\times$ fundamental $\times$ (−1)

, (4.7.55)

where all indices involving μ and ν are $SU(N_f)$ indices ranging from $1, ..., N_f$, and those that appear in exponents or subscripts of B or D are antisymmetrised among themselves; indices involving α and β are $SU(2)$ indices ranging from $1, 2$; and C_1 is the invariant of the $U(1)$ factor in the flavour symmetry (see Section 4.7.4 for more details). We conjecture that the non-zero Poisson brackets of (4.7.55) are given by:

$$\begin{aligned}
\{A^{\mu_1}{}_{\nu_1}, A^{\mu_2}{}_{\nu_2}\} &= \delta^{\mu_1}{}_{\nu_2} A^{\mu_2}{}_{\nu_1} - \delta^{\mu_2}{}_{\nu_1} A^{\mu_1}{}_{\nu_2}, \\
\{a_{\alpha_1\beta_1}, a_{\alpha_2\beta_2}\} &= \epsilon_{\alpha_1\beta_2} a_{\alpha_2\beta_1} + \epsilon_{\beta_1\beta_2} a_{\alpha_2\alpha_1} + \epsilon_{\alpha_1\alpha_2} a_{\beta_2\beta_1} + \epsilon_{\beta_1\alpha_2} a_{\beta_2\alpha_1}, \\
\{A^{\mu}{}_{\nu}, B^{\mu_1\cdots\mu_n}{}_{\alpha}\} &= \delta^{[\mu_1}{}_{\nu} B^{\mu_2\cdots\mu_n]\mu}{}_{\alpha}, \\
\{A^{\mu}{}_{\nu}, D_{\mu_1\cdots\mu_n\,\alpha}\} &= \delta^{\mu}{}_{[\mu_1} D_{\mu_2\cdots\mu_n]\nu\,\alpha}, \\
\{a_{\alpha\beta}, B^{\mu_1\cdots\mu_n}{}_{\alpha_1}\} &= B^{\mu_1\cdots\mu_n}{}_{(\alpha}\,\epsilon_{\beta)\alpha_1}, \\
\{a_{\alpha\beta}, D_{\mu_1\cdots\mu_n\,\alpha_1}\} &= D_{\mu_1\cdots\mu_n(\beta}\,\epsilon_{\alpha)\alpha_1}, \\
\{C_1, B^{\mu_1\cdots\mu_n}{}_{\alpha}\} &= +B^{\mu_1\cdots\mu_n}{}_{\alpha}, \\
\{C_1, D_{\mu_1\cdots\mu_n\alpha}\} &= -D_{\mu_1\cdots\mu_n\alpha}, \\
\{B^{\mu_1\cdots\mu_n}{}_{\alpha}, D_{\nu_1\cdots\nu_n\beta}\} &= C_1{}^{n+\sigma}\,\delta^{[\mu_1}{}_{[\nu_1}\cdots\delta^{\mu_n]}{}_{\nu_n]}\,\epsilon_{\alpha\beta},
\end{aligned} \tag{4.7.56}$$

where $(\cdot)/[\cdot]$ indicates a symmetrisation/antisymmetrisation over the enclosed indices with no numerical prefactor; and C_1 is normalised such that there are no additional numerical coefficients in (4.7.56). All other Poisson brackets between (4.7.55) that are not listed in (4.7.56) vanish.

4.7.5.3 Kite family

The kite family are magnetic quivers for one cone in the Higgs branch of $5d$ $\mathcal{N} = 1$ SQCD with parameters satisfying the following subset of (4.7.46), "region 4" of [72]:

$$2 < |k| = N_c - \frac{N_f}{2} + 2, \tag{4.7.57}$$

with N_f even. There is an additional Higgs branch cone with a magnetic quiver that does not conform to the structure of (4.7.58) for $N_f \geq 2$, but it is the closure of a nilpotent orbit.[36] The family is given

[36] Note also that for the exceptional case of $k = 1$, the magnetic quiver does not take the form of (4.7.58).

by

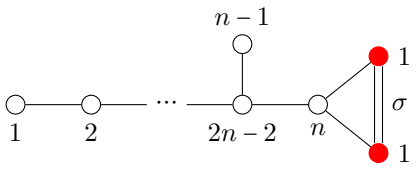

(4.7.58)

for $n \geq 2$, where a red node indicates that it is unbalanced, and σ indicates the multiplicity of the hypermultiplet stretching between the two unbalanced $U(1)$ nodes. Generically, we can read off that this quiver has global symmetry $SO(4n) \times U(1)$. There are 4 generating representations, as can be found from the HWG:

$$HWG = \frac{1 - \mu_{2n}^2\, t^{2(n+\sigma)}}{(1-t^2)(1-\mu_{2n}^2\, t^{2n})(1-\mu_{2n}\, q\, t^{n+\sigma})(1-\frac{\mu_{2n}}{q}\, t^{n+\sigma})\prod_{i=1}^{n-1}(1-\mu_{2i}\, t^{2i})}, \tag{4.7.59}$$

where $\mu_1, ..., \mu_{2n}$ are the highest weight fugacities for the $SO(4n)$ factor in the global symmetry, and q is the fugacity for the $U(1)$ charge. Explicitly, the generators are:

Generator	Δ	$SO(4n) \times U(1)$ representation
$a_{\mu\nu}$	1	adjoint (0)
C_1	1	trivial $\times\,(0)$
s_α^+	$\frac{n+\sigma}{2}$	spinor $\times\,(+1)$
s_α^-	$\frac{n+\sigma}{2}$	spinor $\times\,(-1)$

, (4.7.60)

where α and β spinor indices going from $1, ..., 2^{2n-1}$; any other indices are vector indices going from $1, ..., 4n$, antisymmetrised with those appearing alongside them in a given subscript; and C_1 is the invariant of the $U(1)$ factor in the flavour symmetry (see Section 4.7.4 for more details). The spinor representation of $SO(4n)$ is real/pseudo-real for even/odd n. We conjecture that the non-zero Poisson brackets of (4.7.60) are given by:

$$\begin{aligned}
\{a_{\mu\nu}, a_{\rho\sigma}\} &= \delta_{\nu\rho} a_{\mu\sigma} - \delta_{\mu\rho} a_{\nu\sigma} + \delta_{\mu\sigma} a_{\nu\rho} - \delta_{\nu\sigma} a_{\mu\rho}, \\
\{a_{\mu\nu}, s_\alpha^\pm\} &= (\gamma_{\mu\nu})_{\alpha\beta}\, s_\beta^\pm, \\
\{C_1, s_\alpha^\pm\} &= \pm\, s_\alpha^\pm, \\
\{s_\alpha^+, s_\beta^-\} &= \begin{cases} {C_1}^{n+\sigma-2}\, (\gamma_{\mu\nu})_{\alpha\beta}\, a_{\mu\nu} & \text{if } n \text{ even}, \\ {C_1}^{n+\sigma-1}\, \Omega_{\alpha\beta} & \text{if } n \text{ odd}, \end{cases}
\end{aligned} \tag{4.7.61}$$

where C_1 is normalised such that there are no additional numerical coefficients in (4.7.61); and $\Omega_{\alpha\beta}$ is the invariant skew-symmetric two form of $Sp(k = 2^{2n-2})$ (4.3.4). All other Poisson brackets between (4.7.60) that are not listed in (4.7.61) vanish.

4.7.5.4 Truck family

The truck family is the magnetic quiver for the Higgs branch of $5d$ $\mathcal{N} = 1$ SQCD with parameters satisfying the same subset of (4.7.46) as the kite family, (4.7.57) ("region 4" of [72]), but with N_f

odd.[37] The family is given by

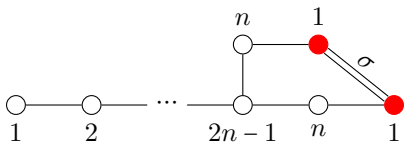

(4.7.62)

for $n \geq 2$, where a red node indicates that it is unbalanced, and σ indicates the multiplicity of the hypermultiplet stretching between the two unbalanced $U(1)$ nodes. Generically, we can read off that this quiver has global symmetry $SO(4n+2) \times U(1)$. There are 4 generating representations, as can be found from the HWG:

$$HWG = \frac{1 - \mu_{2n}\,\mu_{2n+1}\,t^{2(n+\sigma)}}{(1-t^2)(1-\mu_{2n}\,\mu_{2n+1}\,t^{2n})(1-\mu_{2n}\,q\,t^{n+\sigma})(1-\frac{\mu_{2n+1}}{q}\,t^{n+\sigma})\prod_{i=1}^{n-1}(1-\mu_{2i}\,t^{2i})}, \tag{4.7.63}$$

where $\mu_1, ..., \mu_{2n+1}$ are the highest weight fugacities for the $SO(4n+2)$ factor in the global symmetry, and q is the fugacity for the $U(1)$ charge. Explicitly, the generators are:

Generator	Δ	$SO(4n+2) \times U(1)$ representation
$a_{\mu\nu}$	1	adjoint (0)
C_1	1	trivial $\times\,(0)$
s^α	$\frac{n+\sigma}{2}$	left spinor $\times\,(+1)$
s_α	$\frac{n+\sigma}{2}$	right spinor $\times\,(-1)$

, (4.7.64)

where α and β spinor indices going from $1, ..., 2^{2n}$; any other indices are vector indices going from $1, ..., 4n+2$, antisymmetrised with those appearing alongside them in a given subscript; and C_1 is the invariant of the $U(1)$ factor in the flavour symmetry (see Section 4.7.4 for more details). The left and right spinors of $SO(4n+2)$ are complex representations, and conjugate to one another, hence the raised and lower indices respectively. We conjecture that the non-zero Poisson brackets of (4.7.64) are given by:

$$\begin{aligned}
\{a_{\mu\nu}, a_{\rho\sigma}\} &= \delta_{\nu\rho}a_{\mu\sigma} - \delta_{\mu\rho}a_{\nu\sigma} + \delta_{\mu\sigma}a_{\nu\rho} - \delta_{\nu\sigma}a_{\mu\rho}, \\
\{a_{\mu\nu}, s^\alpha\} &= (\gamma_{\mu\nu})^\alpha{}_\beta\, s^\beta, \\
\{a_{\mu\nu}, s_\alpha\} &= s_\beta\, (\gamma_{\mu\nu})^\beta{}_\alpha, \\
\{C_1, s^\alpha\} &= +\, s^\alpha, \\
\{C_1, s_\alpha\} &= -\, s_\alpha, \\
\{s^\alpha, s_\beta\} &= C_1{}^{n+\sigma-1}\,\delta^\alpha{}_\beta,
\end{aligned} \tag{4.7.65}$$

where the spinor indices on the $\gamma_{\mu\nu}$ and δ are determined as in Section 4.7.4; and C_1 is normalised such that there are no additional numerical coefficients in (4.7.65). All other Poisson brackets between (4.7.64) that are not listed in (4.7.65) vanish.

[37] Note that for $k = \frac{1}{2}$, the magnetic quiver does not take the form (4.7.62), and instead takes the form of (4.7.1) for $N_f = 2n+7$ (where this n is that used in (4.7.1), not to be confused with the n of (4.7.62).

Chapter 5

Conclusion

The author hopes that this thesis serves as a helpful and pedagogical introduction to the study of $3d$ $\mathcal{N} = 4$ Coulomb branches $\mathcal{C}$; in particular, to the use of existing tools (such as magnetic quivers, Hasse diagrams and the monopole formula) along with new techniques developed by the author and Amihay Hanany (such as quiver addition and the amendment to the BGS algorithm) to make progress with determining the topological global symmetry and Poisson brackets of $\mathcal{C}$. The methods discussed combine the physical and mathematical interpretation of $\mathcal{C}$, utilising and developing the bridge between these two fields to draw conclusions about both symplectic singularities and the physics of the underlying theory.

In principle, a quiver should encode everything about a theory. The ideal result of the avenues of study discussed would be an algorithm to determine the global symmetry and Poisson brackets via simple graph theory computations using the quiver data. The works of [10] and [11], the subjects of this thesis, make progress towards this. The former, presented in Chapter 3, helps to understand the failings of a previous algorithm to find the global symmetry of certain Coulomb branches from their Coulomb quivers, and provides an amended algorithm which solves these failures in the cases discussed. This not only sheds light on some underlying physics, but takes a step closer to finding an algorithm which works unfailingly to find the full global symmetry for all quivers. The latter, presented in Chapter 4, computes Poisson brackets for certain Coulomb branches. These brackets relate to the symplectic form on $\mathcal{C}$ and help us to learn of the singularity structure; the Poisson bracket vanishes along a singular subset of the variety. We hope that Chapter 2 provides a concise and understandable introduction to all the ideas and concepts needed to understand the results presented in Chapters 3 and 4.

There are many further directions that can (and the author hopes will) be explored, developing on the contributions of this thesis. We first discuss some possible directions stemming from the results of Chapter 3. Firstly, the notion of experiencing an enhanced symmetry is noteworthy in itself; it would be interesting to investigate the properties of these quivers further and see if they hold any other surprising or fruitful properties. Those with simple Hasse diagrams[1] would be obvious candidates to start with, as a simple singularity structure can be an indicator of a simpler symplectic singularity. Secondly, the amended algorithm to find the global symmetry from the quiver (presented in Section

[1] We computed the Hasse diagrams for many of the quivers in Chapter 3 but chose not to include them in [10] or this note, as they were not pertinent to the main message.

3.7) still does not work for every quiver that we are interested in studying, but is a good stepping-stone to the end goal of an algorithm which does. It would be nice to build on our amendment to continue to make progress towards this goal. Thirdly, the conjectured symmetries present in this chapter can be used to provide support for future developments of brane systems for more complicated quivers, and their corresponding quiver subtraction rules.

Chapter 4 is the first to display the Poisson brackets for lengthy magnetic quivers of 5 and $6d$ theories at infinite coupling; in the literature, Poisson brackets are largely computed for Coulomb branches of abelian or low rank gauge theories. The conjecture prescribed in Chapter 4 allows us to compute them in any theory for which the generators and relations of the Hilbert series are known. In this thesis we did this for a certain subset of such quivers, but there are many others one could compute. In particular, it would be interesting to compute the brackets of quivers lying lower down in the Hasse diagram of the quivers in Chapter 4. Analysis of these brackets in comparison to those for the original quiver can help us to understand where the degeneracies in the symplectic form occur.

With that we conclude the outlook, and the thesis. Cheers for reading.

Appendix A

Discrete Projections

As mentioned in Section 3.2.1 (and at multiple subsequent points in Chapter 3) the Coulomb branches of quivers containing nodes with an adjoint hypermultiplet can be realised as discrete quotients of the Coulomb branches of quivers with a bouquet of $U(1)$ nodes (3.2.1) [71, 83, 84, 62]. In this appendix, we explain how this can be verified, and see it in practise with an example.

Suppose we have two quivers A and B which are conjectured to satisfy the relation

$$\mathcal{C}(B)/S_n = \mathcal{C}(A), \tag{A.0.1}$$

due to B having some S_n outer automorphism. The way we prove this conjecture to the best of our ability is to show the equality of Hilbert series. This is done by calculating the Hilbert series for $\mathcal{C}(B)$, and finding some S_n action on its generators and relations that obtains the Hilbert series of $\mathcal{C}(A)$. To be more precise, on the left hand side of (A.0.1) we are trying to calculate the S_n gauged Coulomb branch of B. This Coulomb branch should be S_n invariant, and so this gauging is realised by finding some action of S_n on the Coulomb branch and performing the corresponding Molien sum on the Hilbert series of $\mathcal{C}(B)$ to find the Hilbert series of $\mathcal{C}(B)/S_n$ such that it matches the Hilbert series of $\mathcal{C}(A)$, which can just be computed in the usual manner using the monopole formula.

Schematically, this Molien sum (which is responsible for making an object gauge invariant) over our discrete group $G = S_n$ goes like

$$HS(\mathcal{C}(B)/G) = \frac{1}{|G|}\sum_{g\in G} g \cdot HS(\mathcal{C}(B)). \tag{A.0.2}$$

where HS stands for Hilbert series and $\cdot$ is an action of G. The action of G on a Hilbert series is fully determined by the action on its generators and relations. Each element of G will in general act differently, and the contributions from each of these actions are summed together before their total is divided by the cardinality of G. To find the action of G, we need to analyse and understand its representations and characters. This is just an exercise in the theory of finite groups. The example we show here will be that of $G = S_2 = \mathbb{Z}_2$, for which the game is a bit easier as there are just two one dimensional representations. However the method can be extended and applied to any finite group, provided the representations and characters are known and understood.

Example Consider the magnetic quiver of the next to minimal nilpotent orbit of B_3:

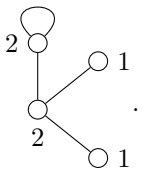

(A.0.3)

In this case, the conjecture (3.2.1) tells us that

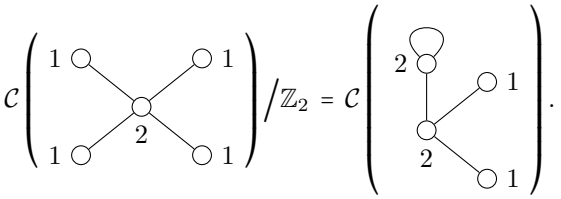

(A.0.4)

Let's see how to show this. First, let's compute the Hilbert series of the quiver on the right hand side, which we call $Q_{\text{n.min}B_3}$, so we know what we are looking to obtain from the left hand side via the discrete quotient. We can find the HWG of Q_{nminB_3}, which completely encodes the refined Hilbert series, to be

$$HWG_{B_3}(Q_{\text{n.min}B_3}) = PE[\mu_2 t^2 + \mu_1^2 t^4] = \frac{1}{(1-\mu_2 t^2)(1-\mu_1^2 t^4)}, \tag{A.0.5}$$

where the B_3 subscript on HWG is used to illustrate that $\{\mu_1, \mu_2, \mu_3\}$ are the Dynkin label (i.e. highest weight) fugacities for B_3.

Now it's time to realise this as the $\mathbb{Z}_2$ quotient of the minimal nilpotent orbit of d_4, which is the Coulomb branch of the quiver on the left hand side of (A.0.4), that we'll call Q_{minD_4}. The HWG of this quiver can be easily computed to be

$$HWG_{D_4}(Q_{\text{min}D_4}) = PE[\tilde{\mu}_2 t^2] = \frac{1}{1-\tilde{\mu}_2 t^2}, \tag{A.0.6}$$

where as before the D_4 subscript on HWG tells us that $\{\tilde{\mu}_1, \tilde{\mu}_2, \tilde{\mu}_3, \tilde{\mu}_4\}$ are the Dynkin label fugacities for D_4. The goal now is to find a $\mathbb{Z}_2$ action on (A.0.6) that will reproduce (A.0.5). However in order to do this, we need to have (A.0.6) in terms of the same fugacities as (A.0.5); we must decompose the adjoint representation of D_4 into irreducible representations of B_3.[1] Writing the characters of D_4 in terms of fundamental weight fugacities $\{x_1, x_2, x_3, x_4\}$ and those of B_3 in terms of $\{x_1, x_2, x_3\}$, one finds that under the fugacity map $x_4 \to x_3$ the adjoint representation of D_4 decomposes into the sum of the adjoint and fundamental representations of B_3:

$$\tilde{\mu}_2 \to \mu_2 + \mu_1. \tag{A.0.7}$$

Based on this, we guess that the HWG of the minimal nilpotent orbit of d_4, i.e. $\mathcal{C}(Q_{\text{min}D_4})$, in terms of B_3 Dynkin label fugacities is

$$HWG_{B_3}(Q_{\text{min}D_4}) = PE[(\mu_2 + \mu_1) t^2] = \frac{1}{(1-\mu_2 t^2)(1-\mu_1 t^2)}. \tag{A.0.8}$$

We need to check that this is correct, as it could be that these representations of B_3 will actually overcount the representations of D_4 we wanted, and to correct this we'd need to impose relations.

[1] The tabulations of the branching rules, among many other useful for results, for several Lie groups can be found in [97].

The way to check for this is to turn (A.0.8) into a refined or unrefined Hilbert series, and compare it to that obtained from using the monopole formula on $Q_{\min D_4}$ (after the appropriate fugacity map in the refined case). Here, under performing this check we see that (A.0.6) and (A.0.8) yield the same Hilbert series, and so (A.0.8) is indeed the correct HWG for the minimal nilpotent orbit of D_4 in terms of B_3 fugacities.

Now all that's left to do is find the $\mathbb{Z}_2$ action that when used in a Molien sum on (A.0.8) will yield (A.0.5). The action on the generators will fully determine the action everywhere, and we can see here our generators are $\mu_1 t^2$ and $\mu_2 t^2$. The group $\mathbb{Z}_2$ has two elements: the identity and some other element which squares to the identity, e.g. $\{1, -1\}$. So our Molien sum looks like

$$HWG_{B_3}(Q_{\min D_4}])/\mathbb{Z}_2 = \frac{1}{2} \sum_{g\in\{1,-1\}} PE[g\cdot\mu_1 t^2 + g\cdot\mu_2 t^2]. \tag{A.0.9}$$

The representations of $\mathbb{Z}_2$ that μ_1 and μ_2 are in determine the action of $\mathbb{Z}_2$ on them. There are just two representations of $\mathbb{Z}_2$: the trivial representation and the sign representation. The trivial representation is obviously invariant under all group elements, and the sign representation is mapped to plus or minus itself by the elements 1 or -1 of $\mathbb{Z}_2$ respectively. It turns out that if μ_1 is in the sign representation and μ_2 is in the trivial representation, we reproduce (A.0.5):

$$\begin{aligned} HWG(Q_{\min D_4})/\mathbb{Z}_2 &= \frac{1}{2}\left(PE[1\cdot\mu_1 t^2 + 1\cdot\mu_2 t^2] + PE[-1\cdot\mu_1 t^2 + -1\cdot\mu_2 t^2]\right) \\ &= \frac{1}{2}\left(PE[\mu_1 t^2 + \mu_2 t^2] + PE[-\mu_1 t^2 + \mu_2 t^2]\right) \\ &= PE[\mu_2 t^2 + \mu_1^2 t^4] \\ &= HWG(Q_{nminB_3}). \end{aligned} \tag{A.0.10}$$

This completes the proof of the equality of Hilbert series for $\mathcal{C}(Q_{\min D_4})/S_2$ and $\mathcal{C}(Q_{\text{n.min}B_3})$, and hence validating the conjecture (A.0.4) to the best of our ability.[2] □

[2] We say only to the best of our ability as the Hilbert series is not a complete characterisation of the Coulomb branch moduli space, but at present it is the most complete encapsulation that we have.

Appendix B

Tensor, Symmetric and Antisymmetric Products

In Sections 4.6 – 4.7, we use the antisymmetric property of the Poisson bracket to constrain the representations that the output can lie in. In this appendix, we outline how this works in practise.

Suppose we want to find the Poisson bracket between two generators g_1 and g_2, which lie in the representations R_1 and R_2 of some group G respectively. Appropriate indices on g_1 and g_2 will reflect the components of the respective representations. The Poisson bracket in some sense intertwines g_1 and g_2, and so the result must lie in the tensor product representation $R_1 \otimes R_2$ in all cases. If $R_1 = R_2$, the antisymmetry of the Poisson bracket means that the result $\{g_1, g_2\}$ not only lies in the tensor product $R_1 \otimes R_1$, but in fact in the second rank antisymmetric product of R_1: $\Lambda^2(R_1) = \Lambda(R_1 \otimes R_1) \subset R_1 \otimes R_1$. But how do we compute this?

In general $R_1 \otimes R_2$ is not an irreducible representation. The weights lying in $R_1 \otimes R_2$ are those obtained by adding all weights of R_2 to each weight of R_1. These weights form several irreducible representations of G, and this is the tensor product decomposition of $R_1 \otimes R_2$. That is, if the weights of the representation R are denoted by w_i^R for $i = 1, ..., d_R = \dim(R)$, then

$$\left\{ w_i^{R_1 \otimes R_2} \;\middle|\; i = 1, ..., d_{R_1}\, d_{R_2} \right\} = \left\{ w_j^{R_1} + w_k^{R_2} \;\middle|\; j = 1, ..., d_{R_1},\ k = 1, ..., d_{R_2} \right\} \tag{B.0.1}$$

and we write

$$R_1 \otimes R_2 = \bigoplus_i c_i \, \tilde{R}_i \tag{B.0.2}$$

where c_i are non-negative integer coefficients, to illustrate how the tensor product representation decomposes into the irreducible representations $\tilde{R}_i$ of G. Sometimes the direct sum symbol is dropped and we just write

$$R_1 \otimes R_2 = \sum_i c_i \, R_i. \tag{B.0.3}$$

Example Consider $G = SU(2)$, $R_1 = \mu$[1] whose weights are $\{w_i^{\mu}\} = \{(1), (-1)\}$, and $R_2 = \mu^2$ whose weights are $\{w_i^{\mu^2}\} = \{(2), (0), (-2)\}$. The tensor product $\mu \otimes \mu^2$ then contains the weights

$$\begin{aligned}\left\{w_i^{\mu\otimes\mu^2} \;\middle|\; i = 1,...,6\right\} &= \left\{w_j^{\mu} + w_k^{\mu^2} \;\middle|\; j = 1,2,\ k = 1,2,3\right\} \\ &= \{(3), (1), (-1), (1), (-1), (-3)\},\end{aligned} \tag{B.0.4}$$

and thus we see that

$$\mu \otimes \mu^2 = \mu^3 + \mu. \tag{B.0.5}$$

□

In the case where $R_1 = R_2 = R$, we can consider the symmetric and antisymmetric parts of such a product. We can see that in this case the weights of the tensor product can be decomposed as follows:

$$\begin{aligned}\left\{w_j^R + w_k^R \;\middle|\; j,k = 1,...,d_R\right\} &= \left\{w_j^R + w_k^R \;\middle|\; j \le k = 1,...,d_R\right\} + \left\{w_j^R + w_k^R \;\middle|\; j > k = 1,...,d_R\right\} \\ &\equiv \left\{w_i^{S^2(R)} \;\middle|\; i = 1,...,d_{S^2(R)}\right\} + \left\{w_i^{\Lambda^2(R)} \;\middle|\; i = 1,...,d_{\Lambda^2(R)}\right\},\end{aligned} \tag{B.0.6}$$

and under these definitions of the second rank symmetric product $S^2(R)$ and the second rank antisymmetric product $\Lambda^2(R)$ that

$$R \otimes R = S^2(R) + \Lambda^2(R). \tag{B.0.7}$$

One can see that the dimensions of the second rank symmetric and antisymmetric products are

$$\begin{aligned}d_{S^2(R)} &= \frac{d_R(d_R+1)}{2}, \\ d_{\Lambda^2(R)} &= \frac{d_R(d_R-1)}{2}.\end{aligned} \tag{B.0.8}$$

Example Consider $G = SU(2)$ and $R = \mu^2$. If we label the weights $w_j^{\mu^2}$ for $j = 1,2,3$ without loss of generality as

$$w_1^{\mu^2} = (2), \quad w_2^{\mu^2} = (0), \quad w_3^{\mu^2} = (-2), \tag{B.0.9}$$

then the second rank symmetric product is specified by the weights

$$w_{ij}^{S^2(\mu^2)} \equiv w_i^{\mu^2} + w_j^{\mu^2} \tag{B.0.10}$$

for

$$(i,j) = \{(1,1), (1,2), (1,3), (2,2), (2,3), (3,3)\}, \tag{B.0.11}$$

giving

$$w_{ij}^{S^2(\mu^2)} = \{(4), (2), (0), (0), (-2), (-4)\}. \tag{B.0.12}$$

Similarly the second rank antisymmetric product is specified by the weights

$$w_{ij}^{S^2(\mu^2)} \equiv w_i^{\mu^2} + w_j^{\mu^2} \tag{B.0.13}$$

for

$$(i,j) = \{(2,1), (3,1), (3,2)\}, \tag{B.0.14}$$

[1] Here we use the Dynkin label notation for a representation: see Section 2.6.2.

giving

$$w_{ij}^{\Lambda^2(\mu^2)} = \{\,(2)\,,\,(0)\,,\,(-2)\,\}. \tag{B.0.15}$$

Thus we conclude from (B.0.12) and (B.0.15) that

$$\begin{aligned} S^2(\mu^2) &= \mu^4 + 1, \\ \Lambda^2(\mu^2) &= \mu^2. \end{aligned} \tag{B.0.16}$$

□

Bibliography

[1] E. Noether, *Invariante variations probleme*, *Math.–Phys. Kl.* **235–257** (1918) . pages 9, 33

[2] A. Beauville, *Symplectic singularities*, *Inventiones Mathematicae* **139** (Mar., 2000) 541–549, [math/9903070]. pages 9, 10, 14, 24, 27, 104

[3] H. Nakajima, *Towards a mathematical definition of Coulomb branches of* 3*-dimensional* $\mathcal{N} = 4$ *gauge theories, I*, *Adv. Theor. Math. Phys.* **20** (2016) 595–669, [1503.03676]. pages 9, 11, 28, 103

[4] D. Gaiotto and E. Witten, *S-Duality of Boundary Conditions In N=4 Super Yang-Mills Theory*, *Adv. Theor. Math. Phys.* **13** (2009) 721–896, [0807.3720]. pages 9, 11, 14, 24, 29, 30, 31, 33, 34, 35, 54, 116

[5] A. Braverman, M. Finkelberg and H. Nakajima, *Towards a mathematical definition of Coulomb branches of* 3*-dimensional* $\mathcal{N} = 4$ *gauge theories, II*, *Adv. Theor. Math. Phys.* **22** (2018) 1071–1147, [1601.03586]. pages 10

[6] M. R. Douglas and G. W. Moore, *D-branes, quivers, and ALE instantons*, hep-th/9603167. pages 10, 14, 21

[7] S. Cremonesi, A. Hanany and A. Zaffaroni, *Monopole operators and Hilbert series of Coulomb branches of* $3d$ $\mathcal{N} = 4$ *gauge theories*, *JHEP* **01** (2014) 005, [1309.2657]. pages 11, 14, 33, 36, 38

[8] G. Ferlito, A. Hanany, N. Mekareeya and G. Zafrir, *3d Coulomb branch and 5d Higgs branch at infinite coupling*, *JHEP* **07** (2018) 061, [1712.06604]. pages 11, 14

[9] A. Bourget, S. Cabrera, J. F. Grimminger, A. Hanany, M. Sperling, A. Zajac et al., *The Higgs mechanism — Hasse diagrams for symplectic singularities*, *JHEP* **01** (2020) 157, [1908.04245]. pages 11, 47, 48, 50

[10] K. Gledhill and A. Hanany, *Coulomb branch global symmetry and quiver addition*, *JHEP* **12** (2021) 127, [2109.07237]. pages 11, 12, 36, 50, 54, 115, 132, 147

[11] K. Gledhill and A. Hanany, *Poisson Brackets for some Coulomb Branches*, 2210.02966. pages 11, 12, 28, 36, 103, 147

[12] R. Brylinski and B. Kostant, *Nilpotent orbits, normality, and Hamiltonian group actions*, *arXiv Mathematics e-prints* (Mar., 1992) math/9204227, [math/9204227]. pages 11, 41, 55, 60, 62, 90, 125

[13] A. Bourget, J. F. Grimminger, A. Hanany, R. Kalveks, M. Sperling and Z. Zhong, *Magnetic Lattices for Orthosymplectic Quivers*, *JHEP* **12** (2020) 092, [2007.04667]. pages 11, 23, 44

[14] S. Cabrera, A. Hanany and A. Zajac, *Minimally Unbalanced Quivers*, *JHEP* **02** (2019) 180, [1810.01495]. pages 11, 54, 71

[15] N. Mekareeya, K. Ohmori, Y. Tachikawa and G. Zafrir, *E_8 instantons on type-A ALE spaces and supersymmetric field theories*, *JHEP* **09** (2017) 144, [1707.04370]. pages 11, 54, 84

[16] A. Bourget, S. Giacomelli, J. F. Grimminger, A. Hanany, M. Sperling and Z. Zhong, *S-fold magnetic quivers*, *JHEP* **02** (2021) 054, [2010.05889]. pages 11, 49, 50, 51, 54, 63

[17] D. Gaiotto, A. Neitzke and Y. Tachikawa, *Argyres-Seiberg Duality and the Higgs Branch*, *Communications in Mathematical Physics* **294** (Mar., 2010) 389–410, [0810.4541]. pages 11, 103, 125

[18] M. Bullimore, T. Dimofte and D. Gaiotto, *The Coulomb Branch of 3d $\mathcal{N} = 4$ Theories*, *Commun. Math. Phys.* **354** (2017) 671–751, [1503.04817]. pages 11, 42, 103

[19] M. Dedushenko, Y. Fan, S. S. Pufu and R. Yacoby, *Coulomb Branch Operators and Mirror Symmetry in Three Dimensions*, *JHEP* **04** (2018) 037, [1712.09384]. pages 11, 29, 103

[20] C. Beem, D. Ben-Zvi, M. Bullimore, T. Dimofte and A. Neitzke, *Secondary Products in Supersymmetric Field Theory*, *Annales Henri Poincaré* **21** (Apr., 2020) 1235–1310, [1809.00009]. pages 11, 103, 109

[21] O. Bergman and D. Rodríguez-Gómez, *The Cat's Cradle: deforming the higher rank E_1 and $\tilde{E}_1$ theories*, *JHEP* **02** (2021) 122, [2011.05125]. pages 14

[22] M. van Beest, A. Bourget, J. Eckhard and S. Schafer-Nameki, *(Symplectic) Leaves and (5d Higgs) Branches in the Poly(go)nesian Tropical Rain Forest*, *JHEP* **11** (2020) 124, [2008.05577]. pages 14

[23] M. Van Beest, A. Bourget, J. Eckhard and S. Schäfer-Nameki, *(5d RG-flow) Trees in the Tropical Rain Forest*, *JHEP* **03** (2021) 241, [2011.07033]. pages 14

[24] M. Bullimore and D. Zhang, *3d $\mathcal{N} = 4$ Gauge Theories on an Elliptic Curve*, *SciPost Phys.* **13** (2022) 005, [2109.10907]. pages 14

[25] C. Closset, S. Schäfer-Nameki and Y.-N. Wang, *Coulomb and Higgs branches from canonical singularities. Part I. Hypersurfaces with smooth Calabi-Yau resolutions*, *JHEP* **04** (2022) 061, [2111.13564]. pages 14

[26] M. Akhond, F. Carta, S. Dwivedi, H. Hayashi, S.-S. Kim and F. Yagi, *Exploring the orthosymplectic zoo*, *JHEP* **05** (2022) 054, [2203.01951]. pages 14, 23

[27] F. Carta, S. Giacomelli, N. Mekareeya and A. Mininno, *A tale of 2-groups: $D_p(USp(2N))$ theories*, 2208.11130. pages 14

[28] J. Distler, G. Elliot, M. J. Kang and C. Lawrie, *Isomorphisms of 4d N=2 SCFTs from 6d*, 2212.11983. pages 14

[29] H.-C. Kim and S. S. Razamat, *Star shaped quivers in four dimensions*, 2302.05113. pages 14

[30] J. Wess and J. Bagger, *Supersymmetry and supergravity*. Princeton University Press, Princeton, NJ, USA, 1992. pages 14, 15

[31] P. Goddard, J. Nuyts and D. I. Olive, *Gauge Theories and Magnetic Charge*, *Nucl. Phys. B* **125** (1977) 1–28. pages 14, 30

[32] V. Borokhov, A. Kapustin and X.-k. Wu, *Topological disorder operators in three-dimensional conformal field theory*, *JHEP* **11** (2002) 049, [hep-th/0206054]. pages 14, 30, 31

[33] J. Harris, *Algebraic Geometry: A First Course*. Graduate Texts in Mathematics. Springer, 1992. pages 14, 25, 36

[34] S. Cabrera and A. Hanany, *Quiver Subtractions*, *JHEP* **09** (2018) 008, [1803.11205]. pages 14, 49, 50

[35] A. M. Polyakov, *Quark confinement and the topology of gauge groups*, *Nucl. Phys.* **B234** (1983) 269. pages 21, 29, 34

[36] N. Seiberg and E. Witten, *Gauge dynamics and compactification to three-dimensions*, in *Conference on the Mathematical Beauty of Physics (In Memory of C. Itzykson)*, pp. 333–366, 6, 1996. hep-th/9607163. pages 21, 29, 30

[37] S. Benvenuti, A. Hanany and N. Mekareeya, *The Hilbert Series of the One Instanton Moduli Space*, *JHEP* **06** (2010) 100, [1005.3026]. pages 22

[38] A. Hanany and R. Kalveks, *Quiver Theories for Moduli Spaces of Classical Group Nilpotent Orbits*, *JHEP* **06** (2016) 130, [1601.04020]. pages 22, 23, 62, 66, 125

[39] S. Cabrera and A. Hanany, *Branes and the Kraft-Procesi transition: classical case*, *JHEP* **04** (2018) 127, [1711.02378]. pages 23, 49, 125

[40] S. Cabrera, A. Hanany and M. Sperling, *Magnetic quivers, Higgs branches, and 6d $\mathcal{N}$ = (1, 0) theories — orthogonal and symplectic gauge groups*, *JHEP* **02** (2020) 184, [1912.02773]. pages 23, 49

[41] M. Akhond, F. Carta, S. Dwivedi, H. Hayashi, S.-S. Kim and F. Yagi, *Five-brane webs, Higgs branches and unitary/orthosymplectic magnetic quivers*, *JHEP* **12** (2020) 164, [2008.01027]. pages 23

[42] A. Bourget, J. F. Grimminger, M. Martone and G. Zafrir, *Magnetic quivers for rank 2 theories*, *JHEP* **03** (2022) 208, [2110.11365]. pages 23

[43] A. Bourget, A. Dancer, J. F. Grimminger, A. Hanany, F. Kirwan and Z. Zhong, *Orthosymplectic implosions*, *JHEP* **08** (2021) 012, [2103.05458]. pages 23

[44] M. Akhond, F. Carta, S. Dwivedi, H. Hayashi, S.-S. Kim and F. Yagi, *Factorised 3d $\mathcal{N}$ = 4 orthosymplectic quivers*, *JHEP* **05** (2021) 269, [2101.12235]. pages 23

[45] A. Bourget, J. F. Grimminger, A. Hanany, R. Kalveks, M. Sperling and Z. Zhong, *Folding orthosymplectic quivers*, *JHEP* **12** (2021) 070, [2107.00754]. pages 23

[46] M. Sperling and Z. Zhong, *Balanced B and D-type orthosymplectic quivers — magnetic quivers for product theories*, *JHEP* **04** (2022) 145, [2111.00026]. pages 23

[47] S. Nawata, M. Sperling, H. E. Wang and Z. Zhong, *Magnetic quivers and line defects — On a duality between 3d $\mathcal{N}$ = 4 unitary and orthosymplectic quivers*, *JHEP* **02** (2022) 174, [2111.02831]. pages 23

[48] A. Hanany and E. Witten, *Type IIB superstrings, BPS monopoles, and three-dimensional gauge dynamics*, *Nucl. Phys. B* **492** (1997) 152–190, [hep-th/9611230]. pages 24, 49, 103, 111

[49] A. Hanany and R. Kalveks, *Quiver Theories and Formulae for Nilpotent Orbits of Exceptional Algebras*, *JHEP* **11** (2017) 126, [1709.05818]. pages 24, 125

[50] B. Fu, *A survey on symplectic singularities and resolutions*, *arXiv Mathematics e-prints* (Oct., 2005) math/0510346, [math/0510346]. pages 25

[51] K. A. Intriligator and N. Seiberg, *Mirror symmetry in three-dimensional gauge theories*, *Phys. Lett. B* **387** (1996) 513–519, [hep-th/9607207]. pages 30, 42, 49, 103, 111

[52] J. de Boer, K. Hori, H. Ooguri and Y. Oz, *Mirror symmetry in three-dimensional gauge theories, quivers and D-branes*, *Nucl. Phys. B* **493** (1997) 101–147, [hep-th/9611063]. pages 30

[53] V. Borokhov, A. Kapustin and X.-k. Wu, *Monopole operators and mirror symmetry in three-dimensions*, *JHEP* **12** (2002) 044, [hep-th/0207074]. pages 30

[54] V. Borokhov, *Monopole operators in three-dimensional N=4 SYM and mirror symmetry*, *JHEP* **03** (2004) 008, [hep-th/0310254]. pages 30

[55] N. Seiberg and E. Witten, *Monopoles, duality and chiral symmetry breaking in N=2 supersymmetric QCD*, *Nucl. Phys. B* **431** (1994) 484–550, [hep-th/9408099]. pages 30

[56] N. Seiberg and E. Witten, *Electric - magnetic duality, monopole condensation, and confinement in N=2 supersymmetric Yang-Mills theory*, *Nucl. Phys. B* **426** (1994) 19–52, [hep-th/9407087]. pages 30

[57] G. 't Hooft, *On the phase transition towards permanent quark confinement*, *Nuclear Physics B* **138** (1978) 1–25. pages 31

[58] M. K. Benna, I. R. Klebanov and T. Klose, *Charges of Monopole Operators in Chern-Simons Yang-Mills Theory*, *JHEP* **01** (2010) 110, [0906.3008]. pages 33

[59] D. Bashkirov and A. Kapustin, *Supersymmetry enhancement by monopole operators*, *JHEP* **05** (2011) 015, [1007.4861]. pages 33

[60] A. Hanany and R. Kalveks, *Highest Weight Generating Functions for Hilbert Series*, *JHEP* **10** (2014) 152, [1408.4690]. pages 41

[61] S. Cremonesi, G. Ferlito, A. Hanany and N. Mekareeya, *Coulomb Branch and The Moduli Space of Instantons*, *JHEP* **12** (2014) 103, [1408.6835]. pages 42, 43

[62] A. Bourget, A. Hanany and D. Miketa, *Quiver origami: discrete gauging and folding*, *JHEP* **01** (2021) 086, [2005.05273]. pages 43, 58, 60, 90, 96, 149

[63] A. Hanany and A. Zajac, *Ungauging Schemes and Coulomb Branches of Non-simply Laced Quiver Theories*, *JHEP* **09** (2020) 193, [2002.05716]. pages 44

[64] H. Kraft and C. Procesi, *Minimal singularities in gln.*, *Inventiones mathematicae* **62** (1980/81) 503–515. pages 47

[65] H. Kraft and C. Procesi, *On the geometry of conjugacy classes in classical groupes.*, *Commentarii mathematici Helvetici* **57** (1982) 539–602. pages 47

[66] B. Fu, D. Juteau, P. Levy and E. Sommers, *Generic singularities of nilpotent orbit closures*, *arXiv e-prints* (Feb., 2015) arXiv:1502.05770, [1502.05770]. pages 47

[67] J. F. Grimminger and A. Hanany, *Hasse diagrams for 3d $\mathcal{N}$ = 4 quiver gauge theories — Inversion and the full moduli space*, *JHEP* **09** (2020) 159, [2004.01675]. pages 47, 52

[68] A. Bourget, J. F. Grimminger, A. Hanany and Z. Zhong, *The Hasse diagram of the moduli space of instantons*, *JHEP* **08** (2022) 283, [2202.01218]. pages 47, 51

[69] G. Ferlito, A. Hanany, N. Mekareeya and G. Zafrir, *3d Coulomb branch and 5d Higgs branch at infinite coupling*, *Journal of High Energy Physics* **2018** (July, 2018) 61, [1712.06604]. pages 48, 49, 132, 137, 138, 139

[70] K. A. Intriligator, *RG fixed points in six-dimensions via branes at orbifold singularities*, *Nucl. Phys. B* **496** (1997) 177–190, [hep-th/9702038]. pages 48, 132

[71] A. Hanany and G. Zafrir, *Discrete Gauging in Six Dimensions*, *JHEP* **07** (2018) 168, [1804.08857]. pages 49, 58, 149

[72] S. Cabrera, A. Hanany and F. Yagi, *Tropical Geometry and Five Dimensional Higgs Branches at Infinite Coupling*, *JHEP* **01** (2019) 068, [1810.01379]. pages 49, 132, 141, 143, 144, 145

[73] S. Cabrera, A. Hanany and M. Sperling, *Magnetic quivers, Higgs branches, and 6d N=(1,0) theories*, *JHEP* **06** (2019) 071, [1904.12293]. pages 49, 71, 141

[74] A. Bourget, J. F. Grimminger, A. Hanany, M. Sperling and Z. Zhong, *Magnetic Quivers from Brane Webs with O5 Planes*, *JHEP* **07** (2020) 204, [2004.04082]. pages 49

[75] A. Bourget, J. F. Grimminger, A. Hanany, M. Sperling, G. Zafrir and Z. Zhong, *Magnetic quivers for rank 1 theories*, *JHEP* **09** (2020) 189, [2006.16994]. pages 49

[76] A. Hanany and N. Mekareeya, *The small E_8 instanton and the Kraft Procesi transition*, *Journal of High Energy Physics* **2018** (July, 2018) 98, [1801.01129]. pages 49, 132

[77] A. Hanany and M. Sperling, *Magnetic quivers and negatively charged branes*, *JHEP* **11** (2022) 010, [2208.07270]. pages 49

[78] A. Bourget, S. Cabrera, J. F. Grimminger, A. Hanany and Z. Zhong, *Brane Webs and Magnetic Quivers for SQCD*, *JHEP* **03** (2020) 176, [1909.00667]. pages 49

[79] H. Kraft and C. Procesi, *On the geometry of conjugacy classes in classical groups.*, *Commentarii Mathematici Helvetici* **57** (1982) 539–602. pages 49

[80] S. Cabrera and A. Hanany, *Branes and the Kraft-Procesi Transition*, *JHEP* **11** (2016) 175, [1609.07798]. pages 49, 125

[81] A. Bourget, J. F. Grimminger, A. Hanany, M. Sperling and Z. Zhong, *Branes, Quivers, and the Affine Grassmannian*, 2102.06190. pages 50, 55, 62, 63, 66, 100

[82] A. Bourget and J. F. Grimminger, *Fibrations and Hasse diagrams for 6d SCFTs*, *JHEP* **12** (2022) 159, [2209.15016]. pages 51

[83] A. Hanany and M. Sperling, *Discrete quotients of 3-dimensional $\mathcal{N}$ = 4 Coulomb branches via the cycle index*, *JHEP* **08** (2018) 157, [1807.02784]. pages 58, 59, 149

[84] A. Hanany and A. Zajac, *Discrete Gauging in Coulomb branches of Three Dimensional $\mathcal{N} = 4$ Supersymmetric Gauge Theories*, *JHEP* **08** (2018) 158, [1807.03221]. pages 58, 60, 63, 90, 149

[85] L. Bhardwaj, *On the classification of 5d SCFTs*, *JHEP* **09** (2020) 007, [1909.09635]. pages 71

[86] G. Zafrir, *Brane webs, 5d gauge theories and 6d $\mathcal{N} = (1, 0)$ SCFT's*, *JHEP* **12** (2015) 157, [1509.02016]. pages 71

[87] E. Lerman, R. Montgomery and R. Sjamaar, *Examples of singular reduction*, p. 127–156. London Mathematical Society Lecture Note Series. Cambridge University Press, 1994. 10.1017/CBO9780511526343.008. pages 119

[88] A. F. McMillan, *On embedding singular poisson spaces*, 2011. 10.48550/ARXIV.1108.2207. pages 119

[89] A. McMillan Fraenkel, *Extensions of Poisson Structures on Singular Hypersurfaces*, *arXiv e-prints* (Oct., 2013) arXiv:1310.6083, [1310.6083]. pages 119

[90] J. McKay, *Graphs, singularities, and finite groups*, *Proc. Sympos. Pure Math.* **37** (1980) 183–186. pages 120

[91] J. McKay and D. Ford, *The Geometric Vein*. Springer-Verlag, 1982. pages 120

[92] S. Benvenuti, B. Feng, A. Hanany and Y.-H. He, *Counting BPS Operators in Gauge Theories: Quivers, Syzygies and Plethystics*, *JHEP* **11** (2007) 050, [hep-th/0608050]. pages 120, 121, 123

[93] A. Hanany and D. Miketa, *Nilpotent orbit Coulomb branches of types AD*, *JHEP* **02** (2019) 113, [1807.11491]. pages 125

[94] A. Hanany and A. Pini, *HWG for Coulomb branch of 3d Sicilian theory mirrors*, 1707.09784. pages 132, 137, 138, 139

[95] B. Feng, A. Hanany and Y.-H. He, *Counting gauge invariants: The Plethystic program*, *JHEP* **03** (2007) 090, [hep-th/0701063]. pages 133

[96] O. Bergman and G. Zafrir, *Lifting 4d dualities to 5d*, *JHEP* **04** (2015) 141, [1410.2806]. pages 141

[97] R. Slansky, *Group Theory for Unified Model Building*, *Phys. Rept.* **79** (1981) 1–128. pages 150